

Molecular Mechanisms Involved in Inflammatory Bowel Disease and Colorectal Cancer: Novel Therapeutic Strategies

DOCTORAL THESIS

Daniel Roca Lema

2021

Programa de Doctorado en Biología Molecular

Director: Dr. Angélica Figueroa Conde-Valvís

Codirector: Dr. Olaia Martínez Iglesias



UNIVERSIDADE DA CORUÑA

The directors of this doctoral thesis, Dr. Angélica Figueroa Conde-Valvís, group leader of Epithelial Plasticity and Metastasis Group at the Instituto de Investigación Biomédica de A Coruña (INIBIC), and and Dr. Olaia Martínez Iglesias.

CERTIFIE THAT

This work, entitled ‘Molecular Mechanisms Involved in Inflammatory Bowel Disease and Colorectal Cancer: Novel Therapeutic Strategies’, was carried out by Daniel Roca Lema under their supervision at the Instituto de Investigación Biomédica de A Coruña (INIBIC), and gathers the conditions of originality and scientific rigor that are required to be publicly defended and which qualify for an international PhD.

And for the record and to all appropriate purposes, I sign this certificate in A Coruña, on October 19, 2021.

Signed: Angélica Figueroa Conde-Valvís
(Director and tutor)

Signed: Olaia Martínez Iglesias
(Codirector)

Signed: Daniel Roca Lema
(PhD student)



Part of this research has been carried out during a predoctoral stay in 2019 at the *Klinischen Abteilung für Gastroenterologie und Hepatologie, Medizinische Universität Wien* (Vienna, Austria), under the supervision of Dr. Christoph Gasche. This predoctoral stay was funded by the inMOTION programme INDITEX-UDC 2019.

A Abdulia

A mis abuelos

A mis padres

Agradecimientos

Durante mis años de universidad siempre dije que en cuanto acabara la carrera no quería saber nada más de estudiar ni de la universidad, que no haría un doctorado ni loco, etc. Años antes también había dicho que no me quería ir a estudiar fuera y que prefería quedarme cerca de casa. También tenía claro que quería quedarme en España y no irme a vivir al extranjero. Al final el tiempo y la vida se han empeñado en quitarme siempre la razón y he terminado estudiando en León, trabajando en Reino Unido y terminando este doctorado. Ha sido un largo camino el que me ha llevado hasta aquí, un camino que, por supuesto no he recorrido solo, por lo que me gustaría dar las gracias a todas aquellas personas que lo han hecho posible y que me han acompañado a lo largo del mismo.

En primer lugar, me gustaría dar las gracias a mi directora, Angélica Figueroa, por haber hecho posible que esta tesis se llevara a cabo. Gracias por darme total libertad desde el primer día para trabajar en el laboratorio, por fomentar que aprendiéramos de nuestros errores y buscar soluciones por nosotros mismos. Por promover que vale más intentarlo y fallar que no haberlo intentado, creo que eso ha de estar en la base de cualquier científico. Sabes que comparto tu visión optimista tanto del trabajo como de la vida, aunque seamos de los pocos en el grupo, y que sobre todo admiro tu dedicación a la investigación.

Gracias también a mi codirectora Olaia. Por haber peleado conmigo día tras día desde que comencé en el laboratorio hasta que tuviste que marchar y por haberme enseñado gran parte de lo que he aprendido a lo largo de este doctorado. Sé que no he sido el mejor alumno ni el más ortodoxo, pero quiero que sepas que tengo un cariño especial por haber dado mis primeros pasos en la investigación a tu lado. Me hace mucha ilusión ser tu primera tesis dirigida.

A todas las instituciones que han hecho posible que esta tesis se haya llevado a cabo: CICA-INIBIC, Complejo Hospitalario Universitario de A Coruña, Universidad de A Coruña, Fundación Profesor Novoa Santos, Diputación de A Coruña, Inditex y Universidad de Viena.

A los todos los donantes de las muestras, puesto que su ayuda y colaboración son fundamentales para la investigación.

A Carlos, Juan, Manu y Montse de la cafetería del Materno, por todas las risas y buenos momentos que me habéis hecho pasar durante mi tiempo en el INIBIC, sois muy grandes.

Thanks also to all the members of the Department of Gastroenterology and Hepatology at the Vienna University Hospital. In particular to Dr. Christoph Gasche to Dr. Vineeta Khare and Anita Krnjic, for sharing with me all their experience and knowledge and accepting me as one more member of the group from the beginning. Also, for all the help they have given me since the end of my stay, both with the sending of material and the revision of publications, including this thesis. Thank you, as well, to all the other members that welcomed me from the first day and

made my stay the most profitable: Max, Adrian, Michaela, Rayko, Kristine, I will always remember the lab retreat in St. Sebastian and all the good times during my time there.

A Tom, por ser la persona que quizás durante más tiempo me ha acompañado a lo largo de este camino y que pese a nuestros altos y bajos sé que me seguirá acompañando en el futuro. Espero que pronto encuentres a alguien que te acompañe también en tu camino.

Gracias por supuesto a todos mis compañeros de laboratorio. A Andrea Díaz, por los miles de momentos que hemos vivido juntos durante los últimos años, tanto los buenos como los malos, por las mil anécdotas que nos ayudaron a sobrellevar los días menos fáciles. A Marta la lagarta, que, aunque compartimos poco tiempo tiene el récord de mayor número de anécdotas en el laboratorio, toda una leyenda, además eres un ejemplo de valentía. A Jenny, por haber sido compañera de fatigas durante este tiempo, por ser esa cara amable en la mejor U de todo el laboratorio, siempre envidiaré no haber sido de inflamación ya lo sabes. A las nuevas generaciones del laboratorio, Maca y Andrea, no os voy a desear que os vaya bien porque habéis aprendido del mejor así que no tenéis más remedio de que os vaya genial. Mucho ánimo jaja.

Gracias a Alba. Porque si hay algo por lo que de verdad ha valido la pena esta tesis has sido tú. Gracias por aparecer en mi vida en el peor momento, por haber creído en mí y haberme devuelto la ilusión. Por cada tarde después del labo tirados en el campo, en el cine, yendo a Riazor, a Santa Cristina. Por Ámsterdam, Viena, León y Gijón. Por cada una de las mil preguntas que me solventabas cada día en el laboratorio y que han hecho posible que llegara hasta aquí. Porque eres un ejemplo de compromiso, esfuerzo, sensibilidad y superación, te mereces todo lo bueno que te pase en la vida. Espero que cuando mires atrás dentro de unos años y leas esto de nuevo recuerdes todos los momentos que hemos podido disfrutar juntos durante este tiempo, porque yo también lo haré. Te quiero.

Y, por último, gracias a mi familia. A mis tíos y primos. A mi cuñado, por ser uno más de la familia y como un hermano para mí. A mis abuelos. A abuelo José y abuela Obdulia, la única que no podrá leer estas líneas, pero que desde donde este sé que sigue apoyándose incondicionalmente como lo hacía siempre. A abuelo Miro y abuela Rosi, por ser mis segundos padres, todo lo que os pueda escribir aquí es poco, es un orgullo ser vuestro nieto, sois mi ejemplo a seguir, gracias por haberme cuidado siempre. A Paula, por haberme acompañado en cada paso de mi vida, por ser mi confidente y mi contrapunto, por todos los ataques de risa en la cocina que me acompañaran siempre, gracias. A mis padres, porque, aunque ningún agradecimiento será nunca suficiente para devolver todo lo que han hecho por mí, esta tesis es por ellos y para ellos. Gracias por todo el esfuerzo y sacrificios que habéis hecho para que haya podido llegar hasta aquí. Espero poder algún día ser capaz de devolveros la mínima parte de todo el cariño y dedicación que me habéis dado. Por vosotros, os quiero.

Daniel Roca Lema

Abstract

Chapter One

Inflammatory bowel disease (IBD) is characterized by chronic inflammation in the gastrointestinal tract and represents an important risk factor for the onset of colorectal cancer (CRC). Hakai is an E3 ubiquitin-ligase involved in tumour progression and metastasis of carcinomas through the degradation of E-cadherin. The loss of E-cadherin is the hallmark of EMT, a key process at early stages of carcinoma progression. In this work we investigated the expression of Hakai in all the different stages of CRC as well as its potential role in IBD. Our results show that Hakai is a potential biomarker for CRC progression and its expression is increased even at early TNM-stages of tumorigenesis. Interactome analysis of Hakai in CRC cells allowed us to identify a novel Hakai-interacting protein named FASN, a protein reported to be associated to IBD. We described that Hakai increases FASN ubiquitination and degradation, resulting in the regulation of FASN-mediated lipid accumulation. Moreover, we showed that Hakai is downregulated in inflammatory tissues by using different IBD mice models and that IFN- γ downregulates Hakai expression in CRC cells. Our findings open a new research field to better understand the mechanisms involved in intestinal inflammation and cancer bowel disease.

Chapter Two

CRC is one of leading causes of mortality in western countries and new strategies are required for its treatment. Natural products comprise a vast diversity of biologically active substances with high therapeutic potential including compounds widely used in anticancer chemotherapy. Polysaccharide-rich extracts from fungal origin, for example, have proven their antitumoral effects in different previous studies. In the present study, we aim to evaluate the possible antitumor effect on CRC cells of a series of fungal polysaccharide-rich extracts, obtained from autochthonous fungi of Galicia. We identified two extracts from *Trametes versicolor* (TV) and *Grifola frondosa* (GF) which exhibited inhibition of human colon cancer cell proliferation and induced cytotoxicity. Furthermore, both fungal extracts significantly inhibited oncogenic potential, cell migration and invasion in CRC cells as well as increased E-Cadherin expression and reduced metalloproteinase activity. Finally, our results also showed that the combination of the extracts with one the most clinical used agents for colorectal cancer, 5-fluorouracil, increases cell cytotoxicity, opening the door to further research for the use of fungal extracts as adjuvant treatment in cancer.

Resumen

Capítulo uno

La enfermedad inflamatoria intestinal (EII) se caracteriza por una inflamación crónica del tracto gastrointestinal y representa un factor de riesgo importante para el desarrollo del cáncer colorrectal (CCR). Hakai es una E3 ubiquitina-ligasa involucrada en la progresión tumoral y metástasis de carcinomas a través de la degradación de E-cadherina. La pérdida de E-cadherina es el sello distintivo de la EMT, un proceso clave en las etapas más tempranas de la progresión de los carcinomas. En este trabajo se investiga la expresión de Hakai en todos los diferentes estadios del CCR, así como su potencial papel en la EII. Los resultados muestran que Hakai es un potencial biomarcador de la progresión del CCR con una expresión aumentada incluso en las primeras etapas de la carcinogénesis. El análisis del interactoma de Hakai en células de CCR permitió identificar una nueva proteína que interactúa con Hakai, FASN, una proteína asociada con el desarrollo de la EII. En este trabajo se describe que Hakai aumenta la ubiquitinación y degradación de FASN, ocasionando la regulación de la acumulación de lípidos mediada por FASN. Además, se demuestra que Hakai está regulado negativamente en los tejidos inflamatorios de diferentes modelos animales de EII y que IFN- γ regula negativamente la expresión de Hakai en células CCR. Nuestros hallazgos abren un nuevo campo de investigación para comprender mejor los mecanismos involucrados en la inflamación y el cáncer intestinales.

Capítulo dos

El CCR es una de las principales causas de mortalidad en los países occidentales y se requieren nuevas estrategias para su tratamiento. Los productos naturales comprenden una gran diversidad de sustancias biológicamente activas con un alto potencial terapéutico, incluidos compuestos ampliamente utilizados en la quimioterapia contra el cáncer. Los extractos ricos en polisacáridos de origen fúngico, por ejemplo, han demostrado sus efectos antitumorales en diferentes estudios previos. En el presente trabajo pretendemos evaluar el posible efecto antitumoral sobre las células de CCR de una serie de extractos fúngicos ricos en polisacáridos, obtenidos de hongos autóctonos de Galicia. Se identificaron dos extractos de *Trametes versicolor* (TV) y *Grifola frondosa* (GF) con capacidad citotóxica y de inhibición de la proliferación de células de CCR. Además, ambos extractos fueron capaces de inhibir significativamente el potencial oncogénico, la migración celular y la invasión en las células CRC, así como elevar los niveles de expresión de E-Cadherina y reducir la actividad de las metaloproteinasas. Finalmente, nuestros resultados también muestran que la combinación de los extractos con uno de los agentes más utilizados en la clínica para el cáncer colorrectal, el 5-fluorouracilo, aumenta la citotoxicidad celular, abriendo la puerta a nuevas investigaciones para el uso de extractos de hongos como tratamiento adyuvante en el cáncer.

Resumo

Capítulo Un

A enfermidade inflamatoria intestinal (EII) caracterízase pola inflamación crónica do tracto gastrointestinal e representa un importante factor de risco para o desenvolvemento do cancro colorrectal (CRC). Hakai é unha E3 ubiquitina-ligasa implicada na progresión tumoral e metástase de carcinomas a través da degradación da E-cadherina. A perda de E-cadherina é o selo distintivo de TMS, un proceso clave nas primeiras fases da progresión dos carcinomas. Neste traballo, investigábase a expresión de Hakai en todas as diferentes etapas do CRC, así como o seu potencial papel na EII. Os resultados mostran que Hakai é un biomarcador potencial da progresión do CRC cunha expresión aumentada incluso nas fases iniciais da carcinoxénese. A análise do interactoma de Hakai nas células CRC identificou unha nova proteína que interactúa con Hakai, FASN, unha proteína asociada ao desenvolvemento da EII. Neste traballo, descríbese que Hakai aumenta a ubiquitinación e degradación de FASN, provocando a regulación da acumulación de lípidos mediada por FASN. Ademais, móstrase que Hakai está regulado negativamente nos tecidos inflamatorios de diferentes modelos animais de IBD e que o IFN- γ regula negativamente a expresión de Hakai nas células CCR. Os nosos descubrimentos abren un novo campo de investigación para comprender mellor os mecanismos implicados na inflamación intestinal e no cancro.

Capítulo dous

O CRC é unha das principais causas de mortalidade nos países occidentais e son necesarias novas estratexias para o seu tratamento. Os produtos naturais comprenden unha gran variedade de substancias biolóxicamente activas con alto potencial terapéutico, incluídos compostos moi utilizados na quimioterapia contra o cancro. Extractos ricos en polisacáridos de orixe fúngica, por exemplo, demostraron os seus efectos antitumorais en diferentes estudos anteriores. No presente traballo pretendemos avaliar o posible efecto antitumoral sobre as células CRC dunha serie de extractos de fungos ricos en polisacáridos, obtidos a partir de fungos autóctonos de Galicia. Identificáronse dous extractos de *Trametes versicolor* (TV) e *Grifola frondosa* (GF) con capacidade citotóxica e de inhibición da proliferación de células CRC. Ademais, ambos extractos foron capaces de inhibir significativamente o potencial oncoxénico, a migración celular e a invasión das células CRC, así como aumentar os niveis de expresión da E-Cadherina e reducir a actividade das metaloproteinasas. Por último, os nosos resultados tamén mostran que a combinación dos extractos cun dos axentes máis empregados na clínica para o cancro colorrectal, o 5-fluorouracilo, aumenta a citotoxicidade celular, abrindo a porta a novas investigacións sobre o uso de extractos de fungos como tratamento adxuntivo no cancro.

Index

Introduction: Chapter I.....	1
1. Epidemiology of Colorectal Cancer (CRC)	1
2. CRC Risk factors.....	3
3. Staging of CRC	4
4. Molecular Bases of CRC.....	6
5. Colorectal cancer pathways	11
5.1. Molecular classification of colorectal cancer	14
6. Epithelial to Mesenchymal Transition in CRC	15
6.1. EMT is associated to tumour progression and metastasis.....	18
6.2. E-cadherin regulation during EMT	20
6.3. E3 ubiquitin-ligase Hakai	20
7. Pathophysiology of inflammatory bowel disease (IBD)	25
7.1. Ulcerative colitis	28
7.2. Crohn's disease.....	30
7.3. Genetic factors in IBD.....	33
7.4. Gut microbiota in IBD.....	34
7.5. Role of fatty acids in inflammatory bowel disease: FASN and ILF3	35
7.6. Animal models for the study of IBD	39
Hypothesis and Objectives: Chapter I.....	43
Materials and Methods: Chapter I.....	45
1. Human tissues samples.....	45
2. Mice tissues samples.....	46
3. AOM/DSS Model of Colitis-Associated Cancer.....	46
4. DSS Model of Acute Colitis.....	47
5. Interleukin-10 knockout mouse model of colitis	47
6. Histology and Immunohistochemistry	47
7. Deparaffinization of Formalin-Fixed Paraffin-Embedded (FFPE) tissue and total RNA purification.....	51
8. Exosome extraction.....	51
9. RNA extraction from exosomes	52
10. Microarray Data Mining in NCBI's Gene Expression Omnibus (GEO)	53
11. Interactome.....	54
11.1. Large-scale Immunoprecipitation	54
11.2. In gel protein digestion	54

11.3. Mass Spectrometric Analysis (DDA acquisition).....	55
11.4. Interactome Analysis.....	56
12. Plasmids, Antibodies, and materials	56
13. Cell lines	58
14. Western blotting	58
15. RNA extraction and RT-qPCR.....	62
16. Plasmid transfection.....	67
17. Viral transduction.....	67
18. Immunofluorescence	73
19. RNA silencing transient	74
20. Immunoprecipitation	75
21. Analysis of Protein Stability by the Cycloheximide	76
22. Ubiquitin-proteasome assays: proteasome, lysosome or autophagy inhibition	76
23. Oil-red staining assay	76
24. Statistical analysis.....	77
Results: Chapter I	79
1. Hakai is a biomarker of tumour progression in colorectal cancer	79
1.1. Exosome analysis of serum samples from colorectal cancer patients.....	82
2. Hakai expression in human samples of Ulcerative Colitis and Crohn’s disease.....	84
3. Hakai expression in different Inflammatory Bowel Disease (IBD) mouse models.....	85
4. Hakai interactome	89
5. Effect of Hakai overexpression on FASN and ILF-3	93
6. Effect of Hakai silencing on FASN and ILF-3	94
7. Hakai interacts with FASN	97
8. Silencing Hakai increases FASN half-life	102
9. Hakai effect on FASN ubiquitination	103
10. Hakai inhibits lipid accumulation via FASN	105
11. IFN- γ affect Hakai-FASN interaction.....	106
12. FASN upregulation in inflamed tissue from an AOM/DSS Colitis-associated colorectal cancer model.....	108
Discussion: Chapter I.....	111
Conclusions: Chapter I.....	119
Introduction: Chapter II.....	123
1. Fungal extracts with antitumor effect in colorectal cancer: general characteristics.....	123
2. General medical properties of Fungi.....	125
3. Functional composition of Fungi	129

4. Antitumoral activity of Fungi.....	133
5. Antitumoral activity of the Basidiomycetes: <i>T. versicolor</i> and <i>G. frondosa</i>	138
5.1. <i>Trametes versicolor</i>	139
5.2. <i>Grifola frondosa</i>	144
Hypothesis and Objectives: Chapter II	149
Materials and Methods: Chapter II	151
1. Material	151
2. Cell lines	153
3. Mycoplasma test	153
4. Cytotoxicity assay	155
5. Sonication.....	156
6. Phase contrast microscopy	157
7. Proliferation Assay	157
8. Soft agar anchorage-independent cell growth	158
9. Wound healing assay.....	159
10. Invasion assay.....	161
11. Western Blot, Immunofluorescence and RT-qPCR.....	162
12. Gelatine zymography	163
13. Statistical analysis.....	165
Results: Chapter II	167
1. Screening of different fungal extracts from different species on the effect over viability of colorectal cancer cells	167
2. Evaluation of specific modifications in the extraction, composition and/or processing of fungal extracts.....	173
3. Screening of different fungal extracts from different species on the effect on the cell phenotype of colorectal cancer cells	181
4. Effect of <i>Trametes versicolor</i> and <i>Grifola frondosa</i> extracts on viability and proliferation of colon cancer cells	183
5. Effect of <i>Trametes versicolor</i> and <i>Grifola frondosa</i> extracts on the anchorage-independent cell growth of LoVo cells	186
6. Effect of <i>Trametes versicolor</i> and <i>Grifola frondosa</i> extracts on cell migration in LoVo colon cancer cells.....	188
7. Effect of <i>Trametes versicolor</i> and <i>Grifola frondosa</i> extracts on cell invasion in LoVo colon cancer cells.....	190
8. Effect of TV and GF extracts on E-cadherin and mesenchymal markers protein expression	191
9. Effect of TV and GF extracts on mRNA expression of E-cadherin and their transcription repressors.....	194

10. Effect of TV and GF extracts on the expression of cell cycle regulators pRb, p21 and CDK2	196
11. Effect of TV and GF extracts on metalloproteinase activity and mRNA expression	197
12. TV and GF extracts increases the effect of the chemotherapy drug 5-fluorouracil.....	199
Discussion: Chapter II.....	203
Conclusions: Chapter II.....	211
Bibliography	213
Appendixes.....	263
Appendix A	264
Appendix B	265
Appendix C	285

Figure Index

Figure 1. Worldwide Incidence and mortality rates of each cancer type in 2020 for both sexes and all ages.....	1
Figure 2. Descriptive epidemiology of colorectal cancer.....	2
Figure 3. Staging and prognosis for different stages of colorectal cancer.....	6
Figure 4. The biological hallmarks of cancer and facilitators (in black italics) of their acquisition.....	8
Figure 5. Schematic representation of all the different Colorectal cancer pathways.....	12
Figure 6. Detailed sequence of all the molecular mechanisms and mutations underlying the most common Colorectal carcinogenesis pathways.....	13
Figure 7. Schematic representation of the evolution of the molecular pathogenesis from colitis to carcinoma.....	14
Figure 8. Schematic representation of the Consensus Molecular Subgroups (CMS) classification of colorectal cancer.....	15
Figure 9. Molecular insides of the EMT program.	17
Figure 10. Model for Hakai regulation of E-cadherin.	22
Figure 11. Schematic representation of the contribution of EMT to the multiple histological manifestations of IBD.....	27
Figure 12. Schematic representation of the underlying molecular mechanisms of ulcerative colitis.....	30
Figure 13. Schematic representation of the underlying molecular mechanisms of Crohn’s disease.	32
Figure 14. Immunohistochemistry (IHC) Image Analysis Toolbox.	49
Figure 15. Distribution of the wells in the plate for testing all the conditions in viral transduction.....	69
Figure 16. Expression of Hakai in human samples of colorectal cancer, adenoma, and healthy epithelial tissue.	80
Figure 17. Expression of epithelial and mesenchymal markers in colorectal cancer, adenoma, and healthy epithelial tissue.	82
Figure 18. Expression of Hakai in human samples of Ulcerative Colitis, Crohn’s disease, Colorectal Adenocarcinoma stage IV and its healthy tissue pairs.	84
Figure 19. Expression of Hakai in mouse samples of the AOM/DSS Colitis-associated colorectal cancer model.	86
Figure 20. Expression of Hakai in mouse samples of the Acute DSS Colitis model.	87

Figure 21. Expression of Hakai in mouse samples of the IL-10 KO model.	87
Figure 22. Gene expression of Hakai in AOM/DSS and IL-10 KO mouse models.	89
Figure 23. Protein-protein interaction network of the identified Hakai interactome.	92
Figure 24. Effect of Hakai overexpression on FASN and ILF-3.	94
Figure 25. Effect of Hakai silencing on cell phenotype and FASN and Hakai expression.	95
Figure 26. Effect of Hakai silencing on FASN and ILF-3.	96
Figure 27. Hakai immunoprecipitation in HCT-116 with basal levels of expression.	97
Figure 28. Coimmunoprecipitation of FASN and Hakai.	98
Figure 29. FASN immunoprecipitation in HCT-116 co-transfected with Src and Hakai.	99
Figure 30. Attempted co-immunoprecipitation between ILF3 and Hakai.	100
Figure 31. Effect of Hakin-1 inhibitor over the coimmunoprecipitation of FASN and Hakai....	101
Figure 32. Effect of Hakin-1 inhibitor over the expression of FASN in HCT-116.	101
Figure 33. Effect of Hakai silencing on FASN half-life.	103
Figure 34. FASN is degraded by Hakai by ubiquitination via lysosome.	104
Figure 35. Hakai inhibition of lipid accumulation via FASN.	105
Figure 36. IFN- γ induces FASN expression through Hakai downregulation.	107
Figure 37. Expression of Hakai and FASN in mouse samples of the AOM/DSS Colitis-associated colorectal cancer model.	107
Figure 38. Schematic representation of the five phyla of fungi.....	124
Figure 39. Schematic illustration of therapeutic applications of medicinal mushrooms.	126
Figure 40. Scheme of the different compounds found in mushrooms with beneficial health properties.	129
Figure 41. Multiple signalling pathways possibly involved in the anti-tumoral effect of β -glucans	135
Figure 42. Crosstalk among signal transduction pathways in which Ganoderic acids participates in autophagy and apoptosis.	136
Figure 43. Working model of α -amanitin antibody-drug conjugates.	137
Figure 44. Picture of <i>Trametes versicolor</i>	139
Figure 45. Antitumoral molecular mechanisms of PSP, PSK and other extracts from <i>Trametes versicolor</i>	142
Figure 46. Antitumoral molecular mechanisms of β -glucans from <i>Grifola frondosa</i>	145

Figure 47. Representative image of how the Image J software automatically recognises the wound area.	161
Figure 48. Effect of different fungal extracts over cell viability of colorectal cancer cells after 24 h of treatment.	168
Figure 49. Effect of different fungal extracts over cell viability of colorectal cancer cells after 48 h of treatment.	169
Figure 50. Effect of different fungal extracts over cell viability of colorectal cancer cells after 72 h of treatment.	170
Figure 51. IC50 determination from the dose-response graphs of the extracts over cell viability.	172
Figure 52. Effect of different fungal extracts over cell viability of colorectal cancer cells after 72 h of treatment.....	174
Figure 53. IC50 determination from the dose-response graphs of the extracts over cell viability.	175
Figure 54. Effect of different fungal extracts on cell viability of colorectal cancer cells after 72 h of treatment.	177
Figure 55. Effect of different fungal extracts on cell viability of colorectal cancer cells after 72 h of treatment.	178
Figure 56. Effect of sonication on fungal extract effectivity in colorectal cancer cells.	179
Figure 57. Effect of different fungal extracts on cell viability of colorectal cancer cells after 72 h of treatment.	180
Figure 58. Effect of different fungal extracts on the cell phenotype of colorectal cancer cell line.	182
Figure 59. Effect of different fungal extracts on the cell phenotype of colorectal cancer cell line.	183
Figure 60. Effect of TV and GF extracts on cell viability of LoVo and HT-29 cells.	184
Figure 61. Effect of TV and GF extracts on cell proliferation in LoVo and HT-29 cells.	185
Figure 62. Effect of TV and GF extracts over anchorage-independent growth of LoVo cells...	187
Figure 63. Effect of TV and GF extracts in cell migration of LoVo cells.	189
Figure 64. Effect of TV and GF extracts over cell invasion of LoVo cells.	191
Figure 65. Effect of TV and GF extracts in protein expression of epithelial and mesenchymal markers measured by Western blot.	193
Figure 66. Effect of TV and GF extracts on protein expression of E-Cadherin measured by Immunofluorescence.	194
Figure 67. Effect of TV and GF extracts in mRNA expression of E-Cadherin and transcriptional factors measured by RT-qPCR.	195

Figure 68. Effect of TV and GF extracts in protein expression of p21, pRb and CDK2 by Western blot.	197
Figure 69. Effect of TV and GF extracts in metalloproteinase activity and mRNA expression.	199
Figure 70. Effect of the combined treatment of TV and GF extracts in combination with 5-Fluorouracil on in colorectal cancer cell viability.	200
Figure 71. Effect of TV and GF extracts in non-transformed epithelial cells viability and in combination with 5-Fluorouracil.	202

Table Index

Table 1. List of antibodies used with their reference and technique in which they were used.	57
Table 2. Components and volumes for the elaboration of the HCEC-1CT cells growth medium.	58
Table 3. List of components included in the Laemmli Buffer 5x.....	60
Table 4. List of components included polyacrylamide gels.	61
Table 5. List of components of the First-Strand cDNA Synthesis kit.	63
Table 6. List of components of the mix for the retro transcription.....	64
Table 7. List of primers used with their forward and reverse sequences.	66
Table 8. Dilutions used for transduction evaluation.	71
Table 9. List of proteins identified in Hakai interactome.	91
Table 10. List of proteins identified in Hakai interactome by Hakin-1 treatment.	92
Table 11. List of species from which each extract was obtained.....	152
Table 12. List of components included in the mix for PCR.....	154
Table 13. List of references of all the antibodies used.....	162
Table 14. List of primers used for PCR and their sequences.....	163
Table 15. List of components used for the zymography gels and their volumes.....	164
Table 16. IC50 values in LoVo cells with each extract for 72 h treatment. Data is expressed in $\mu\text{g/ml}$	173
Table 17. IC50 values in LoVo cells with each extract for 72 h treatment. Data is expressed in $\mu\text{g/ml}$	176
Table 18. IC50 values for TV and GF for each time of treatment. Data is expressed in $\mu\text{g/ml}$	185

List of abbreviations

°C	Degree Celsius
μl	Microlitre
5-FU	5-fluorouracil
AMPK	Activated protein-kinase
AOM	Azoxymethane
ATCC	American Type Culture Collection
ATP	Adenosine triphosphate
BCA	Bicinchoninic Acid
Bcl-2	B-cell lymphoma-2
BrdU	Bromodeoxyuridine (5-bromo-2'-deoxyuridine)
BSA	Bovine serum albumin
BSA	Bovine serum albumin
CBL	Casitas B-lineage lymphoma
CD	Crohn's disease
CDH1	Cadherin 1, E-cadherin
cDNA	Complementary deoxyribonucleic acid
CIMP	CpG Island Methylator Phenotype
CIN	Chromosomal instability
CMS	Consensus molecular subtype
CO ₂	Carbon dioxide
CRC	Colorectal cancer
DAB	3,3'- Diaminobenzidine
DAPI	4',6-diamidino-2-phenylindole
DC	Dendritic cells
DEPC	Diethyl pyrocarbonate
DMEM	Dulbecco's Modified Eagle's Medium
DMSO	Dimethyl sulfoxide
DNA	Deoxyribonucleic acid
DSS	Sodium dextran sulphate

ECIS	European Cancer Information System
ECM	Extracellular matrix
EGF	Epidermal growth-factor
EGFR	Epidermal growth-factor receptor
EMT	Epithelial-mesenchymal transition
FASN	Fatty acid synthase
FBS	Fetal bovine serum
FDA	U.S. Food and Drug Administration
FFPE	Formalin-fixed paraffin-embedded
g	Gravitational force equivalent (g-force)
GA	Ganoderic acid
GAPDH	Glyceraldehyde 3-phosphate dehydrogenase
GF	<i>Grifola frondosa</i>
GLOBOCAN	Global Cancer Observatory
H&E	Hematoxylin and eosin
Hakin-1	Hakai inhibitor 1
HCC	Hepatocellular carcinoma
HDI	Human Development Index
HPLC	High performance liquid chromatography
HPRT	Hypoxanthine guanine phosphoribosyl transferase
HRP	Horseradish peroxidase
HTS	High throughput screening
HYB	Hakai-pY-binding
IBD	Inflammatory Bowel Disease
IC ₅₀	Half maximal inhibitory concentration
IECs	Intestinal epithelial cells
IFN	Interferon
IHC-P	Immunohistochemistry for paraffin embedded samples
IL	Interleukin
ILF3	Interleukin Enhancer Binding Factor 3
JAMs	Junction adhesion molecules

KRAS	Kirsten Rat Sarcoma Virus
m ⁶ A	N ⁶ -Methyladenosine
mA	Milliampere
MAPK	Mitogen-Activated Protein Kinases
MET	Mesenchymal-epithelial transition
mg/kg	Milligrams per kilogram
miRNA	Micro ribonucleic acid
ml	Millilitre
mM	Millimolar
MMPs	Matrix metalloproteinases
MMPs	Metalloproteinases
MOI	Multiplicity of infection
mRNA	Messenger RNA
MSI	Microsatellite instability
MSI	Microsatellite Instability
MTT	3-(4,5-dimethylthiazol-2-yl)-2,5-diphenyltetrazolium bromide
MYC	MYC proto-oncogene, bHLH transcription factor
NaCl	Sodium chloride
NANOG	Nanog homeobox
NEM	N-ethylmaleimide
ng	Nanogram
nm	Nanometre
nM	Nanomolar
nmol	Nanomole
No	Number
NSCLC	Non-small-cell lung carcinoma
PBCs	Peripheral blood cells
PBS	Phosphate-buffered saline
PBST	Phosphate-buffered saline, 0.1% Triton X-100
PCR	Polymerase Chain Reaction
PIK3CA	Phosphatidylinositol-4,5-bisphosphate 3-kinase catalytic subunit alpha

PKD1	Protein kinase D1
pmol	Picomole
PMSF	Phenylmethylsulfonyl fluoride
pRB	Phospho Retinoblastoma protein
PSF	Polypyrimidine tract-binding protein-associated splicing factor
PSK	Polysaccharide-K
PSP	Polysaccharide-Peptide
pTyr	Tyrosine-phosphorylated, phosphotyrosine
PVDF	Polyvinylidene difluoride
qPCR	Quantitative polymerase chain reaction
RB	Retinoblastoma protein
RING	Really interesting new gene
RNA	Ribonucleic acid
RPL13	Ribosomal protein L13
RPLP0	Ribosomal protein lateral stalk subunit P0
rpm	Revolutions per minute
RPMI	Roswell Park Memorial Institute
RT	Room temperature
RT-PCR	Reverse Transcription Polymerase Chain Reaction
RT-qPCR	Quantitative Reverse Transcription Polymerase Chain Reaction
SCFA	Short-chain fatty acids
SD	Standard deviation
SDS	Sodium dodecyl sulfate
SDS-PAGE	Sodium dodecyl sulfate-polyacrylamide gel electrophoresis
SEM	Standard error of the mean
siRNA	Small interfering ribonucleic acid
Slug	Snail family transcriptional repressor 2
Snai1	Snail family transcriptional repressor 1
Src	Proto-oncogene tyrosine-protein kinase Src
TBST	Tris buffered saline, 0.1% Triton X-100
TBST	Tris buffered saline-Tween 20

TGF- β	Transforming growth factor- β
TLR	Toll-like receptor
TNF	Tumour necrosis factor
TNM	Tumour Node Metastases
Tris-HCl	Tris-hydrochloride
TUNEL	Terminal deoxynucleotidyl transferase dUTP nick end labelling
TV	<i>Trametes versicolor</i>
Twist1	Twist basic helix-loop-helix transcription factor 1
Twist2	Twist basic helix-loop-helix transcription factor 2
UC	Ulcerative colitis
V	Volt
VEGF	Vascular endothelial growth factor
WHO	
ZEB1	Zinc finger E-box-binding homebox 1
ZEB2	Zinc finger E-box-binding homebox 2
μg	Microgram
μm	Micrometre
μM	Micromolar
PPAR- γ	Peroxisome proliferator- activated receptor gamma

CHAPTER I

Introduction: Chapter I

1. Epidemiology of Colorectal Cancer (CRC)

Cancer is one of the main causes of mortality and morbidity in the world, with approximately 19,3 million new cases in 2020. The number of new cases is expected to increase in the next two decades to 30,2 million a year in 2040. The number of tumour-related deaths in 2020, according to the data provided by the WHO, accounts to 9.96 million. The tumours responsible for the highest number of deaths worldwide are lung cancer (18,0% of all cancer deaths), colorectal cancer (9,4%), liver cancer (8,3 %) and stomach cancer (7,7 %).

Colorectal cancer is the fourth type of cancer with the highest incidence worldwide for both sexes and all ages according to the Global Cancer Observatory (GLOBOCAN) in his last report of 2020 (*Cancer Today*, n.d.). Taking into account the mortality rate, colorectal cancer is the second type of cancer that causes the most deaths in the world (**Figure 1**). On the European scale, according to the European Cancer Information System (ECIS) colorectal cancer leads the incidence chart for all cancers, while occupies the second place as the type of cancer with the highest mortality (*Data explorer | ECIS*, n.d.).

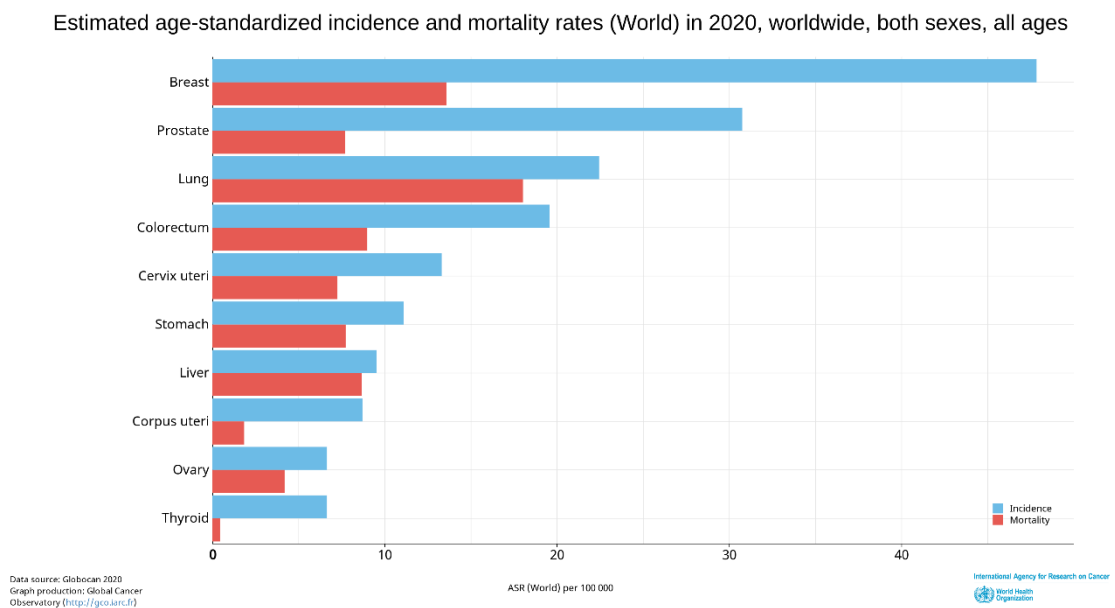


Figure 1. Worldwide Incidence and mortality rates of each cancer type in 2020 for both sexes and all ages. Source: GLOBOCAN 2020, Graph production: Global Cancer Observatory

The number of annual cases of colorectal cancer worldwide for 2020 accounts to 1.931.590 (10 %), while the 5-year prevalence is 5.253.335 (10,4 %). Incidence rates are approximately 3 times higher in developed countries than in developing countries; however, there is less variation in mortality rates, even though the highest values are in countries with the lowest human development index (HDI). The incidence of colorectal cancer is highly variable, ranging from 6 to 8 times, depending on the world region. It is a disease that could be considered as a marker of socio-economic development since in countries with periods of accelerated development, incidence rates increase uniformly with increasing HDI (**Figure 2**) (Bray et al., 2018).

Increases in disease incidence in some countries are generally influenced by changes in dietary patterns, obesity or lifestyle factors, while decreases in mortality observed in more developed countries are a reflection of improvements in survival through the adoption of better practices in the diagnosis and treatment of cancer (Siegel et al., 2019). Among this practices, the changing patterns in relation with risk factors like smoking, alcohol and body fatness as well as the increasing use of CRC screening stand out (Wolf et al., 2018)(Bray et al., 2018).

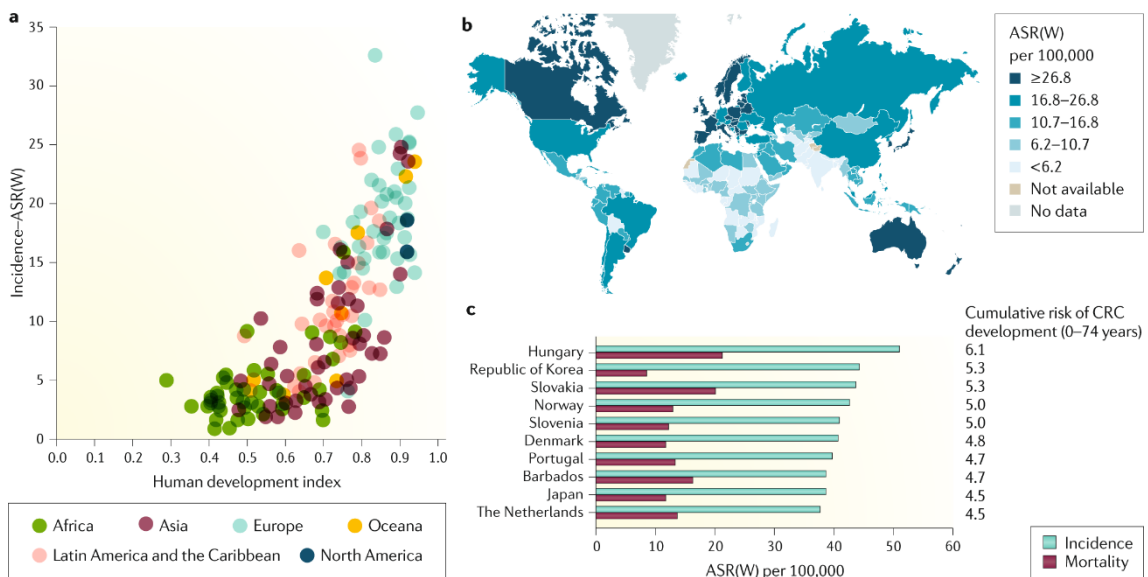


Figure 2. Descriptive epidemiology of colorectal cancer. Incidence rates of CRC are higher in countries with higher values of human development index (HDI) associated to a western dietary pattern, sedentary lifestyle and increasing obesity. Source: (Keum & Giovannucci, 2019)

2. CRC Risk factors

The aetiology of CRC is multifactorial, being the result of a complex interaction between genetic susceptibility and different biological and environmental factors. These risk factors can be divided into modifiable and non-modifiable.

Non-modifiable risk factors for CRC include age, inflammatory bowel disease, and a personal history of adenomas and/or CRC. Age has a tendency to increase the incidence from the age of 50 and is difficult to find people younger than 40 years with this type of cancer. However, in subjects with a genetic predisposition or underlying diseases, such as inflammatory bowel disease (Crohn's disease and ulcerative colitis), the age of presentation is usually before the 4th decade.

Regarding the personal history of adenomas, the presence of previous adenomas in an individual is associated with an increased risk of development CRC, although it is true that not all adenomas are malignant. The risk of recurrence of adenomas is associated with the number, size, villous component, and degree of dysplasia. The standardized incidence ratio (SIR) for CRC is 2.23 for patients with previous advanced adenomas and 0.68 for patients with previous non-advanced adenomas. The 10-year cumulative probabilities of colorectal cancer are, respectively, 2.05% and 6.22% (Cottet et al., 2012).

There is also an increased risk for those individuals with inherited diseases such as Familial Colonic Polyposis (FCP) or Lynch syndrome. Although the vast majority of CRCs are sporadic (85-90%), up to 15-20% may present family aggregation (Henrikson et al., 2015) and 5-10% are hereditary (Jiao et al., 2014).

Regarding the modifiable risk factors for CRC, the following should be highlighted: diet, gut microbial dysbiosis, consumption of fats, obesity, smoking, alcohol, cholecystectomy and radiation. These risk factors are predisposing in the development of CRC (Botteri et al., 2008; Kyrgiou et al., 2017; Nakatsu et al., 2015). However, there are modifiable risk factors that can be considered protective of the CRC, such as fibre, vegetables and fruits, calcium and vitamin D, antioxidants and physical activity (Keum & Giovannucci, 2019).

3. Staging of CRC

The TNM (Tumour Node Metastases) Classification of Malignant Tumours is a globally recognised standard for classifying the extent of spread of cancer. In the case of CRC, when the diagnosis is confirmed, it is essential to establish the correct stage of the disease development for adequate and optimal therapeutic planning. In addition, TNM classification allows the prognosis to be established and the results of the treatment to be evaluated. The most acceptable TNM (Tumour Node Metastases) classification, is from AJCC (American Joint Committee on Cancer) tumour staging system (Amin, 2016). TNM refers to three aspects, tumour size (T), regional lymph node metastasis (N), and distant metastasis (M). Each of these parameters is subclassified depending on different features (**Figure 3**).

Primary tumour (T):

- Tx: primary tumour cannot be evaluated.
- T0: no evidence of primary tumour
- Tis: carcinoma in situ; intraepithelial or invasion of the lamina propria.
- T1: tumour invades submucosa.
- T2: tumour invades own muscular layer.
- T3: tumour invades through the muscular layer the subserosa or pericolonic or perirectal tissues in areas without peritoneum.
- T4a: the tumour penetrates through the visceral peritoneum.
- T4b: directly invades other adjacent organs or structures (includes invasion of other colon segments).

Regional lymph nodes (N):

- Nx: regional nodes cannot be evaluated.
- N0: there are no metastases in regional lymph nodes.
- N1: metastases in 1 to 3 regional lymph nodes.
- N1a: metastasis in 1 regional lymph node.
- N1b: metastasis in 2-3 regional lymph nodes.
- N1c: tumour deposits in the subserosa, mesentery, or in non-peritoneal pericolonic tissues or perirectal tissue, in the absence of regional lymphatic metastases.

- N2: metastasis in 4 or more regional lymph nodes.
- N2a: metastasis in 4 to 6 regional lymph nodes.
- N2b: metastasis in 7 or more regional lymph nodes.

Distant metastases (M):

- MX: the existence of metastases cannot be evaluated.
- M0: no distant metastases.
- M1: there are distant metastases.
- M1a: metastasis confined to a single organ or a single site (lung, liver, ovary, non-regional nodes ...).

The definition of the tumour stage using the characteristics described by TNM classification is complemented by the classification in a numerical system.

Stage 0 or carcinoma *in situ*: it is the earliest phase of CRC. The tumour cells are located in the most superficial part of the mucosa and in no case pass through it. It does not affect lymph nodes.

Stage I: the tumour affects the wall of the colon or rectum without trespassing the muscle layer. There is no involvement of lymph nodes.

Stage II: the tumour has infiltrated all the layers of the wall of the colon or rectum. It can invade surrounding organs. Nodal involvement is not observed.

Stage III: the tumour may or may not affect all layers of the colon or rectum. It is defined by the presence of lymph node involvement. No presence of metastasis.

Stage IV: the cancer has spread affecting distant organs such as liver, lung or bones, that is, there is a presence of metastasis.

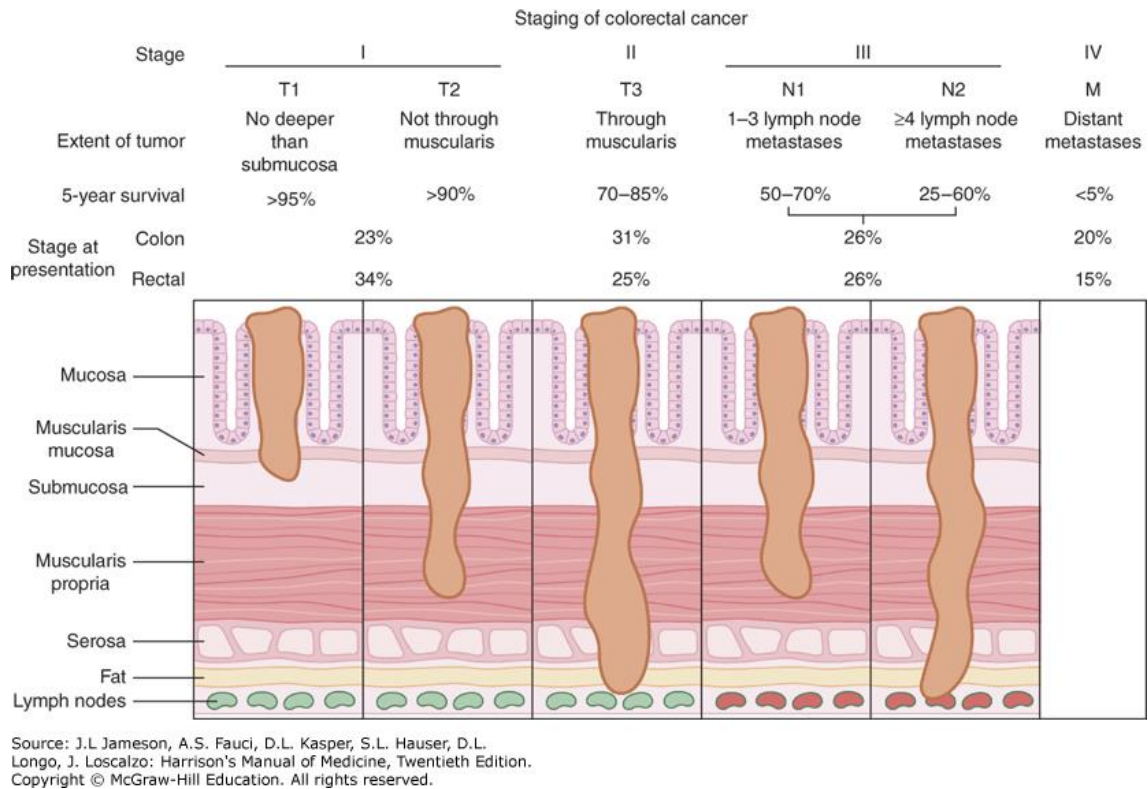


Figure 3. Staging and prognosis for different stages of colorectal cancer. Tumour staging depends on the extension of the tumour and is related with survival rates. In colorectal cancer, tumour staging is determined by the presence of invasion at the lamina propria and the serosa apart from the presence of affected lymph nodes and metastases. Source: (*COLORECTAL CANCER | Harrison's Manual of Medicine*, n.d.)

4. Molecular Bases of CRC

The vast majority of colorectal cancer cases (> 90%) correspond to adenocarcinomas, tumours that originate from glandular epithelial cells. These epithelial cells have a characteristic structure, forming layers of cells that are linked together by cellular contacts, including tight junctions, adherent junctions, gap junctions, and desmosomes. At the same time, epithelial cells are in contact with the basement membrane through cell-substrate contacts such as hemidesmosomes and focal adhesions. All these junctions are responsible for the maintenance of the epithelial structure, thus marking the separation with the connective tissue, also known as stroma. This epithelial structure is of vital importance for the health of the host and global homeostasis.

Epithelial cells have a characteristic feature known as apico-basal polarity, so that the apical zone is oriented towards the lumen and the basal zone towards the basement membrane. The loss of this peculiar structure of the epithelial tissue is the point from which carcinomas arise.

Most colorectal cancers (CRC) initiate from adenomatous polyps, which appear in the colon when the mechanisms that regulate epithelial cell renewal are altered. Multiple anatomopathological, epidemiological and observational evidence supports the existence of a polyp-carcinoma sequence (Vogelstein’s model) in the pathogenesis of CRC (Fearon & Vogelstein, 1990). It has been shown that colorectal carcinogenesis is a multi-step process in which the accumulation of genetic alterations in epithelial cells gives them a series of biological capabilities that allow tumour development.

As healthy epithelial cells progressively evolve towards a neoplastic state, they acquire a series of distinctive capacities that will allow them to first become tumorigenic and finally malignant. These eight hallmarks of cancer are: sustaining proliferative signalling, evading growth suppressors, resisting cell death, enabling replicative immortality, inducing angiogenesis, activating invasion and metastasis, deregulating cellular energetics and avoiding immune destruction (Figure 4).

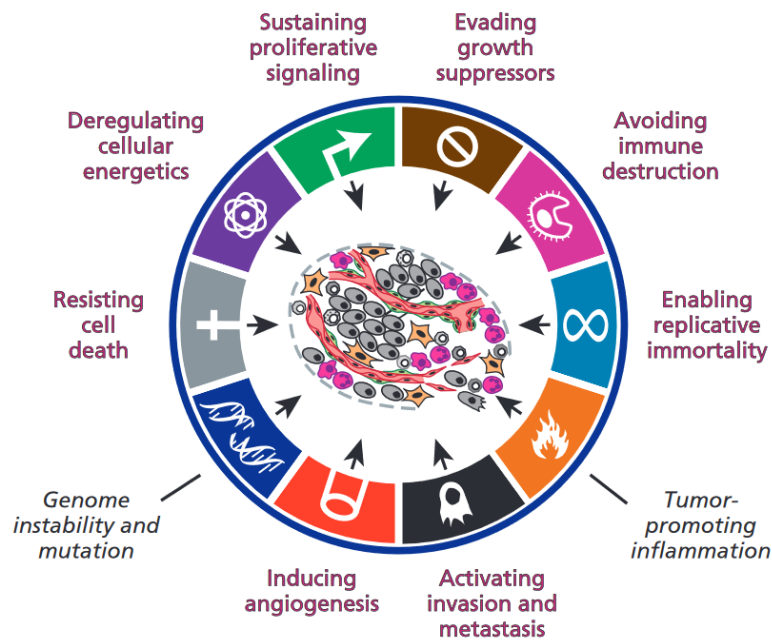


Figure 4. The biological hallmarks of cancer and facilitators (in black italics) of their acquisition. Source: (Hanahan & Weinberg, 2011)

Sustaining proliferative signalling: Normal cells depend on growth signals to be able to divide and proliferate during embryonic development, physiological growth, and homeostatic maintenance of tissues. On the other hand, tumour cells are capable of generating their own growth stimuli (autocrine signals), thus reducing the dependence on the stimuli of the cellular microenvironment and proliferating inappropriately. The most important mutations that sustain proliferative signalling in human cancers include epidermal growth factor (EGF) receptor and signal transducers in the down-stream KRAS – RAF – MEK – MAPK pathway.

Evading growth suppressors: essential tissue homeostasis is governed by a balance between growth signals and antiproliferative signals. These antiproliferative signals are mainly regulated by two monitoring systems of the growth and cell division cycle, retinoblastoma protein (pRb) and p53 protein. pRb along with several "cyclin-dependent" kinase-inhibitor proteins modulate proliferative activity from external signals transmitted through cell surface receptors. Meanwhile, p53 protein is responsible for monitoring cell division only when the physiological state of the cell is appropriate, it is activated especially in reaction to abnormal physiological situations or in the presence of severe genomic damage.

Resisting cell death: Another barrier that prevents aberrant cell proliferation is the mechanisms of programmed cell death, among which apoptosis and autophagy stand out. Under normal conditions, these programs are activated in response to an inadequate proliferation or migration capacity, as well as to cellular damage or incorrect localization. In cancer cells, these mechanisms are variably nullified or attenuated, allowing proliferative expansion and phenotypic evolution to states of intensified malignancy.

Enabling replicative immortality: Another chronic proliferation control mechanism resides in the structure of mammalian chromosomes. A cell population has a limited number of divisions after which it is unable to continue multiplying and reaches a state of senescence. This limit is marked by telomeres, short sequences present at the ends of chromosomes that are shortened with each replicative cycle and that, at a certain point, activate cell cycle arrest pathways or apoptosis. Cancer cells in some cases bypass this proliferative barrier that represents telomere erosion by expressing a telomere-

extending enzyme called telomerase. This enzyme in conditions of homeostasis has the function of preserving the replication capacity of normal embryonic and tissue stem cells.

Inducing angiogenesis: Like any other organ, tumours need a continuous supply of oxygen, glucose, and other nutrients, as well as eliminating metabolic waste for normal cell function. Without this contribution, cells die from ischemia. The excessive cell proliferation that takes place in tumours causes the blood nutrient requirements to grow rapidly and therefore the network of capillaries necessary to supply them must also grow accordingly. This growth of new vessels is known as angiogenesis and is activated by the tumour cells themselves, which, in hypoxic situations, activate systems that regulate the transcription of hundreds of genes involved in promoting angiogenesis.

Activating invasion and metastasis: The main characteristic that defines the malignancy of cancer cells is their ability to invade adjacent tissues, extravasate and migrate to distant organs to form micrometastases. There are many programs involved in the acquisition of these capacities, both intrinsic to the cell itself and dependent on the tumour microenvironment. The most relevant one is the epithelial-mesenchymal transition (EMT), which is associated with cell migration and tissue invasion during normal organogenesis. The activation of these distinctive capacities can take place at multiple points during tumour development, being sometimes an early event, and other times a late event.

Deregulating cellular energetics and metabolism: The high proliferative activity of tumour cells and the alteration of the multiple control mechanisms that have been previously mentioned leads to a very high energy expenditure. This fact has been known for almost 90 years, when Otto Warburg observed that certain cancer cells had a greater absorption of glucose. Today we know that tumour cells enhance multiple cellular energy pathways to obtain energy, from oxidative phosphorylation to aerobic glycolysis or even the use of lactate.

Avoiding immune destruction: Finally, the umpteenth barrier that incipient neoplasms have to overcome is to elude the vigilance and activity of the immune system, which would otherwise eventually eliminate these malignant cells. In this case, the

immunological mechanisms that are involved in the early stages of tumour progression are still unknown. On the one hand, because the antigens expressed by tumour cells have immune system tolerance as they are autoantigens, and only in the case of expressing embryonic or highly mutated antigens they will produce an immune response. Furthermore, the fact that immunodeficiency contexts do not markedly increase the incidence of human cancers also suggests a lack of immunological surveillance for early neoplasms. However, it has been documented in surgical resections of tumours that those tumours with a greater immune infiltrate have a better prognosis than those with little infiltration. This suggests that some types of cancer do have to deal with immune recognition and attack during the stages of neoplastic progression and, in response, acquire immunoevasive strategies. In any case, the rules governing the immune control of cancer are still ambiguous.

The acquisition by neoplastic cells of all these distinctive capabilities discussed above is a process that is possible primarily through two clearly established mechanisms. On the one hand, the development of genomic instability and the consequent generation of random mutations in genes, and on the other hand, the inflammation level of malignant and premalignant lesions caused by cells of the immune system.

Genomic instability and random mutations are routine events in the cell genome. They are caused by reaction products of normal metabolism, environmental damage, or errors during cell replication itself. The resulting defects are monitored by the cell and activate repair mechanisms for such damage. Irreparable damage causes the elimination of cells, a task orchestrated by p53, which has therefore been named the "guardian of the genome". The failure of this complex machinery, designed to monitor and repair genomic damage, results in the accumulation of mutations and genetic rearrangements of the genome, thus allowing the efficient acquisition of the hallmark cancer capabilities.

With regard to CRC, it is not considered a single disease but rather a heterogeneous group of diseases caused by a different genetic and epigenetic basis (Inamura, 2018). The progression of CRC will consist of multiple steps, transforming a normal cell into a neoplastic one, and although there is a preferred sequence, what is important is the accumulation of mutational changes, which will determine the final phenotype (Dekker et al., 2019).

The genetic alterations associated with its pathogenesis include epigenetic mechanisms (DNA methylation) and genomic instability. Genomic instability can be further divided into chromosomal instability (CIN) and microsatellite instability (MSI) (Grady & Carethers, 2008; Ogino & Goel, 2008). Genomic instability includes deletions of chromosomal regions, which involve loss of genes that may be related to negative cell cycle regulation (tumour suppressor genes); gene mutations that can activate or inactivate different proteins; gene amplifications that lead to overexpression of specific genes; or even the complete loss or gain of an entire chromosome. On the other hand, among epigenetic alterations is DNA methylation, which involves silencing of genes. This silencing is caused by the hypermethylation of repetitive CG dinucleotides (CpG islands) in the promoters of tumour suppressor genes.

CIN is produced by irregularities in chromosomal structure and copy number. These abnormalities are supposed to be occasioned by mitosis errors, for example, deficient mitotic checkpoint proteins or irregular centrosome number (Bakhoum et al., 2014).

MSI is caused by a malfunction in the DNA mismatch repair (MMR) process that is responsible for error correcting during DNA replication. When this process is impaired causes alterations in the length of microsatellite (short nucleotide tandem repeats in DNA sequences) (Pawlik et al., 2004).

5. Colorectal cancer pathways

Most CRC carcinogenesis begins from a benign precursor lesion or polyp. From this starting point, carcinogenesis may follow three different pathways: 1) adenoma–carcinoma sequence, 2) serrated pathway, and 3) inflammatory pathway (**Figure 5**).

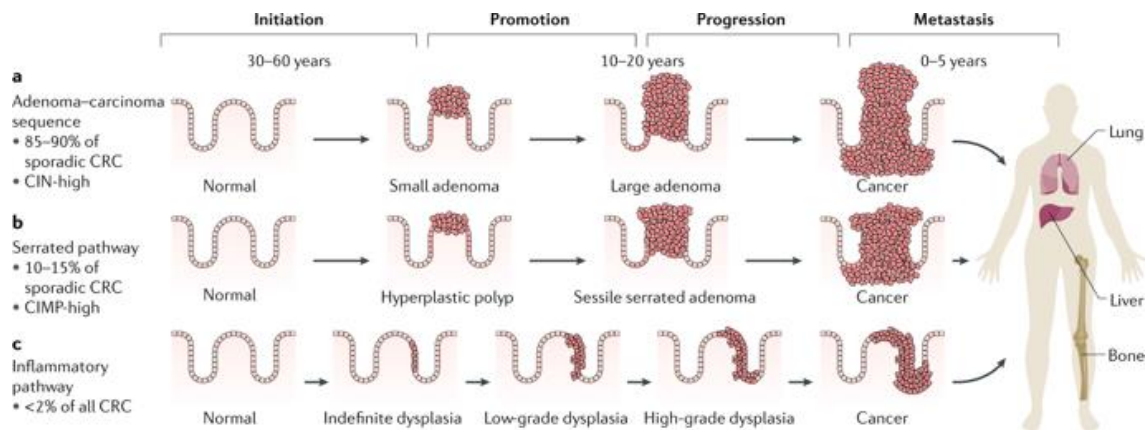


Figure 5. Schematic representation of all the different Colorectal cancer pathways and their time course depending on their molecular origin and evolution. Source: (Keum & Giovannucci, 2019)

- Adenoma-carcinoma pathway: The classic pathway that explains the majority of CRCs is the adenoma-carcinoma sequence, also known as the CRC chromosomal instability (CIN) pathway. It involves mutations in more than one gene, and the progression of CRC is determined by the sequence of these mutations. This pathway starts with the formation of a small adenoma from normal epithelial cells, which arises as a result of the gradual accumulation of genetic and epigenetic alterations, and which would eventually evolve into cancer. Inside this whole process, some genes play a key role. For example, the inactivation of APC tumour suppressor gene, which is the main responsible for the increased cell proliferation and adenoma development. Familial Adenomatous Polyposis (FAP) is the hereditary syndrome linked with APC mutation. On the other hand, mutations over the oncogene KRAS, also promote adenoma growth. Finally, the inactivation of TP53 tumour suppressor gene gives rise to the progression to CRC (Keum & Giovannucci, 2019) (**Figure 6**).

- Serrated pathway: it is linked to the so-called CpG island methylator phenotype (CIMP). Epigenetic alterations are changes in the expression of a gene, without affecting the DNA sequence. These changes are generally caused by DNA methylation or histone modification. DNA methylation often occurs at the 5'-CG-3' dinucleotide (CpG). If methylation affects the promoter region of the gene, it causes gene silencing and represents an alternative mechanism for the loss of function of tumour suppressor

genes and carcinogenesis. This pathway is characterised by the development of CRC from hyperplastic polyps known as serrated adenomas. These hyperplastic polyps are derived from normal cells but in this case the mutation of the oncogene BRAF is defined as the initial point for cell abnormal proliferation due to the inhibition of apoptosis (Kedrin & Gala, 2015; Leggett & Whitehall, 2010). From this event, the serrated lesions can progress towards hyperplastic polyps, which are very likely to undergo methylation in the CpG islands. The rate of mutations in TP53 is lower in this type of cancers (**Figure 6**).

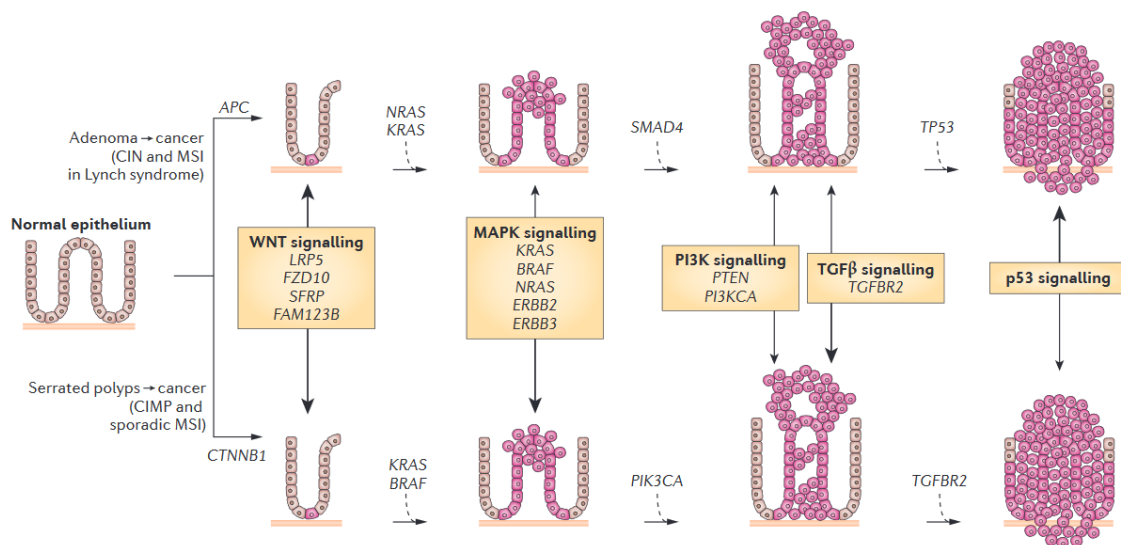


Figure 6. Detailed sequence of all the molecular mechanisms and mutations underlying the most common Colorectal carcinogenesis pathways, the adenoma-carcinoma sequence, and the serrated pathway. Source: (Kuipers et al., 2015)

- Inflammatory pathway: an alternative described pathway is the one associated with chronic inflammation and inflammatory bowel disease (IBD). The sequence of this carcinogenic process evolves from normal epithelial cells, through a series of low- to high-grade dysplasia's, until CRC finally arises. In contrast to the adenoma-carcinoma pathway, the order in which gene alteration occurs differs. In the inflammatory sequence TP53 mutations normally appear early in the process while APC mutations not always happen, or they occur later (Itzkowitz & Yio, 2004) (**Figure 7**).

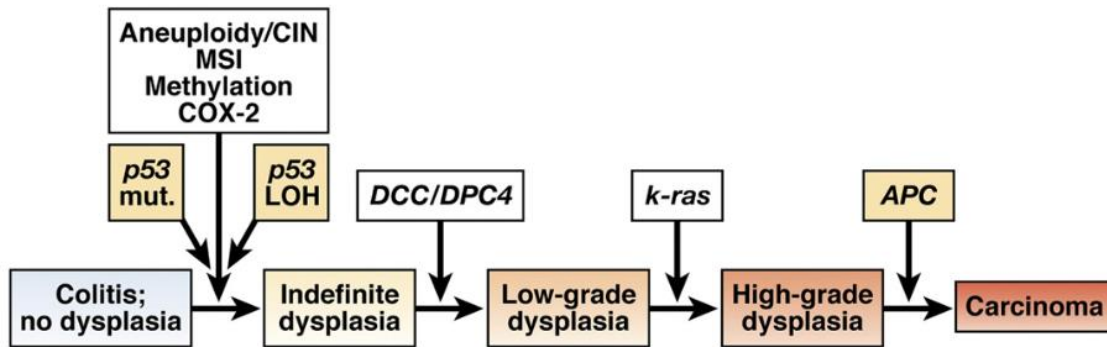


Figure 7. Schematic representation of the evolution of the molecular pathogenesis from colitis to carcinoma in the inflammatory pathway of colorectal cancer. Source: (Ullman & Itzkowitz, 2011)

As mentioned above, immune cell infiltration (inflammation) is another major way in which cells acquire the distinctive capabilities of cancer. Recently, it has been described that infiltrating immune cells (IIC) help paracrinely transmit proliferative and survival signals, proangiogenic factors, suppress cytotoxic T lymphocytes, and facilitate local invasion and metastasis. Although it is still unknown how and why they work, to a large extent, these immunological mechanisms are known to be clearly associated with contexts of chronic tissue inflammation or wound healing. In these cases, damage signals are emitted that attract IICs in order to induce and contribute to processes such as induction of angiogenesis and stimulation of cell survival, proliferation, and migration/invasion. These traits represent distinctive capabilities that may inadvertently promote neoplastic initiation and/or progression of incipient cancer cells present in inflammatory tissue microenvironments.

5.1. Molecular classification of colorectal cancer

The molecular classification of colorectal cancer has evolved significantly in recent years. Until now, the main criteria were the genomic phenotypes of microsatellite instability (MSI) and chromosomal instability (CIN), which do not overlap and provide prognostic and predictive information. MSI+ tumours are associated with a good outcome for patients in the early stages, which is probably related to the high burden of mutations and the infiltration of cytotoxic immune cells. In the metastatic setting, patients with

MSI + tumours have a poor prognosis but respond well to inhibition of immune checkpoints. Most colorectal cancers are characterized by chromosomal instability, and aneuploidy is one of the factors that predicts a poor prognosis (Sveen et al., 2018). Recently, a more detailed classification of primary colorectal cancer has been proposed based on intrinsic gene expression profiles, which has resulted in the four biologically distinct consensus molecular subtypes (CMS): CMS1 MSI-immune, Epithelial and canonical CMS2, epithelial and metabolic CMS3, and mesenchymal CMS4 (Dienstmann et al., 2017).

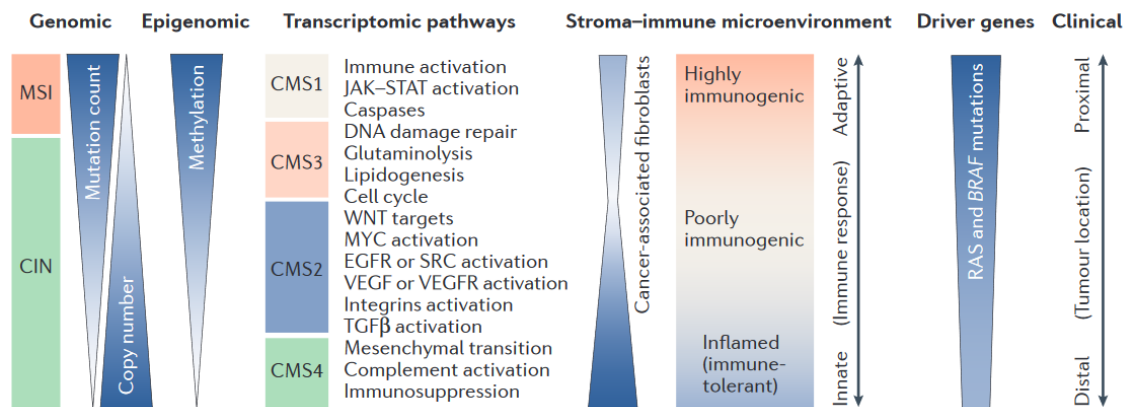


Figure 8. Schematic representation of the Consensus Molecular Subgroups (CMS) classification of colorectal cancer including their major genomic and epigenomic characteristics, pathways, and driver genes. Source: (Dienstmann et al., 2017)

6. Epithelial to Mesenchymal Transition in CRC

As previously mentioned, one of the distinctive capacities that cancer cells acquired during tumour development process is the ability to invade and metastasize. It is estimated that metastases are responsible for 90% of cancer deaths (Mehlen & Puisieux, 2006). The main regulatory mechanism that allows the activation of these cellular capacities is a process known as epithelial-mesenchymal transition (EMT), which takes place at the early stages of carcinoma progression. During EMT, cells lose their epithelial phenotype and progressively acquire a mesenchymal phenotype, which is the main characteristic that define this process. This phenotypic change is linked to the loss of apico-basal polarity of the cells, as well as the adhesions both cell-to-cell and cell-to-

substrate. Cells also reprogram gene expression and develop multiple biochemical changes that enable them to acquire a mesenchymal phenotype. As a result, cells that undergo the epithelial-mesenchymal transition acquire a greater degree of motility and invasiveness due to reorganization of the actin cytoskeleton. The increased motility and invasiveness are essential elements in the development of metastasis, as cells are able to migrate individually, invade the surrounding tissue, extravasate and travel to distant sites to metastasise (J. Yang et al., 2020).

The initial concept of epithelial-mesenchymal transformation was introduced by Elizabeth Hay, who in 1967 became aware of her involvement in embryonic development, with additional evidence of a highly coordinated and specific series of events that define the transition between epithelial and mesenchymal cells (Hay, 1970, 1995).

During the EMT process, different cell and tissue adhesion molecules play a fundamental role. There are different markers of epithelial phenotype, but perhaps the prototype and best characterized marker of the EMT process is the loss of the epithelial marker E-cadherin (Takeichi, 1988). E-cadherin is a transmembrane protein that has an extracellular domain that forms homophilic interactions in a calcium-dependent manner with other extracellular E-cadherin domains, thus allowing cell-cell adhesion. In addition, it presents a highly conserved cytoplasmic domain that is connected to the actin cytoskeleton through various catenin's, such as α -catenin, β -catenin, and p120-catenin. This cytoplasmic domain is involved in intracellular signalling. E-cadherin is a tumour suppressor whose loss is associated with EMT, the transition from adenoma to carcinoma, a low degree of tumour differentiation, and it is also an indicator of poor patient prognosis (Vleminckx et al., 1991). In addition, other EMT markers have been described that characterize the epithelial phenotype, such as cytokeratin's, (CK18, CK19 or CK20) and the mesenchymal phenotype, such as Vimentin, Fibronectin, ZEB-1, Snail, Slug or Twist (J. Yang et al., 2020).

Cell surface proteins such as E-cadherin and integrins, which mediate the connection between neighbouring cells and with the basement membrane respectively, are replaced by N-cadherin and integrins that provide the cells with transitory unions inducing them to the mesenchymal phenotype and to a higher migratory potential. This

“cadherin switch” is one of the hallmarks of EMT (Wheelock et al., 2008). The components of the cytoskeleton are reorganized while the intermediate cyokeratin filaments are replaced by Vimentin.

The resulting mesenchymal phenotype is characterized by morphological and molecular changes such as the acquisition of elongated fibroblast-like form, upregulation of mesenchymal markers (N-cadherin, Vimentin, smooth muscle actin) and components of the extracellular matrix (collagen $\alpha 1$ and $\alpha 2$), downregulation of epithelial cell surface markers and components of the cytoskeleton (E-cadherin, claudins, occludins, cyokeratin’s), upregulation and/or nuclear translocation of specific transcription factors (Snail, Slug, ZEB1/2, Twist1/2), resistance to apoptosis and increased capacity for invasion and migration through the extracellular matrix (**Figure 9**).

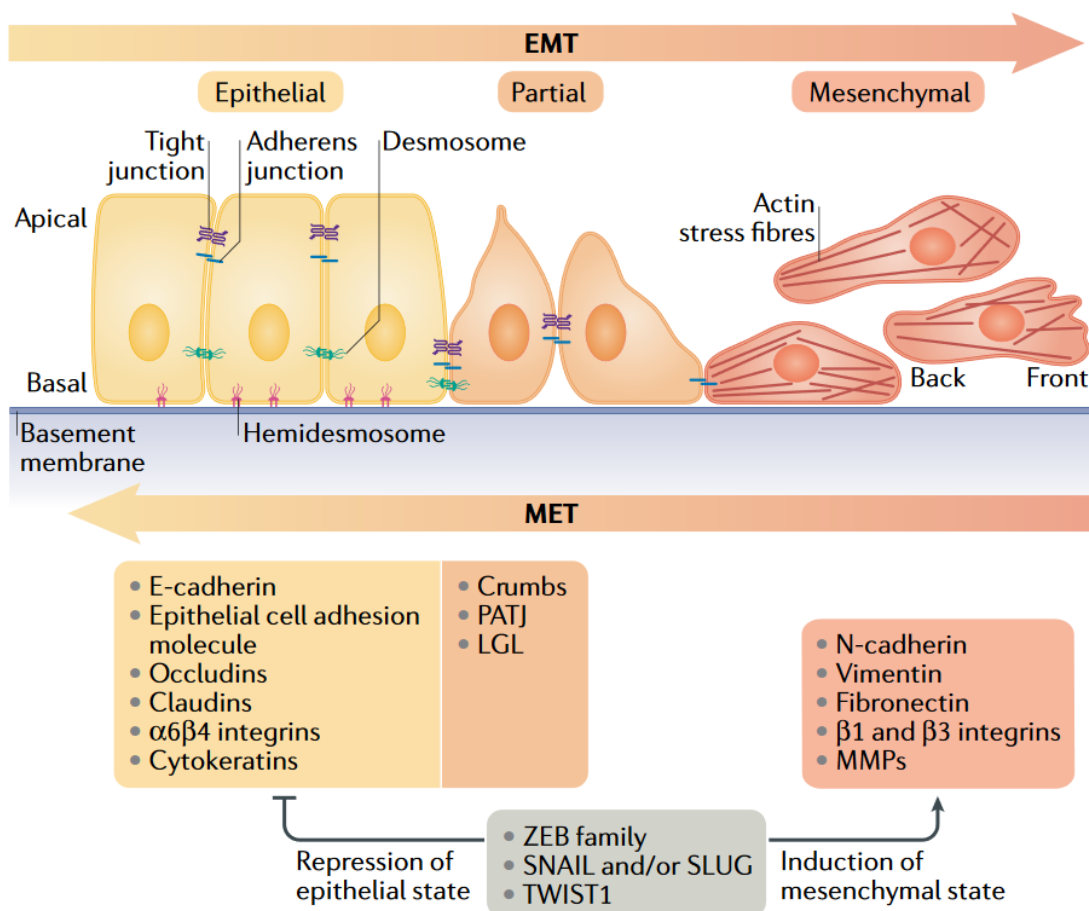


Figure 9. Molecular insides of the EMT program. Epithelial cells are induced by EMT-inducing transcription factors (ZEB, SNAIL and TWIST) to disassemble cell–cell junctions and the apical–basal cell polarity leading to the acquisition of mesenchymal features. During EMT, cells become

motile by reorganization of their actin cytoskeleton and acquire invasive capacities. Source: (Dongre & Weinberg, 2019)

EMT takes place in three different biological contexts, with different functional consequences: 1) Type I EMT, associated with developmental processes; 2) Type II EMT, associated with tissue healing and regeneration processes; and 3) Type III EMT, which is associated with tumour progression (Kalluri & Weinberg, 2009). This Type III consists of changing cancer cells of epithelial origin into tumour cells with mesenchymal characteristics capable of invading and spreading leading to the formation of metastases. These last two types of EMT are similar in conductive growth factors and in the secretion of proteases that allow these cells to reshape the surrounding extracellular matrix.

The process of EMT is a reversible and transitory process. It has been shown that once cancer cells colonize new tissues and reach distant organs, the reverse process of mesenchymal-epithelial transition (MET) occurs, leading to macrometastasis. The alternation between an epithelial phenotype and a mesenchymal phenotype is called epithelial plasticity and is an essential mechanism in the development of metastasis (Thiery, 2002)(Aparicio et al., 2015).

Although it is very well established that the process of EMT takes place in colon adenocarcinomas, it has been described that EMT is relevant in many other cancers of epithelial origin, such as kidney or prostate cancer among others (Heerboth et al., 2015).

6.1. EMT is associated to tumour progression and metastasis

In its initial stage, carcinomas are characterized by an increased epithelial cell proliferation and angiogenesis. The subsequent appearance of invasiveness occurs at the beginning of the final stage of the process, which ultimately leads to metastatic spread.

Among the genetic controls and biochemical mechanisms underlying the acquisition of this invasive phenotype, the activation of an EMT program has been proposed as a critical mechanism. In this context, the coordinated and orderly induction of a complete EMT does not occur, but instead, highly variable environmental signals, together with the genetic heterogeneity of the tumour, can lead to various degrees of

epithelial plasticity and the reactivation of migration programs associated with development, which causes the induction of individual or collective cell migration. This suggests that EMT is not only a mechanism for local dissemination of tumour cells from a primary site, but also a program with the properties necessary for tumour progression (Kalluri & Weinberg, 2009).

The molecular regulation of EMT is very complex, as it involves many signalling pathways acting independently or interconnected. Most of them converge in the control of E-cadherin expression, whose downregulation is the key molecular event in this process since it leads to the loss of intercellular junctions and destabilization of the epithelial architecture. Among the most important mechanisms in EMT regulation, it is worth highlighting E-cadherin transcriptional factors (TF), such as SNAIL, ZEB and TWIST and different pathways as TGF- β or Wnt/ β -catenin.

EMT is not only responsible for the control of the epithelial cell phenotype and the structure of the epithelium. It also controls other important pathways in the progression of carcinoma to metastasis like cell invasion. Cell invasion has been shown to be a key element in the development of metastasis and is controlled by different oncogenic signalling pathways, including EMT. It has been previously documented that the acquisition of EMT characteristics is decisive for the cellular invasion that takes place during cell progression (Kang & Massagué, 2004).

Extracellular matrix metalloproteinases (MMPs), especially MMP-9 and MMP-2, are the main mediators in the process of cell invasion. Metalloproteinases control important cellular events such as extracellular matrix (ECM) degradation and remodelling, cell proliferation, apoptosis, and morphological changes (Itoh & Nagase, 2002). In cancer, metalloproteinases allow cell progression by degrading ECM as well as stimulating and inducing cell invasion and EMT. Each type of MMP is specific for a different type of ECM substrate, for example, MMPs 1, 8, and 13 are collagen specific while MMPs 2 and 9 are gelatine specific (Jackson et al., 2010). According to several findings, there is a strong association between EMT and MMPs during tumour progression through three different mechanisms. Increased MMPs in the tumour microenvironment can directly induce EMT in epithelial cells, while tumour cells subjected to EMT can induce MMP activity and expression thereby facilitating cell

invasion, and epithelial cells can undergo EMT to through increased production of MMPs.

6.2. E-cadherin regulation during EMT

As mentioned above, E-cadherin is a key marker of EMT, and the regulation of its expression is of great importance in the control of tumour progression processes. The study of its regulation is therefore of vital importance, since its loss marks the early stages of cancer before metastasis occurs. E-cadherin could be regulated at three different levels: genetic or epigenetic regulation, transcriptional regulation, post-translational regulation (Reinhold et al., 2010).

Within regulation at the genetic or epigenetic level, the expression of E-cadherin can be affected by methylation processes on the CpG islands of its promoter, a process that has already been mentioned previously. Likewise, genomic instability can affect the expression of E-cadherin either by mutations at the chromosomal level in which the gene is lost or mutations at the genetic level that can activate or inactivate that gene (Y. N. Liu et al., 2005). Regulation can also take place at the transcriptional level. This type of regulation is very well studied and different transcriptional repressors of E-cadherin are known, such as Snail, Slug, Twist or Zeb. Furthermore, posttranscriptional mechanisms are also reported during EMT (Aparicio et al., 2013).

Within the regulation at the post-translational level, we can find the processes of phosphorylation, glycosylation, ubiquitination, and proteolysis. The proteolysis of E-cadherin is mediated, among others, by the metalloproteinases MMP-2 and MMP-9. N-acetylglucosaminyltransferase-III (GnT-III) has also been shown to be able to regulate the expression of E-cadherin through its glycosylation (Pinho et al., 2012)(Pinho & Reis, 2014). Finally, the phosphorylation of tyrosine residues of E-cadherin is mediated by EGF, FGF receptors and s-Src kinase, between others (Dupre-Crochet et al., 2007).

6.3. E3 ubiquitin-ligase Hakai

The degradation of E-cadherin dependent on phosphorylation is in turn associated with a process of ubiquitination. The ubiquitination process consists of adding one or more ubiquitin molecules to a target protein, and it may have different consequences. Although the most studied is the degradation of the target protein via the proteasome,

ubiquitination can also alter its cellular location, affect its activity, and promote or prevent protein interactions. This protein degradation system via ubiquitin-proteasome was first described in 1980 (Hershko et al., 1979, 1980), deserving of the Nobel Prize in Chemistry in 2004.

During the ubiquitination process three enzymes are involved. The ubiquitin activating enzyme (E1), responsible for the activation of ubiquitin; the ubiquitin-conjugating enzyme (E2) responsible for transferring ubiquitin; and the ubiquitin-ligase enzyme (E3) capable of specifically recognizing the target substrate.

In 2002, the first post-translational regulator of the stability of the E-cadherin protein was described (Fujita et al., 2002). This regulator, called Hakai for its Japanese meaning of “destruction”, was described as an E3 ubiquitin-ligase that mediates ubiquitination and degradation of E-cadherin in a phosphorylation-dependent manner, causing its disappearance from cellular contacts, and therefore the alteration of the cellular unions. Following internalization, E-cadherin is degraded into the lysosomes by means of Rab5 and Rab7 GTPases, and the mesenchymal phenotype is maintained by the reduction of E-cadherin recycling by Rab11-containing recycling endosomes (Mosesson et al., 2008; Palacios et al., 2005). The recognition of E-Cadherin by Hakai is dependent on the phosphorylation of its tyrosine residues by tyrosine kinase v-Src, then Hakai binds to the cytoplasmic domain of E-Cadherin and mediates its internalization and subsequent ubiquitin-dependent degradation (**Figure 10**).

To date, E-cadherin is the only described Hakai substrate that is directly involved in the EMT process. However, it has also been observed that Hakai interacts with other Src-phosphorylated proteins such as DOK-1 and Cortactin, although the biological significance of this interaction is still unknown. Moreover, Hakai was found to be ubiquitously expressed, even in tissues such as lymph nodes or skeletal muscle where E-cadherin is completely absent, suggesting that Hakai may have additional substrates (Fujita et al., 2002). In 2009, Figueroa and collaborators identified polypyrimidine tract-binding protein-associated splicing factor (PSF) as a novel Hakai-interacting protein. The authors observed that PSF colocalized with Hakai at the nucleus, promoting PSF RNA-

binding ability and acting in an E3-ubiquitin ligase-independent manner (Figueroa, Fujita, et al., 2009; Figueroa, Kotani, et al., 2009).

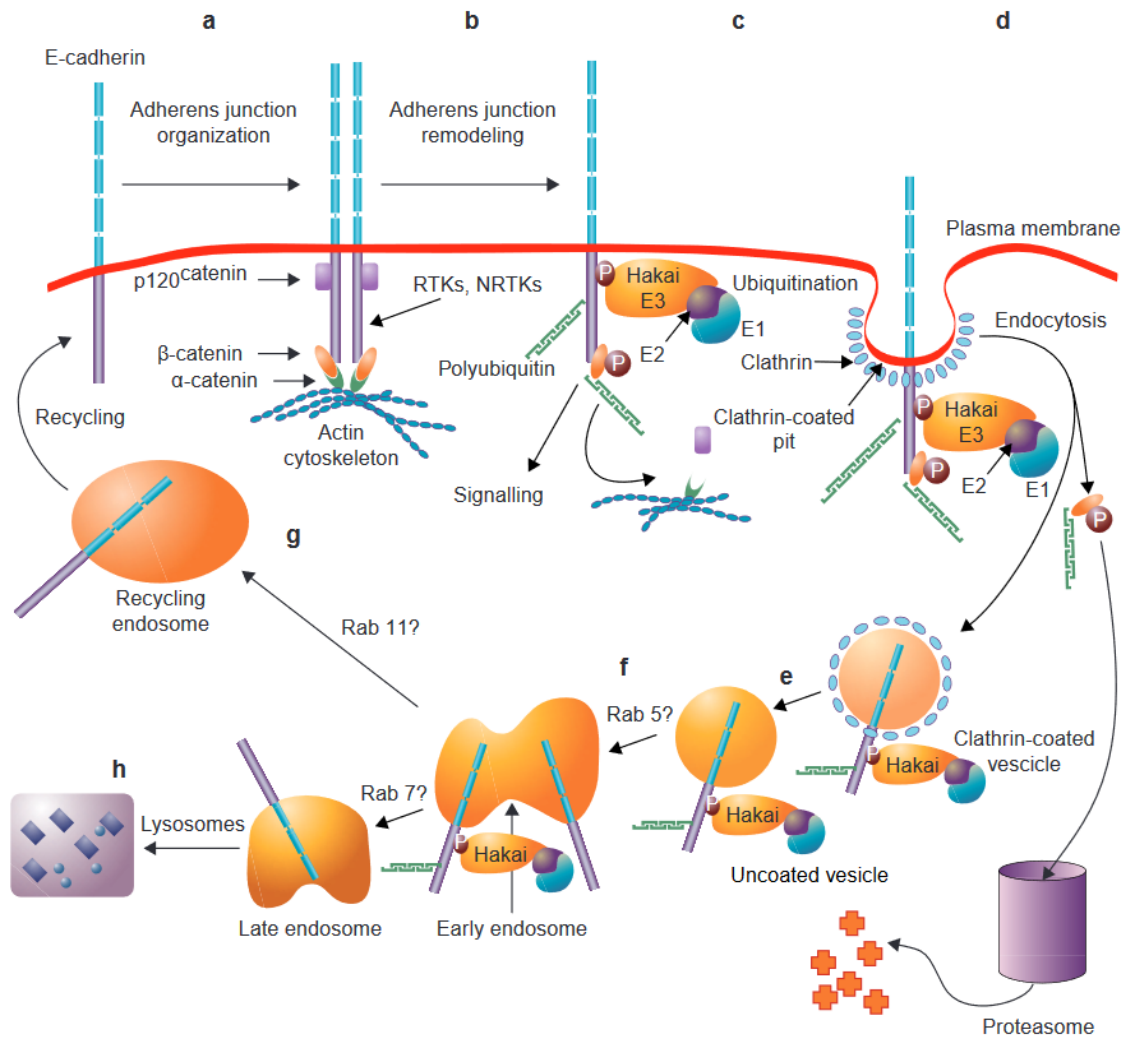


Figure 10. Model for Hakai regulation of E-cadherin. Tyrosine-phosphorylated E-cadherin is recognized and ubiquitinated by E3 ubiquitin-ligase Hakai. E-cadherin then suffers endocytosis through Rab5 and Rab7 GTPases, and finally is degraded by lysosomes. Recycling of E-cadherin through Rab11 is diminished, thus maintaining the mesenchymal phenotype. Source: (Pece & Gutkind, 2002).

In breast cancer cells, it was observed that Hakai interacted with estrogenic receptor alpha (ER α) and inhibited its activity by competing with ER α coactivators SRC-1 and SRC-2, which are necessary for ER α transactivation (Gong et al., 2010). In hepatocellular carcinoma (HCC), Hakai was described to interact with Ajuba, a tumour suppressor that acts as a negative regulator of Wnt signalling pathway, inducing its degradation through neddylation. Moreover, these authors also observed that Hakai interacted with β -catenin and induced its nuclear translocation (M. Liu et al., 2018). In

last years, novel Hakai-regulated proteins have been identified (Díaz-Díaz et al., 2017). In a recent publication, Hakai has been shown to form a protein interaction complex with Hsp90 chaperone and Annexin A2. Interestingly, in this study authors observed that Hakai not only interacts with Annexin A2 but also reduces its expression, suggesting it may be a novel substrate for E3 ubiquitin-ligase Hakai (Díaz-Díaz et al., 2020).

Hakai has also been described to interact with RNA and play a regulatory role in epitranscriptomics, during m6A methylation. It was initially observed to form a complex with WTAP, Virilizer and other members of the m6A methylation complex in HeLa cells (Horiuchi et al., 2013), and this interaction of Hakai with different members of m6A methylation complex was further reported in *Arabidopsis thaliana* (Růžička et al., 2017). Later on, Hakai was reported to regulate mouse embryonic stem cell (mESC) self-renewal by forming a complex with Zc3h13, WTAP and Virilizer, thus promoting m6A methylation of nuclear RNA (Wen et al., 2018). Moreover, recent studies carried out in *Drosophila melanogaster* and human cells demonstrated that Hakai is a conserved component of the methyltransferase complex. Hakai was observed to colocalize and interact with and stabilize other members of the m6A writer complex, through its ubiquitination domain. However, it was observed Hakai-mediated stabilization of m6A writer complex subunits is independent of its ubiquitin-ligase activity (Bawankar et al., 2021; Y. Wang et al., 2021). It is through this very same mechanism that Hakai also has been linked with the regulation of the immune microenvironment of periodontitis where Hakai is believed to regulate TNF cytokine and its receptors (X. Zhang et al., 2021). Therefore, considering this described role of Hakai in epitranscriptomics, as well as its interaction with other proteins besides E-cadherin, it has been considered that Hakai may be involved not only in EMT but also in other cellular processes.

E3 ubiquitin-ligase Hakai was initially described as a RING-type E3 ligase that resembled the Cbl family, which have three different domains: an N-terminal phosphotyrosine (pTyr)-binding domain, a central RING finger domain and a proline-rich domain at the C-terminal region. However, although Hakai contains the same domains, their linear order is different, as the RING domain is located at the N-terminal region, followed by the pTyr-binding and the C-terminal proline-rich domains (Fujita et al., 2002). Moreover, it was also observed that the mechanism for the recognition of

tyrosine-phosphorylated substrates is different between Hakai and Cbl ligases. In 2012, Mukherjee and collaborators observed that Hakai formed an atypical pTyr-binding domain, as it exhibited a homodimeric configuration formed as a result of the anti-parallel dimerization of two Hakai monomers interacting in a zinc-coordinated manner. The dimerization process results in the formation of a phosphotyrosine-binding pocket that recognizes tyrosine-phosphorylated substrates such as E-cadherin (Mukherjee et al., 2012). This unusual pTyr-binding domain of Hakai, which comprises amino acids 106-206, was called HYB (for Hakai-pY-binding), and its dimeric structure is essential for the interaction with tyrosine-phosphorylated substrates (Mukherjee et al., 2014). It is important to mention that, to date, the HYB domain has only been described in Hakai and the testis-specific E3 ubiquitin-ligase ZNF645. Although ZNF645 is able to interact with E-cadherin, it does not interact with other described Hakai substrates such as Cortactin, thus suggesting they could exhibit different substrate specificities (Y. Q. Liu et al., 2010). Therefore, due to its distinctive structural features, the HYB domain has been proposed as a promising therapeutic target for cancer treatment (Aparicio et al., 2012; Mukherjee et al., 2012, 2014).

The excessive degradation of E-cadherin, such as that produced when Hakai is overexpressed, is related to the process of invasion and metastasis, suggesting its participation in tumour progression.

The role of Hakai during tumour progression has been described in various publications. Its overexpression has been associated with increased cell proliferation *in vitro* as well as induction of tumour progression and metastasis *in vivo* (Castosa et al., 2018; Figueroa, Kotani, et al., 2009) (Figueroa, Fujita, et al., 2009). Most of the information on the importance of Hakai in cancer has been described in colorectal cancer but there are also references to its role in the regulation of other cancers such as lung or liver cancer (M. Liu et al., 2018; Zi Liu et al., 2018)(Aparicio et al., 2012). Recently, specifically designed inhibitors against Hakai have been shown to effectively inhibit tumour growth and progression of colorectal cancer both *in vitro* and *in vivo* (Martinez-Iglesias et al., 2020).

Due to the key role Hakai plays in regulating a marker as important as E-cadherin for the EMT process, it has been considered as a potential therapeutic target against

cancer. Based on the fact that the loss of E-cadherin is the hallmark of EMT and allows epithelial cells to lose their polarity, their cell-cell junctions as well as gain migratory and invasive capacity, searching for compounds that are capable of controlling their degradation through its main post-translational regulator seems a very promising alternative.

Furthermore, the use of Hakai as a therapeutic target would have the advantage of the high specificity of such treatment. This is because as E3 ubiquitin-ligase, it has a very high degree of specificity for its substrates and therefore its eventual inhibition would not cause many side effects. This contrasts with other treatments already developed within the ubiquitin-proteasome pathway such as bortezomib or carfilzomib (D. Chen et al., 2011; Ziogas et al., 2017). Both inhibitors were designed against proteasome subunits, thus inhibiting the degradation of multiple proteins, which has been very useful in the treatment of some cancers but at the cost of high cytotoxicity due to their low specificity. More specifically, these types of inhibitors have shown great results in the treatment of haematological malignancies, however, the clinical efficacy for solid tumours has been limited (Huang et al., 2014; Roeten et al., 2018).

7. Pathophysiology of inflammatory bowel disease (IBD)

The link between inflammation and tumorigenesis is well-established for CRC and, as previously mentioned, a specific pathway of carcinogenesis has been described. IBD is a chronic inflammatory condition that affects the gastrointestinal tract, and it comprises two main clinical entities: Crohn's disease (CD) and ulcerative colitis (UC). These two diseases, historically, have been studied together because of their common symptoms and treatment but nowadays it is clear that they represent two distinct pathophysiological entities. IBD is an important risk factor for the development of CRC and the incidence and characteristics are similar for both pathologies. In the case of ulcerative colitis, the risk of CRC is increased 2.4-fold (Jess et al., 2012) and in the case of Crohn's disease the risk increases 2.5-fold (Canavan et al., 2006). The cumulative risk increases with the passage of time of both diseases, being 2,1 % at 10 years, 8,5 % at 20 years and 17,8 % at 30 years for patients with UC and 2,9% at 10 years for patients with Chron's disease (Eaden et al., 2001).

Both CD and UC are complex diseases that involve a great interrelation between the immune system, the intestinal microbiota and multiple environmental factors. Besides, there are also findings of some genetic alterations that predispose to a greater risk of both diseases, but especially CD (De Souza & Fiocchi, 2016). In this way, it is considered that this group of diseases occurs in subjects with a certain genetic predisposition, in which the previously described factors trigger an uncontrolled inflammatory reaction in the digestive tract. Although important advances have been made in the knowledge of these diseases, the main events or triggers and their sequence until the appearance of intestinal lesions are still unknown.

In the pathophysiology of IBD, several immunological mechanisms have been observed that are involved in its appearance (Maloy & Powrie, 2011; Ramos & Papadakis, 2019). Among them, it should be noted, anomalies in the epithelial barrier, alterations in the mechanisms of autophagy, dysregulation of the recognition systems for external agents, changes in innate immunity, altered immune effector systems and changes in adaptive immune response.

The intestinal epithelial barrier represents one of the principal areas of interaction of the human body with the outside, as well as with the intestinal microbiota. This barrier, despite being composed of a single line of epithelial cells (enterocytes), has an essential role in the pathophysiology of IBD as it is responsible for key functions such as mucus and antimicrobial peptides secretion, release of cytokines and recognition of molecular patterns of external agents.

Disruption of the epithelial barrier leads to an inflammatory response as part of the physiological wound healing process aimed to repair the damaged tissue and restore the normal structure and functionality of the intestine (H. Jiang et al., 2018). This wound healing and tissue repair process is mediated by type 2 EMT, as described above (**Figure 11**). Epithelial cells gain motility through this program and migrate to the site of injury to restore tissue integrity. The study of biopsies from sites of active inflammation in UC patients showed an enrichment in the EMT pathway, specially E-Cadherin, in active lesions compared to inactive or normal colon tissue (Lovisa et al., 2019). This fact was also associated with a higher metastatic potential at the active site of ulceration and potentially suggesting the use of the EMT as a molecular marker to determine cancer

risk in patients with active UC lesions (Zhao et al., 2015). In CD, immunohistochemistry analysis of CD characteristic fistulae, revealed that EMT transcription factors might play a critical role in the development of these structures. Snail was highly expressed in the nuclei of cells forming non-epithelialized fistulae, which do not show a layer of epithelial cells but instead are covered by a thin layer of myofibroblast-like cells that represent epithelial cells that have undergone EMT (Botaille et al., 2008).

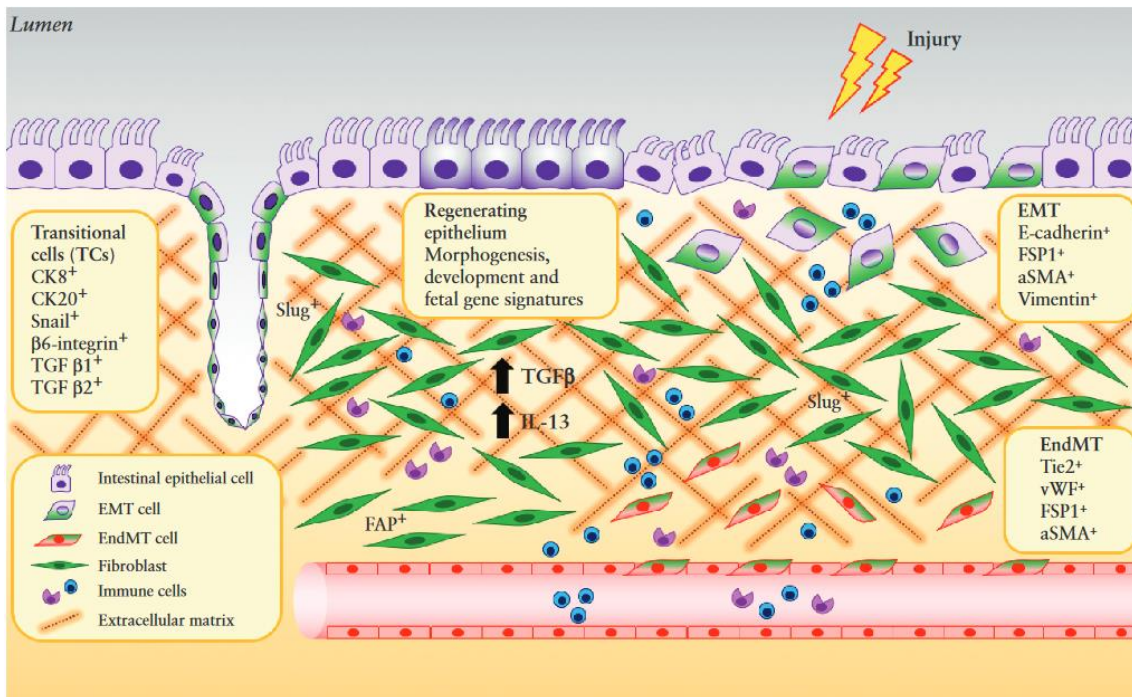


Figure 11. Schematic representation of the contribution of EMT to the multiple histological manifestations of IBD. EMT is activated in IBD in response to injury contributing to the fibrogenic process by generating epithelial-derived fibroblasts that are responsible for tissue scarring. Source: (Lovisa et al., 2019)

Autophagy consists of a series of cellular mechanisms with a main role in "cell recycling" as well as in the recognition and processing of molecules from external microbial agents. Its activity, and therefore its alterations, are relevant since they influence cytokine signalling and antibacterial defence (Park et al., 2017). Its relevance is demonstrated by observing that certain genetic variants in some of the main proteins of the autophagy process, specifically the T300A polymorphism of the ATG16L1 gene, confers a higher risk of CD and is related to alterations at the level of Paneth cells

(Stappenbeck & McGovern, 2017). Although this variant is the main one, up to 12 other variants have been described that may be relevant in IBD (Lassen & Xavier, 2017).

The immune system has external agent recognition systems that try to identify common molecular patterns of the multiple microorganisms that are usually in contact with the gastrointestinal mucosa surface. The main pathways that have been identified in the pathophysiology of IBD involve Toll-like receptors (TLRs) within extracellular receptors and NOD2 between intracellular mechanisms. Some missense variants of this NOD2 gene have been described to over-activate NF- κ B conferring susceptibility to CD and representing a solid molecular model for pathogenic mechanism of CD (JP et al., 2001).

Innate immunity comprises all the cells and mechanisms in charge of the recognition and control of pathogens, and its alterations have been associated with different pathologies. Its main role is to maintain homeostasis with the external environment, so that the immune response is generated only against harmful agents. In IBD, macrophages and dendritic cells show a pro-inflammatory profile with the overexpression of receptors and cytokines, which favours the perpetuation of the inflammatory process (Bernardo et al., 2018).

Since the role of these alterations varies according to if they are analysed in UC or CD, an independent approximation is needed to identify most relevant to each of the pathologies.

7.1. Ulcerative colitis

UC is characterized by inflammation of the mucosa, normally initiating in the rectum, and extending to the colon on a continuous basis. Inflammation in UC is typically limited to the mucous layer, causing superficial damage to the intestinal wall. The incidence of UC globally is estimated at 0,15-57,9 cases per 100.000 person-years, with a prevalence ranging from 2,42-505,0 cases per 100.000 person-years (Ng et al., 2017).

When considering UC, the main pathophysiological mechanisms involved in this disease include different alterations like changes in the epithelial barrier and in the intestinal mucosa (Kobayashi et al., 2020). The expression of activated peroxisomal proliferator receptor gamma (PPAR- γ), a negative modulator of inflammation

mediated by nuclear factor kappa-light-chain-enhancer of activated B cells (NF- κ B), is downregulated in the epithelial cells of patients with UC, which is considered to have a possible role in the onset of the disease (Decara et al., 2020; Dubuquoy et al., 2006).

In addition to this, autoantibodies have also been studied as diagnostic markers and potential drivers of inflammation, such as those directed against colonocyte-associated tropomyosin, although these findings are insufficient to suggest a clear autoimmune origin of UC (Geng et al., 1998; Jodeleit et al., 2020). What has been proven is the increased risk of UC patients for other autoimmune diseases, which shows that autoimmunity could play an important role in this pathology, but a more in-depth study is still necessary. (Wilson et al., 2016).

Expression of trefoil factors have been also found as an alteration in UC patients. These factors belong to a family of proteins related to goblet cells and are produced in response to damage to the intestinal mucosa. Differential expression of this proteins have been described in UC patients (Aamann et al., 2014; Hensel et al., 2014), and have been proposed as a biomarker of mucosal healing (Srivastava et al., 2015). Other findings include the inflammatory infiltrate of neutrophils in the intestinal mucosa and at the crypt level, as well as the expression in dendritic cells of costimulatory molecules that contribute to triggering an abnormal immune response after disruption of the intestinal barrier, even in patients in remission (Bennike et al., 2015; Dinallo et al., 2019).

This pro-inflammatory immune cell infiltrate present at the intestinal mucosa is responsible for the origin of several cytokines (IL-13, TNF, IFN- γ , IL-23, IL-9, and IL-36) (**Figure 12**) with a central function in the pathogenesis of UC. Among them, TNF is the most important as it plays an integral role in the pathogenesis of UC and is elevated in patients suffering from this disease. Overexpression of TNF causes a significant decrease in intestinal barrier resistance and therefore TNF produced in the inflammatory infiltrate of the lamina propria results in barrier defects characteristic of UC (Lissner et al., 2015). In fact, different studies have demonstrated the efficacy of anti-TNF treatment in the treatment of subgroups of patients with UC (Rutgeerts et al., 2005).

In the inflammatory immune cell infiltrate of patients with UC it is also common to find dendritic cells that secrete costimulatory molecules that contribute to triggering an abnormal immune response after disruption of the intestinal barrier. Among their main functions, these cells can metabolize vitamin A to produce retinoic acid and thus induce the expression of integrin $\alpha 4\beta 7$ in both T and B lymphocytes. In this way, these lymphocytes, which will pass into the systemic circulation, will be able to bind to their respective ligand (MAdCAM-1)(Figure 12) and thus subsequently extravasate towards the intestinal mucosa (Fischer et al., 2016).

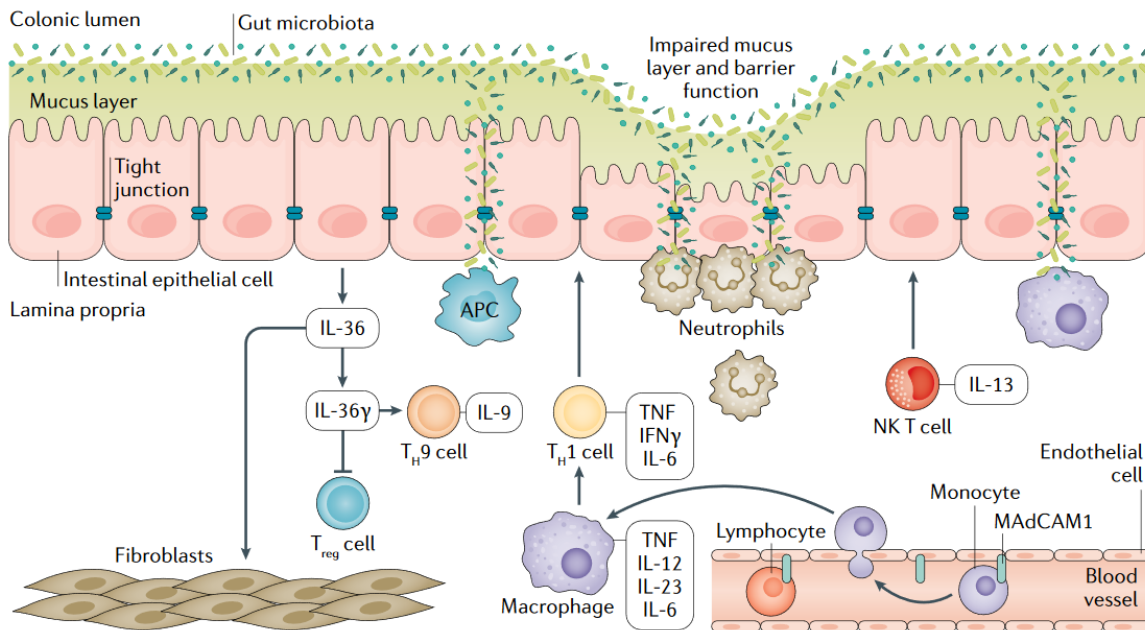


Figure 12. Schematic representation of the underlying molecular mechanisms of ulcerative colitis. In UC Intestinal epithelium is disrupted due to an Impaired mucus layer and barrier function, then, the microbiota that cross the barrier, activates macrophages and antigen-presenting cells (APCs) inducing expression of chemokines. This fact initiates an inflammatory cascade that leads to the chronicity of the disease. .Source: (Kobayashi et al., 2020)

7.2. Crohn's disease

CD would be the second major disease of IBD. It is an inflammatory bowel disease that can affect any part of the digestive tract and is characterized by intermittent patchy lesions along any part of the digestive tract, instead of the continuous lesions caused by UC. CD is characterized by transmural inflammation (involving all layers of the intestinal wall) that leads to the development of fibrosis, stenosis, and fistulas. The incidence of

CD globally is estimated at 0,09-29,3 cases per 100.000 person-years, with a prevalence ranging from 0,9-322,0 cases per 100.000 person-years.

As in UC, CD is caused by a combination of multiple factors and with great interindividual variability of all of them, including genetic susceptibility, environmental factors and intestinal microbiota, which conditions an altered immune response and an alteration in the intestinal epithelium barrier function (Roda et al., 2020). The intestinal epithelium, as in UC, has an important role in the origin of CD. Certain alterations of the intestinal mucosa layer, such as those observed as a consequence to some emulsifiers in the diet (Chassaing et al., 2015) or due to mutations in the primary component of the mucin barrier MUC2 (Boltin et al., 2013), can condition an increase in bacterial translocation. Within this process, the autophagy mechanisms of the intestinal epithelium are involved in the control of the spread of these bacteria, since they activate the defence mechanisms against intracellular fragments of bacterial peptidoglycans through the transcription of genes associated with NF- κ B and MAPK (Benjamin et al., 2013). The influence of this process has been observed by finding certain hypomorphic mutations, such as ATG16L1 and IRGM, which are responsible for abnormal bacterial clearance and antigen-specific T-cell responses and have been identified as relevant risk factors for the development of CD (Jostins et al., 2012).

Polymorphisms in genes that encode binding proteins, such as E-cadherin, guanine- α 12 nucleotide-binding protein subunit, and zonula occludens 1 in intestinal epithelial cells (IEC) or their altered expression may lead to increased permeability of the gut barrier which is characteristic of IBD. Specifically, reduced expression of claudins 5 and 8 or increased expression of pore-forming claudin 2 in IEC have been described in active CD (Weber et al., 2008; Zeissig et al., 2007).

Within the innate immune response, alterations in multiple cell populations have also been described. Dendritic cells, within their antigen presentation work, show an activated profile with expression of TLR2 and TLR4 together with costimulatory receptors. In the homeostatic state, these dendritic cells are stimulated by the TGF β produced by intestinal epithelial cells (IECS) and initiate the secretion of the anti-inflammatory cytokine IL-10, thus, maintaining homeostasis and regulating crosstalk between innate and adaptative immune response (Peterson & Artis, 2014).

The innate immune system also plays an essential role in maintaining the integrity of the intestinal epithelial barrier and the gut homeostasis. It responds to different stimuli such as microorganisms or luminal antigens that can come from the diet with the secretion of different cytokines TNF- α , IL-17, IL-22 and IFN- γ that bridge the innate and adaptive immune systems (**Figure 13**). An increase of different innate immune cells (IIC) subtypes was located in the epithelium and the lamina propria of the ileum of patients with CD has been found and indicates a potential role for these cells in IBD pathogenesis (Geremia & Arancibia-Cárcomo, 2017). CD patients who present inflammation in the ileum and colon also contain a higher number of innate immune cells (IICs) than those without inflammation (Geremia & Arancibia-Cárcomo, 2017).

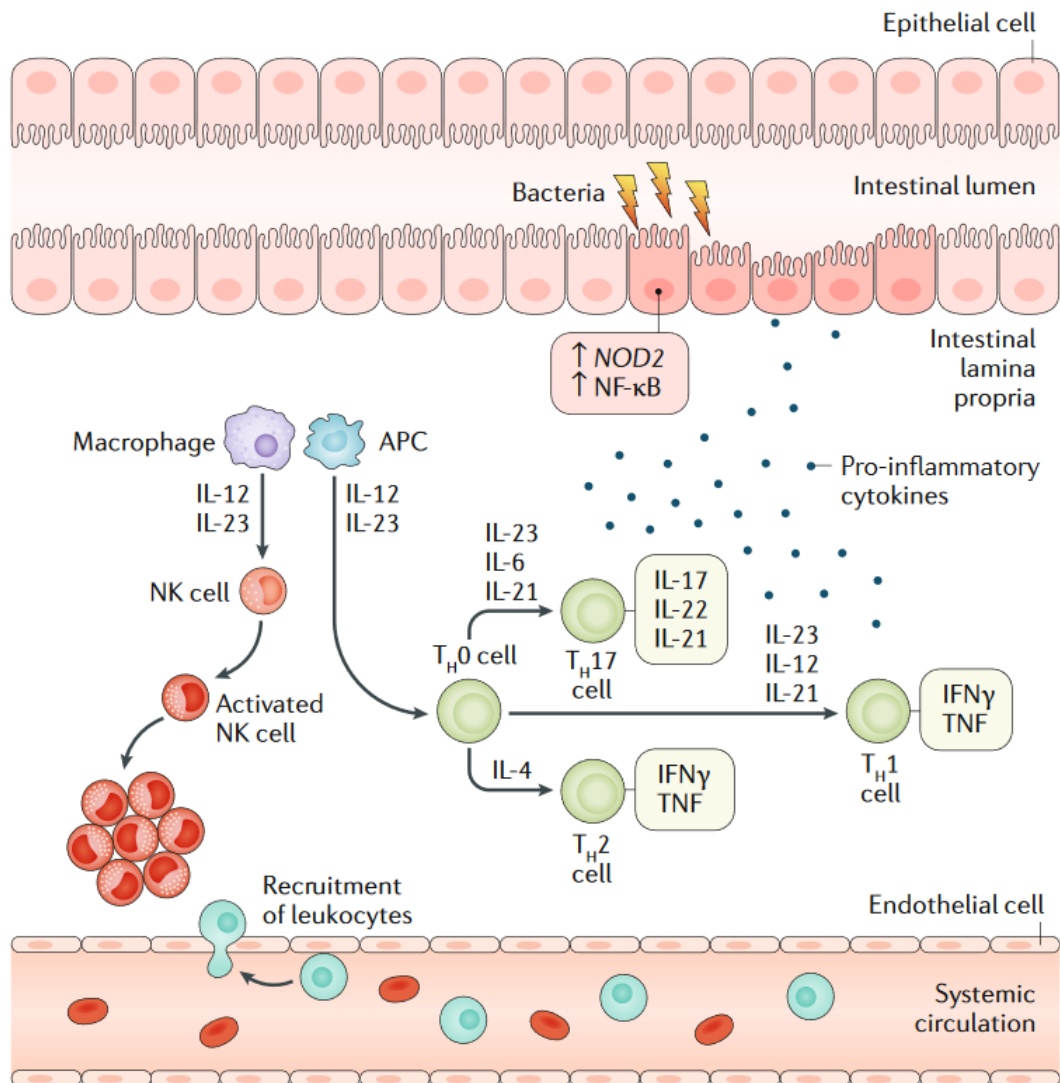


Figure 13. Schematic representation of the underlying molecular mechanisms of Crohn's disease. In CD, epithelial barrier dysfunction results luminal contents entering the lamina propria, which leads to dendritic cells activating inflammatory T cell types that produce

proinflammatory cytokines. These contents also induce macrophages that activate NK cells, resulting in perpetuation of the intestinal inflammation. Source: (Roda et al., 2020)

Furthermore, these inflamed areas contain a higher level of IFN- γ -producing IICs, this proinflammatory cytokine activates the adaptive immune system by activating macrophages, increasing antigen processing, and favouring persistent immune activation of T-cells (Neurath, 2014).

7.3. Genetic factors in IBD

The influence of genetic predisposition in IBD is observed in the fact that the presence of a relative with the disease is the most important risk factor for the development of IBD (Borren et al., 2018), with 12% of affected relatives in patients with IBD (Moller et al., 2015). Different genetic alterations that may be involved in its pathophysiology have been studied in UC, the main ones being those located in TNF- α , MDR1 and TLRs (Sarlos et al., 2014). The genetic component of CD appears to be greater than in UC (Moller et al., 2015), this fact is illustrated by twin studies in both monozygotic and dizygotic twins which show that concordance rates were higher in monozygotic twins (17% for UC and 55% for CD) than in dizygotic twins (6% for UC and 4% for CD) (Spehlmann et al., 2012; Van Dongen et al., 2012). The functions of the main genes associated with CD are usually related to the detection of bacterial pathogens and different alterations in innate immunity, as well as the function of Th17 lymphocytes (NOD2, ATG16L1, LRRK2, IRGM, IL23R, HLA, STAT3, JAK2) and intestinal mucus (MUC2) (Jostins et al., 2012; McGovern et al., 2015). In any case, only 13% of the hereditary component of the disease can be explained by genetic factors, so this highlights the role of other aspects such as the environment and epigenetic changes (Torres et al., 2017; Uniken Venema et al., 2017). In addition to this, genetic studies have not found a clear association with the location of the disease, except for NOD2 and ileal location which have been detected in genome-wide association studies. The abnormal interactions between the ileal microbiota and mucosal immunity due to coding variations of NOD2 was observed in intestinal epithelial cells (IECs) from NOD2 deficient mice that presented impaired bacteria- killing ability (Sidiq et al., 2016). Lastly, patients that present very early onset inflammatory bowel disease (VEO-IBD) present various monogenetic mutations among which stands out IL-

10 and IL-10 receptor genes that show highly penetrant Mendelian- like inheritance (Zhu et al., 2017).

7.4. Gut microbiota in IBD

During the last 10 years, the study of intestinal dysbiosis or alteration of the composition of intestinal microbiome has been of great importance in the study of the IBD. This intestinal microbiome is largely determined by environmental changes and the differences in their composition have been observed both in patients with UC and CD (Sonnenburg & Bäckhed, 2016).

In patients with CD, a lower representation of the firmicute and bacteroid rigs and an overrepresentation of enterobacteria has been described in the intestinal microbiota (Pascal et al., 2017). In addition, some specific bacteria such as those corresponding to the adherent-invasive species *E. coli* and *Faecalibacterium prausnitzii* have been linked with concrete effects on CD pathology. The presence of *E. coli* has been associated with a greater overcolonization of epithelial cells and therefore with the promotion of CD development. For its part, the detection of *Faecalibacterium prausnitzii* in patients has been associated with a greater degree of protection against CD due to the production of butyrate (Palmela et al., 2018; Sokol et al., 2008).

The study of the microbiome of patients with active CD, inactive CDs and healthy individuals, showed that individuals with active CD have an altered intestinal flora with an enrichment in bacteria of the Gender *Escherichia* and a decrease in the abundance of phylos firmicutes, which is linked with greater vascular and paracellular permeability (Libertucci et al., 2018).

On the other hand, in UC, a lower population of some bacteria has been described as *Roseburia hominis* and *Faecalibacterium prausnitzii*, but no particular species has been directly associated with active UC (Halfvarson et al., 2017). Short chain fatty acids (AGCC), such as butyrate, are metabolites produced by various bacterial species and have protective properties on the intestinal barrier, as well as anti-inflammatory properties. Several studies have described that these metabolites are reduced in patients with UC and therefore present an imbalance in the homeostasis of the mucosa (Schulthess et al., 2019). For example, butyrate, an inhibitor of histone

deacetylase, has been shown to maintain the function of the intestinal barrier by means of a downregulation, mediated by IL-10, of the Poros Claudin 2 protein, which increases the permeability of the narrow joints. In experimental models of colitis, the substitution of butyrate by histone inhibitors deacetylase produced an improvement of colitis (L. Zheng et al., 2017).

The treatment of this intestinal dysbiosis by faecal transplants has not proven to be effective in the treatment of the CD. In the case of UC, certain positive results have been observed as the achievement of remission in some patients and UC subjected to multiple faecal transplants, or the effective treatment of colitis induced by *difficile* clostridium but in general is not effective for the cure of patients with UC (Moayyedi et al., 2015; Paramsothy et al., 2017; Rossen et al., 2015).

Despite advances in the understanding of the microbiota, there are important limitations since most bacteria are difficult to culture or are not completely known, and it is difficult to define the exact role of the microbiota in this pathology, since they could act as an intermediate agent between some factors such as diet, pollution or exposure to other infectious agents and maintain the relationship with intestinal homeostasis within an individual genetic predisposition (Somineni & Kugathasan, 2019).

7.5. Role of fatty acids in inflammatory bowel disease: FASN and ILF3

As has been discussed so far, epithelial cells play a fundamental role in the pathogenesis of IBD, triggering the local immune response and acting as a protective barrier between the intestinal lumen and the immune cells. Maintaining the integrity and functionality of the epithelium are key aspects in the development of IBD. In this sense, there is a wide range of fatty acids of vital importance in the physiology of intestinal epithelial cells as well as in their inflammatory processes (Donnet-Hughes et al., 2001; Miller, 2012).

Short-chain fatty acids (SCFA), especially butyrate, is an important energy source of the cells of the intestinal mucosa. Butyrate is produced at the intestinal flora through fermentation from carbohydrates and endogenous substrates. Low levels or absence of butyrate has been associated with intestinal inflammation processes (Venegas et al., 2019), while its presence has been shown to have beneficial effects on intestinal inflammation caused by UC (Russo et al., 2019). Among the mechanisms responsible for

this effect would be its participation in biochemical processes such as the detoxification of xenobiotics or the synthesis of mucus. In addition, butyrate has been reported to reduce the paracellular permeability of the colon by enhancing the activation of peroxisome proliferator receptor γ (PPAR γ).

Long-chain fatty acids also contribute considerably to the function and pathology of intestinal epithelial cells. In particular, polyunsaturated fatty acids (PUFAs), such as ω -3 and ω -6 PUFAs, have the ability to modulate inflammatory processes. Ω -3 fatty acids have been shown to affect tight junction permeability of intestinal epithelial cells and decrease oxidative stress in UC patients (Scaiola et al., 2017). By competing with ω -6 fatty acids, ω -3 attenuates sodium dextran sulphate (DSS)-induced colitis in animal models by reducing mucosal inflammatory cytokine levels and suppressing T-cell activation in the intestine. Recently, conjugated linoleic acid (CLA) was also shown to ameliorate DSS colitis in a mouse model by activating PPAR γ , resulting in repression of tumour necrosis factor α (TNF α) expression and activation of NF κ B, while transforming growth factor β (TGF β) is induced. In UC patients, PPAR γ showed decreased expression in colon epithelial cells, and reversal of PPAR γ expression in mice with DSS-induced colitis markedly attenuated the disease (Y. Chen et al., 2019).

Biosynthesis of long-chain fatty acids is catalysed by the Fatty acid synthase (FASN). FASN is a very well structured multienzyme complex responsible for the “de novo” synthesis of long chain fatty acids from the NADPH-dependent condensation of acetyl-CoA and malonyl-CoA. Under normal conditions, in lipogenic tissues the synthesis of fatty acids takes place in order to store energy in the form of triglycerides. In fasting, FASN expression and activation are inhibited, malonyl-CoA values decrease, and fatty acid oxidation is activated. During lipogenesis, malonyl-CoA acts by inhibiting the enzyme complex carnitine palmitoyltransferase-18 (CPT-1), a shuttle of long-chain fatty acids from the cytoplasm to the mitochondrial matrix, where beta-oxidation takes place (Bartlett & Eaton, 2004).

Regarding the role of FASN in IBD, its expression has been detected in some benign and preneoplastic lesions of the prostate, breast, lung, stomach, colon, and skin nevi (Röhrig & Schulze, 2016). Several studies have also documented the overexpression of this protein in inflammatory disorders, especially in UC. In a study with 90 patients,

30 with active ulcerative colitis, 30 with ulcerative colitis in remission and 30 healthy control subjects, it was shown that FASN is significantly overexpressed in pathological and normal mucosa of UC patients, mainly in the acute phase, compared to healthy controls (Consolazio et al., 2006). Moreover, a specific inhibitor designed against FASN alleviated the severity of colon damage and inhibited the activation of inflammatory pathways in DSS-induced colitis in a mouse animal model. Among the main pathways downregulated by this inhibitor are those activated by the proinflammatory cytokines TNF- α , interleukin IL-1 β and IL-6 (Fafián-Labora et al., 2019; Matsuo et al., 2014).

The expression of FASN by mucosal cells affected by UC has also been related to the production of membrane phospholipids for the increased cell turnover of proliferative cells involved in the wound healing process of UC lesions. In relation to this, Pizer et al. (E S Pizer et al., 1998) showed parallel expression of FASN and Ki-67, a proliferation antigen, in human tissues with rapid growth rates, and treatment of cultured fibroblasts with growth factor significantly increased FASN expression levels (Hsu et al., 1993).

Finally, this link between FASN and cell proliferation has been also documented on multiple occasions in relation to its role in tumour progression. The synthesis of fatty acids is a common process in most neoplasms since they are part of the structural lipids of the membranes. It is currently accepted that the synthesis of fatty acids allows tumour cells to maintain a high proliferative activity.

The expression of FASN is decreased in most human tissues and is only elevated in situations that require de novo synthesis of fatty acids such as in the liver and adipose tissue and is regulated by the type of diet and fatty acid needs. However, unlike the nutritional control of FASN mediated by insulin, glucagon, and other hormones related to metabolism (Fukuda et al., 1999), FASN expression in cancer is mainly regulated by kinase-dependent signalling pathways: phosphatidyl inositol 3-kinase / protein kinase B (PI3K / Akt) and mitogen-activated protein kinase (MAPK), through the transcription factor SREBP-1c (sterol regulatory element binding protein 1-c). These signalling pathways are specifically controlled through different receptors such as growth factor receptor (GFR), epidermal growth factor receptor (EGFR) and the epidermal growth factor receptor 2 (HER2) (Fhu & Ali, 2020). Studies with MAPK and PI3K inhibitors in

breast cancer (MCF-7) and colon cancer (HCT116) cell lines showed a decrease in SREBP-1c values, FASN transcription and acid synthesis fatty.

It has been described in different types of tumours, such as breast, prostate, colorectal, bladder and lung, that FASN can be detected in sections of tumour tissue and that the intensity of the staining increases correlatively with the stage of the disease. Conversely, healthy tissues adjacent to the tumour rarely express detectable amounts of FASN (Buckley et al., 2017). Serum studies of patients with breast, prostate, colon and ovarian cancer have shown elevated FASN values compared to healthy subjects as well as the existence of a correlation between these values and tumour staging (Notarnicola et al., 2012; Y. Y. Wang et al., 2004).

These clinicopathological data indicate that high values of FASN expression facilitate the growth and proliferation of malignant cells thanks to the de novo synthesis of fatty acids that will form part of the plasma membrane of proliferating tumour cells.

ILF3, also known as NF90, encodes a double-stranded RNA binding protein that regulates gene expression and stabilizes mRNAs. Through union to different cellular RNA, ILF3 participates in various cellular functions such as the stabilization of mRNAs, the inhibition of translation and biogenesis of non-coding RNAs (U. Jayachandran et al., 2015; L. Shi et al., 2007). The role of ILF3 in IBD has not yet been studied thoroughly, but there is evidence that prove its upregulation in patients with IBD with respect to control subjects. These observations were obtained by immunohistochemical analysis of colon samples belonging to patients suffering from IBD and healthy controls (Normand et al., 2018).

In cancer, ILF3's study is still emerging, but it was discovered that it regulates the stability of the mRNA of the vascular endothelial growth factor in breast cancer, as well as that it regulates the cell cycle of hepatocellular carcinoma cells through the modulation of The stability of the mRNA of cyclin E1 (W. Jiang et al., 2015). However, much of its activity in cancer remains to be characterized. The cause and the consequence of the abundance of ILF3 in cancer are not well elucidated.

7.6. Animal models for the study of IBD

AOM/DSS mouse model

Described for the first time in 1996, the azoxymethane (AOM)/DSS mouse model represents an exceptional model that faithfully mimics the pathological changes of "adenoma-carcinoma" development observed in colitis-associated human CRC, for which reason its use has been common in studies on inflammatory colorectal carcinogenesis (I. Okayasu et al., 1996).

DSS is a sulphated polymer with cytotoxic capacity on intestinal epithelial cells and macrophages. The mechanism by which DSS induces intestinal inflammation is the alteration of the monolayer lining of the intestinal epithelium, which leads to the entry of luminal bacteria and associated antigens into the mucosa and allows the dissemination of pro-inflammatory intestinal contents into the underlying tissue (Kiesler et al., 2001). For induction of colitis-related colonic tumours in mice by DSS treatment, long-term administration or repeated cycle treatment is required to generate chronic inflammation. When the oral administration of DSS is carried out cyclically, the mice develop a chronic colitis that can last several weeks after the cessation of administration. Chronic lesions are usually characterized by the presence of prominent lymphoid follicles and the presence of epithelial dysplasia. Consequently, in the most advanced stages of this intestinal inflammatory process, animals treated with DSS show a high incidence of colonic cancer. In addition, enteral DSS favours the increase of gram-negative anaerobic bacteria, which together with the erosive potential on the intestinal barrier and the inappropriate response of macrophages would favour the appearance of intestinal lesions (Wirtz et al., 2017).

Subcutaneous administration of AOM, a potent carcinogen, induces the formation of tumours predominantly in the distal colon of rats and mice, specifically the presence of tubular adenomas, dysplasia and colitis with ulceration of the mucosa at week 20 of treatment (Tanaka et al., 2003). The metabolism of this carcinogen generates cytotoxic substances for colonocytes within a few hours of induction. This initiation stage is characterized by changes in intestinal epithelial homeostasis that lead to increased proliferation. In parallel, AOM can introduce mutations that confer a high

potential for neoplastic transformation to intestinal cells that escape apoptosis. A progressive increase in the formation of aberrant crypt foci (FCA), the appearance of mutations in KRAS, COX-2, iNOS and β -catenin, and microsatellite instability in the colon of animals induced with AOM have been observed. Upregulation of COX-2 and iNOS is associated with increased inflammation as well as an increased risk of cancer development (De Robertis et al., 2011).

These phenotypic characteristics of oncogenic progression by administration of AOM are histopathological similar to the progression of human colorectal carcinogenesis (hCRC). However, unlike what happens in humans, tumours induced by AOM show a low frequency in APC mutations (<10%) and non-existent for p53 and DCC, despite the fact that the former has been described as of great importance in the development of colonic neoplasms associated with colitis (Pan et al., 2017).

Acute colitis DSS model

The DSS model, initially described in 1990, is one of the most widely used experimental models today due to its simplicity and reproducibility (Isao Okayasu et al., 1990). It also exemplifies morphologically and symptomatically the epithelial damage observed in human ulcerative colitis.

In this model, intestinal inflammation is not directly induced by DSS, but rather acts as a chemical toxin for the intestinal epithelium, causing damage to the epithelial barrier. The mechanism by which DSS induces intestinal inflammation is the alteration of the monolayer lining of the intestinal epithelium, which leads to the entry of luminal bacteria and associated antigens into the mucosa and allows the dissemination of pro-inflammatory intestinal contents into the underlying tissue (Kiesler et al., 2001). The administration of varying concentrations of DSS in drinking water causes colonic lesions in mice, rats and hamsters that mimic Ulcerative Colitis (UC). The lesions affect the intestinal mucosa and submucosa with the presence of ulcerations, more evident in the left colon and progressing distally (Chassaing et al., 2014). The administration of DSS can be carried out in the form of a high-concentration monocycle in order to simulate conditions similar to those that would occur in acute colitis and its severity can be altered by varying both the duration of the cycle and the concentration of DSS

(Chassaing et al., 2014). This type of model can lead to drastic weight loss in animals and the presence of diarrhoea, regarding the type of lesions observed, highlights the depletion of mucin and goblet cells, epithelial erosion, ulceration and infiltration of granulocytes in the lamina propria and submucosa (Eichele & Kharbanda, 2017).

IL-10 deficient mice

Since IL-10 is a potent suppressor of cytokine synthesis by macrophages, natural killer cells, and T cells, its absence in IL-10-deficient mice results in a lack of control of normal intestinal immune responses against enteric antigens, leading to chronic inflammation through continuous overproduction of cytokines such as INF- γ , TNF- α , and IL-12 (Kühn et al., 1993).

This mouse knockout model has a biallelic mutation (- / -) in the IL-10 gene that causes spontaneous enterocolitis at 12 weeks of age, is highly reproducible and influenced by the environment (Kühn et al., 1993). This intestinal inflammation is especially intense if the animals are in contact with potential enteropathogens. In contrast, mice kept in conditions of maximum sterility do not develop colitis. This is because intestinal inflammation in the mutants originates from uncontrolled immune responses stimulated by enteric antigens and that IL-10 is an essential immunoregulator in the intestinal tract. The mucosal surface of the intestine is exposed to high concentrations of antigens derived from food and microorganisms, which leads to continuous stimulation of the intestinal immune system.

The more sensitive strains of IL-10 (- / -) mice can develop pancolitis accompanied by anaemia and significant loss of body weight. Histologically, the presence of transmural lesions and the loss of intestinal barrier function stand out (Elson et al., 1995). Mice deficient for IL-10 are unable to attenuate the response of Th-1 lymphocytes due to the elevated colonic levels of the cytokines INF- γ , TNF- α and IL-12, generating chronic inflammation. This in turn is accompanied by an aberrant expression of class II molecules of the major histocompatibility complex in the epithelium that promotes a massive exposure of lymphoid cells in the mucosa to luminal antigens and components of the bacterial cell wall such as LPS, reinforcing the inflammatory process.

Macrophages and CD4 + lymphocytes activated by different luminal components have been suggested to be the main causes of colitis in IL-10 (-/-) mice (Jankovic et al., 2010). The immunopathological characteristics of this model of spontaneous colitis mimic CD. Furthermore, 60% of the animals kept under conventional conditions develop colonic tumours in the most advanced stages of the disease (Tanikawa et al., 2012).

Hypothesis and Objectives: Chapter I

The E3 ubiquitin-ligase Hakai plays an important role during EMT and tumour progression by downregulating E-cadherin at cell-cell contacts. Based on the background described and the previous results obtained by our research group, it is proposed to study, in depth, the expression of the E3 ubiquitin-ligase Hakai at early stages of tumour progression of CRC and its possible role in inflammatory bowel disease (IBD). The general hypothesis of this study would be:

- Hakai could be implicated at early events of CRC progression and might be implicated in the in the development of preneoplastic inflammatory conditions as IBD.

In order to confirm this hypothesis, we propose the following specific objectives:

- **Objective 1-** To analyse Hakai expression in pairs of human colon healthy tissues compared to adenoma and to different TNM stages (I-IV) from colon adenocarcinomas.
- **Objective 2-** To carry out a Hakai interactome to search for potential novel Hakai-interacting proteins involved in inflammatory processes.
- **Objective 3-** To study the possible role of Hakai *in vitro* by its action on novel inflammatory-related targets in colorectal cancer.
- **Objective 4-** To analyse *in vivo* the role of Hakai in different IBD mice models.
- **Objective 5-** To analyse Hakai expression in human samples of UC and CD patients.

Materials and Methods: Chapter I

1. Human tissues samples

Human colon cancer biopsies were obtained from the Pathological Anatomy Department from the “Complejo Hospitalario Universitario A Coruña” (CHUAC), under informed consent signed from all patients and research investigation was approved by the Research Ethics Committee from A Coruña-Ferrol (ethical protocol code: 2017/570) following standard ethical procedures of the Spanish regulation (Ley Orgánica de Investigación Biomédica, 14 July 2007). Paraffin samples were provided by CHUAC Biobank integrated in the Spanish Hospital Platform Biobanks Network. The biopsies collected were from a total of 35 patients and included different colon cancer stages, adenoma and normal colon tissues (normal colonic mucosa, n = 26; adenoma, n = 9; colorectal cancer, n = 26 of all stages).

Human biopsies from patients with Chron’s Disease and Ulcerative Colitis were also obtained from the Pathological Anatomy Department from the “Complejo Hospitalario Universitario A Coruña” (CHUAC), under informed consent signed from all patients and research investigation was approved by the Research Ethics Committee from A Coruña-Ferrol (ethical protocol code: 2018/257) following standard ethical procedures of the Spanish regulation (Ley Orgánica de Investigación Biomédica, 14 July 2007). Paraffin samples were provided by CHUAC Biobank integrated in the Spanish Hospital Platform Biobanks Network. A total number of 18 patients were analysed, 10 biopsies from patients with Chron’s Disease and 8 biopsies from patients with Ulcerative Colitis.

Serum samples from colorectal cancer patients were provided by CHUAC Biobank integrated in the Spanish Hospital Platform Biobanks Network. Research investigation was approved by the Research Ethics Committee from A Coruña-Ferrol (ethical protocol code: 2017/570). A total of 62 patients were used for this study, 25 of them diagnosed as healthy individuals (meaning absence of neoplastic disease), 26 of them diagnosed with colorectal cancer (in different stages) and 11 of them diagnosed with colon adenoma.

2. Mice tissues samples

Mouse biopsies from C57BL/6J and C57BL/6 IL10 KO mice were kindly provided by A.o. Univ. Prof. Dr. Christoph Gasche from the Department of Internal Medicine III, Division of Gastroenterology and Hepatology, Medical University of Vienna, Vienna, Austria. The total number of samples used was 30.

3. AOM/DSS Model of Colitis-Associated Cancer

This mice model was carried out in C57BL/6J mice, in which the development of colorectal cancer associated with inflammation is promoted through the use of a chemical induction with a carcinogen (Azoxymethane, AOM) and an inflammatory agent (Dextran Sodium Sulphate, DSS). It is an ideal model for studying chronic inflammation-associated carcinogenesis that significantly reduces the time required for the onset of CRC and with great power and reproducibility.

Subcutaneous administration of AOM induces tumour formation predominantly in the distal colon of mice. The initiation stage is characterized by changes in the homeostasis of the intestinal epithelium that led to increased proliferation. In parallel, the AOM can introduce mutations that confer a high potential for neoplastic transformation to intestinal cells that escape apoptosis.

DSS is a sulphated polymer with cytotoxic capacity on intestinal epithelial cells and macrophages. The administration of variable concentrations of DSS in drinking water causes colonic lesions that mimic Ulcerative Colitis in mice. The lesions affect the intestinal mucosa and submucosa with the presence of ulcerations. When oral administration of DSS is cyclically terminated, mice develop chronic colitis that can last for several weeks after cessation of administration.

The AOM was delivered by a single intraperitoneal injection at a concentration of 10 mg/kg. Subsequently, after one week, 4 cycles of DSS would be applied in 1.7% drinking water. DSS cycles were 5 days, leaving 14 days rest between cycles. The mice would be euthanized 14 days after the last DSS cycle.

4. DSS Model of Acute Colitis

This animal model is similar to the AOM/DSS Model described before (Isao Okayasu et al., 1990). The main differences are that in this model there is no use of a carcinogenic agent like AOM and that the DSS is used only in a single cycle of longer duration (8 days) and concentration (3%) that mimics the symptoms of Acute Colitis. Animals were sacrificed 4 days before the end of the DSS cycle. Chronic, relapsing, or acute models of inflammation can be achieved by modifying the DSS concentration and the timing of the administration. The advantages of this model are its short duration compared to other models, as well as its simplicity and reproducibility.

5. Interleukin-10 knockout mouse model of colitis

IL-10 KO mutant mice spontaneously develop chronic inflammatory bowel disease (IBD). In the case of the Interleukin-10 defective model, this is characterized by the use of genetically modified mice in which the Interleukin-10 gene, responsible for the inhibition of cytokine synthesis, has been eliminated resulting in the appearance of enterocolitis in the presence of intestinal bacteria and imbalance in the function of the intestinal mucosa. As a result, we have mice that develop colitis and colorectal cancer mimicking the steps of inflammatory bowel disease associated cancer in humans.

6. Histology and Immunohistochemistry

Immunohistochemistry is an immunodetection technique that makes an antigen visible at its specific location at the tissue or cellular level. This is done by using secondary antibodies marked with an enzyme whose activation will allow the visualization of the enzyme product at the site of formation of the antigen-antibody complex with the primary antibody. For the immunohistochemistry, sections of the paraffin blocks were made in serial sections of 4 μm thick in a Leica RM2155 microtome (Leica Biosystems). The paraffin cuts obtained were placed on slides and stored at room temperature. The day before the use, the slides were placed in a stove at 37°C overnight. The next day, samples were transferred to a stove for one hour at 60 °C to facilitate paraffin dissolving,

then deparaffinization and rehydration of the tissues was performed, which consists of the following steps:

- Xylol 10 min
- Xylol 10 min
- Hydration 100° ethanol 10 min
- Hydration 96° ethanol 10 min
- Hydration 70° ethanol 10 min
- Final hydration in distilled water for 10 min

Samples has to receive this treatment to remove any embedding media remains. Residual embedding media can cause an increased nonspecific or reduced staining.

The samples were then subjected to a heat-induced epitope retrieval in a pressure cooker (Retriever 2100) with citrate buffer pH 6 (Dako, S2031) or Tris / EDTA buffer pH 9 (Dako, S2375) following the manufacturer's recommendations and depending on the indications of the antibody producer. This process was carried out to unmask the antigen and to allow recognition and access for antigen-antibody binding increasing staining intensity. After the heat treatment, the samples were allowed to cool for 15 minutes and were washed with distilled water. After that they were washed with washing buffer (PBS/Tween-20 0.1%) for 10 min. Then samples were dried carefully with a paper tissue, trying not to touch the sample, before they were marked with a hydrophobic pen (Dako Pen, Dako). Surrounding the sample with this hydrophobic ink, allowed us to confine the liquid during immunofluorescence staining and therefore use fewer volume of the reagents.

The next step was treating the samples with an inhibitor of the action of endogenous peroxidase (Dako) for 15 min. The reason for this is that the enzyme attached to the secondary antibody and that will reveal the formation of the antibody-antigen complexes, is also a peroxidase so blocking endogenous peroxidase activity will eliminate any non-specific background staining.

Subsequently, one wash was performed with the wash buffer for 10 min, and then the samples were blocked with a Bovine Serum Albumin (BSA)/0.1% Tritón X-100 (TX-100) solution for 30 min to avoid nonspecific binding of the primary antibody.

Finally, the preparations were incubated overnight at 4°C with the indicated antibodies (**Table 1**) diluted in blocking buffer. For this incubation a wet chamber to avoid the evaporation of the primary antibody solution was used.

After the incubation, three 10 min washes were performed with the wash buffer, followed by incubation with the peroxidase-conjugated polyclonal secondary antibody (Dako) for 60 min. After another three 5 min washes with wash buffer, it was incubated with a 1:50 dilution of the diaminobenzidine chromogen (DAB) (Dako), which acts as a substrate for peroxidase (conjugated to the secondary antibody), giving a coloured brown product that reveals the presence of bound secondary antibody, and therefore the presence of protein in the tissue sections studied. The enzymatic reaction of DAB was stopped with distilled water.

Finally, to see the distribution of the antibody-protein reactions within the cellular context, a Gill III (Merck) haematoxylin counterstain was performed for 30 seconds. Gill III haematoxylin is a progressive stain, in which the incubation time is used to define the final staining, to avoid that the staining of the nuclei does not interfere with the marking of the markers analysed by immunohistochemistry. After the counter staining, the preparations were finally dehydrated, and mounted with DePex resin (VWR). The dehydration protocol was:

- Hydration 70° ethanol 1 min
- Hydration 96° ethanol 1 min
- Hydration 100° ethanol 1 min
- Xylol 1 min
- Xylol 1 min

Pictures from the slides were taken with an Olympus microscope (Olympus BX61) in the indicated objectives in figure legends. The quantification of the preparations was carried out with the ImageJ computer program, specifically we used an Immunohistochemistry (IHC) Image Analysis Toolbox created by (Jie Shu et al., 2010). This software allowed us to use an objective method for quantification of the positive signal areas of the samples either using a predefined model included in the program or creating our own model using our own positive control. The idea behind this toolbox is

to isolate and select the positive colour pixels of the image while the background colour pixels are eliminated. The program includes the possibility of using an automatic statistical colour detection model for DAB staining or a semi-automatic colour selection model in which you can train the program using your own positive controls to identify the positive colour pixels. In brief, using this software eliminates human subjective mistakes when trying to quantify statistically the positive signal of a sample.

The program also has the possibility of creating a custom model of staining detection by using a personal positive control. In our case, we tried both systems and decided that the quantification was more precise when using our own positive control. To optimize this process, several positive controls were used in order to find the one more appropriate for the differentiation of positive staining and background haematoxylin. By using this model, we could show the program which positive pixels we want to isolate for quantification as shown in **Figure 14**, and the program will replicate this pattern in all the other images automatically.

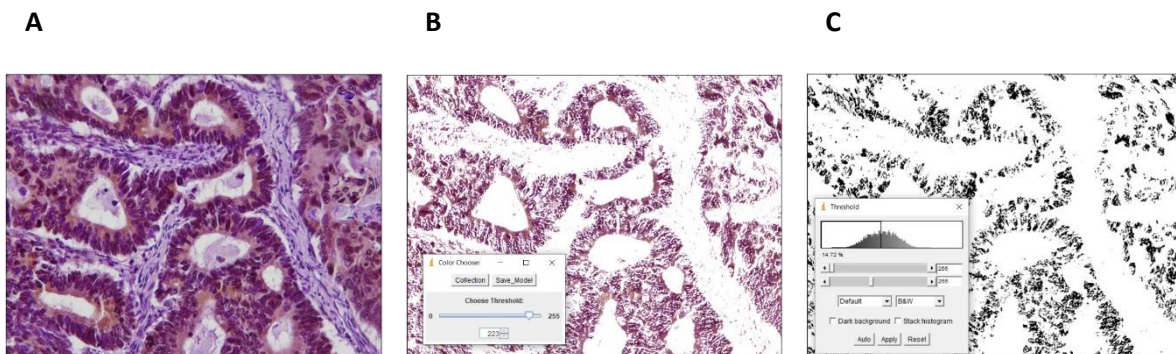


Figure 14. **A**, Raw image from a Hakai immunohistochemistry taken by microscopy. **B**, Processed image from a Hakai immunohistochemistry where we eliminate the background staining. **C**, Processed image from a Hakai immunohistochemistry where we quantify the intensity of the staining.

For this analysis five representative photos of each of the histological preparations were used and the percentage of tissue that presented a positive signal (brown) in relation to the total area of the tissue studied was quantified. The results were represented statistically as the mean of quantifications of the five analysed samples (mean \pm SEM).

7. Deparaffinization of Formalin-Fixed Paraffin-Embedded (FFPE) tissue and total RNA purification

In order to remove paraffin, FFPE tissue sections were put in a 1,5mL microcentrifuge tube, on which 1mL of 100% xylene was added. After vortexing and centrifuging (13400 rpm/min for 2 min), xylene was removed and added 1mL of ethanol (96-100%) to the pellet, and again vortexing and centrifuging (13,400 rpm/min for 2 min). Ethanol was removed and the precipitate tissues were dry up at room temperature for 10 min (to remove any residue of ethanol). Samples were resuspended into 240µl of Buffer PKD (proteinase K digest buffer, QIAGEN) and 10µl of proteinase K, mixed by vortexed. Samples were incubated at 56° for 15 min, then at 80° for 15 min.

For total RNA purification, samples were incubated on ice for 3 min, centrifuged for 15 min at 13,400 rpm/min, and the supernatants were transferred to a new microcentrifuge tube. Samples were incubated with 25µl of DNase Booster Buffer (QIAGEN) and 10µl of DNase I for 15 min at room temperature, and then 500µl of RBC Lysis Solution (QIAGEN) and 1200µl of ethanol (100%) were added and mixed by pipetting. The samples were transferred to RNeasy MinElute spin column (QIAGEN) and centrifugated for 15 sec at 10000 rpm/min. Two washing steps were performed adding 500µl of Buffer RPE to the RNeasy Min Elute spin column, and centrifuged for 15 sec and 2 min, respectively. The RNeasy Min Elute spin column were centrifuged at 13400 rpm/min for 5 min to eliminate the residual ethanol. Finally, the RNA was eluted by add 30µl RNase-free water directly to the spin column following by centrifugation at 13400 rpm/min for 1 min.

8. Exosome extraction

Exosomes are extracellular vesicles (EV) that are produced in the endosomes of most eukaryotic cells and secreted, then they can be found in biological fluids such as blood, urine, or spinal fluid. Exosomes contain in their interior all the specific molecular constituents of their original cells, such as: proteins, RNA, miRNA, DNA and lipids.

For the extraction of exosomes from serum samples of healthy and colorectal cancer patients from different stages, we used the exosome isolation kit ExoGAG

(NasasBiotech), which is based in the use of precipitation solution that interacts with the glycosaminoglycans (GAGs) present in exosomes allowing to separate and isolate them from samples like blood, serum or urine.

The protocol started by collecting 500 μ l of serum sample for each patient. Serum samples were stored at -80°C and were allowed to defreeze before starting the protocol. A first centrifugation at 2000 g for 10 minutes was performed in order to remove any cells or cells debris from the sample. The supernatant was then transferred into a new 1.5 ml tube (Eppendorf) and pellet was discarded. After that 1000 μ l of ExoGAG precipitation reagent was added to the tube before mixing the tube by inversion to homogenize the solution until it turned blue. Subsequently, samples were incubated for 5 minutes at 4°C and then centrifugated at 16000 g for 15 minutes at 4°C . Finally, the supernatant is removed, and we will keep the dark blue pellet formed.

9. RNA extraction from exosomes

For RNA extraction from the isolated exosomes, we used the Total Exosome RNA & Protein Isolation Kit (Invitrogen). The kit is based on an Acid-Phenol:Chloroform extraction (Chomczynski and Sacchi, 1987) combined with a final step of RNA purification with filter of glass-fibre.

The pellet obtained from exosome isolation was resuspended with 200 μ l of ice-cold Exosome Resuspension Buffer and incubated for 10 minutes to allow the pellet to dissolve. After that, samples were pipetted up and down carefully to homogenize the solution. Then one volume of 2X Denaturing Solution pre-warmed at 37°C was added to each sample and then mix thoroughly. Mixture was incubated on ice for 5 minutes. Once the incubation was finished one volume of Acid-Phenol:Chloroform was added to each sample and samples were mixed again by vortexing for 60 seconds. Then samples were centrifugated for 5 minutes a 16000 g at room temperature to form an upper aqueous phase and a lower organic phase. These phases were carefully separated by aspiration of the upper phase and transference to a new tube, lower phase was discarded.

The next part of the protocol consists on purify the ARN and isolate it from the aqueous phase that was recovered. For that 1.25 volumes of 100% ethanol are added

to each sample and mixed vigorously. After that a Filter Cartridge was putted inside a Collection Tube (supplied in kit), one tube for each sample processed. Subsequently, 700 μ l of the lysate/ethanol mix were loaded inside the Filter Cartridge and tubes were centrifugated at 10000 g for 15 seconds. Then 700 μ L miRNA Wash Solution 1 were added to the filter and tubes were again centrifugated at 10000 g for 15 seconds. Finally, two washes were carried out applying 500 μ L of Wash Solution 2/3 in the filter and centrifuging at 10000 g for 15 seconds. In this step the purified ARN should be attached to the filter and the last step was transferring the Filter Cartridge into a fresh Collection Tube in which the final ARN was collected. For recovering the ARN from the filter 50 μ L of preheated (95°C) Elution Solution were added and tube was centrifuged at full speed for 30 seconds. The final ARN sample was stored at -20°C for its posterior use.

10. Microarray Data Mining in NCBI's Gene Expression Omnibus (GEO)

Data from Hakai expression from both a gene-centric and an experiment-centric perspective in the GEO Database was examined paying special attention to its possible regulation under inflammatory conditions in the intestine. Following this line of thought, we filtered all the data sets available looking for microarrays of models of colitis associated cancer (CAC). After the initial filtration, the resulting studies were filtered again to eliminate the ones that included any treatment over the model that could interfere in our evaluation of the physiological process.

The final studies selected were analysed using GEO2R, an interactive tool that permits comparing two or more groups of samples in a GEO Dataset in order to identify genes that could be differentially expressed across the experimental conditions. This allowed us to the distribute all the information of the data set attending to our interest and then search for the expression of Hakai in the subgroups that we created. The results are presented as a table of genes ordered by significance.

11. Interactome

11.1. Large-scale Immunoprecipitation

Cells for large-scale immunoprecipitation were seeded in four 150 mm dishes for each point of the experiment. Then for 48 h cells were treated with 50 μ M of DMSO in the case of control samples and 50 μ M of Hakai inhibitor in the case of experimental points. This Hakai inhibitor is a specific inhibitor designed against the HYB domain of Hakai, responsible for the recognition of phosphorylated substrates for their labelling with ubiquitin. After that, 40 μ L of protein A from the Dynabeads (ThermoFisher) were resuspended in 500 μ L of prefiltered PBS-T 0.1 %. Then, the suspension was incubated depending on the sample with 5 μ g of control IgG or 5 μ g of Hakai antibody (Bethyl) for 2 h at 4° C, this incubation was done in rotation for facilitating bead-antibody complex formation.

At the same time, total protein was extracted and quantified from the initial 150 mm plates as previously described. Once the incubation of the antibody with the beads was complete, 0.1% filtered PBS-T was used for three washes of the beads and 7 mg of total protein was loaded into the beads for each point of the experiment. Beads and total protein were incubated under rotation at 4° C overnight. The next day, beads were washed two times with filtered lysis buffer and samples were prepared as described above. Finally, 10 μ L of each sample was loaded onto a 10% SDS-PAGE gel, electrophoresed and stained with silver staining reagent.

11.2. In gel protein digestion

Gel protein digestion was performed in the Proteomic Platform at the Instituto de Investigación Sanitaria de Santiago de Compostela. Briefly, the previously prepared samples were loaded into 10% SDS-PAGE gel and subjected to electrophoresis. Samples were allowed to penetrate 3 mm into the resolving gel and then the run was stopped. The band was stained with Sypro-Ruby (Lonza) fluorescent stain, extracted from the gel and processed for digestion in the gel (Shevchenko et al., 1996). The gel pieces were processed as described in Alvarez et al., 2019.

After that, the samples were reduced in 10 mM dithiothreitol dissolved in 50 mM Ammonium Bicarbonate (AMBIC) (Sigma-Aldrich). Then samples were alkylated with iodoacetamide 55 mM dissolved in AMBIC 50 mM (Sigma-Aldrich). The gel pieces were rinsed with AMBIC 50 mM in 50% methanol (HPLC grade, Scharlau) and acetonitrile (HPLC grade, Scharlau) was added for dehydration. Finally, they were dried in a SpeedVac (Thermo Fisher Scientific) and digested with porcine trypsin (Promega) to a final concentration of 20 ng / μ L in AMBIC 20 mM for a final overnight incubation at 37°C. The peptides were extracted in 40 μ L of 60% acetonitrile in 0.5% formic acid for 20 minutes in triplicate, then combined and concentrated using the SpeedVac (Thermo Fisher Scientific).

11.3. Mass Spectrometric Analysis (DDA acquisition)

The separation of peptides was done by Reverse phase chromatography. The 400 micro nanoLC liquid chromatography system (Eksigent Technologies, ABSciex) combined with a Triple Time-of-flight (TOF) 6600 high speed mass spectrometer (ABSciex) were used for creating a gradient. Analysis of peptides was performed on the C18CL reverse phase column (150 x 0.30 mm, 3 μ m, 120 Å) (Eksigent, ABSciex). The YMC-TRIART C18 (3 μ m, 120 Å) trap column (YMC Technologies) was paired in-line with the analytical column.

The charge pump flow was 10 μ L/min 0.1% of formic acid. The flow rate of the micropump was 5 μ L/min under gradient elution conditions (mobile phase A was 0.1% formic acid in water; mobile phase B was 0.1% formic acid in acetonitrile). The peptides were separated using a 90-minute gradient ranging from 2% to 90% of mobile phase B (mobile phase A: 0.1% formic acid, 2% acetonitrile; mobile phase B: 0.1% formic acid, 100% acetonitrile). The injected sample volume was 4 μ L.

Acquisition of data was performed on a Triple TOF 6600 system (ABSciex). The ion spray voltage floating (ISVF) was 5500 V, the curtain gas (CUR) was 25, the ion source gas 1 (GS1) was 25, and the collision energy used (CE) was 10. The TF 1.7.1 analyst software was used for instrument operation (ABSciex). A switching criterion was used for ions greater than the mass/charge ratio (m/z) 350 and less than m/z 1400, with a mass tolerance of 250 ppm, a charge state of 2-5 and a threshold of abundance of more

than 200 accounts (cps). Previous target ions were excluded for 15 s. The instruments were calibrated automatically every 4 h using PepCalMix (Sciex) calibrating peptides (Álvarez et al., 2019).

11.4. Interactome Analysis

To discriminate specific from unspecific interactions, the identified proteins in each immunoprecipitation (HAKAI and IgG antibody) were analysed with the Significance Analysis of INteractome (SAINT) score SAINTexpress. SAINT models the distribution of true and false interactions using label-free quantitative data from affinity purification coupled to mass spectrometry bait and negative control experiments and calculates the posterior probability of a true interaction for each prey-bait pair from the quantitative data. Results from each experiment were analysed using their corresponding negative control. Preys with SAINT probability score cut-off of 1 detected by at least two exclusive spectral counts were deemed high confidence HAKAI interacting proteins.

12. Plasmids, Antibodies, and materials

Plasmids used for cell transfection were pcDNA-Flag-Hakai, pcDNA 3.1, pBSSR-HA-Ubiquitin and pSG-v-Src which were kindly provided by Yasuyuki Fujita (Hokkaido University, Japan).

For human immunohistochemistry Hakai dilution was 1:700 and for the other antibodies 1:1000. Commercial kit for immunohistochemistry was Dako EnVision+ System, Peroxidase (EnVision+ System, HRP) purchased to Agilent Technologies, Inc. For western blot dilutions were 1:1000. References and companies where the antibodies were purchased for each technique are included in (**Table 1**).

MG132 (M8699), Cycloheximide (O1810) and Oil red O solution (O1391) were all products purchased to Sigma-Aldrich.

Table 1. List of antibodies used with their reference and technique in which they were used.

Antibody	Reference	Technique	Dilution
Hakai	Non-commercial, provided by Yasuyuki Fujita (Hokkaido University, Japan)	Immunocytochemistry	1:700
E-Cadherin	Cell signalling, 24E10	Immunocytochemistry	1:1000
Cortactin	Millipore, 05-180	Immunocytochemistry	1:1000
N-cadherin	Abcam, ab18203	Immunocytochemistry	1:1000
FASN	Santa Cruz Biotechnology, sc-48357	Immunocytochemistry	1:1000
GAPDH	Invitrogen, 39-8600	Western blot	1:1000
Hakai	Invitrogen, 36-2800	Western blot	1:1000
E-Cadherin	BD Transduction Laboratories, 610182	Western blot	1:1000
β-actin	Abcam, ab8227	Western blot	1:1000
β-catenin	Cell Signalling	Western blot	1:1000
FASN	Santa Cruz Biotechnology, sc-48357	Western blot	1:1000
NF90 (ILF-3)	Santa Cruz Biotechnology, sc-377406	Western blot	1:1000
HA (12CA5)	Sigma-Aldrich, 11583816001	Western blot	1:1000
LC3 I/II	Cell Signalling	Western blot	1:1000
N-Cadherin	Abcam ab18203	Western blot	1:1000
Vimentin	Cell Signalling Technology D21H3	Western blot	1:1000
E-Cadherin	BD Transduction Laboratories, 610182	Immunofluorescence	1:200
Hakai	Invitrogen, 36-2800	Immunofluorescence	1:500
Mouse IgG HRP Linked	GE healthcare NA934	Secondary antibody	1:10000
Rabbit IgG HRP Linked	GE healthcare NA931	Secondary antibody	1:10000
Mouse IgG Alexa Fluor 488	Life Technologies A28175	Secondary antibody	1:10000

13. Cell lines

SW620 and HCT 116 cells lines were cultured in Dulbecco's Modified Eagle Medium (DMEM), HT-29 cell line was cultured in McCoy's 5A medium, CaCo2 cells were cultured in Eagle's Minimum Essential Medium (EMEM), all of them containing 1% penicillin/streptomycin and 10% of heat-inactivated fetal bovine serum (FBS). HCEC-1CT cells were grown in a special medium describe in the table above (**Table 2**). Cells were grown at 37 °C in a humidified incubator with 5% CO₂. Cells were also tested regularly for mycoplasma contamination and all cells used were negative for mycoplasma test. SW620 is a cell line derived from a metastatic site of colorectal adenocarcinoma while HCT 116, HT29 and Caco2 were obtained from colon adenocarcinomas. HCEC-1CT cell line is derived from human colon epithelial cells and immortalized by retroviral transduction (Roig et al., 2010).

Table 2. Components and volumes for the elaboration of the HCEC-1CT cells growth medium.

Amount	Reagent
500ml	DMEM
10ml	10x medium 119
90ml	Sterile H ₂ O
10ml	Cosmic calf serum CCS
0,6ml	Gentamycin (50mg/ml)
100µl	EGF
100µl	Hydrocortisone
5,2ml	Insulin/trenserrin/Na selenite
10ml	Hepes 1M

14. Western blotting

For protein extraction, 8×10^5 cells were counted and plated in 60mm dishes, after 24 h cells were treated with 100 or 250 µg/ml of fungal extracts diluted in growth medium and incubated for 72 h at 37°C in a CO₂ incubator. Then, medium was removed by suction and cells were washed with PBS and scrapped from the plate before they were

collected by pipetting and transferred to a 1.5 ml tube (Eppendorf). Whole cell pellets were prepared by centrifugation at 5000 g for 5 minutes and PBS were removed.

For protein extraction, briefly, cells were lysed for 30 min at 4°C in 0.3 ml of 1% Triton X-100 lysis buffer (20 mM Tris-HCL [pH 7.5], 150 mM NaCl, and 1% Triton X- 100) containing 5µg/ml leupeptin (Sigma), 50 mM phenylmethanesulphonyl fluoride (PMSF) (Sigma), and 7.2 trypsin inhibitor units (TIU) for aprotinin (Sigma). After centrifugation at 14000 g for 10 min, supernatant containing the protein was transferred to a new 1.5 ml tube (Eppendorf) and pellet was discarded.

Protein concentration was measured using Pierce BCA Protein Assay Kit (Thermo Fisher Scientific). This assay is based in the biuret reaction in which takes place the chelation of copper with protein in an alkaline environment to form a light blue complex. The reason is because peptides with 3 or more amino acid residues form a coloured chelate complex with Cu ions in an alkaline medium containing sodium potassium tartrate. This Cu chelate reacts with bicinchoninic acid (BCA) resulting in a purple-coloured product (BCA/copper). The complex is water soluble and exhibits a strong linear absorbance at 562 nm. The quantification of the protein concentration is possible because the absorbance of the compound is proportional to protein concentration. After the reaction takes places, the absorbance is measured at a λ of 570 nm in the spectrophotometer NanoQuant InfiniteM200 (Tecan).

Before loading the protein samples in the BCA assay plate, a calibration curve was created from known concentrations of bovine serum albumin protein (BSA), in a range of 0 to 10 mg/ml. This curve will allow us to correlate the absorbance values of our samples to the absorbance of the samples from the calibration curve. Then, both reagents from the BCA kit, reagent A and reagent B, were mixed in a 50:1 dilution following the manufacturer's instructions, and 200 µl of the mix was added to each well. The volume of sample added to each well of the plate was 2 µl. The plate was incubated at 37°C for 30 min before it was taken to the spectrophotometer to measure the absorbance.

After that, calculations were made from the absorbance values in order to prepare samples with 20 µg of protein load which then were completed by adding

loading buffer Laemmli 5X (Sigma-Aldrich) at a final concentration of 1X. Composition of Laemmli buffer is included in (**Table 3**). Finally, the samples were heated to 95°C for 10 min to denature the proteins. Protein denaturation involved the loss of three-dimensional conformation, which allowed the proteins to resolve into a one-dimensional gel according to their molecular size. This way, the samples were ready to be loaded into a gel, or to be frozen at -20°C for later use.

Table 3. List of components included in the Laemmli Buffer 5x

Loading Buffer Laemmli 5x
10% de dodecilsulfato sódico (SDS)
50% de glicerol
10% de β -mercaptoetanol
0.1% de azul de bromofenol
200mM de Tris-HCl pH 6.8

To analyse protein expression, electrophoresis in Sodium dodecyl sulphate (SDS) polyacrylamide gels (SDS-PAGE) was used. SDS-PAGE is a type of electrophoresis, in which proteins are denatured by heat and the action of both β -mercaptoethanol and SDS. β -mercaptoethanol acts by reducing disulphide bridges typical from tertiary protein structures and SDS breaks the non-covalent interactions responsible for the tertiary and quaternary structure, completely denaturing the proteins. The denatured proteins become negatively charged by action of SDS, and because of this fact the SDS-protein complex migrates from the anode to the cathode proportionally to the mass. The molecular weight of the protein can be therefore determined by comparing its migration to a molecular size marker. The electrophoresis was carried out in an electrophoresis cuvette (BioRad), with running buffer (Trizma base 0.25 M, glycine 1.92 M and 1% SDS), using 80 volts (V) for 20 min and 180 V for 1 h.

Gels used for electrophoresis were 10% or 12% polyacrylamide, depending on the resolution we needed for each protein target, and the composition is indicated in (**Table 4**).

Table 4. List of components included polyacrylamide gels.

Reactive	Resolving gel 10%	Resolving gel 12%	Stacking gel
0.5M Tris-HCl pH 6.8	-	-	1.25 ml
1.5M Tris-HCl pH 8.8	2.5 ml	2.5 ml	-
40% acrilamide/bisacrilamide (29:1)	2.5 ml	3 ml	500 μ l
10% SDS	100 μ l	100 μ l	50 μ l
Tetramethylethylenediamine (TEMED)	15 μ l	15 μ l	5 μ l
Ammonium persulfate (APS)	30 μ l	30 μ l	50 μ l
50% glycerol	2 ml	2 ml	-
H ₂ O	3 ml	2.5 ml	3.2 ml

After the electrophoresis, the same cuvette was used for the transference of the migrated proteins from the gel to a polyvinylidene difluoride (PVDF) membrane (Millipore). For that a transfer buffer (Base Trizma 0.25 M, 1.92 M glycine and 20% methanol) in distilled water was prepared, and the cuvette was programmed for 200 milliamps (mA) for 1 h as transfer conditions. Previously the PVDF membranes were activated with methanol for 30 seconds and washed with distilled water.

Protein detection in the membrane was carried out by immuno-detection. First, membranes were incubated in a blocking solution (5% milk in Tris-saline buffer (TBS)), for 1 h at room temperature. Then, they were incubated overnight at 4°C with the primary antibody at the dilutions indicated in Table x, specific against the proteins of interest, dissolved in blocking solution at the most appropriate concentration following manufacturers information.

The next day, membranes were washed 3 times with TBS with Tween 20 detergent (TBS-T) (Sigma-Aldrich) at 0.05% for 10 min each time. Subsequently, the membranes were incubated with the secondary antibody, suitable for each case depending of the species in which the primary antibody was produced, diluted 1:10000 in the blocking solution for 1h in agitation at room temperature. After incubation of the membranes with the secondary antibody, another three 10 minutes washes with TBS-T were performed to eliminate any possible rest of antibody. The list of antibodies used for western blotting are included in (Table 1).

Finally, immunoreactive proteins were detected with the Amersham chemiluminescence development kit ECL™ Western Blotting Analysis System (GE Healthcare). The reaction is based on the fact that radish peroxidase bounded to the secondary antibody, is able to transform the luminol substrate into 3-amino phthalate. This enzymatic product emits light at 428 nm, which allows its visualization using the imager (Amersham Imager 600, GE Healthcare). Experiments were repeated at least three times. Images were quantified by densitometry and results are expressed as mean \pm S.D and fold induction is represented compared to untreated cells.

15. RNA extraction and RT-qPCR

For the analysis of gene expression by RT-qPCR cells were plated in a six-well culture plate (Corning) with an initial number of 3×10^5 cells/well. 24 h after seeding, the cells were subjected to the corresponding treatment in each case. After this time, the RNA extraction protocol was started.

RNA extraction was performed with the TriPure Isolation reagent (Roche). It is based is the single-step RNA isolation method developed by Chomczynski and Sacchi and allows to isolate total RNA by one only liquid phase separation. This reagent consists of a solution based on phenol and guanidine isothiocyanate (GITC), which stabilizes the RNA and prevents its degradation by the action of RNAses.

Protocol started by adding 1 ml of PBS to each well of the cell culture plate, the cells were detached with the help of a spatula, and the cell suspension was collected into a 1.5 ml tube (Eppendorf). After centrifugation at 5000 g for 5 minutes, the supernatant was removed by aspiration, and we kept the cellular pellet. Following the manufacturer's recommendations, 1 ml of TriPure was added to each tube and after passing the cell suspension through the pipette several times for homogenization, samples were incubated for 5 min at room temperature. Then, 300 μ l of chloroform (Sigma) was added to each tube before it was vortexed for 15 s. After centrifugation of the mix at 12,500 g during 15 min at 4°C, two phases were obtained, an aqueous upper phase, and an organic lower phase, with an interface. For extraction of RNA, the colourless aqueous upper phase containing RNA was collected into a new 1.5 ml tube.

In order to precipitate this RNA, 500 µl of isopropanol (Sigma) per tube was added and then mixed by inversion of the tube several times. After that the samples were incubated for 10 min at room temperature for allowing the precipitate to form. Samples were then centrifuged at 12500 g for 10 min at 4°C to precipitate the RNA, and after removing the supernatant a wash with 1 ml of 70% ethanol was performed. The pellet was detached from the bottom of the tube by vortexing and then centrifuged again at 7500 g for 5 min at 4°C.

Finally, the RNA-containing precipitate was allowed to dry and resuspended in 15 µl of distilled water treated with diethyl pyro carbonate (DEPC) (Applied Biosystems), an RNase inhibiting agent. Once the RNA was extracted, a quantification was performed on the NanoDrop ND-1000 kit (Thermo Fisher Scientific) to determine its concentration, using a λ of 260 nm. At the same time, the purity of the RNA extraction was evaluated, as well as the level of degradation of the sample, which is determined by the ratio between the absorbance 260/280 nm and 260/230 nm respectively, selecting those samples whose ratios were proximal to 2.0.

The extracted RNA was subjected to a reverse transcription process to obtain complementary DNA (cDNA) to analyse the expression levels of mRNA under the experimental conditions indicated in each case. To carry out the reverse transcription, calculations were made from the values obtained in the quantifications to use 500 ng of RNA from each of the samples. The First-Strand cDNA Synthesis kit (NZYTech) was used to obtain the cDNA using a combination of oligo(dT)₁₈ primers and random hexamers. The components of this kit are indicated in **(Table 5)**.

Table 5. List of components of the First-Strand cDNA Synthesis kit.

Component	Composition
NZYRT Enzyme Mix (1)	Reverse Transcriptase and Ribonuclease Inhibitor
NZYRT 2× Master Mix (2)	Primers, dNTPs, MgCl ₂ and RT buffer
NZY RNase H (<i>E. coli</i>)	RNase H (from <i>E. coli</i>)
DEPC-treated H ₂ O	DEPC-treated H ₂ O

A mixed of all the components with the RNA was made, following the manufacturers recommendations, as indicated in (**Table 6**).

Table 6. List of components of the mix for the retro transcription.

Component	Volume
NZYRT 2× Master Mix 10 μL	10 μL
NZYRT Enzyme Mix 2 μL	2 μL
RNA (500 ng) × μL	× μL
DEPC-treated H ₂ O up to 20μL	up to 20μL

The samples were incubated at 25° C for 10 min, resulting in RNA denaturation. Then, they were incubated 30 min at 50° C for retro-transcription. After this time, the reaction was stopped by inactivating the enzyme reverse transcriptase (Enzyme Mix) at 85° C for 5 min. After this first cycle, samples were cooled to 4° C and 1μl of RNase H was added per tube. The last step was a 20 min incubation at 37° C, in order to eliminate the RNA not back transcribed. The obtained cDNA was stored at -20° C.

Quantification of the expression levels of the genes under study was performed with the LightCycler 480 SYBR Green I Master kit (Roche) in the LightCycler 480 II thermocycler (Roche). The SYBR Green I Master contains the buffer, deoxynucleotide triphosphates (dNTPs), a thermostable DNA polymerase, and SYBR 'Green. SYBR 'Green is a fluorescent dye capable of binding to the double stranded DNA, emitting 1000 times more fluorescence than when it is free in solution. The reaction product of each complete cycle of PCR is a new double-stranded DNA molecule, to which SYBR' Green binds, so the increase in fluorescence intensity is proportional to the amount of newly synthesized DNA as product. PCR Quantification is based on the sample cycle threshold (Ct) values, which is defined as the number of cycles required for the fluorescence signal to be greater than the background fluorescence. The lower the Ct value will indicate the fewer number of cycles necessary to capture the fluorescence emitted by the SYBR 'Green, which means a greater number of double-stranded DNA molecules present in the sample to be analysed.

Since SYBR' Green binds to any DNA molecule in double chain, it was necessary to carry out the melting curves, which are characteristics of the PCR product, as they depend on the size and composition of the amplicon. These curves allow us to certify the quality of the amplification, and to certify that we are correctly amplifying our template because during PCR some by-products like the primer dimers can be formed. If our primers are not well designed or the PCR conditions are not ideal, primers can bind each other and be amplified. The amplification of these structures could lead to an increase in fluorescence intensity due to the unspecific binding of SYBR' Green. By performing this melting curve analysis, we can check that our amplification is specific and that the values of fluorescence are correct.

For this purpose, a denaturation was carried out at 95°C for 5 seconds, followed by another stage at 65°C for 1 min to allow again the hybridization of all the strands, thus reaching the maximum of fluorescence. The temperature was then raised to 95°C, to get the temperature at which half the DNA strands are dissociated, which is called melting temperature (T_m). The T_m must be kept constant for each of the genes used. The variations in T_m values may be due to the non-specific binding of primers and the primer-dimer structures that we mentioned before, among other causes, and those samples showing these variations must be discarded as the amplification product is different from the amplicon of interest.

The data obtained was analysed, and the relative levels of expression were calculated with the software qbase⁺ (Biogazelle). For relativization of gene expression we used HPRT and RPLP0 genes as housekeeping's (Table 8). Conceptually, reference genes or housekeeping's are used to correct changes in RT-qPCR measurements due to experimental variations, such as the quality of the starting RNA or the reverse transcription reaction. This is possible because these reference genes maintain a constitutive expression because they are charged with basic cellular functions and do not vary their expression depending on the experimental conditions.

The conditions for the qPCR were as following:

- 95° C for 10 min. DNA polymerase activation.
- Amplification 40 cycles:

- 95° C for 10 sec. Denaturation
- 50 – 65° C (depending on the oligos) 10 sec. Annealing
- 72° C. 5 sec. Elongation
- Melting. 1 cycle
 - 95° C for 5 sec.
 - 65° C for 60 sec.
 - Ramping increase until 95° C (Ramp rate °C/s: 0.03)
- Cooling for 10 sec at 40°C

Primers used (Sigma) are listed in (Table 7).

Table 7. List of primers used with their forward and reverse sequences.

Gene	Forward primer (5'-3')	Reverse primer (5'-3')
GAPDH	GTGCTGAGTATGTCGTGGAGTCTAC	GGCGGAGATGATGACCCTTTTGG
RN18S	CGATGCGGCGGCGTTATTC	ATCTGTCAATCCTGTCCGTGTCC
CD163	CCTCCTCATTGTCTTCCTCCTGTG	CATCCGCCTTTGAATCCATCTCTTG
CD68	TCCAAGATCCTCCACTGTTG	ATTTGAATTTGGGCTTGGAG
TNF-α	ATGAGAAGTTCCCAAATGGC	CTCCACTTGGTGGTTTGCTA
Hakai	CGCAGACGAATTCCTATAAAGC	CCTTCTTCATCACCAGGTGG
RPL13A	CTCAAGGTGTTTGACGGCATCC	TACTTCCAGCCAACCTCGTGAG
RPLP0	TGGTCATCCAGCAGGTGTTCTGA	ACAGACTGGCAACATTGCGG
TGF-β1	CCCTATATTTGGAGCCTGGA	CTTGCGACCCACGTAGTAGA
IL-6	CTCTGGGAAATCGTGAAAT	CCAGTTTGGTAGCATCCATC
IL-1β	CACAGCAGCACATCAACAAG	GTGCTCATGTCCTCATCCTG
CCL5	AGATCTCTGCAGCTGCCCTCA	GGAGCACTTGCTGCTGGTGTAG
COL1A1	GCTGAGATGGCAACAGGGCTA	TTGATGGACGGGAATGAACA
CCL20	CGACTGTTGCCTCTCGTACA	GAGGAGGTTACAGCCCTTT
FASN	TTCTACGGCTCCACGCTCTTCC	GAAGAGTCTTCGTGAGCCAGGA
NF90 (ILF3)	GCGCGAATTCAGGCTATGAATGCCCT GAT	GCGCGGATCCCGGCAAGCCCATGTCGTG TA

16. Plasmid transfection

All the transfections of the different plasmids used in these experiments were performed using Lipofectamine 2000 Transfection Reagent (Invitrogen) and Opti-MEM media following manufacturer's protocol. HCT-116 cells were seeded in p100 or MW-6 plates, depending of the experiment, at a confluence that would reach approximately 40-50 % one day before transfection.

For transfection day, we prepared two different tubes for the calculated volumes of lipofectamine and plasmid and then they were diluted in 125 μ L of Opti-MEM each in the case of transfection of MW-6 plates, or 500 μ L in the case of transfection in p100 plates; then the tubes were incubated for 5 min. A ratio of 1:2 in volume between plasmid and Lipofectamine was used for transfection.

After the 5-minute incubation, lipofectamine and plasmid tubes were mixed together by pipetting the volume from the lipofectamine tube into the plasmid tube, then the tube was incubated again for 20 min.

During incubation time, cells were washed with sterile saline serum and 1,25 mL and 5 mL of Opti-MEM were added to the MW-6 and p100 plates respectively. The transfection mix, including both lipofectamine and plasmid was then added to the cells and incubated for 6 hours in the CO₂ incubator at 37 ° C. Once the 6-hour incubation was over, cells were washed again with saline serum and the Opti-MEM was replaced with the normal culture medium of that cell line.

Finally, after changing the medium, transfection was maintained for the indicated times before scraping all plates and preparing the extracts. When transfection was carried out using multiple plasmids for one single experiment, an empty vector was used to complete the transfection system until reaching the same quantity of plasmid and lipofectamine for each of the points of the experiment.

17. Viral transduction

Generation of stable cell lines with overexpression or silencing of Hakai was carried out by lentiviral transduction. Due to the viral nature of integration into the host genome,

this method for generating stable cell lines is highly effective. Lentiviruses include in the viral vector a reverse transcriptase which transforms the viral RNA into double-strand DNA and an integrase that is able to insert the viral DNA into the host genome. The integrated DNA replicates with the host genome, allowing sustainable expression of the gene of interest. Lentiviruses have the advantage over other viruses that are capable of transducing cells that are not in mitosis, also lentiviruses represent a great advantage due to the higher efficiency of transduction compared to standard transfection in epithelial cells.

In addition to our gene of interest the viral vector must include for co-transduction, a marker of selection that produces resistance to a drug. This resistance will allow us to carefully monitor the integration of the transgene into the target cell's genome, after the transduction protocol, cells would be selected for positive integration by adding the antibiotic to which cells that have integrated the viral vector would be resistant.

In this way, independently to percentage of transduced cells, when antibiotics are included to the selection medium, they would kill all cells that have not incorporated the lentiviral vector and those cells that survive can be expanded to create stable cell line.

Normally, the protocol would start by the transfection of the viral vector containing our gene of interest, the resistance gene, a reporter gene and all the viral machinery for integration and encapsulation. This transfection would take place in a cell line easy to transfect like HEK-293 cells. Viral vector would integrate into the HEK-293 genome and start expressing. Inside the cells, generated viral particles will start packaging and being released to the medium. After 48 h from the transfection, HEK-293 medium containing the viral particles would be collected for its use in the target cells.

In our case, viral particles were directly bought from Dharmacon, Horizon Discovery Group. We bought lentiviral particles for Hakai constitutive overexpression (Precision LentiORF CBLL1), and for Hakai inducible silencing (SMARTvector Inducible Lentiviral shCBLL1). The constitutive overexpression is controlled by a human cytomegalovirus promoter (hCMV). The inducible silencing is controlled by an inducible

promoter with Tetracycline Response Elements (TRE3G), that activates under the presence of Doxycycline by the Tet-On 3G protein.

In this way, we save some steps from the process of establishing stable cell lines, but we still should set up the best conditions for using the viral particles. Before transducing our target cells with the viral particles, we had to find the best conditions for the transduction including cell density, presence or absence of serum in the medium, concentration of polybrene and time of transduction as included below. Then after defining all the variables, a transduction with a positive control of transduction is needed in order to determine the functional titration of the viral particles.

The protocols for the transduction of cells with viral particles for Hakai overexpression and silencing are very similar and have many parts in common so we will first explain the protocol for the overexpression of Hakai and then specify the specific differences when trying to silence it.

17.1. Transduction for Hakai overexpression:

An MTT proliferation assay was performed as described in “Material and Methods Chapter One” in order to see how all the conditions mentioned affect cell viability of HT-29 cells. We used two 96-well plates, one was for evaluation of a time of 6 h of transduction incubation and the other one for the evaluation of overnight transduction incubation. In each plate we evaluated three different cell densities (5×10^3 cells/well, 7.5×10^3 cells/well and 1×10^4 cells/well), taking into account the presence or absence of FBS and also with a gradient of concentration of Polybrene (Hexadimethrine bromide) (Sigma) (0 – 14 $\mu\text{g/ml}$, with a 2 $\mu\text{g/ml}$ increasing concentration). For that we distributed the plate as shown in (**Figure 15**).

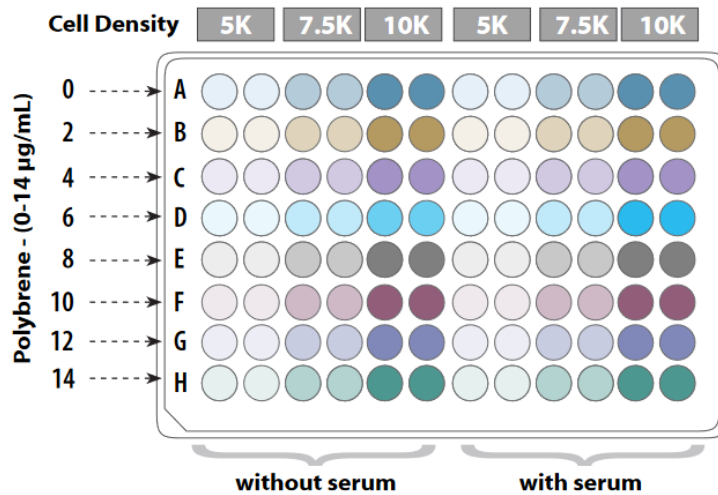


Figure 15. Distribution of the wells in the plate for testing all the conditions.

The criteria for selecting the optimal conditions were:

- The right cell density should be the one that gives a confluency between 40% and 80% the day before seeding. In our case we seeded 1×10^4 cells/well of HT-29 cells
- The highest transduction efficiency is achieved when the concentration of serum is the lowest as possible. As the viability of our HT-29 cells was not significantly affected by the absence of FBS it was not used serum for transduction.
- Polybrene is a cationic polymer that is used to increase transduction efficiency by neutralizing the charge repulsion between virions and sialic acid on the cell surface. As it may have cell toxicity depending on the cellular type, it is recommended to use the highest concentration of Polybrene possible without affecting cell viability. In our case the highest concentration (14 µg/ml) did not significantly affect cell viability of HT-29 cells, so we choose it.
- If there is no evidence of enhanced toxicity during overnight incubation for transduction compared to the 6 h incubation, overnight incubation should be used due to higher efficiency. In our case there was no significant difference in viability between incubations, so we chose overnight incubation.

In conclusion, our experimental conditions were:

- A density of 1×10^4 cells/well
- No serum
- 14 $\mu\text{g/ml}$ Polybrene
- Overnight incubation

Once all conditions were defined, determination of the functional titer of the viral particles was the next step. The functional titer is cell-line specific and may differ from the titrating provided by the manufacturer as they use HEK-293 cells. Functional titer was determined by counting GFP-positive colonies after transduction of the HT-29 cell with control lentiviral particles with the optimal conditions previously determined.

For transduction, HT-29 cells were trypsinized, counted and seeded in 96-well plate as previously described. Cells were incubated overnight at 37°C in a CO_2 incubator. The next day, 5-fold series dilutions of the control lentiviral particles were made in medium without serum and containing a concentration of 14 $\mu\text{g/ml}$ of Polybrene. The concentrations were prepared as shown in **Table 8**:

Table 8. Dilutions used for transduction evaluation.

Well	Dilution factor
1	5
2	25
3	125
4	625
5	3125
6	15625
7	78125
8	390625

After preparing all the mixes, they were allowed to form lentiviral-Polybrene complexes for 5 minutes at room temperature. Then medium was removed from the

96-well plate by aspiration and 25 μ l of each dilution was added to the wells and incubated overnight. The next day, we added 75 μ l of normal growth medium on top of the 25 μ l that were already in each well. After that, cells were incubated for another 48h.

Once the incubation was finished, plate was taken to the fluorescence microscope for counting positive GFP colonies. For the calculation of the functional titer from the number of positive colonies we used the following formula:

- Functional titering = Number of GFP-positive colonies x Dilution factor \div 0.0025 ml (volume used)

Determining the functional titer of the viral particles is key for a good transduction, as we can calculate the volume of viral particles we need for a certain multiplicity of infection (MOI). MOI is defined as the number of transduction units (TU) per cell that we use in a given transduction. Normally a reduced MOI of 0.3 is used to produce populations of cells with only one integration event per cell. The higher the MOI the higher would be percentage of transduced cells, however, it also would increase the possibility of multiple integration in the genome which can lead to undesired effects depending on the future applications. The cells that were not transduced would then be removed by resistance antibiotic selection.

Prior to antibiotic selection it is necessary to perform a kill curve. This curve allows us to determine the minimum concentration of antibiotic that is able to kill 100 % of our wild type cell line. For that, series of increasing concentrations (2 – 18 μ g/ml) of the antibiotic are tested in different wells for a period of 6 days. After that time, cells are visualized at a microscope, searching for the minimum concentration that is able to kill all the cells in the well, in our specific case this value was 12 μ g/ml of Puromycin. In this way, when selecting for positive transduction in transduced cells, we will be sure that by using the determined concentration of antibiotic any non-transduced cell will be dead and we will only keep the desired cells.

The final transduction of the HT-29 cells was finally done with a MOI of 0.3 TU/cell under the optimal conditions already calculated and following the same steps as we mentioned for the transduction of the control viral particles. The only difference is that instead of finishing the experiment with the colony counting cells, in that same

point we changed growth medium for a selection medium including the resistance antibiotic at a pre-determined concentration.

Cells were kept under these selecting conditions while being expanded until the adequate cell number was achieved in order to freeze and archive the stable cell line. After that, cells were finally used for Western blot assay in order to confirm overexpression or silencing of Hakai.

17.2. Transduction for Hakai silencing:

In the case of the silencing of Hakai, the only difference from the previous protocol was that after cell transduction with the different dilutions we cannot directly check for positive GFP colonies, we also needed to add doxycycline to the growth medium to induce the expression of the promoter as we mentioned. For that, 0.5 µg/ml of doxycycline was added to the medium, and cells were incubated for 72 h before being tested.

18. Immunofluorescence

Immunofluorescence is an assay used to detect a protein in biological samples like tissue or cells by recognising a specific antigen which also allows to determine the subcellular localization of the protein. The base for immunofluorescence is the specificity of antibodies and the use of chemically labelled secondary antibodies with fluorescent dyes which are visible under a fluorescence microscope.

To perform the immunofluorescence assay, cells were plated in 25 mm round crystal slides previously sterilized by U.V overnight inside a 12-well culture plates (Corning) with a density of 3×10^4 cells/well. After 24h hours, cells were subjected to the corresponding treatment in each case. To process the slides two washes with PBS were performed, and cells were fixed with 1 ml of 4% Paraformaldehyde (PFA-PBS) solution for 15 min. Then, two washes with PBS were performed to discard any rest of PFA and cells were permeabilized with 1 ml of 0,5% Triton X 100/PBS for 15 min at room temperature. After that, cells were incubated with 3% BSA-PBS blocking buffer overnight at 4°C.

The next day, after removing the blocking buffer, cells were washed with PBS once and they were incubated with the E-Cadherin primary antibody (BD Transduction Laboratories) dilution (1:200) in blocking buffer for 2 h at room temperature. After the incubation three washes of 5 min were carried out with PBS, and they were incubated for 1 h at room temperature and in the dark with the Mouse IgG Alexa Fluor 594 (Life Technologies) secondary antibody (1:500). After the incubation time, the preparations were washed with PBS another three times and incubated with a 1:1000 dilution of Hoechst 33342 (Thermo Fisher Scientific) in PBS for 10 min in the dark to mark the nuclei of the cells. Finally, a last PBS wash was performed and mounted in Prolong Gold Antifade mounting medium (Thermo Fisher Scientific). The results were observed in the fluorescence microscope “Monitorized reflected Fluorescence System” (Olympus), taking 5 representative photographs of each of the samples (magnification 100x).

19. RNA silencing transient

In addition to stably silencing Hakai using viral infections, transient silencing was also performed by interfering RNA. The siRNA oligonucleotides for Hakai were Hakai-1 (5' CTCGATCGGTCAGTCAGGAAA) and Hakai-2 (5' CACCGCGAACTCAAAGAACTA). HCT-116 cells were transfected with the interference RNA's by using Lipofectamine 2000 Transfection reagent (Invitrogen). For transfection cells were seeded in MW-6 plates at a confluence of $2,5 \times 10^5$ cells/well and a tube was prepared with 2 μ L of 100 μ M oligonucleotides of interference RNA (200 pmol) and lipofectamine in ratio of 1:2 as in the previously described transfection protocol.

As a control of transfection, we used commercial Mission Universal Non-coding siRNA (Sigma-Aldrich), specifically, 10 μ L of 20 μ M commercial siRNA stock with 4 μ L of lipofectamine. Finally, cell extracts were prepared 72 hours after transfection and used for assessing protein expression.

20. Immunoprecipitation

For carrying immunoprecipitation assays cells were plated at 2×10^6 cells/plate in 100 mm dishes (Corning), transfected after 24 or 48 h and kept for 2 more days in culture as the protocol was carried out 48 h after transfection. Initially, cells were washed twice with ice-cold PBS-T 1% (PBS supplemented with 1% of Tween-20), scrapped in ice with 1 mL PBS-T and collected into ice-cold 1,5 mL tubes.

Once all plates were scrapped, cells were isolated into pellets by a 3 min centrifugation at 4000 rpm and 4 °C. After centrifugation, pellets were lysed with 1 mL lysis buffer (20 mM Tris-HCl pH 7,5, 150 mM NaCl and 1% Triton X-100) supplemented with 10 µg/ml aprotinin (Sigma-Aldrich), 10 µg/ml leupeptin (Sigma-Aldrich), 1 mM phenylmethylsulphonyl fluoride (PMSF) (Sigma-Aldrich) and 125 mg/mL N ethylmaleimide (Sigma-Aldrich) in rotation at 4 °C for 30 min. PMSF, leupeptin and aprotinin are protease inhibitors and N-ethylmaleimide (NEM) is a cysteine protease inhibitor used to preserve the native cell ubiquitination and it was added only when the pellets were used for ubiquitination assay.

Cell lysates were centrifuged at 14000 rpm after the incubation and transferred to a new ice-cold tube. In parallel, 60 µl of agarose beads were incubated with 2 µg of the desired antibody for 30 minutes at 4°C and under rotation. As control, 2 µg of normal mouse/rabbit IgG (Santa Cruz Biotechnology) were incubated also with agarose beads. Protein A Agarose Beads (Santa Cruz) were used when the antibody used for immunoprecipitation was from rabbit and Protein G Plus-Agarose (Santa Cruz) when the antibody used for immunoprecipitation was from mouse. After the incubation step, beads were washed with 1 ml of lysis buffer and subsequently centrifuged at 3000 rpm for 2 minutes at 4°C.

The final step consists in another incubation, in this case the antibody-conjugated beads were incubated under rotation for 2 hours with 900 µl of the protein lysates at 4°C. The rest of the protein lysates, 100 µl, were used as a protein input control. After the last incubation of the antibody-conjugated beads with the protein lysate, beads were centrifugated at 3000 rpm for 2 minutes and then washed with 1ml of lysis buffer for two times.

For sample preparation, Laemmli buffer was added to each tube including the ones used for protein input control and then heated for 5 minutes at 95°C for protein denaturation and elution from the antibody-bead complex.

21. Analysis of Protein Stability by the Cycloheximide

Experiments with cycloheximide (CHX) were used to study protein half-life as CHX acts as a protein biosynthesis inhibitor. HT-29 cells were seeded in 6-well plates at a density of 3×10^5 cells/well and treated with 10 µg/ml of cycloheximide for the indicated time course. Cycloheximide was added 72 h after the stimulation of HT-29 shCBL1 cells with doxycycline to induce silencing of Hakai. Once the treatment with CHX was over, cells were collected and lysed for the analysis of protein expression by western blot.

22. Ubiquitin-proteasome assays: proteasome, lysosome or autophagy inhibition

Proteasome inhibitor MG132 (Sigma-Aldrich, St. Louis, MO, USA) was added for 6 h using 10 µM and 30 µM. Lysosome degradation inhibitor Chloroquine (Sigma-Aldrich, St. Louis, MO, USA), was added for 24 h at 50 µM and for 6 h at 100 µM indicated concentrations. Autophagy inhibitor 3-Methyladenine (Sigma-Aldrich, St. Louis, MO, USA) was added for 24 h at 5 mM and 10 mM. Protein synthesis inhibitor cycloheximide (Sigma-Aldrich) was used at 10 µg/mL for the indicated times.

23. Oil-red staining assay

Oil red O is a lysochrome dye used for staining of neutral triglycerides and lipids that imparts a red-orange colour to them. To perform oil-red staining assay, cells were seeded in 8-well chambers (Millicell EZ SLIDE 8-well glass, Millipore) at a cell density of 10×10^4 cells per well. First, we prepared a working solution of 0.5 % Oil red O solution in 100 % 2-propanol and dilute it 6:4 in diH₂O to get 60 % Oil red O, 40 % H₂O. Media was removed from the cells and a PBS wash was performed before adding 4 % paraformaldehyde for 30 minutes at room temperature. Then paraformaldehyde was

removed, and cells were washed twice with distilled water. The next step was to add directly the working solution of oil-red and incubate cells with it for 15 minutes, after that time the working solution was removed, and cells were washed five time with diH2O. Finally, we removed the deionized water (diH2O) form the last wash and use mounting medium (Dako, Agilent Technologies) to mount the preparation with a cover slip. After that the samples were ready to be seen under a light microscope (Olympus BX61).

24. Statistical analysis

Statistical significance of data was determined by applying a two-tailed Student t-test or ANOVA depending on the data. Shapiro-Wilk test was used to check a normal distribution and Levene test to assess the equality of variances. Results obtained are expressed as mean \pm SD or mean \pm SEM. Quantification of human IHQ did not follow a normal distribution therefore we used Kruskal-Wallis with Tukey correction test. Significance of the Student t-test and Kruskal-Wallis with Tukey correction test among the experimental groups indicated in the figures is shown as * $P < 0.05$, ** $P < 0.01$ and *** $P < 0.001$.

Results: Chapter I

1. Hakai is a biomarker of tumour progression in colorectal cancer

Hakai has been shown to play an important role in tumour progression through the regulation of EMT processes, specifically due to its ubiquitination of E-cadherin, a process that mediates its degradation. Given that previously obtained results in our research group had shown that Hakai was clearly up-regulated in human colon adenocarcinomas compared to normal tissues, we wanted to determine if this expression of Hakai was correlated to the stage of the disease.

The over-expression of Hakai in colorectal cancer samples with respect to healthy adjacent epithelial tissue has previously been described by immunohistochemistry (Abella et al., 2012)(Rodríguez-Rigueiro et al., 2011). Here, we deepen the study of the role of Hakai in colorectal cancer by comparing sample pairs of colon adjacent healthy tissue to different Classification of Malignant Tumors (TNM) stages (I-IV) of colon adenocarcinomas and to adenoma.

Immunohistochemistry assays were performed for the evaluation of Hakai expression in all the colon tissue samples previously classified as healthy, adenoma or TNM stages by a pathologist.

The results showed that Hakai staining intensities were increased gradually from healthy colon tissue to adenoma and to stages I to IV of colorectal adenocarcinoma (**Figure 16A, B**). This Hakai overexpression was significantly noticeable even in the first stages of the tumour progression including adenoma and stage I adenocarcinoma. At the same time the biggest differences in Hakai staining intensity were for the TNM-stages III and IV on which Hakai increased expression had the highest significant value. Interestingly, Hakai localization was markedly increased in the nucleus of the cells, but also significantly at a cytoplasmic level.

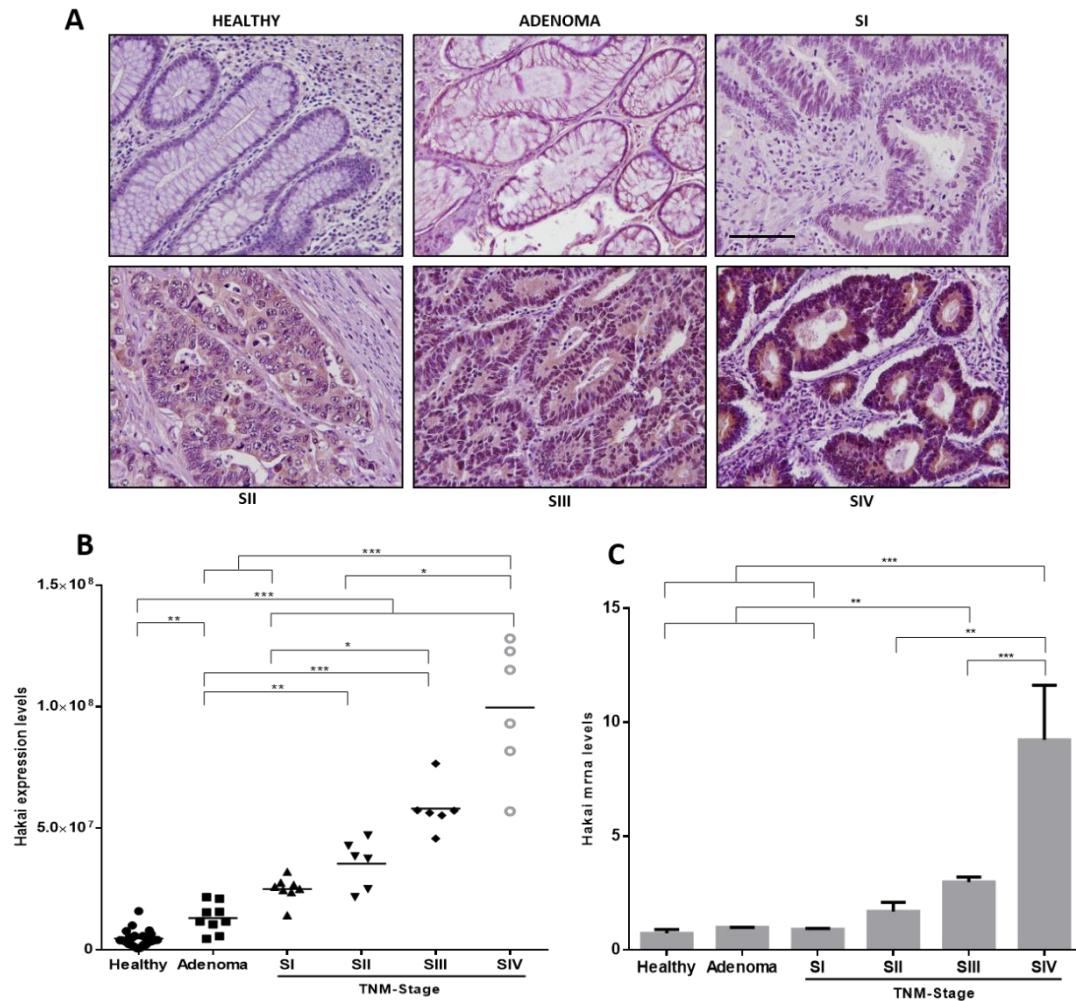


Figure 16. Expression of Hakai in human samples of colorectal cancer, adenoma and healthy epithelial tissue. **A**, Immunohistochemistry staining of Hakai in non-transformed colonic mucosa, adenoma, and colorectal cancer (TNM stages I-IV). Images obtained with 20x objective. Scale bar 125 μ m. **B**, Quantification of the staining intensity of Hakai in epithelial cells at different colorectal cancer stages, adenoma and healthy colon tissues (normal colonic mucosa, n = 26; adenoma, n = 10; colorectal cancer, n = 20 of all stages). Five pictures of each sample were taken and quantified. Data are represented as scatter plot. Values are means \pm SEM of staining intensity signal scoring per area. Quantification and calibration of the images were performed with Immunohistochemistry (IHC) Image Analysis Toolbox software for Image J. Kruskal-Wallis with Tukey correction test analyses show statistical differences in colorectal cancer (TNM, SI-IV) respect to paired healthy samples (*p < 0.05; **p < 0,01; ***p < 0,001). **C**, Expression of Hakai mRNA levels normalized to control RPL13A mRNA were measured in normal colonic mucosa, adenoma, and colorectal cancer (normal colonic mucosa, n = 12; adenoma, n = 3; colorectal cancer, n = 12 of all stages). Scale bar 50 μ m.

This same regulation was observed when analysing the Hakai mRNA expression levels from the corresponding samples by RT-qPCR (**Figure 16C**). In this case expression of Hakai mRNA suffered a significant increase in TNM stages III and IV, which points to a late transcriptional regulation of Hakai during tumour progression.

In addition to Hakai, we also evaluated different epithelial and mesenchymal markers like E-Cadherin, N-Cadherin and Cortactin. E-cadherin is a specific target for Hakai, and its loss is associated in colorectal cancer to poor prognosis and marks the transition from adenoma to carcinoma. N-Cadherin and Cortactin are both mesenchymal markers and they are also regulated by Hakai expression, in fact cortactin has been described as a direct target of Hakai (Mukherjee et al., 2012).

In these samples, E-Cadherin expression was high in normal colon epithelial tissue with a strong staining in cell contacts that is less clear in the adenoma tissue. E-Cadherin expression was reduced in all the samples of the TNM stages with the exception of TNM-stage IV in which the expression was recovered but without the characteristic cell contacts staining and more presence in the cytoplasm (**Figure 17**). N-Cadherin expression is almost not detectable in healthy tissue, adenoma and stages I and II while in stages III and IV the staining increased gradually. Cortactin, despite the fact it's been described to be a substrate for Hakai it is also described as a mesenchymal marker. In this case, Cortactin did not show any significant change in expression between all the samples considered in the staging (**Figure 17**). Taking into consideration these results, we can conclude that Hakai may be a potential molecular biomarker for colon cancer progression.

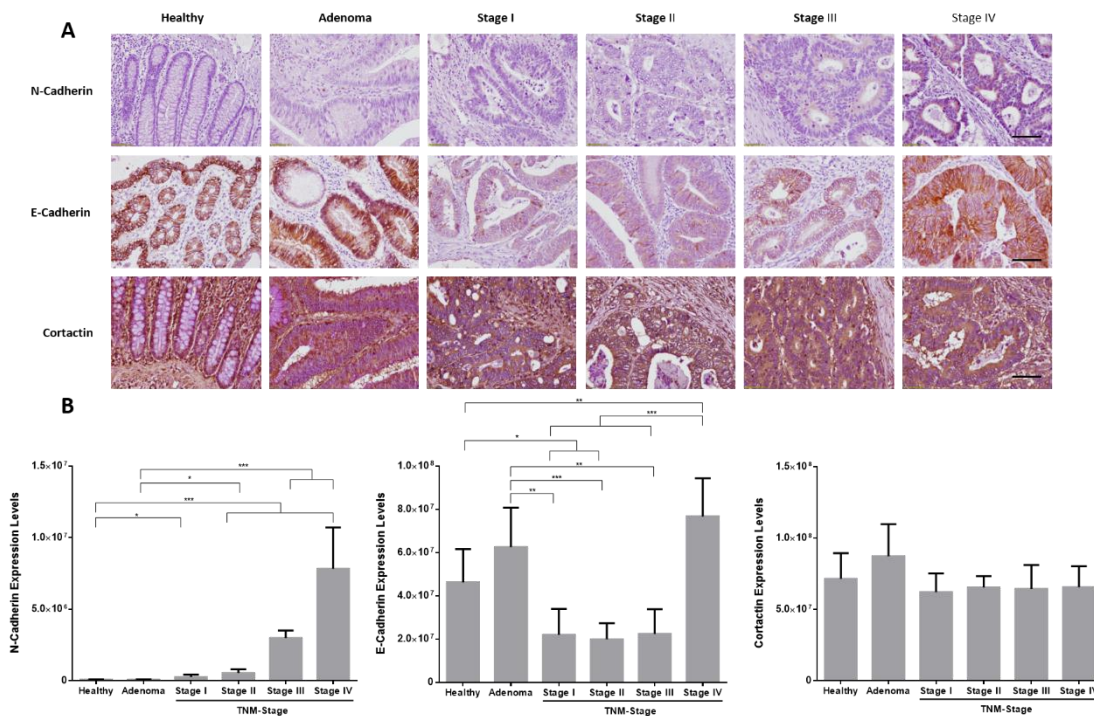


Figure 17. Expression of epithelial and mesenchymal markers in colorectal cancer, adenoma and healthy epithelial tissue. **A**, Immunohistochemistry staining of N-Cadherin, E-Cadherin and Cortactin in human samples from normal colonic epithelium, adenoma, and colon cancer (TNM stages I-IV). Photographs were taken with 20x objective. **B**, Quantification of N-Cadherin, E-Cadherin and Cortactin intensity levels in colorectal cancer cells at different colon cancer stages and in adenoma and healthy colon tissues (normal colonic mucosa, n = 8; adenoma, n = 2; colorectal cancer, n = 8 of all stages). Five images of each sample were taken and quantified. Data are represented as bar plot. Values are means \pm SD of staining intensity signal scoring per area. Quantification and calibration of the images were performed with Immunohistochemistry (IHC) Image Analysis Toolbox software for Image J. Kruskal-Wallis with Tukey correction test analyses show statistical differences in colorectal cancer (TNM, SI-IV) respect to paired healthy samples (*p < 0.05; **p < 0,01; ***p < 0,001). Scale bar 50 μ m.

1.1. Exosome analysis of serum samples from colorectal cancer patients

In view of the results obtained in the study of the expression of Hakai by immunohistochemistry from different stages of colorectal cancer, adenoma and adjacent healthy tissue, Hakai appeared to be a potential biomarker of tumour progression in colorectal cancer.

Despite the existence of a good correlation between the expression levels detected by immunohistochemistry and the staging of the different patient samples, the fact that an intestinal biopsy is necessary to determine the Hakai expression levels greatly limited its potential application as a biomarker due to the procedure. Due to this fact, the study of Hakai expression levels from serological samples from healthy patients with adenoma and colorectal cancer was proposed as an alternative.

The type of approach that was decided to use for the study of these sera was the isolation and purification of exosomes. Exosomes could be described as extracellular vesicles with a lipid bilayer membrane structure that are present both in tissues and in biological fluids and that contain the specific molecular components of their cells of origin: proteins, RNA, DNA and lipids. The function of these exosomes in the body is very varied, and the mechanisms involved are still being studied, but their importance in different intercellular communication processes such as inflammation, immune responses, coagulation, cancer and host interactions has been demonstrated. -microbe. The study of the content of these exosomes has proven to be of great importance in cancer diagnosis and constitutes a technique with great advantages, among which its non-invasiveness stands out.

For this study, serological samples were available from 62 patients (11 patients with adenoma, 26 with colorectal cancer, and 25 healthy) from which the exosomes were first isolated to then extract their RNA and use it in RT-qPCR for the study of Hakai levels. Unfortunately, the results obtained were not conclusive given that the levels of RNA extracted from the exosomes were too low that when analysing them by PCR, amplification values of both Hakai and the different housekeeping's were obtained at cycles, and it could not be considered specific.

Different optimization methods of the entire process were tested to reduce the number of PCR cycles necessary for the detection of the different markers of interest. On the one hand, it was improved the performance in the purification and isolation of exosomes, different RNA extraction kits that could obtain a greater amount of it from isolated exosomes, loading a greater amount of sample both in retro transcription and in the PCR wells, all without reaching sufficient levels for the detection of Hakai specifically.

2. Hakai expression in human samples of Ulcerative Colitis and Crohn's disease

Given that the upregulation of Hakai was observed even in early stages of the tumoral progression, including adenoma and TNM-stage I colorectal adenocarcinoma, we decided to analyse whether Hakai may also have an important role in inflammatory and preneoplastic disorders like Ulcerative Colitis and Crohn's disease. These two processes are chronic inflammatory conditions of the gastrointestinal tract in which the inflammatory damage increases the risk of developing pre-neoplastic and neoplastic conditions.

For this purpose, we used human samples from patients with Ulcerative Colitis and Crohn's disease as well as human samples from patients with colorectal adenocarcinoma stage IV and its pairs of histologically normal tissue adjacent to the tumour as controls. Immunohistochemistry assays were performed to analyse Hakai levels of expression.

Hakai staining intensity in inflammatory bowel disease samples was significantly upregulated compared to adjacent normal tissue but not at as high as the staining intensity observed in the colorectal adenocarcinoma stage IV samples (**Figure 18**).

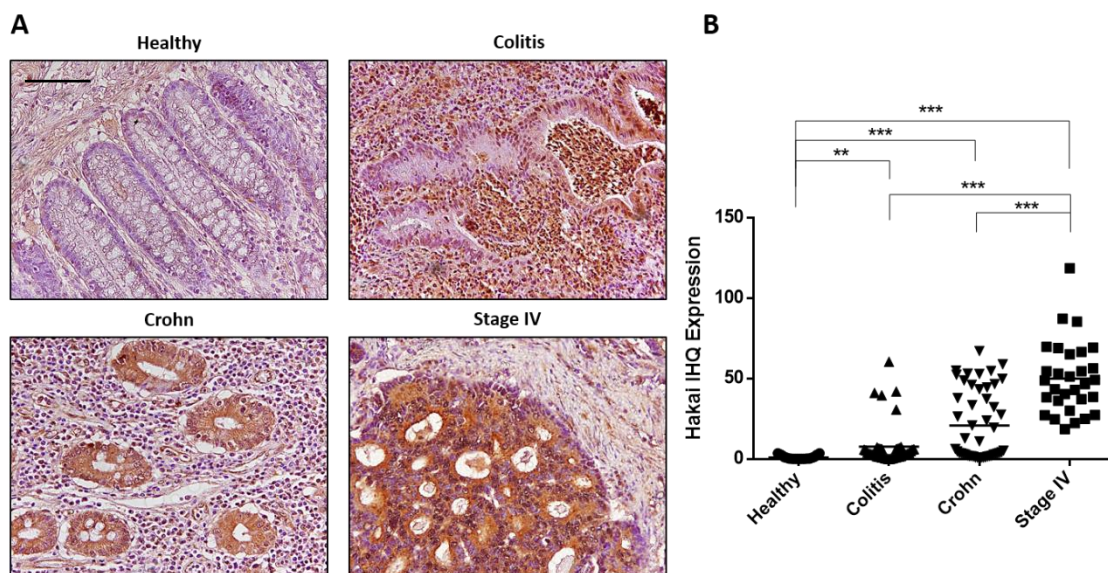


Figure 18. Expression of Hakai in human samples of Ulcerative Colitis, Crohn's disease, Colorectal Adenocarcinoma stage IV and its healthy tissue pairs. A, Immunohistochemistry staining of Hakai in non-transformed colonic mucosa, Ulcerative Colitis, Crohn's disease and Colorectal Adenocarcinoma stage IV. Images obtained with 20x objective. Scale bar 125 μ m. **B,**

Quantification of the staining intensity of Hakai in non-transformed colonic mucosa, Ulcerative Colitis, Crohn's disease and Colorectal Adenocarcinoma stage IV tissues (non-transformed colonic mucosa, n = 6; Ulcerative Colitis, n = 8; Crohn's disease, n = 10; Colorectal Adenocarcinoma stage IV, n = 6). Five pictures of each sample were taken and quantified. Data are represented as scatter plot. Values are means \pm SEM of staining intensity signal scoring per area. Quantification and calibration of the images were performed with Immunohistochemistry (IHC) Image Analysis Toolbox software for Image J. Kruskal-Wallis with Tukey correction test analyses show statistical differences in Ulcerative Colitis, Crohn's disease and Colorectal Adenocarcinoma stage IV respect to paired non-transformed colonic mucosa samples (*p < 0.05; **p < 0,01; ***p < 0,001). Scale bar 50 μ m.

Moreover, the differences in staining intensity between patients with the same condition were noticeable. Some Ulcerative Colitis and Crohn's disease patients showed high levels of expression of Hakai proximal to the colorectal adenocarcinoma stage IV samples, and some other patients had very low levels of expression of Hakai. These differences may be explained in part by the fluctuational characteristics over time of these diseases, and in the patients were in an acute phase or a remission phase.

3. Hakai expression in different Inflammatory Bowel Disease (IBD) mouse models

Given the previous results on which we detected higher levels of Hakai expression on Ulcerative Colitis and Crohn's disease human samples, we decided to investigate whether E3-ubiquitin-ligase Hakai could be related to the inflammatory processes. To do so, we performed three different mouse models that mimic different origins and stages of the IBD disease.

The first model analysed was the AOM-DSS model of colitis-associated cancer. This model replicates the tumour development process of the human Colitis-Associated Colorectal Cancer (CAC) by using the combination of a proinflammatory agent (DSS) and a carcinogenic compound (AOM). The second animal model in which we studied the role of Hakai was the Acute Colitis mouse model, which recapitulates the key aspects of severe periods of human ulcerative colitis by the treatment of the animals with long exposure periods to the proinflammatory agent (DSS). Finally, the third mouse model was based in the utilization of genetically modified mice IL-10 KO which are deficient for

the IL-10 gene. These mice spontaneously develop a chronic inflammatory bowel disease (IBD) due to the important control that IL-10 has over gut microbiota. The absence of IL-10 modulates cellular immune response and reduces mice tolerance towards bacterial antigens of enteric bacteria which causes the inflammatory process.

Whole intestine samples from the three different mouse models were processed and used for immunohistochemistry assay against Hakai. The staining with Hakai revealed the same pattern of expression for the three models. Comparing to control healthy mouse, animals submitted to inflammatory conditions showed a significant decreased expression of Hakai in their gut epithelium. As shown in (Figure 19), Hakai expression was significantly reduced in the inflamed tissue of the AOM-DSS model, on the contrary, the expression of Hakai in tumoral tissue from the Colitis-associated colorectal cancer model was markedly upregulated. Similarly, in (Figure 20) Hakai is also downregulated in the inflamed tissue corresponding to the Acute-Colitis mouse model. Finally, in the IL-10 KO mouse model the inflamed intestinal tissue, again presented lower expression levels of Hakai (Figure 21). This was seen in all models despite the fact the origin of the inflammation was totally different.

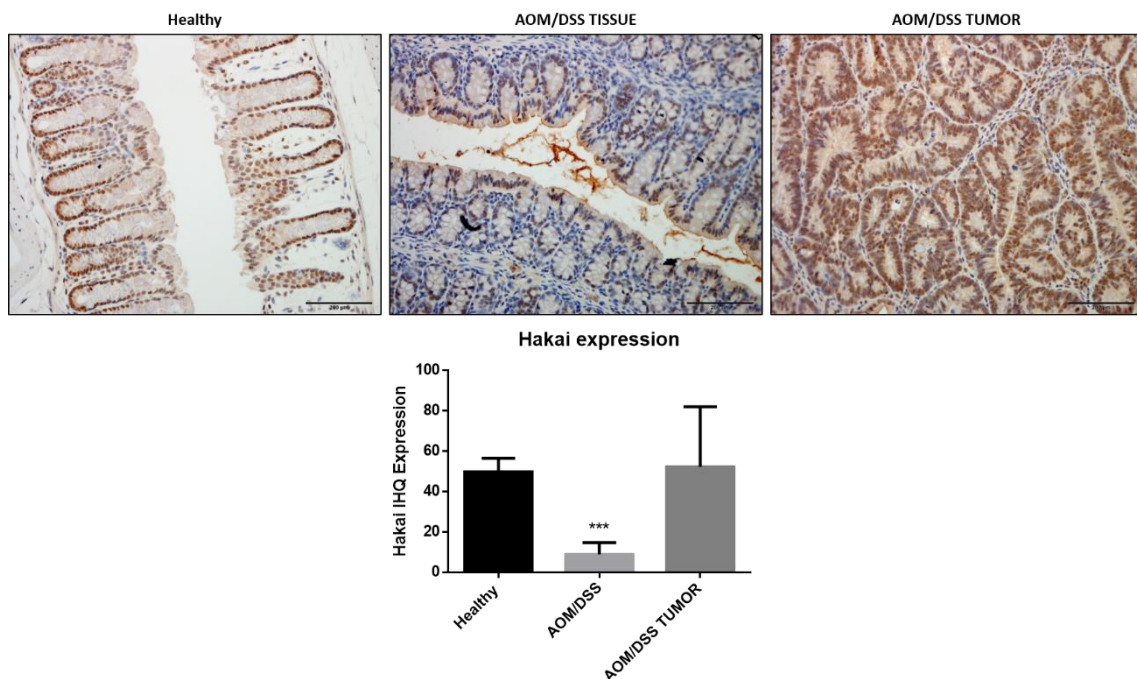


Figure 19. Expression of Hakai in mouse samples of the AOM/DSS Colitis-associated colorectal cancer model. Immunohistochemistry staining of Hakai in healthy non-treated mouse colonic mucosa and in gut sections of AOM/DSS-treated mouse (inflamed epithelium and tumours).

Images obtained with 20x objective. (Healthy mice, n = 7; AOM/DSS-treated mice, n = 14). Five pictures of each sample were taken and quantified. Data are represented as scatter plot. Values are means \pm SEM of staining intensity signal scoring per area. Quantification and calibration of the images were performed with Immunohistochemistry (IHC) Image Analysis Toolbox software for Image J. Kruskal-Wallis with Tukey correction test analyses show statistical differences in AOM/DSS-inflamed tissue respect to paired healthy samples (* $p < 0.05$; ** $p < 0,01$; *** $p < 0,001$). Scale bar 125 μm .

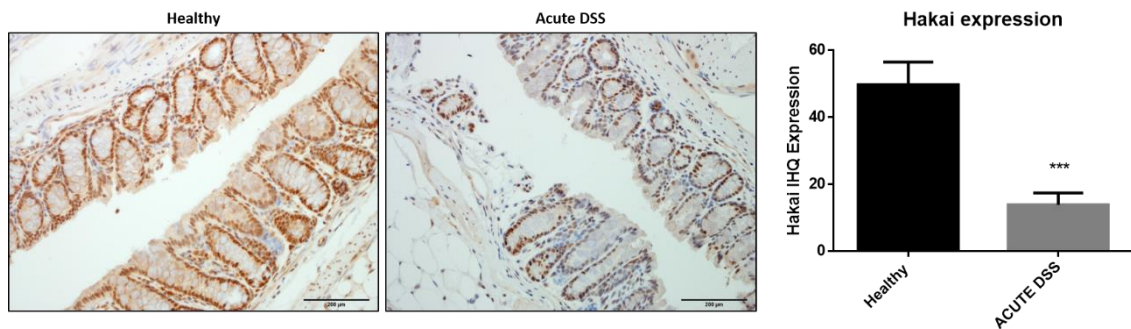


Figure 20. Expression of Hakai in mouse samples of the Acute DSS Colitis model. Immunohistochemistry staining of Hakai in healthy non-treated mouse colonic mucosa and in gut sections for DSS-treated mouse (inflamed epithelium). Images obtained with 20x objective. (Healthy mice, n = 7; DSS-treated mice, n = 3). Five pictures of each sample were taken and quantified. Data are represented as scatter plot. Values are means \pm SEM of staining intensity signal scoring per area. Quantification and calibration of the images were performed with Immunohistochemistry (IHC) Image Analysis Toolbox software for Image J. Kruskal-Wallis with Tukey correction test analyses show statistical differences in DSS-inflamed tissue respect to paired healthy samples (* $p < 0.05$; ** $p < 0,01$; *** $p < 0,001$). Scale bar 125 μm .

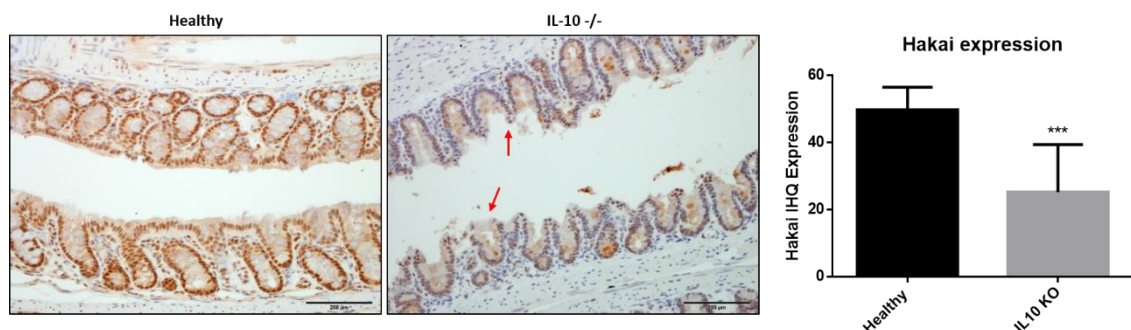


Figure 21. Expression of Hakai in mouse samples of the IL-10 KO model. Immunohistochemistry staining of Hakai in healthy non-treated mouse colonic mucosa and in gut sections for IL-10

deficient mice (inflamed epithelium). Images obtained with 20x objective. (Healthy mice, n = 7; IL-10 deficient mice, n = 6). Five pictures of each sample were taken and quantified. Data are represented as scatter plot. Values are means \pm SEM of staining intensity signal scoring per area. Quantification and calibration of the images were performed with Immunohistochemistry (IHC) Image Analysis Toolbox software for Image J. Kruskal-Wallis with Tukey correction test analyses show statistical differences in IL-10 KO inflamed tissue respect to paired healthy samples (*p < 0.05; **p < 0,01; ***p < 0,001). Scale bar 125 μ m.

Taken all together these results, on one hand confirm previous results observed regarding Hakai overexpression in tumour tissue when compared to adjacent non tumour tissue. On the other hand, they point out a clear regulation of Hakai under different inflammatory conditions, with a great reduction in Hakai expression in the inflamed epithelium. On the contrary, the high expression of Hakai in the epithelium of healthy untreated mouse was not observed in human tumour-adjacent healthy tissue (**Figure 16**).

Then we decided to analyse the gene expression of Hakai in AOM/DSS and IL-10 KO mouse models by using microarray data from similar experiments in NCBI's Gene Expression Omnibus (GEO). This approach was possible thanks to the Gene Expression Omnibus (GEO) database of microarray. We analysed the gene expression of Hakai in different reported mouse models including the acute colitis, colitis-associated colorectal cancer, or the IL-10 KO model. We observed, as shown in (**Figure 22**), that Hakai mRNA levels were reduced in the inflamed tissue of both the DSS (**Figure 22A, B**) and the IL-10 KO (**Figure 22C**) models. Also, we appreciated that although in the AOM/DSS model (**Figure 22A**), Hakai gene expression was reduced, in the inflamed tissue it tended to increase again during tumour progression from low grade dysplasia to adenocarcinoma. Taking together these results suggest that mRNA and protein expression of Hakai are clearly downregulated under a proinflammatory environment in the intestinal tissue regardless of origin of that inflammation. Moreover, this regulation seems to be taking place already at a transcriptional level considering the results of the microarray data.

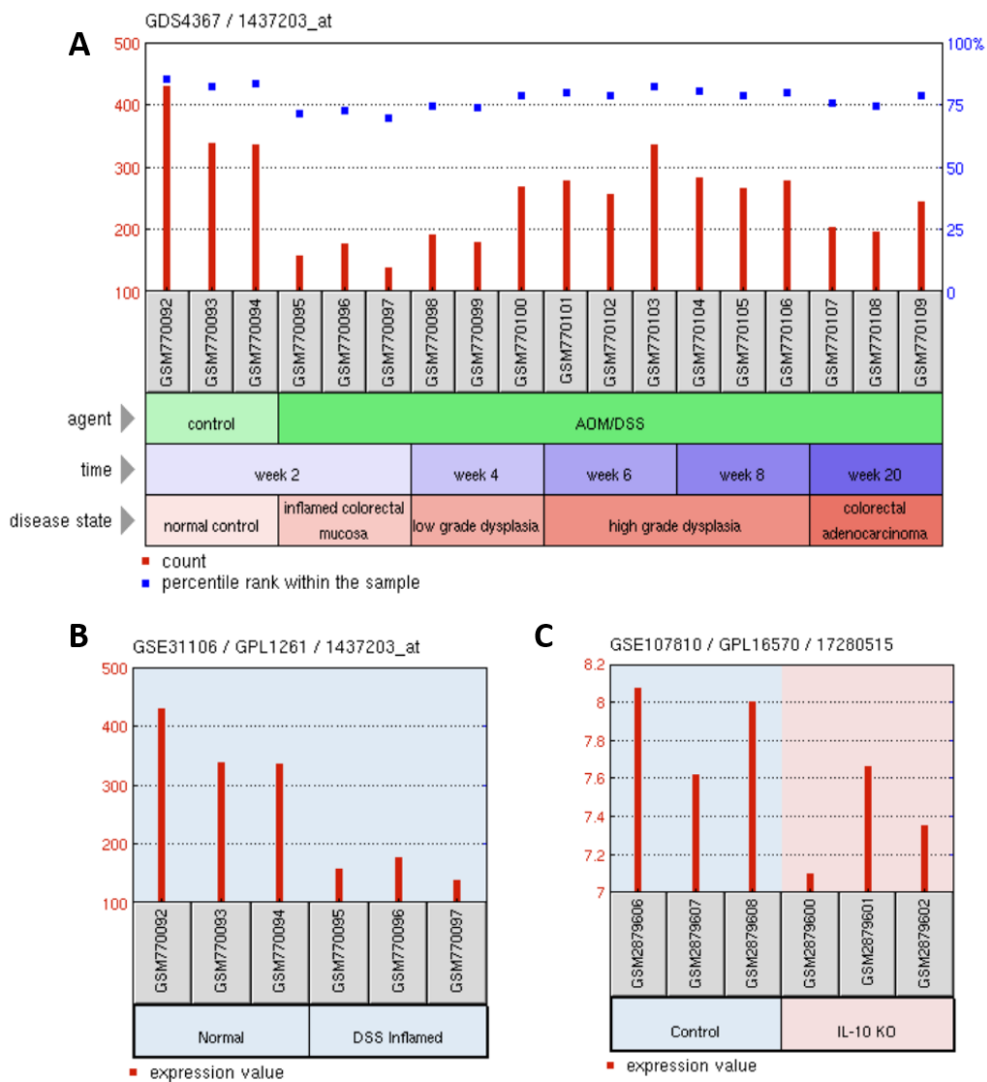


Figure 22. Gene expression of Hakai in AOM/DSS and IL-10 KO mouse models. A, Gene expression of Hakai during temporal analysis of mouse colon tissue from AOM/DSS-induced model of ulcerative colitis-associated colorectal cancer. **B,** Hakai gene expression differences between normal control and DSS inflamed mucosa in mouse. **C,** Hakai gene expression in colon tissue from IL-10 WT and IL-10 KO mice. Data from GEO database accession numbers: GDS4367, GSE31106 and GSE107810.

4. Hakai interactome

Observations carried out in inflammatory animal models suggested that Hakai could play a role in the regulation of intestinal inflammatory processes. This fact led us to propose

the realization of a large-scale immunoprecipitation of Hakai to develop a map of its molecular interactions and determine if there could be any link to inflammatory processes. This type of study would allow us to narrow the number of proteins with regulatory functions of the inflammatory process on which Hakai could be involved.

The interactome was performed in HCT-116 colon cancer cells, and immunoprecipitation of endogenous Hakai was carried out. The coimmunoprecipitated proteins then were identified by the IDIS proteomics platform (Instituto de Investigación Sanitaria de Santiago de Compostela). This was performed by using the TripleTOF 6600 system for processing the samples, after having previously separated the peptides using Reverse Phase Chromatography.

Two different conditions were taken into consideration for the development of the interactome. On the one hand a control situation with DMSO treatment, and on the other the treatment with Hakin-1. Hakin-1 is a specific inhibitor designed against the HYB domain of Hakai, responsible for the recognition of phosphorylated substrates for their labelling with ubiquitin. A total of 26 different proteins were identified bound to Hakai by the analysis (**Table 9**). None of the proteins identified remained interacting with Hakai in the samples treated with Hakin-1 inhibitor (**Figure 23**). In addition, two new proteins, KIAA1429 and HMCES, that did not appear among the proteins identified in the control conditions, did appear when treating cells with Hakin-1. A list of the proteins identified are included in **Table 10**. Moreover, STRING analyses were performed, STRING is a biological database that is able to process data from several sources to determine and provide information about both physical and functional properties of proteins (Franceschini et al., 2013). After analysing the identified proteins by STRING, the interaction networks between them were obtained as shown in (**Figure 23A**).

Table 9. List of proteins identified in Hakai interactome.

N	Accession number	Gene code	Protein name	Biological role
1	Q9Z1X4	ILF3	Interleukin enhancer-binding factor 3	Transcription factor (NF45, ILF2) required for T-cell expression of interleukin 2
2	Q16630	CPSF6	Cleavage and polyadenylation specificity factor subunit 6	Subunit of a cleavage factor required for 3' RNA cleavage and polyadenylation processing
3	Q43809	NUDT21	Cleavage and polyadenylation specificity factor subunit 5	Subunit of a cleavage factor required for 3' RNA cleavage and polyadenylation processing
4	Q92841	DDX17	ATP-dependent RNA helicase DDX17	RNA helicases. They are implicated in a number of cellular processes involving alteration of RNA secondary structure
5	P17844	DDX5	ATP-dependent RNA helicase DDX5	RNA helicases. This protein is involved in pathways that include the alteration of RNA structures
6	Q07955	SRSF1	Serine/arginine-rich splicing factor 1	Arginine/serine-rich splicing factor protein family
7	Q16658	FSCN1	Fascin	Member of the fascin family of actin-binding proteins
8	P18206	VCL	Vinculin	Cytoskeletal protein associated with cell-cell and cell-matrix junctions
9	Q2KJG3	NARS	Asparagine tRNA ligase	Asparaginyl-tRNA synthetase
10	Q07666	KHDRBS1	KH domain-containing, RNA-binding, signal transduction-associated protein 1	Member of the K homology domain-containing, RNA-binding, signal transduction-associated protein family
11	P26640	VARS	Valine tRNA ligase	Valyl-tRNA synthetase
12	O00571	DDX3X	ATP-dependent RNA helicase DDX3X	ATP-dependent RNA helicase
13	P40939	HADHA	Trifunctional enzyme subunit alpha	Catalyzes the last three steps of mitochondrial beta-oxidation of long chain fatty acids
14	P49327	FASN	Fatty acid synthase	Catalyzes the synthesis of palmitate from acetyl-CoA and malonyl-CoA, in the presence of NADPH, into long-chain saturated fatty acids
15	P53396	ACLY	ATP-citrate synthase	Primary enzyme responsible for the synthesis of cytosolic acetyl-CoA in many tissues
16	Q16822	PCK2	Phosphoenolpyruvate carboxykinase	Mitochondrial enzyme that catalyzes the conversion of oxaloacetate to phosphoenolpyruvate in the presence of guanosine triphosphate
17	Q13263	TRIM28	Transcription intermediary factor 1-beta	Gene mediates transcriptional control by interaction with the Kruppel-associated box repression domain found in many transcription factors
18	P48643	CCT5	T-complex protein 1 subunit epsilon	Molecular chaperone that is a member of the chaperonin containing TCP1 complex
19	Q16543	CDC37	Hsp90 co-chaperone	Molecular chaperone with specific function in cell signal transduction. It has been shown to form complex with Hsp90
20	P78527	PRKDC	DNA-dependent protein kinase catalytic subunit	Catalytic subunit of the DNA-dependent protein kinase (DNA-PK). It functions with the Ku70/Ku80 heterodimer protein in DNA double strand break repair and recombination
21	P54886	ALDH1L8	Delta-1-pyrroline-5-carboxylate synthase	Catalyzes the reduction of glutamate to delta-1-pyrroline-5-carboxylate, a critical step in the de novo biosynthesis of proline, ornithine and arginine
22	O15371	EIF3D	Eukaryotic translation initiation factor 3 subunit D	The complex binds to the 40S ribosome and helps maintain the 40S and 60S ribosomal subunits in a dissociated state
23	P26373	RPL13	60S ribosomal protein L13	This gene encodes a ribosomal protein that is a component of the 60S subunit
24	Q02878	RPL6	60S ribosomal protein L6	This gene encodes a protein component of the 60S ribosomal subunit
25	Q07020	RPL18	60S ribosomal protein L18	Ribosomes, the organelles that catalyze protein synthesis, consist of a small 40S subunit and a large 60S subunit
26	P60842	EIF4A1	Eukaryotic translation initiation factor 4A-1	Eukaryotic translation initiation factor 4A1

Table 10. List of proteins identified in Hakai interactome by Hakin-1 treatment.

N	Accession number	Gene code	Protein name	Biological role
1	Q96FZ2	HMCE5	Abasic site processing protein	Sensor of abasic sites in single-stranded DNA (ssDNA) required to preserve genome integrity by promoting error-free repair of abasic sites
2	Q69YN4	KIAA1429	Protein virilizer homolog	Mediates N6-methyladenosine (m6A) methylation of RNAs

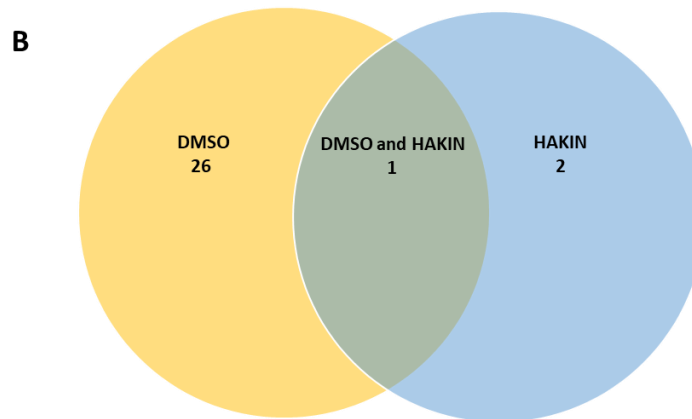
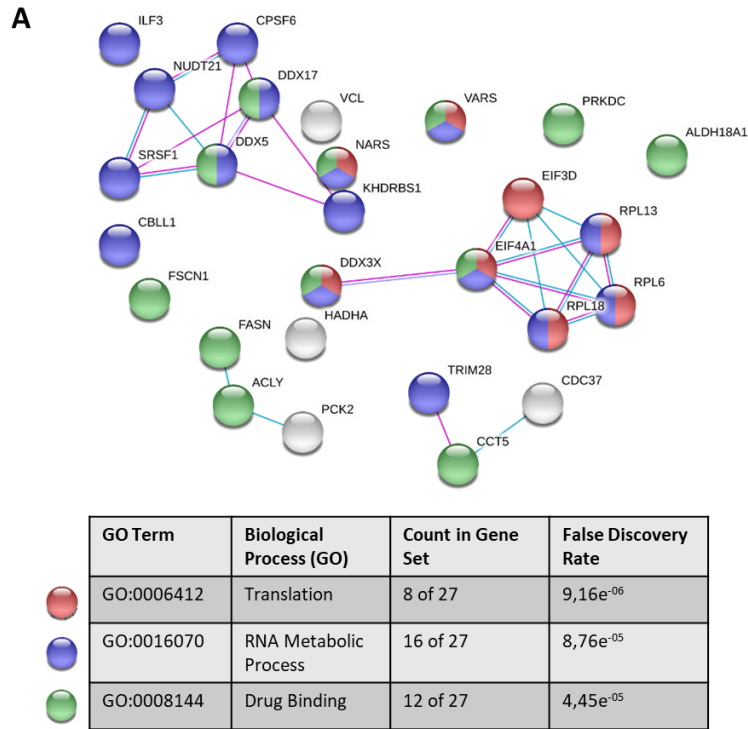


Figure 23. Protein-protein interaction network of the identified Hakai interactome. A, Network of all the proteins identified in the analysis of Hakai immunoprecipitation in HCT-116 cells designed using STRING database. Proteins in green indicate their role in drug binding, red colour indicates that they are implicated in translation and blue colour that they are important for RNA processing. **B,** Venn's diagram of the proteins identified under the different conditions considered for the interactome study. The computer analysis of the raw data obtained was carried out by (Aida - UK) using ProteinPilotTM 5.0.1 software (ABSciex).

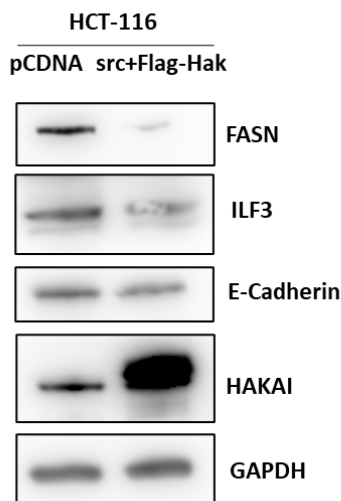
Interestingly, from all the proteins identified in the study, two of the proteins were already described to be involved in inflammatory processes. These two proteins were FASN, or Fatty acid synthase, and ILF-3 (Interleukin enhancer-binding factor 3). We therefore selected these two proteins to determine the possible link between them and Hakai and the potential role in inflammatory process.

5. Effect of Hakai overexpression on FASN and ILF-3

In order to determine the possible connection between Hakai and the selected proteins identified in the interactome we firstly transiently overexpress Hakai. HCT-116 cells were co-transfected with pcDNA-Flag-Hakai and pSG-v-Src plasmids, to achieve a strong overexpression of Hakai, and the effect on FASN and ILF-3 expression was assessed by western blot.

As observed in (**Figure 24**), overexpression of Hakai strongly downregulated FASN expression in HCT-116 cells. This downregulation was also seen in ILF3 when overexpressing Hakai but not with the same marked effect. These results might suggest that Hakai could be playing an important role on FASN regulation. Moreover, it was confirmed that E-Cadherin was downregulated by Hakai overexpression. At the same time, we were interested in studying whether this regulation that we observe in protein expression could be happening as well at mRNA level. To this end, the expression levels of FASN and ILF3 mRNA were studied by RT-qPCR, obtaining as a result that there was no type of regulation at a transcriptional level. This fact suggests that Hakai might be regulating FASN and ILF-3 at a post-translational level.

A



B

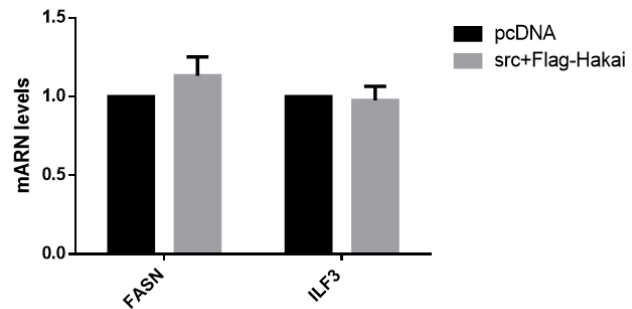


Figure 24. Effect of Hakai overexpression on FASN and ILF-3. **A**, Western blot in HCT-116 cells co-transfected with pcDNA-Flag-Hakai (2 μ g) and pSG-v-Src (0.5 μ g) for 48 h. Cell lysates were subjected to Western Blotting as described in Materials and Methods using the corresponding antibodies. **B**, mRNA levels of FASN and ILF3 were evaluated by performing RT qPCR using RPL13A and GAPDH as a housekeeping's.

6. Effect of Hakai silencing on FASN and ILF-3

Then we decided to analyse the effect of Hakai-silencing in the regulation of the identified proteins. For this purpose, we used two different systems: transient transfection of siRNA Hakai for HCT116 cells and shRNA-Hakai silencing in a puromycin-inducible system by viral transduction for HT29.

We used viral transduction instead of transient transfection in HT29 as these cells are difficult to transfect, we tried to establish both a model of overexpression and a model of silencing, achieving the second one but failing to successfully establish the first one after many tries. Viral transduction is highly efficient due to the viral nature of integration into the host genome and represents a great alternative for hard-to-transfect cells. On the other hand, the fact that we used an inducible system is crucial since Hakai is a vital protein for cell survival, therefore it was not possible to establish a cell line with Hakai silencing, since the cells would end up dying.

We started by studying the effect of Hakai-silencing in cell phenotype as well as on the expression and localization of Hakai by immunofluorescence. At the phenotypic

level, the change that occurs upon induction with doxycycline and the consequent silencing of Hakai is dramatic (**Figure 25**). Hakai silencing caused more three-dimensional cell sheet, showing cells closely attached compared to control cells. This effect on phenotype observed was according to Hakai role in the regulation of the epithelial-to-mesenchymal transition (EMT). The images showing GFP expression in (**Figure 25A**), are a positive control to show that the Tet-On system is induced in those cells as the viral plasmid also contains GFP reporter under the control of the same promoter as the shCBLL1 gene.

Regarding the study of the localization of Hakai expression in this model, a loss of the nuclear localization of Hakai was observed when stimulating with doxycycline (**Figure 25B**).

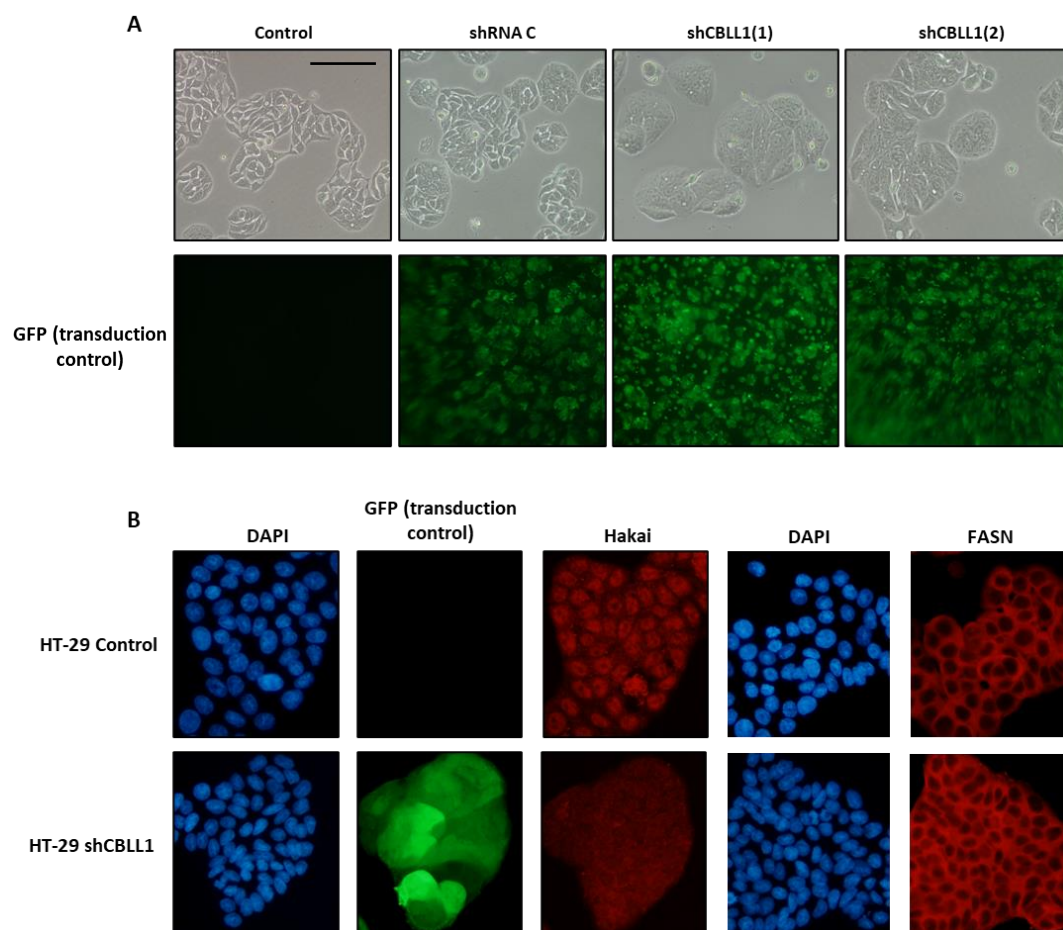


Figure 25. Effect of Hakai silencing on cell phenotype and FASN and Hakai expression. A, Effect of Hakai inducible silencing on HT-29 cell phenotype analysed by optical microscopy images, induction of cells with 1 $\mu\text{g}/\text{ml}$ of Doxycycline was maintained for 72h. Images taken with 10X

magnification. Scale bar 125 μm . **B**, Effect of Hakai silencing over Hakai and FASN subcellular location on stably and inducible transduced HT-29 cells measured by immunofluorescence with anti-Hakai and anti-FASN antibodies. Images taken with 40X magnification.

The analysis of protein expression by western blot showed that silencing of Hakai induce a drastic decrease in Hakai expression (**Figure 26**). Furthermore, this lower expression of Hakai achieves a strong upregulation of the expression of FASN, but the effect on ILF3 was not that evident. This result further suggest that Hakai may regulate FASN expression. As previously shown mRNA expression of FASN was not affected by Hakai silencing (**Figure 26C**), further supporting a possible regulation of Hakai on FASN at a post-translational level.

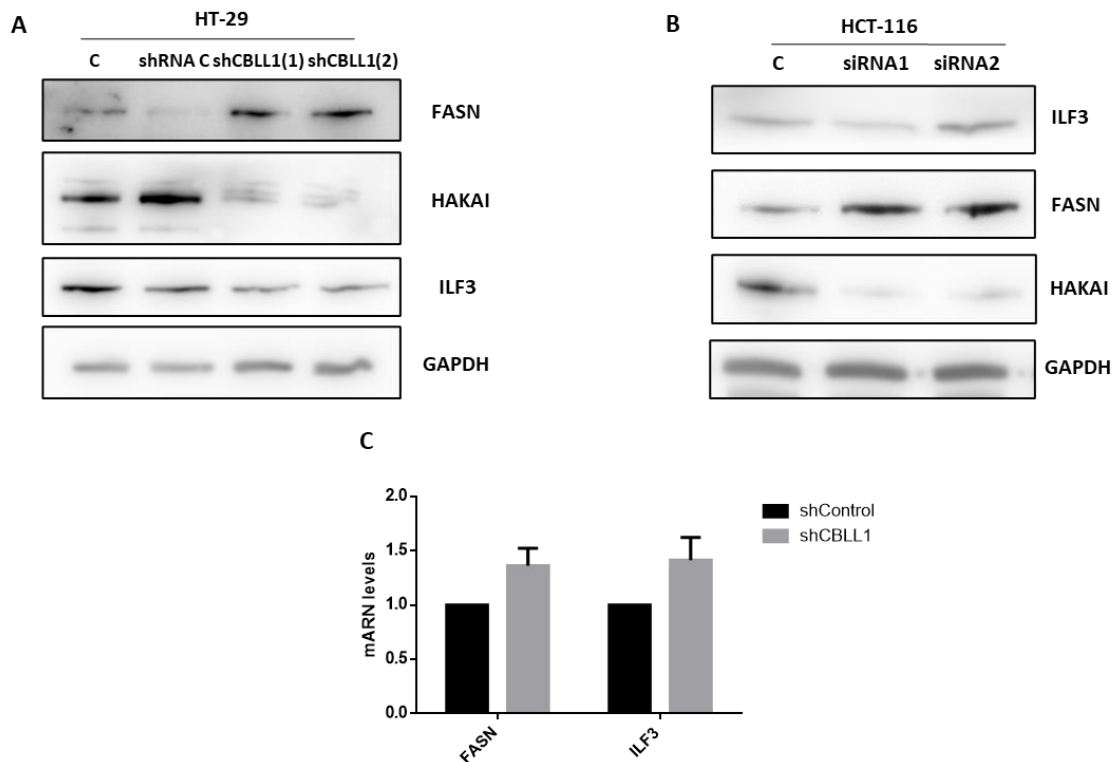


Figure 26. Effect of Hakai silencing on FASN and ILF-3. **A**, Western blot in HT-29 cells using an inducible viral-transduced system with Hakai targeting shRNA and induced for 72h with 1 $\mu\text{g}/\text{ml}$ doxycycline for Hakai silencing. Cell lysates were subjected to Western Blotting as described in Materials and Methods using the corresponding antibodies. **B**, Western blot in HCT-116 cells transiently transfected with Hakai targeting siRNAs. Cell lysates were subjected to Western Blotting as described in Materials and Methods using the corresponding antibodies. **C**, mRNA

levels of FASN and ILF3 were evaluated by performing RT qPCR using RPL13A and GAPDH as a housekeeping's.

7. Hakai interacts with FASN

The next step in our research was to determine the potential molecular mechanism by which Hakai could act in the inflammatory processes. Coimmunoprecipitation is one of the most useful techniques for the study of protein-protein interaction, allowing us to immunoprecipitate the desired protein through its conjugation with sepharose beads and then study by western-blot any other protein that has been precipitated by the fact of having been interacting with the study protein. To confirm the interaction between Hakai and FASN/ILF3 detected by interactome, we carried out immunoprecipitation assays using FASN, ILF3 or Hakai antibody for immunoprecipitation. Then, the possible co-immunoprecipitation was analysed by western-blot analysis.

The first immunoprecipitation was carried out in HCT-116 cells by analysing endogenous immunoprecipitation. As shown in **(Figure 27)** when using Hakai antibody for the immunoprecipitation, the coimmunoprecipitation of FASN was not detected despite having a good level of immunoprecipitation of Hakai.

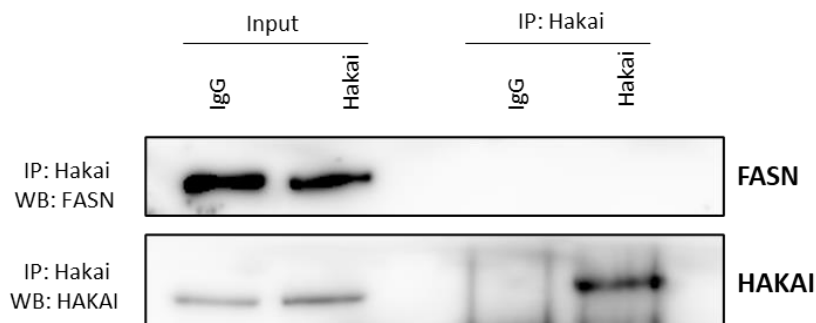


Figure 27. Hakai immunoprecipitation in HCT-116 with basal levels of expression. Protein-protein interaction between Hakai and FASN was evaluated by immunoprecipitation of Hakai, using its basal levels of expression in HCT-116 cells. Hakai immunoprecipitation was performed

by employing anti-Hakai Bethyl antibody. Coimmunoprecipitation was evaluated by western blot as described in materials and methods using the indicated antibodies.

Secondly, since the first approach was not successful, it was decided to analyse the possible interaction between the proteins by the co-transfection of pcDNA-Flag-Hakai. As it is reported that Src induces Hakai, we also transfected pSG-v-Src plasmids in order to increase Hakai protein levels in the cell.

As shown in (**Figure 28**), these conditions clearly favour the interaction, since the co-immunoprecipitation of FASN could be clearly detected when Hakai antibody is used for immunoprecipitation, further demonstrating their interaction. In the first place, the fact that the overexpression of Hakai reduced the global levels of FASN, could suggest that this would make it difficult to detect a possible co-immunoprecipitation. But, on the contrary, even decreasing global levels of FASN, overexpression of Hakai seems to increase the number of interacting complexes Hakai-FASN.

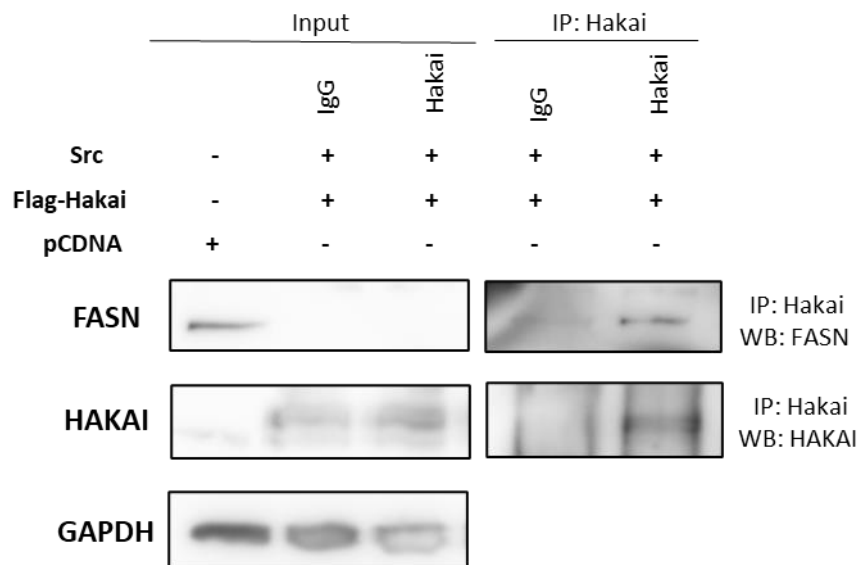


Figure 28. Coimmunoprecipitation of FASN and Hakai. Hakai and FASN protein-protein interaction was evaluated by immunoprecipitation of Hakai, in HCT-116 cells co-transfected with pcDNA-Flag-Hakai (2 µg) and pSG-v-Src (0.5 µg) for 48 h. Hakai immunoprecipitation was performed by using 1,5 µg of anti-Hakai Bethyl antibody. Coimmunoprecipitation was evaluated by western blot as described in materials and methods using the indicated antibodies.

Once the interaction between Hakai and FASN was demonstrated using Hakai antibody for immunoprecipitation, we decided to immunoprecipitate FASN and determine whether co-immunoprecipitation of Hakai was detected. In this case, as shown in **(Figure 29)**, we could not detect the coimmunoprecipitation of Hakai when immunoprecipitating FASN. This could be due to the fact that FASN antibody could interfere with the binding site to Hakai or just simply because the concentration of FASN in the cell is much higher than the concentration of Hakai and only a very small fraction of it was pulled down.

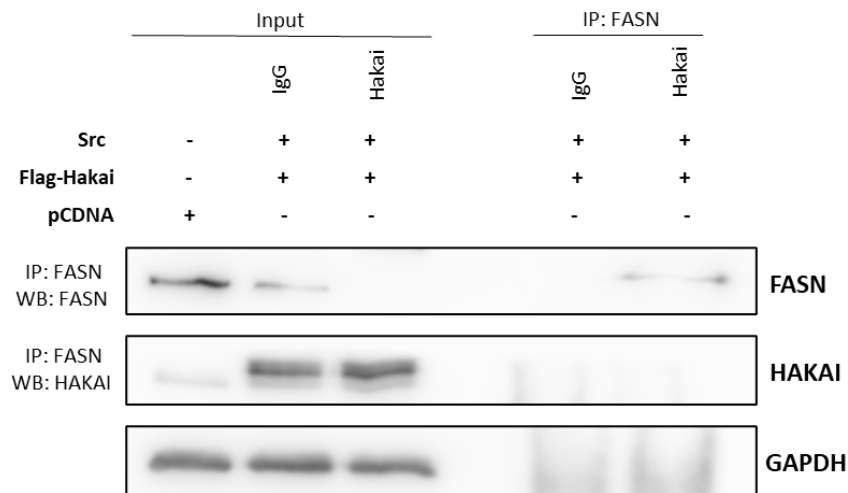


Figure 29. FASN immunoprecipitation in HCT-116 co-transfected with Src and Hakai. The study of protein-protein interaction between Hakai and FASN was evaluated by immunoprecipitation of FASN, in HCT-116 cells co-transfected with pcDNA-Flag-Hakai (2 µg) and pSG-v-Src (0.5 µg) for 48 h. FASN immunoprecipitation was performed by employing 1.5 µg of anti-FASN Santa Cruz Biotechnology antibody. Coimmunoprecipitation was evaluated by western blot as described in materials and methods using the indicated antibodies.

The same procedure was also carried out for ILF3. In this case, as it can be seen in **(Figure 30)**, the interaction was not confirmed. After testing reverse immunoprecipitation, and different conditions, we decided to focus more deeply on the potential significance of Hakai and FASN interaction.

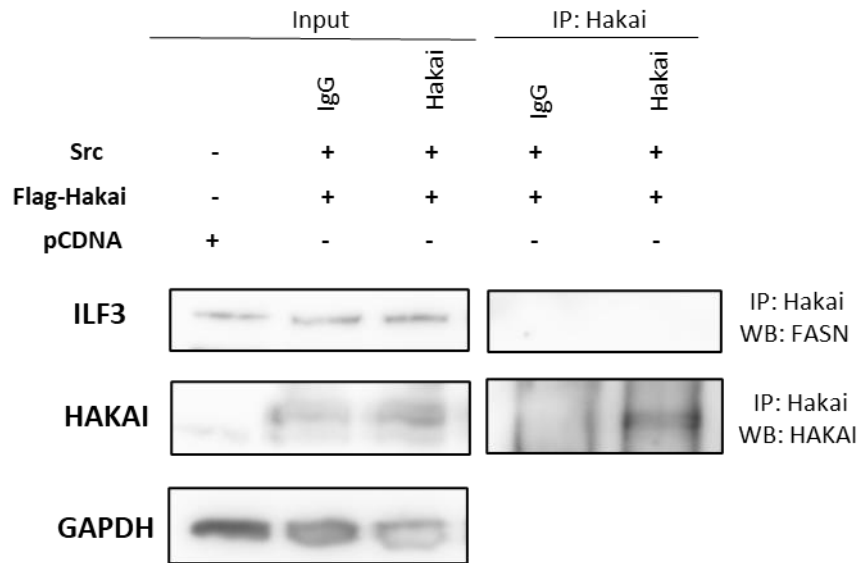


Figure 30. Attempted co-immunoprecipitation between ILF3 and Hakai. Interaction between Hakai and ILF3 was evaluated by immunoprecipitation of Hakai, in HCT-116 cells co-transfected with pcDNA-Flag-Hakai (2 μ g) and pSG-v-Src (0.5 μ g) for 48 h. Hakai immunoprecipitation was performed by employing 1.5 μ g anti-Hakai Bethyl antibody. Coimmunoprecipitation was evaluated by western blot as described in materials and methods using the indicated antibodies.

In relation to this interaction described between Hakai and FASN, an attempt was made to take advantage of the development of these experiments to test the efficacy of Hakin-1. As mentioned, Hakin-1 is a small-molecule inhibitor for Hakai previously used interactome study. This inhibitor had been shown to block the interaction of Hakai and FASN in the interactome study, therefore we decided to determine the potential effect on the interaction using immunoprecipitation assays. Interestingly, FASN band did not completely disappear when using Hakin-1 (**Figure 31**).

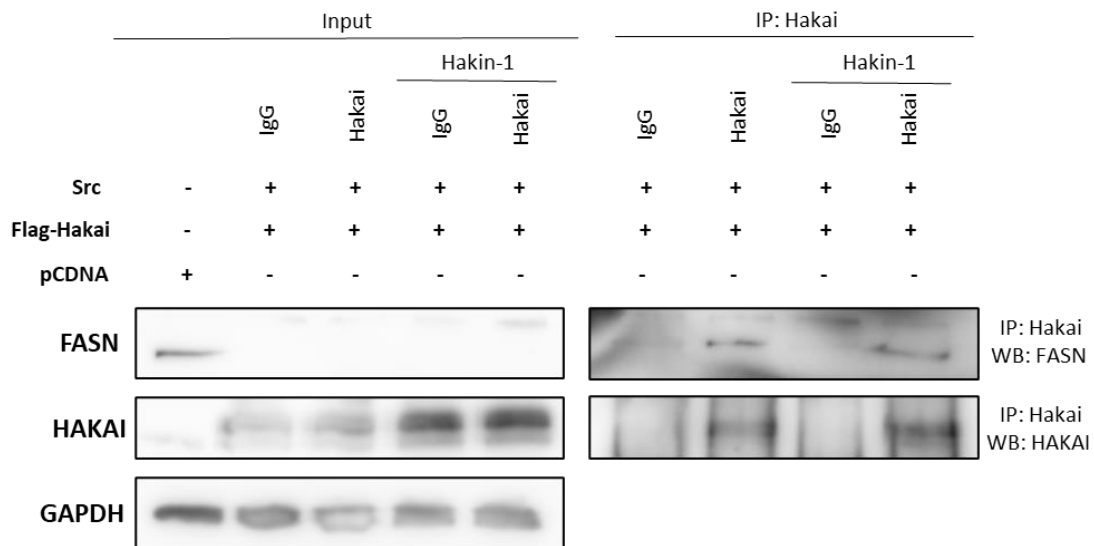


Figure 31. Effect of Hakin-1 inhibitor on the coimmunoprecipitation of FASN and Hakai. Study of the effect of Hakai inhibitor Hakin-1 over the interaction between Hakai and FASN was evaluated by immunoprecipitation of Hakai, in HCT-116 cells co-transfected with pcDNA-Flag-Hakai (2 μ g) and pSG-v-Src (0.5 μ g) for 48 h. Hakai immunoprecipitation was performed by employing 1.5 μ g of anti-Hakai Bethyl antibody. Coimmunoprecipitation was evaluated by western blot as described in materials and methods using the indicated antibodies. Hakin-1 was used at a concentration of 200nM for 48 h in the indicated samples.

Despite that Hakin-1 does not appear to affect FASN-Hakai interaction, the inhibitor does seem to influence the expression of FASN as we can see from (Figure 32). As shown, increasing concentrations of the inhibitor can upregulate the expression of FASN.

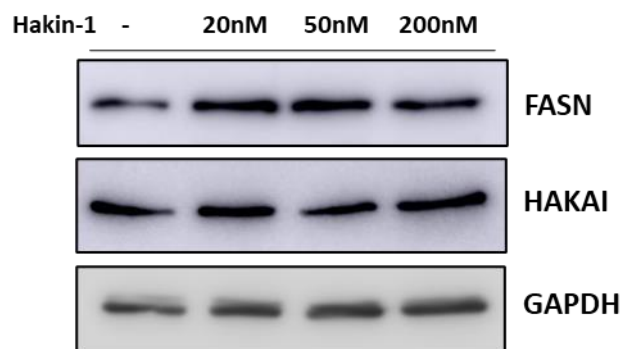


Figure 32. Effect of Hakin-1 inhibitor over the expression of FASN in HCT-116. Hakin-1 was used in increasing concentrations, ranging from 20 nM, 50 nM and 200nM for 48 h in HCT-116 cells.

Taken all together, our results suggest that Hakai and FASN can interact, but further experiments are needed to validate and characterize this interaction.

8. Silencing Hakai increases FASN half-life

The half-life of a protein may vary between a few hours and even days and can be modulated by post-translational modifications. The analysis of the half-life of a protein can help us to study its degradation by evaluating its expression over time and how it varies depending on different factors.

In our case, for the study of the half-life of FASN we used the Cycloheximide (CHX) assay. CHX inhibits protein synthesis by blocking the elongation of translation in eukaryotic cells. Thus, after treating cells with CHX, protein synthesis is inhibited which allows to determine the half-life of proteins.

In addition, this experiment will help us to determine whether Hakai is directly affecting the degradation of FASN in a post-translational level. For this, the Hakai induced silencing cell model was used to determine the influence of Hakai silencing of on FASN half-life.

As shown in **Figure 33**, silencing of Hakai was able to increase FASN half-life for almost two hours, going from 9,5 to 11,5 h, suggesting Hakai influence on FASN degradation.

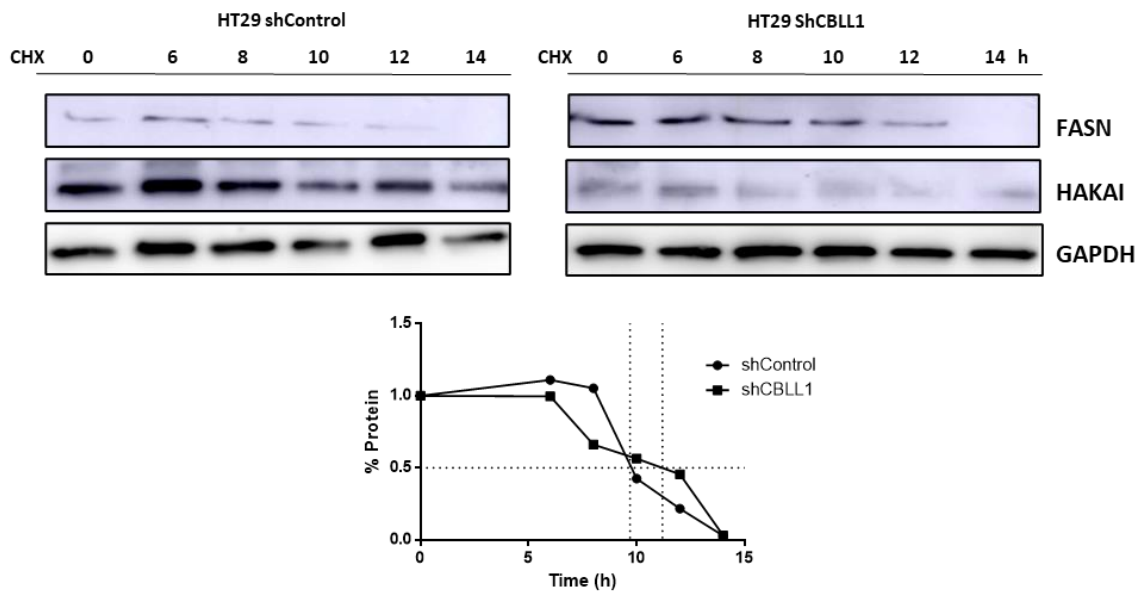


Figure 33. Effect of Hakai silencing on FASN half-life. FASN half-life in HT-29 cell line was determined by treatment with 10 $\mu\text{g/ml}$ Cycloheximide for the indicated time course and compared with FASN half-life in Hakai-silenced HT-29 cells. Viral transduced HT-29 cells were previously induced with 1 $\mu\text{g/ml}$ of Doxycycline for 72 h. Endogenous FASN protein levels were analysed by western blot as described in materials and methods using the indicated antibodies. Quantification of endogenous FASN protein levels and protein half-life are shown in the graph below. Amersham™ Imager 600 software was used for band quantification and GraphPad Prism 6 was used for graph representation.

9. Hakai effect on FASN ubiquitination

The ubiquitination system is responsible for labelling proteins by binding ubiquitin molecules for subsequent protein degradation in the proteasome, especially for short half-life proteins. The protein responsible for the specific recognition of the substrate to be degraded is the E3 ubiquitin ligase enzyme of the ubiquitination complex.

In order to determine whether Hakai is involved in the ubiquitination out of FASN, transfection with pcDNA-Flag-Hakai, pBSSR-HA-Ubiquitin and pSG-v-Src in HCT-116 cells was carried out. Then, FASN immunoprecipitation was performed, and the ubiquitination smear was detected by western blot using anti-HA antibody (**Figure 34A**). The results obtained show (**Figure 34A**) that Hakai overexpression clearly increases the levels of ubiquitination of FASN, suggesting that FASN degradation is mediated, at least in part, by Hakai at a post-translational level.

On the other hand, to further investigate FASN degradation, we evaluated the three described pathways by which ubiquitinated substrates can be degraded: proteasome degradation, lysosome degradation and autophagy system. With that purpose, we used three different inhibitors, the lysosome degradation inhibitor Chloroquine, the autophagy inhibitor 3-Methyladenine (3-MA) and the proteasome inhibitor MG132. Results showed that while MG132 and 3-MA did not increase FASN protein levels in HCT116 cells, Chloroquine treatment was effective elevating FASN protein levels (**Figure 34B**) suggesting that FASN degradation does occur via lysosome degradation.

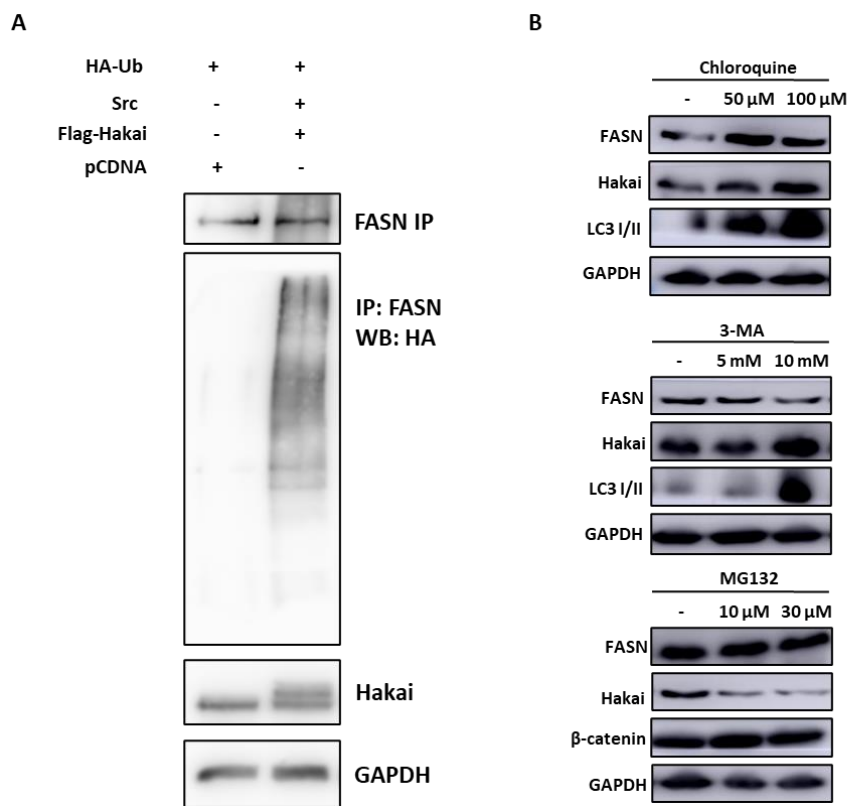


Figure 34. FASN is degraded by Hakai by ubiquitination via lysosome. **A**, Polyubiquitination levels of immunoprecipitated FASN detected by western-blotting using anti-HA antibody in HCT-116 cells co-transfected with pcDNA-Flag-Hakai (2 μ g), pBSSR-HA-Ubiquitin (0.5 μ g) and pSG-v-Src (0.5 μ g) for 48 h. **B**, FASN and Hakai levels in HCT-116 cells treated with the lysosome degradation inhibitor Chloroquine, the autophagy inhibitor 3-Methyladenine and the proteasome inhibitor MG132 at the indicated concentration times described in materials and methods. LC3 I/II levels were analysed as a positive control of chloroquine and 3-MA treatment and β -catenin for MG132 treatment.

10. Hakai inhibits lipid accumulation via FASN

FASN is a multifunctional enzyme that regulates the synthesis of long chain saturated fatty acids (Gang et al., 2016). In the results previously shown, we have demonstrated the role of Hakai as a regulator of FASN at post-translational level. Then, we decided to study whether the expression of Hakai can affect lipid synthesis, the well-described functional role of FASN. For this purpose, Oil Red O was used for detection of specific staining of fatty acids and neutral lipids was used. Two different cell lines were used. On the one hand, Hakai was overexpressed in HCT-116, by transient transfection, and on the other hand the inducible system of Hakai silencing in HT-29. Both cell lines were seeded and staining with Oil Red O was carried out to determine under the microscope if whether differential expression of Hakai could affect lipid accumulation.

As expected, overexpression of Hakai inhibits lipid accumulation (**Figure 35**), while Hakai silencing increased lipid accumulation by the upregulation of FASN. Altogether these results support that Hakai may regulate FASN at posttranslational level, affecting FAS-mediated lipid accumulation.

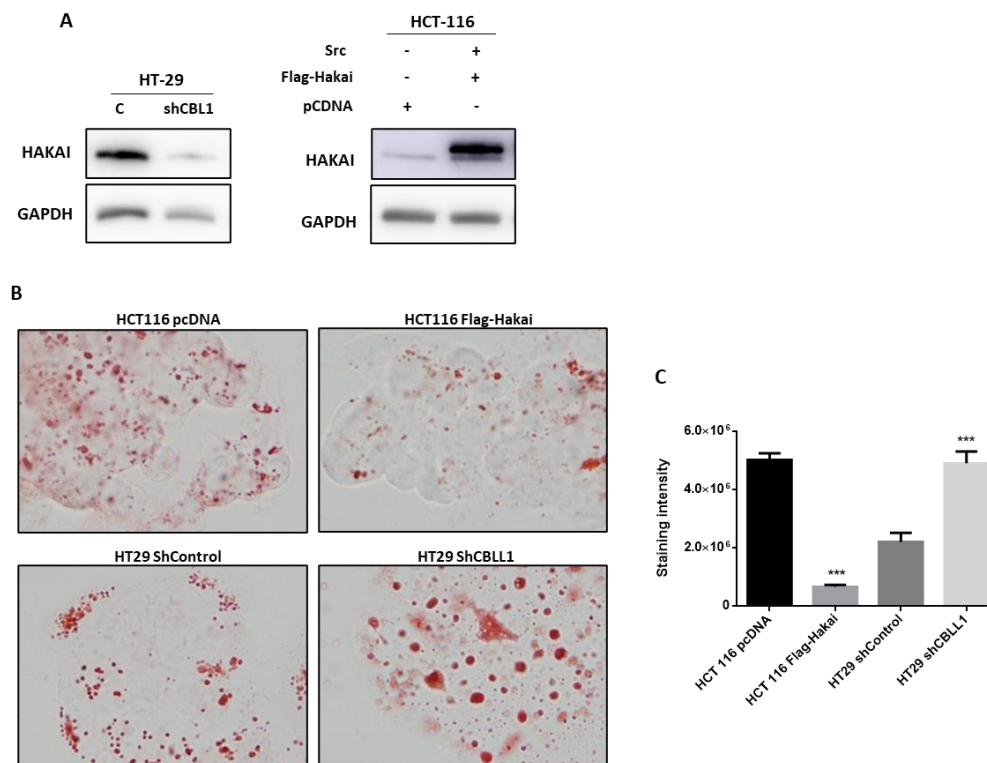


Figure 35. Hakai inhibition of lipid accumulation via FASN. **A**, Hakai levels in HCT-116 cells transfected with pcDNA-Flag-Hakai (2 μ g) and pSG-v-Src (0.5 μ g) and in shRNA-Hakai HT-29

previously induced with 1 µg/ml of Doxycycline for 72 h analysed by western blot as described in materials and methods using the indicated antibodies. **B**, HCT-116 transfected with pcDNA-Flag-Hakai (2 µg) and pSG-v-Src (0.5 µg) and shRNA Hakai HT-29 cells stained with Oil Red O. **C**, Quantification of the staining intensity of Oil Red O. in the different cell samples evaluated in (B). Five pictures of each sample were taken and quantified. Data are represented as bar chart. Values are means ± SD of staining intensity signal scoring per area. Quantification and calibration of the images were performed with Image Analysis Toolbox software for Image J. Kruskal-Wallis with Tukey correction test analyses show statistical differences between overexpression/silencing of Hakai and controls (*p < 0.05; **p < 0,01; ***p < 0,001).

11. IFN-γ affect Hakai-FASN interaction

After observing in the previously mentioned inflammatory animal models, that Hakai expression was regulated during the inflammatory processes, we decided to determine the effect of important reported inflammatory inducers in vitro including H₂O₂, TNF-α, IL-6, and IFN-γ.

Some of these inflammatory inducers, such as IL-6, did not show any effect on in vitro expression in Hakai and others, such as H₂O₂ and TNF-α, appeared to slightly regulate Hakai expression. On the other hand, IFN-γ, cytokine produced by CD4 + T lymphocytes and natural killer cells (NK) with a key role in cellular immunity, shows a significant downregulation of Hakai, especially at long exposure times (**Figure 36A, B**) in colorectal cell lines HT-29 and SW-620.

This downregulation of Hakai under an inflammatory stimulus, was also observed in the animal models. This fact led us to study if this downregulation of Hakai had the same effect on FASN as observed using shRNAs. The results showed that indeed, the downregulation of Hakai caused by the treatment with IFN-γ, produced an increase in the expression of FASN, as we had observed in previous silencing experiments (**Figure 36**).

The effect of IFN-γ on Hakai expression was observed at least in two different cell models, HT-29 and SW-620 and the results were later confirmed by immunofluorescence in HT-29. We tried to go deeper into the IFN-gamma-Hakai-FASN

axis by reversing IFN- γ -downregulation of Hakai by transfecting Hakai, but unlike the results obtained in HT-29 and SW-620, this IFN-gamma effect was not clearly detectable in our HCT-116 transfected line. For this reason, given that the HT-29 and SW-620 models were not transfectable in our experimental conditions, we could not perform this approach.

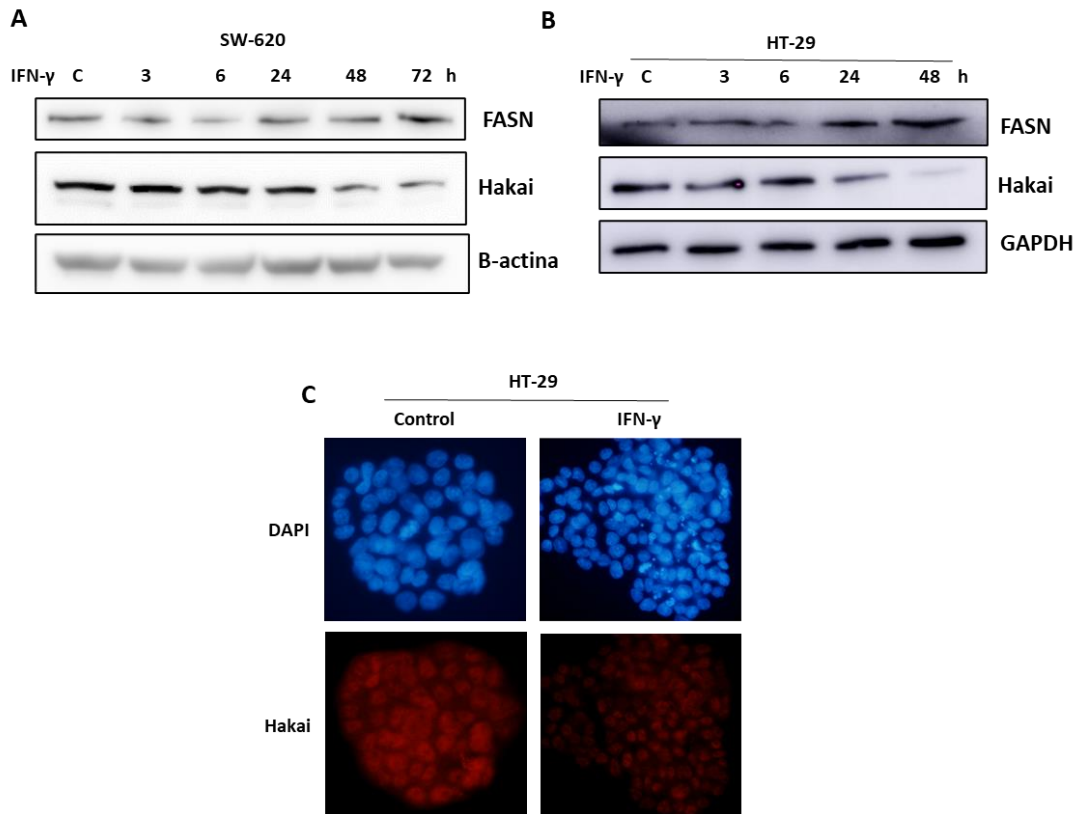


Figure 36. IFN- γ induces FASN expression through Hakai downregulation. A, FASN and Hakai expression in SW-620 cells treated with 10 ng/ml of IFN- γ for the indicated time course analysed by western blot as described in materials and methods using the indicated antibodies. **B,** FASN and Hakai expression in HT-29 cells treated with 10 ng/ml of IFN- γ for the indicated time course analysed by western blot as described in materials and methods using the indicated antibodies. **C,** Effect of 72 h treatment of IFN- γ (10 ng/ml) over Hakai subcellular location on HT-29 cells measured by immunofluorescence with anti-Hakai and antibody. Images taken with 40X magnification.

12. FASN upregulation in inflamed tissue from an AOM/DSS Colitis-associated colorectal cancer model

Given the interesting results obtained on the role of Hakai on FASN, we decided to further study the FASN expression using the AOM/DSS Colitis-associated colorectal cancer model. Immunohistochemical assays were carried out for FASN expression. The immunohistochemical staining showed that those tissues with lower expression of Hakai had higher expression levels of FASN (**Figure 37**) further supporting in vivo the findings described in vitro.

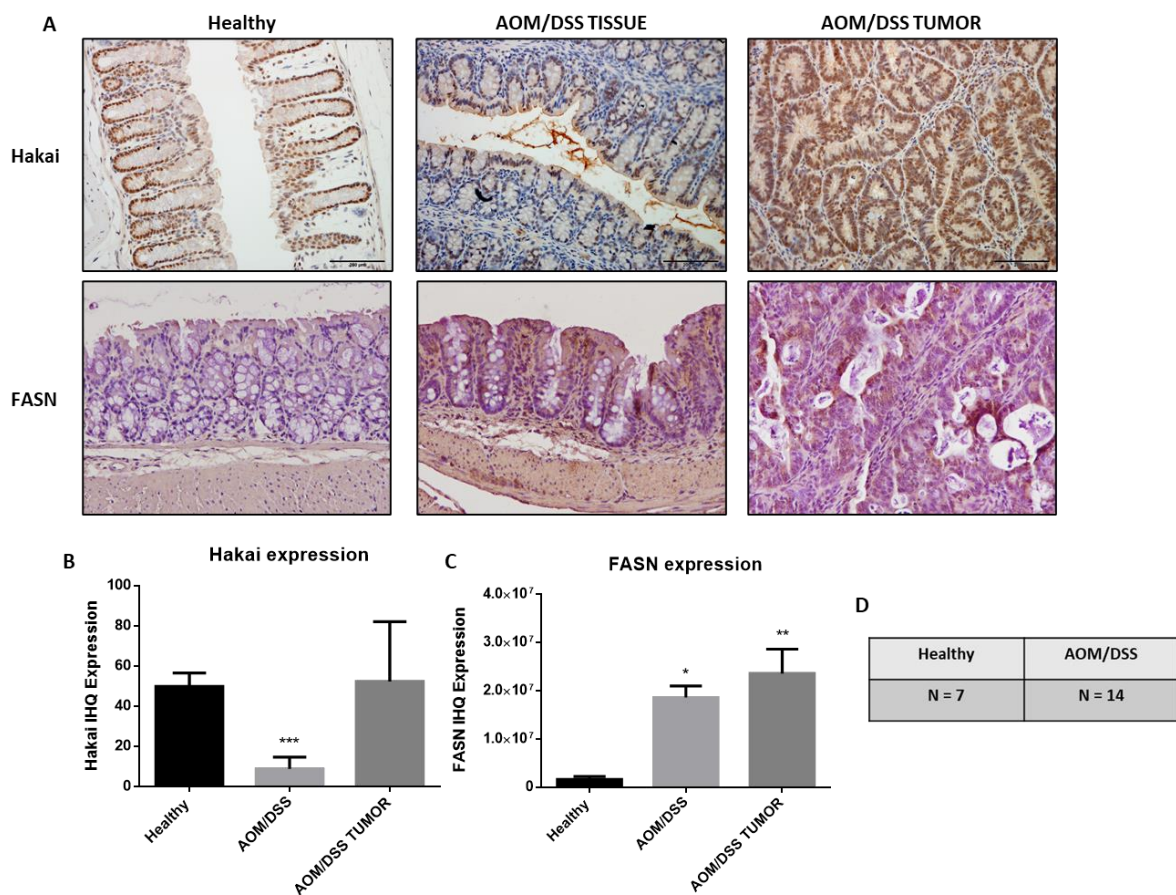


Figure 37. Expression of Hakai and FASN in mouse samples of the AOM/DSS Colitis-associated colorectal cancer model. **A**, Immunohistochemistry staining of Hakai and FASN in healthy non-treated mouse colonic mucosa and in gut sections of AOM/DSS-treated mouse (inflamed epithelium and tumours). Images obtained with 20x objective. Scale bar 125 μ m. **B**, **C**, Quantification of the staining intensity of Hakai and FASN in epithelial cells from healthy non-treated mouse colonic mucosa and gut sections of AOM/DSS-treated mouse (inflamed

epithelium and tumours). Five pictures of each sample were taken and quantified. Data are represented as bar chart. Values are means \pm SEM of staining intensity signal scoring per area. Quantification and calibration of the images were performed with Immunohistochemistry (IHC) Image Analysis Toolbox software for Image J. Kruskal-Wallis with Tukey correction test analyses show statistical differences in inflamed tissue and tumours respect to paired healthy samples (* $p < 0.05$; ** $p < 0,01$; *** $p < 0,001$). **D**, Number of mice included in the study, (Healthy mice, $n = 7$; AOM/DSS-treated mice, $n = 14$).

Discussion: Chapter I

IBD is a chronic inflammatory condition that affects the gastrointestinal tract, and it comprises two main clinical entities: Crohn's disease (CD) and ulcerative colitis (UC) (De Souza & Fiocchi, 2016). It is a disease that is closely linked to CRC, and in fact, its presence is associated with an increased risk of developing colorectal cancer (Yalchin et al., 2021). Both CD and UC are complex diseases that involve a great interrelation between the immune system, the intestinal microbiota, and multiple environmental factors. However, recently, a significant number of publications have begun to highlight the importance of protein ubiquitination in IBD (Cleynen et al., 2014; Weng et al., 2019). Ubiquitin is a highly conserved protein expressed in most of the tissues of the human body whose major function is to selectively label proteins for degradation.

The loss of the integrity and functionality of the intestinal epithelial barrier is a common element both in the development of CRC and in the origin of IBD (Genua et al., 2021). In this sense, intercellular junctions play a fundamental role in maintaining this structure. One of the key proteins within these intercellular junctions is E-cadherin, whose expression is vital for the homeostasis of the intestinal epithelium (Schneider et al., 2010). Specifically, its dysregulation is associated with a greater risk of developing IBD (Daulagala et al., 2019; Zbar et al., 2004) and its role as a tumour suppressor in CRC has also been described since its loss is associated with tumour progression (Christou et al., 2017; Peri et al., 1998).

The E3 ubiquitin-ligase Hakai, was the first described post-translational regulator of the stability of the E-cadherin protein (Fujita et al., 2002). This E3 ubiquitin-ligase mediates ubiquitination and degradation of E-cadherin, causing its disappearance from cellular contacts, and therefore the alteration of the cellular unions. Hakai is overexpressed in colorectal cancer tissues compared to adjacent non-transformed tissues and plays a determining role in processes such as cell proliferation, migration or invasion, key elements in tumour progression (Rodríguez-Alonso et al., 2020). However, Hakai's potential role in the origin and development of IBD is still unknown.

In this study, we focused on determining in greater depth the role of Hakai in the tumour progression of CRC as well as its potential implication in IBD. For this,

immunohistochemical assays were performed in staging of CRC patients and in samples of patients with IBD as well as in different related animal models. In addition, a Hakai interactome was carried out in which FASN, a protein involved in lipid metabolism and whose dysregulation has been linked to IBD, was identified, and validated. Furthermore, we explored the possible mechanism by which this Hakai-mediated regulation of FASN takes place and its possible involvement in IBD.

In this work we have shown that Hakai expression is gradually increased in adenoma and in different TNM stages (I-IV) from colon adenocarcinomas compared to human colon healthy tissues. Interestingly, this regulation can be observed even in very early stages of carcinoma development as in benign colon adenoma samples, protein expression is statistically enhanced compared to normal tissues. This fact suggests that Hakai may not only be involved in the malignant progression of CRC but also at early stages of tumorigenesis acting over cell proliferation (Figuroa, Kotani, et al., 2009). Furthermore, we also analysed Hakai mRNA levels which revealed a significant increased expression in TNM stage III and IV compared to healthy tissues, suggesting that the transcriptional regulation of mRNA Hakai may be a late event during tumour progression. Altogether, our data propose Hakai as a potential novel biomarker for colon cancer progression. However, further investigations are required to elucidate whether Hakai expression could be correlated with patient survival and/or associated with poor outcome or other clinic-pathologic characteristics of colorectal cancer patients.

The great correlation between the expression levels of Hakai and the staging of the different patient samples, contrasts with the disadvantages that the need for an intestinal biopsy for its application entails (Mazouji et al., 2021). Therefore, it was proposed to replicate the results obtained with intestinal biopsies using serological samples instead. This type of approach has great advantages for the analysis of tumour biomarkers, mainly because of its minimal invasiveness and its repeatability (Alix-Panabières, 2020). From this serological samples, isolation and purification of exosomes was carried out, from which RNA was then extracted for analysis by RT-qPCR to evaluate the expression levels of Hakai. Unfortunately, we were not able to obtain conclusive results from this approach as the levels of RNA extracted from the exosomes were too low. Precisely, the methodological constraints of this technique and the low amount of

circulating tumour cells as well as circulating tumour DNA and RNA are some of the main limitations of liquid biopsy and one of the reasons why the technique is not yet a standard tool in the clinical oncologist's arsenal (Vacante et al., 2020). An even greater number of clinical trials are necessary for this type of technique to become a fast, reliable, and non-invasive decision-making tool (Alix-Panabières, 2020).

We also evaluated the expression of the epithelial marker E-cadherin and the mesenchymal marker N-Cadherin in the same patient samples from TNM stages (I-IV). The upregulation of N-cadherin followed by the downregulation of E-cadherin is the hallmark of EMT (Loh et al., 2019), a process in which epithelial cells acquire mesenchymal features and that in cancer is associated with tumour initiation, invasion, metastasis (Pastushenko & Blanpain, 2019). Our results corroborate the cadherin switch between E-cadherin and N-cadherin during colon cancer progression. Furthermore, it was also observed, as previously described, that the loss of E-cadherin coincides with the transition from well-differentiated adenoma to invasive carcinoma (Peri et al., 1998) and that this loss does not occur when adenoma samples are compared with adjacent healthy tissue samples (Berkhout et al., 2006). However, our results did not show significant differences in the expression of another of the substrates reported for Hakai, Cortactin, during the development of colon carcinoma (Mukherjee et al., 2012). Taken together, these data suggest that, as Hakai expression gradually increases during tumour progression, Hakai could be contributing to an invasive phenotype in colon adenocarcinoma by downregulating E-cadherin at early stages of tumour progression.

Since Hakai upregulation seemed to take place in very early stages of tumour development, we further extended our study of Hakai expression to samples for patients with IBD under the hypothesis that its expression could also be altered in this type of diseases associated with CRC development. Our study revealed that in IBD human biopsies, Hakai expression was significantly upregulated in ulcerative colitis and Crohn's disease compared to normal tissues. However, these levels of expression were not as high as the ones detected in TNM-stage IV colorectal adenocarcinoma tissues used as control. The data obtained lead us to hypothesize that Hakai may be implicated in the origin and/or development of preneoplastic inflammatory conditions like IBD. In order

to find out more about the possible role of Hakai in IBD, both animal and in vitro models were established with the aim of trying to establish a clear link between Hakai and IBD.

The analysis of Hakai expression in different IBD mice models showed that Hakai expression is downregulated in inflamed intestinal epithelium compared to healthy epithelium from control mice. Moreover, Hakai expression in tumour tissues from the AOM-DSS colitis-associated cancer mice model presented even higher expression of Hakai than the surrounding inflamed tissue. This downregulation of Hakai in the epithelium of IBD mice models was further confirmed by the analysis of microarray data regarding Hakai gene expression in AOM/DSS and IL-10 KO mouse models from NCBI's Gene Expression Omnibus (GEO) database (Tang et al., 2012).

These results are not according to the expression pattern observed in IBD human samples suggesting that Hakai regulation in mouse models does not accurately mimic human ulcerative colitis and Chron's disease. Despite the fact that mice models are used routinely for the study of the basic pathophysiological mechanisms of multiple diseases, there are important controversies about how faithful murine models are as a reflection of human inflammatory diseases (Junhee Seok et al., 2013; Takao & Miyakawa, 2015). This idea is supported by Seok et al., who in his study show that despite the similar genomic responses to different acute inflammatory stresses in humans, these similarities are not observed in mouse models. Multiple factors can be responsible for the differences observed between the molecular responses of human and mice regarding to inflammatory diseases including the evolutionary distance and the differences in cellular composition between mice and humans as well as the complexity of the human disease (Cabrera et al., 2006; Davis, 2008; Hayday & Peakman, 2008; Mestas & Hughes, 2004).

In addition, in the present study we identified the Fatty Acid Synthase (FASN) as a novel Hakai-interacting protein in the search for possible Hakai targets associated with the IBD. FASN is responsible for the biosynthesis of long-chain fatty acids and its overexpression has been associated with the development of IBD (Matsuo et al., 2014). In fact, the abnormalities in fatty acid metabolism have been reported in IBD, and are considered as one of the etiological factors for the development of this disease (Shores et al., 2011). Activation of FASN and fatty acid biosynthesis have been also closely related to

malignant transformation of normal tissues (Gansler et al., 1997; Shurbaji et al., 1996) and cancer cell survival, for which it has been considered a promising new target in antineoplastic therapy (Koundouros & Poulogiannis, 2020; Kuhajda et al., 1994). Our own results support these observations regarding to the regulation of FASN in IBD as we shown that FASN expression increases in the mucosa of AOM/DSS Colitis-Associated Cancer mouse model, measured by immunohistochemistry. In human IBD, multiple studies have also showed upregulated expression of FASN in the inflamed epithelium of these patients (Consolazio et al., 2006; Röhrig & Schulze, 2016); in CRC this upregulation also has been described (Rashid et al., 2011).

Our results showed that Hakai interacts with FASN by inducing its ubiquitination and degradation, therefore acting as a negative regulator of FASN-mediated fatty acid accumulation. By developing *in vitro* models of overexpression and silencing of Hakai in CRC cell lines, we showed that overexpression of Hakai induces degradation of FASN while its silencing causes an increase in FASN expression. This regulation of FASN expression led to the consequent regulation of fatty acid levels at the cellular level, as measured by oil-red staining. This could also be seen in the AOM/DSS Colitis-Associated Cancer mouse model where the downregulation of Hakai expression in inflamed intestinal epithelium is accompanied by an increase expression of FASN. Indeed, to the best of our knowledge, this would be the first description of a link between Hakai and IBD despite the fact several studies have already documented the role of Hakai in different cancers (Aparicio et al., 2012; M. Liu et al., 2018; Weng et al., 2019). Importantly, in the tumours developed by mice from the AOM/DSS Colitis-Associated Cancer model, a higher expression of FASN and Hakai was detected, further supporting the implication of both proteins in colon cancer. In fact, several studies support the hypothesis that, in tumour cells, fatty acid synthesis increased by FASN could be linked to proliferation. Additionally, FASN inhibitors have shown significant antitumor effect mainly inducing cell apoptosis (Kuhajda et al., 1994; Ellen S. Pizer et al., 2000). Therefore, our results open a research line to further investigate to what extent Hakai could be involved in tumour progression through FASN. Hakai is not the only E3-ubiquitin ligase that has been associated with the pathophysiology of IBD. RING finger protein 186 (RNF186) is highly expressed in colonic epithelia and regulates protein homeostasis and

intestinal inflammation. Knockout of RNF186 in mice increased intestinal barrier permeability, leading to an increased sensitivity to intestinal inflammation (Fujimoto et al., 2017). Accordingly, our results open the possibility to elucidate whether, in a similar manner, a decrease expression of Hakai in inflamed intestinal epithelia in mice may increase risk of IBD.

Nevertheless, other studies have presented different data regarding the role of FASN in IBD. Heimerl et al. in their analysis of gene expression profile in patients with ulcerative colitis, described that FASN expression was decreased compared to healthy individuals (Heimerl et al., 2006). FASN was also reported to play a crucial role in maintaining the homeostasis of intestinal barrier function, showing that loss of FASN in mouse intestine can initiate intestinal inflammation (Wei et al., 2012). In any case, intestinal homeostasis it's a very complex partnership between intestinal epithelium, host immune system and the microbiota depending on multiple factors that regulate their interaction. Multiple regulatory mechanisms are reported to maintain intestinal homeostasis, and several studies have shown how the alteration of these pathways may precipitate the IBD (Maloy & Powrie, 2011). Therefore, further studies are required in order to elucidate in which specific situation Hakai/FASN axis may contribute to intestinal homeostasis or inflammatory bowel disease, as well as to reveal additional molecules that may help to orchestrate this regulatory process.

In this study, we proved for first time that Hakai mediates degradation of FASN by ubiquitination, but previous studies have already shown an increased ubiquitination mediated proteolysis in colonic biopsy samples from patients with IBD (Cenac et al., 2007; Inoue et al., 2009; Xiao et al., 2020). In fact, Ring finger protein 183 (RNF183), another E3 ubiquitin ligase, have also been identified as an upregulated protein in inflamed IBD mucosa. This E3 ubiquitin ligase has been reported to mediate degradation of I κ B α , a transcriptional inhibitor of NF κ B, a transcription factor that plays a key role in regulating the immune response. This, leads to the activation of NF κ B-p65 in intestinal epithelial cells, further suggesting RNF183 role in NF- κ B pathway in intestinal inflammation (Yu et al., 2016). In a similar way, Hakai could also been implicated in the regulation of immune response as it has been recently associated to immune microenvironment regulation of periodontitis, a chronic inflammatory disease occurring

in periodontal that involves complex interactions between pathogens and immune reactions (Slots, 2017; X. Zhang et al., 2021). In this work, authors show that Hakai is an important regulator of TNF and other cytokines in the immune reaction that occurs in periodontitis. Given that TNF- α is a well-described inflammatory mediator, highly expressed in the inflamed intestines of CD and UC patients (Breese et al., 1994), it could be hypothesized that Hakai could be linked to TNF- α signalling pathway in IBD, but further studies would be needed to establish this relation.

In our effort to comprehend more about the mechanism of Hakai in IBD, we evaluated the effect of different inflammatory stimulus over Hakai expression with the objective of determining if any of them could be, at least in part, responsible for the regulation of Hakai in IBD. As we already present so far, Hakai is responsible for FASN degradation. At the same time, in the AOM/DSS Colitis-Associated Cancer mouse model Hakai is downregulated in epithelial inflamed tissue causing an upregulation of FASN, a protein that has been clearly associated with IBD and tumorigenesis. In this sense, our results show that IFN- γ , a cytokine involved in the regulation of nearly all immune and inflammatory responses (Ivashkiv, 2018), causes downregulation of Hakai *in vitro*. IFN- γ is increased in patients with active CD, and its circulating concentrations correlate with clinical disease activity (Tilg et al., 2002). Furthermore, it has been described that IFN- γ plays an indispensable role in the initiation of colitis, and drives IBD pathogenesis through vascular barrier disruption (R. Ito et al., 2006; Langer et al., 2019). Therefore, our data presents a link between IFN- γ /Hakai/FASN that opens the possibility to further explore the possible mechanism that would connect this axis that could be implicated in the origin and development of IBD. However, IFN- γ has also been reported to have a paradoxical effect on the pathogenesis of several chronic inflammatory disorders, including IBD (S. G. Zheng et al., 2019), and other studies contradict its overexpression in UC (Camoglio et al., 1998). Therefore, a further in-depth study would still be necessary to determine the possible mechanism that would link IFN- γ /Hakai/FASN.

Taken together all the results, we found that the E3 ubiquitin-ligase Hakai increases ubiquitination and degradation of FASN, thereby resulting in the regulation of FASN-mediated lipid accumulation, which is associated to the development of IBD. This mechanism is observed in the AOM/DSS Colitis-Associated Cancer mouse model where

Hakai is downregulated causing an upregulation of FASN. IFN- γ , key for IBD development, could be at least in part responsible for this Hakai downregulation but further studies are needed to deepen into the role of Hakai in IBD in mice models and human biopsies in order to better understand the regulatory mechanism and pathways that may influence intestinal homeostasis and its breakdown in IBD.

Conclusions: Chapter I

1. Hakai expression gradually increased in adenoma and I to IV TNM stages of colorectal adenocarcinoma compared to healthy colon tissues, being a potential novel biomarker for colon cancer progression.
2. FASN is a novel Hakai-interacting protein related to IBD.
3. Hakai regulates FASN ubiquitination and degradation via lysosome, impacting on FASN-mediated lipid accumulation.
4. IFN- γ downregulates Hakai expression *in vitro* and increases FASN expression.
5. Hakai expression is downregulated in inflammatory tissues in different mice models.
6. FASN and Hakai are inversely expressed in inflammatory AOM/DSS mice model.
7. Hakai expression is upregulated in inflamed tissue from UC and CD patients compared to adjacent healthy tissue.

CHAPTER II

Introduction: Chapter II

1. Fungal extracts with antitumor effect in colorectal cancer: general characteristics

Fungi are organisms that belong to the Fungi kingdom, an independent kingdom distinct from both animals and plants. It was differentiated from the latter in 1969 by Robert Whittaker (Whittaker, 1969) based on three basic principles:

- They are non-photosynthetic organisms.
- They feed on nutrients produced by other organisms.
- They differ from plants in their body structures, their methods of reproduction, and their cellular composition.

It is a very wide kingdom with an enormous diversity, it is estimated that there are around 2.2 to 3.8 million fungal species on Earth, of which only about 120,000 have been described (David L. Hawksworth & Lücking, 2017).

Fungi are eukaryotic organisms, generally plurinucleate, whose reproduction can be both sexual and asexual. They are heterotrophic organisms that usually feed by absorption, generally releasing digestive enzymes to the exterior to later absorb the products of digestion.

Five different phyla, each of which includes very different species, make up Fungi kingdom (**Figure 38**): Basidiomycota, Ascomycota, Zygomycota, Chytridiomycota and Glomeromycota (Naranjo-Ortiz & Gabaldón, 2019).

- Basidiomycota includes macroscopic fungi with fruiting bodies visible to the naked eye, to which belong the fungi included in this study.
- Ascomycota is made up by great diversity of fungal species among which stands out the *Penicillium* from which Penicillin was obtained, classical yeasts like *Saccharomyces cerevisiae* or the truffles.
- Zygomycota includes the typical bread mold present on the surfaces of breads, fruits, and vegetables.
- Chytridiomycota is formed by the most simple and primitive fungi. The vast majority are saprophytes.

- Glomeromycota was previously included inside Zygomycota but recently has become an independent phylum. They are characterized by being plant symbiotes forming mycorrhizae.

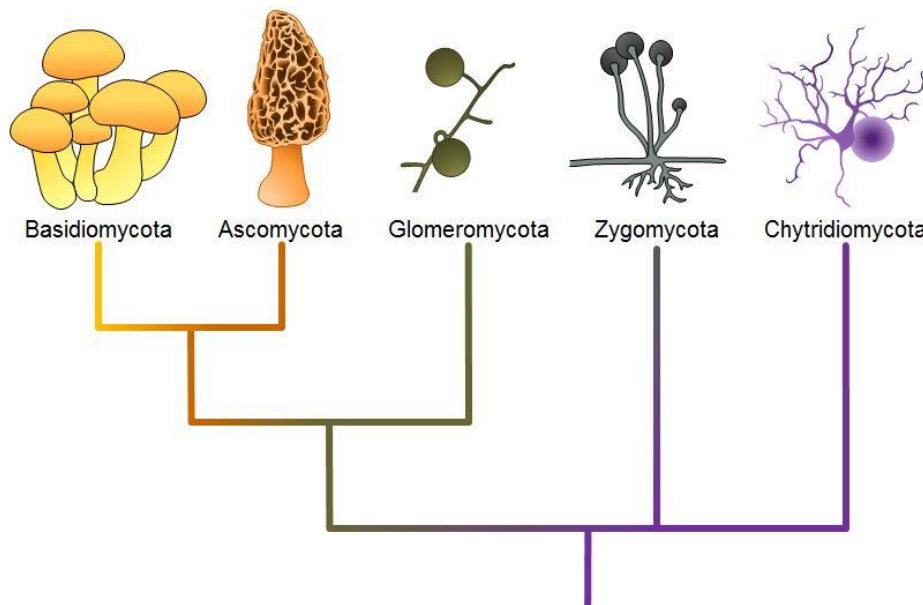


Figure 38. Schematic representation of the five phyla of fungi: Chytridiomycota (Chytrids), the Zygomycota (conjugated fungi), the Ascomycota (sac fungi), the Basidiomycota (club fungi) and Glomeromycota. Source: https://s3.amazonaws.com/microsite-cuny-prod/media/courseware/openstax/m66559/Figure_B24_02_01.jpg.

Fungi are of great importance for man in a wide variety of areas. From an environmental point of view, fungi are organisms of vital importance for the proper functioning of all ecosystems. They are responsible (along with certain bacteria) for the decomposition of organic matter, they play an important role in maintaining the trophic cycle of dead plants and animals (D. L. Hawksworth, 1991) and are essential for maintaining the quality of soils (Perry et al., 1989). At the forest level, some mycorrhizal fungi are used to stimulate the development of plants as well as for the production of fungi of high commercial value such as truffles. Others are appreciated for being enzyme-producing species that are used in different industrial processes, as well as others for helping to control certain pests (Fickers et al., 2005) (Dara et al., 2019). In addition, there are mycorrhizal fungi that are capable of establishing associations with plant roots, which are often necessary for the life of certain plants.

Regarding its relationship with man, there is evidence that proves that the Fungi kingdom has been linked to man since its earliest times, beginning in prehistory, where men already used mushrooms that they collected from nature as food, continuing with the first civilizations of ancient Greece, the Egyptians and the Romans (Abdel-Azeem, 2010). The first settlers in China and Mexico also considered mushrooms as elements of precious value, for their flavours, their therapeutic properties and sometimes for their importance in certain religious rites (Stamets & Zwickey, 2014).

In our days, some species have a high recognition in the gastronomic world, as a result of their appreciated aromas and flavours, while others are used as ingredients or food, yeast from bread dough, fermenters of wine and beer production, cheese ripeners, etc. There are also species that are especially important for their ability to synthesize antibiotics and hormones used in medicine (Fleming, 1929)(COOK & LACEY, 1945), while others are becoming increasingly interesting, due to their functional composition and the therapeutic activities they possess (Sahu et al., 2020). Therefore, Fungi have been of vital importance throughout the years for human progress due to their numerous applications and properties. Among them, it is worth mentioning their medical properties, which will be explained in detail in the following sections.

Of all the phyla that make up the Fungi kingdom, this thesis will be focused on the study of Basidiomycetes and its antitumor effect *in vitro*. Basidiomycetes are the most studied group of fungi in terms of obtaining bioactive compounds.

2. General medical properties of Fungi

Since immemorial time, mushrooms have been used by humans not only as food but also as medicinal agents. Proof of this is the long tradition of the use of mushrooms as therapeutic agents in medicine in eastern countries (China, Japan and Korea, mainly). In addition, mushrooms are currently receiving increasing interest in western societies for their medicinal properties, which in turn is translating into an increasing variety of products obtained from different species of mushrooms that help improve the health status (Chaturvedi et al., 2018; M. Jayachandran et al., 2017).

Of the 120,000 known fungal species, approximately 700 are considered to have medicinal properties. On the contrary, the number of those catalogued as poisonous is 500 species (Wasser, 2011). In addition, it is estimated that medicinal mushrooms are capable of causing many medicinal actions, among which we can find anti-tumour, immunomodulatory, cardiovascular, antibacterial, antiviral, antifungal, antiparasitic, antioxidant, free radical scavenger, anti-hypercholesteraemic, hepatoprotective, antidiabetic, detoxifying and anti-inflammatory drugs (**Figure 39**) (Chaturvedi et al., 2018). The vast majority, if not all species of basidiomycete fungi, are believed to contain biologically active polysaccharides in their fruiting bodies, in their cultured mycelia, and in their culture media (Q. Wang et al., 2017).



Figure 39. Schematic illustration of therapeutic applications of medicinal mushrooms. Source: (Chaturvedi et al., 2018)

The medicinal fungi belonging to the Basidiomycota phylum, therefore, represent an abundant source of natural products with biological activities of interest that are still largely unexploited (Sivanandhan et al., 2017). Of all the fungal species with medicinal properties, only a few have been studied. The most studied species are *Ganoderma lucidum*, *Schizophyllum commune* and *Trametes versicolor* within the inedible species and *Flammulina velutipes*, *Grifola frondosa*, *Hericium erinaceus*, *Lentinus edodes*, *Pleurotus spp.* and *Tremella spp.* within edible species (Elisashvili, 2012).

The therapeutic properties of these fungi are due to several of their cellular compounds, as well as to certain secondary metabolites present in the fruiting bodies, mycelia and their culture media. These metabolites can be very varied in nature: polysaccharides, proteins, complexes formed by both or low molecular weight metabolites such as phenolic compounds, triterpenoids, polyketides, lactones, alkaloids, fatty acids and nucleotides (Lindequist et al., 2005).

Medicinal mushrooms are attracting increasing interest in terms of their cultivation, consumption and study of their bioactive components, to the point that several of their derivatives are at the gates of clinical trials while others are already in the development phase for a future commercialization (Hoeksma et al., 2019; Saxena et al., 2019).

Among the species traditionally considered to be the most useful from the medicinal point of view as well as their therapeutic effects are:

- *Ganoderma lucidum*, commonly known as lingzhi, reishi, or mannentake, has been used for over 4,000 years to promote health and longevity in traditional Chinese medicine (J. Zhang et al., 2010). The pharmacological potential of *G. lucidum* is due to the fact that it has more than 400 bioactive compounds that give it a wide variety of pharmacological effects. It is the most studied medicinal mushroom and numerous products obtained from it have been the subject of clinical trials and are currently available (Cao et al., 2018).
- *Lentinula edodes*, is popularly known in China as xiang gu, and in Japan and more and more places in the world (Europe, America...) as shiitake. Traditional oriental medicine has used this fungus to treat a wide variety of ailments. One of the most important polysaccharides in fungi from a therapeutic point of view, Lentinan was extracted from this fungus. It was isolated in 1970 (Chihara et al., 1970) and exhibits potent antitumor activity, derived from its ability to enhance immune responses. This has led to the fact that, at present, this compound is frequently used as an adjuvant, in chemotherapy in certain cancer patients to help improve their immune response (M. Zhang et al., 2019).

- *Hericium erinaceus*, also known as "lion's mane" by traditional Chinese medicine, this species of mushroom has been used for centuries for its regulatory effect on the human body and psyche. Recently, its being intensively studied in terms of its primary and secondary metabolites and their possible medicinal use. One of the most important is the Erinacine A, which has been shown to possess neuroprotective activities such as the stimulation of nerve growth factor (NGF) synthesis. In addition to its effects on the nervous system, different extracts obtained from this fungus have been shown to have anticancer applications through different mechanisms such as apoptosis, angiogenesis, arrest of the cell cycle or cell migration processes (Blagodatski et al., 2018).
- *Inonotus obliquus*, known as "Chaga" or the "gift from heaven" of Siberian shamans, it is long known in Russia, China, Korea and Japan for its medicinal substances. The body of research regarding this fungus is focused on its anticancer potential both *in vivo* and *in vitro*. *Inonotus obliquus* extracts showed to their effect against colorectal and hepatocellular cancer through regulation of different pathways as Wnt and NF-κB affecting the mechanism of action of apoptosis, immunostimulant and growth arrest (Blagodatski et al., 2018).

In the same way, different compounds have been isolated from other fungi with varied medicinal properties. For example, cordycepin, a compound with antibiotic activity, isolated from *Cordyceps sinensis* (Cunningham et al., 1950), or polysaccharide peptide (PSP) and polysaccharide K (PSK), isolated from the fungus *Trametes versicolor* that have anticancer properties and are currently used as adjuvants combined with chemotherapy or radiotherapy for the clinical treatment of cancer patients (Zhong et al., 2019).

Historically, the study of the medicinal properties of fungi has been limited almost exclusively to Asia, where multiple species and strains have been described. In our case, we will work with native strains of Galicia, which despite belonging to the same species as other fungi studied in Asia, have differences at a phylogenetic level that could affect their composition and properties. Among the autochthonous strains studied are:

Pleurotus ostreatus, *Ganoderma lucidum*, *Trametes versicolor*, *Grifola frondosa*, *Polyporus umbellatus*, *Hericium erinaceus* and *Cordyceps militaris*.

3. Functional composition of Fungi

The population's concern for their state of health is increasing, and this is reflected not only in the follow-up of a balanced diet, but also in the search for functional foods, which contribute to obtaining and preserving an optimal state of health and well-being (Venkatakrisnan et al., 2019). Moreover, public health-related organizations are also constantly looking for strategies to improve eating habits and thus, improve the general global state against chronic diseases such as obesity, atherosclerosis, hypertension, osteoporosis, diabetes and cancer (Locke et al., 2018).

The growing importance of functional foods in today's society has contributed to promoting scientific research on new biologically active natural components for the prevention and treatment of various diseases. Some species of fungi have been shown to contain numerous bioactive substances without presenting any type of health toxicity, which characterizes them as functional foods (Valverde et al., 2015). These substances are described below (**Figure 40**).

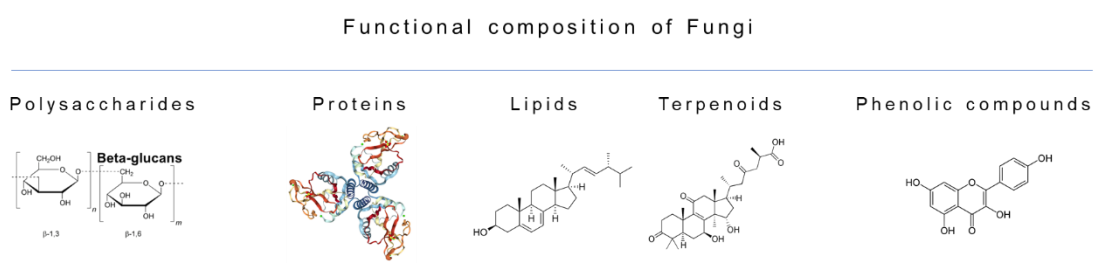


Figure 40. Scheme of the different compounds found in mushrooms with beneficial health properties. Source: Own elaboration

Polysaccharides:

Many of the beneficial health properties of mushrooms are due to their polysaccharide composition. More specifically, in the presence of chitin, β -glucans, β -mannans and

hetero-polysaccharides. The biological activity of polysaccharides, mainly in the last decades, has attracted the attention of the scientific community specially because of their biological effects as immunomodulating and anti-tumour agents.

Undoubtedly, the most studied polysaccharides are the beta-glucans, because of their ability to modulate the immune system. These compounds act through various mechanisms such as induction of haematopoiesis, activation of the cytokine system, inhibition of tumour cell growth and induction of resistance to viral and bacterial infections (Sima et al., 2014).

Among the functional polysaccharides of edible fungi, undoubtedly the most studied are 4: Lentinan, from *L. edodes*; Schizophyllan from *S. commune*; Grifolan, from *G. frondosa* and *Sclerotinia sclerotiorum* glucan (SSG), from *S. sclerotium*. The main reason why they have been studied so much is because of their anti-tumour activity. They are also of special importance for the treatment of certain cancers not only because of their anticancer effects but because of their adjuvant potential of proven efficacy for classic treatments (chemotherapy, radiotherapy, immunotherapy, etc.) (H. Wang et al., 2017) (Rossi et al., 2018).

Proteins:

Different proteins with immunomodulatory as well as antineoplastic activity have been isolated from different species of fungi. We can distinguish various classes of proteins with biological activities such as fungal immunomodulatory proteins (FIPs), glycoproteins, non-glycosylated proteins, peptides, etc.

Numerous glycoprotein complexes have been shown to have immunomodulatory activity as well as anticancer properties. However, mainly two from *T. versicolor* stand out for their demonstrated anticancer activity, both *in vitro* and *in vivo*, and in human trials: Polysaccharide-K (PSK) and Polysaccharide-Peptide (PSP) (Saleh et al., 2017). It has been shown that both are associated with lower risks of mortality when used as an adjunct therapy with chemotherapy and radiotherapy and increased levels of immunoglobulins like CD3. They have been included in several cancer therapies of patients with colorectal cancer, hepatocellular cancer or non-small cell lung cancer, among others, as well as in different phase III clinical trials (Zhong et al., 2019).

Lectins are a type of non-immune proteins that have the ability to bind cells. They are abundant in fruits, vegetables and legumes, as well as fungi. They possess a large number of functional properties such as mitogenic, antiproliferative, or immunostimulant (Coelho et al., 2017).

As for the fungal immunomodulating proteins (FIPs) some of them have been isolated from different species of fungi. They have been shown to have mitogenic and activating effects *in vitro*, on human peripheral blood lymphocytes (hPBLs), thus stimulating the production of cytokines such as IL-2, IFN- γ , and TNF- α . In addition, it has been shown that these proteins are also capable of acting as immunosuppressive agents (W. Y. Chen et al., 2018).

Lipids:

Some components of lipid origin also have functional properties. This is the case of ergosterol and ergosterol peroxide, and certain fatty acids that have anti-tumour, antioxidative, anti-inflammatory and immunosuppressive properties. Ergosterol is a component which is only found in mushrooms. It is present at the cell membranes of yeasts and fungi and it has the same functions as cholesterol in animal cells (Weete et al., 2010). Ergosterol, besides being the precursor of vitamin D2 (ergocalciferol), has proven to have anti-tumour and anti-angiogenesis activity over human lung, breast, and hepatocellular carcinoma. In the last decade, its role in cancer prevention and immune system modulation through blockade of NF- κ B and Mitogen-Activated Protein Kinases (MAPK) signalling pathways has also been described (Shaodan Chen et al., 2017).

Terpenoids:

Many terpenoids are found in plants, marine organisms, and fungi. However, triterpenoids, which have medicinal properties, have only been isolated from fungi. In this regard, one of the most studied fungi is *Ganoderma lucidum*. Studies carried out with triterpenoids isolated from this species have revealed that they possess anti-infective, cytotoxic and immunomodulatory activities. The Ganoderic acid A (GA-A) purified from a methanolic extract from the mycelium of *G. lucidum* was found to have an antineoplastic effect over MDA-MB-231 human breast cancer cells via inhibition of Janus kinase 2 (JAK2) and signal transducer and activator of transcription 3 (STAT3)

signalling pathway (Y. Yang et al., 2018). In the same way, Ganoderic acid DM (GA-DM), induces autophagic apoptosis in non-small cell lung cancer cells by inhibiting the PI3K/Akt/mTOR activity (Xia et al., 2020). Over colorectal cancer, Ganoderic acid D (GA-D) was able to inhibit the energy reprogramming (glucose uptake, lactate production, pyruvate and acetyl-coenzyme production) of colon cancer cells through the regulation of Sirtuin 3 (SIRT3) expression (Zhendong Liu et al., 2018).

Phenolic compounds:

Phenolic compounds are present in a wide variety of living organisms, but especially in plants, because in them they exercise a wide range of responses to genetic and environmental factors.

The phenolic content of fungi is mainly, but not exclusively, of phenolic acids, since there are also other classes of phenolic compounds depending on the species analysed. For example, flavonoids are also present in fungi but represent the least common phenolic compounds in mushrooms (Guo et al., 2012).

Biological activities of phenolic compounds from plants have traditionally been well studied so that their effects are well defined: antioxidants, antibacterial, antiviral, anti-inflammatory, or anticancer. Regarding the anticancer activity of flavonoids isolated from plants, they showed, for example, the induction of apoptosis through activation of caspase-9, caspase-3 and poly ADP Ribose polymers (PARP) cleavage as well as inhibition of nuclear transcription factor NF- κ B and STAT signalling pathway in human leukaemia HL-60 cells (Tanase et al., 2019). The study of these compounds in fungi is much more recent, still, its biological effects are evident. One of the most studied properties is its antioxidant activity, both for its direct beneficial implications on health, as well as for the positive influence on certain chronic diseases, in whose pathogenesis involves the action of free radicals such as heart and brain ischemia, diabetes, arteriosclerosis, rheumatoid arthritis, inflammation and even in the onset of certain types of cancers, as well as in the aging process. This antioxidant activity is due to the fact that these isolated compounds present radical scavenging activities in a dose-dependent manner (Hwang et al., 2016).

In addition to antioxidant activity, the phenolic compounds present in fungi have other less studied effects such as antimicrobial, anticancer, hepatoprotective, and anti-inflammatory effects. Recent studies have evaluated the use of these compounds in the treatment of lung cancer, where the flavonoid kaempferol, has shown to inhibit TGF- β 1-induced EMT and cell migration by recovering the loss of E-cadherin and suppressing the induction of mesenchymal markers as well as the upregulation of matrix metalloproteinase-2 activity. The mechanism is regulated by kaempferol through the inhibition of RAC-alpha serine/threonine-protein kinase (Akt1)-mediated phosphorylation of Smad3 at Thr179 residue, which is vital for its binding to Snail promoter (Muller et al., 2019)(Jo et al., 2015). It also has been studied the combination of these compounds with established treatments for hepatocellular carcinoma like Sorafenib over hepatic cancer cells. This concomitant treatment showed to trigger cell cycle arrest and apoptosis by downregulation of cyclins A, B2 and D1 as well as phosphorylated retinoblastoma and upregulation of Bcl-2, cleaved caspase-3 and cleaved caspase-9 (Bahman et al., 2018).

4. Antitumoral activity of Fungi

Antitumoral properties of fungi were first described in 1957 from extracts of fruiting bodies of *Boletus edulis* and other *Homobasidiomycetes* over sarcoma in mice (BYERRUM et al., 1957). Since then, fungi belonging to a wide variety of species, as well as extracts obtained from them, have been shown to possess antitumoral effects.

There are extracts of fungi that exert their antitumor activity through a single mechanism of action, such as extracts rich in β -glucans, obtained from *Coriolus Versicolor*, whose antitumor activity is due to its immunomodulatory effects. These, include enhanced dendritic and T-cell infiltration into tumours as well as increased expression of cytokines and chemokines such as tumour necrosis factor- α (TNF- α), interleukins like IL-1 β and IL-6, histamine, and prostaglandin E (Chang et al., 2017), or an extract obtained from *Cerrena unicolor*, which exerted its antitumor activity, inhibiting the proliferation of human colon cancer cells HT-29 measured by MTT and inducing apoptosis (Matuszewska et al., 2019).

In contrast, other extracts have more than one mechanism of action. For example, an extract from *Ganoderma lucidum* spores does not only exert its anticancer activity through cytotoxicity mechanisms, like cell cycle arrest, apoptosis or migration inhibition, but also via different ways of immune enhancement (Su et al., 2018). The same pattern could be seen in the extract from *Penicillium sclerotiorum* that showed activation of mitochondrial apoptosis along with both antioxidant and anti-angiogenic properties over cervical cancer cells (Kuriakose et al., 2018).

On the other hand, certain extracts show antitumor activity against a certain cell line, such as some of the extracts obtained from *Botryosphaeria rhodina*, which proved to increase mRNA expression of p53, p27 and induce apoptosis mediated by AMP-activated protein-kinase (AMPK) and transcription factor, FOXO3a in MCF7 breast cancer cell line (Queiroz et al., 2015). Others, such as the organic extract of the *Phellinus baumii* mycelium, has shown to exert a potent inhibition on cell proliferation of different cancer cell lines (i.e. K562, L1210, SW620, HepG2, LNCaP, and MCF-7) (Henan Zhang et al., 2017).

Currently, various compounds with antitumor activity of different nature have been identified: polysaccharides, proteins, steroids, glycopeptides and other protein complexes, alkaloids, phenolic compounds, etc. Among all of them, polysaccharides, especially β -glucans, which have been identified as the main responsible for this effect, stand out clearly. These compounds are capable of inhibiting tumour growth through two pathways: stimulation of the immune system, specifically the innate system, increasing the activity of macrophages, NK cells or T lymphocytes *in vivo* (Shuping Chen et al., 2020) and *in vitro* (Jang et al., 2016; C. C. Lu et al., 2016), and through direct action on the tumour cells themselves, since they are capable of inhibiting their proliferation and inducing apoptosis through the action over PI3K/Akt/mTOR, NF- κ B, and p53-dependent pathways (**Figure 41**) (Xu et al., 2017). This makes them effective against a broad spectrum of cancer cell lines. Zymosan is a β -Glucan derived from *Saccharomyces cerevisiae* which has shown to inhibit the progression of melanoma in mice by reducing tumour size and increasing lymphocyte and macrophage proliferation. This was associated with upregulation of TLR-2, TLR-4 and TNF- α (Taghavi et al., 2018).

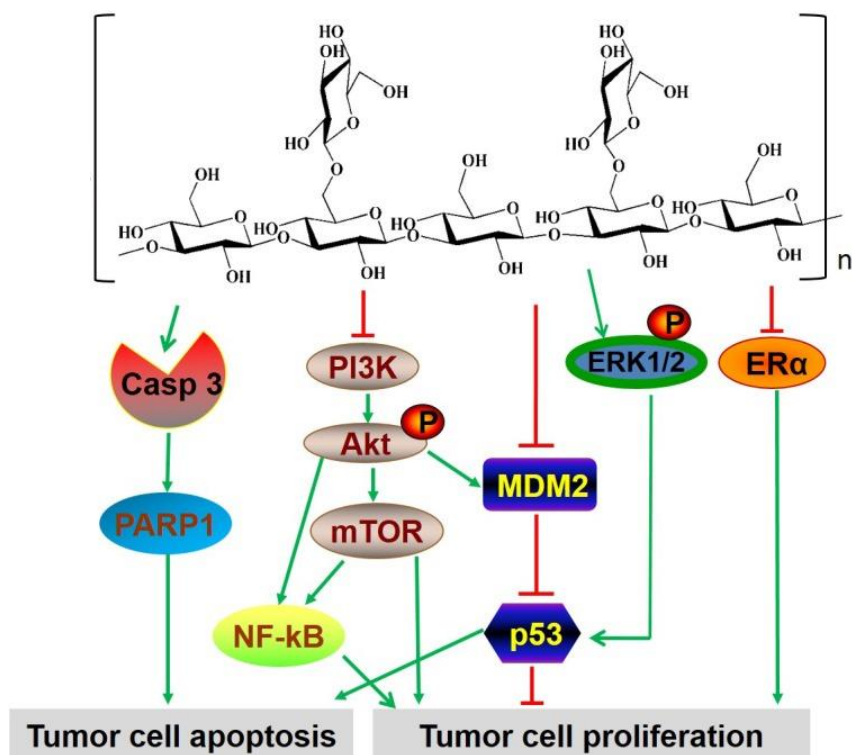


Figure 41. Multiple signalling pathways possibly involved in the anti-tumoral effect of β -glucans isolated from fungi. β -glucans control tumour cells apoptosis and proliferation by promoting and inhibiting different cellular pathways. Source: (Xu et al., 2017)

Others, such as the polysaccharides extracted from *Cerrena unicolor* show antitumor effects on MDA-MB-231 and MCF-7 breast carcinoma cell lines and PC3 prostatic carcinoma cells. This antitumor effect relies on different mechanisms that include, cell cycle arrest (G1 phase) by activating p53 and inhibition of STAT-3 phosphorylation, both related with induction of autophagy and apoptosis (Liang et al., 2019). Finally, purified *Phellinus linteus* proteoglycan has a broader range of action by exerting antiproliferative effects on different cells lines. In human colon (HT-29) and liver (HepG2), treatment with *Phellinus linteus* purified polysaccharides inhibited tumour growth in mouse models through P27kip1-mediated cell cycle arrest. In breast cancer (Mcf-7) the extracts showed to increase PARP cleavage and decrease the expression of Bcl-2. Furthermore, in lung cancer cell lines (NCI-H 460) the same treatment affected the migratory and invasive potential of cells through suppression of the enzymatic activity of MMP-2 and MMP-9, decreasing focal adhesion kinase (FAK)/paxillin,

influencing EMT/Snail and Slug, and affecting the NF- κ B and Nrf2 signalling pathways (W. Chen et al., 2019).

Other compounds of a non-glucidic nature also have antitumor activity. Ganoderic acids DM (GA-DM) and A (GA-A), extracted from species of the genus *Ganoderma*, have demonstrated antitumor effects over human breast cancer cells and non-small cell lung cancer cells. Ganoderic acid DM induced autophagy by inactivating the PI3K/Akt/mTOR pathway in lung cancer cell line A549 at the same time that increased apoptosis by decreasing protein expression levels of Bcl-2 and increasing expression levels of Bax, cleaved caspase-3 and cleaved PARP (Figure 42). In turn, Ganoderic acid A also showed to enhance reactive oxygen species production and the apoptotic index via inhibition of JAK2 phosphorylation and STAT3 downstream activation (Xia et al., 2020; Y. Yang et al., 2018). In fact, many other ganoderic acids (A, C2, D, F, DM, X and Y) are currently at different stages of clinical trials due to their immunomodulatory and antitumor activities (Liang et al., 2019).

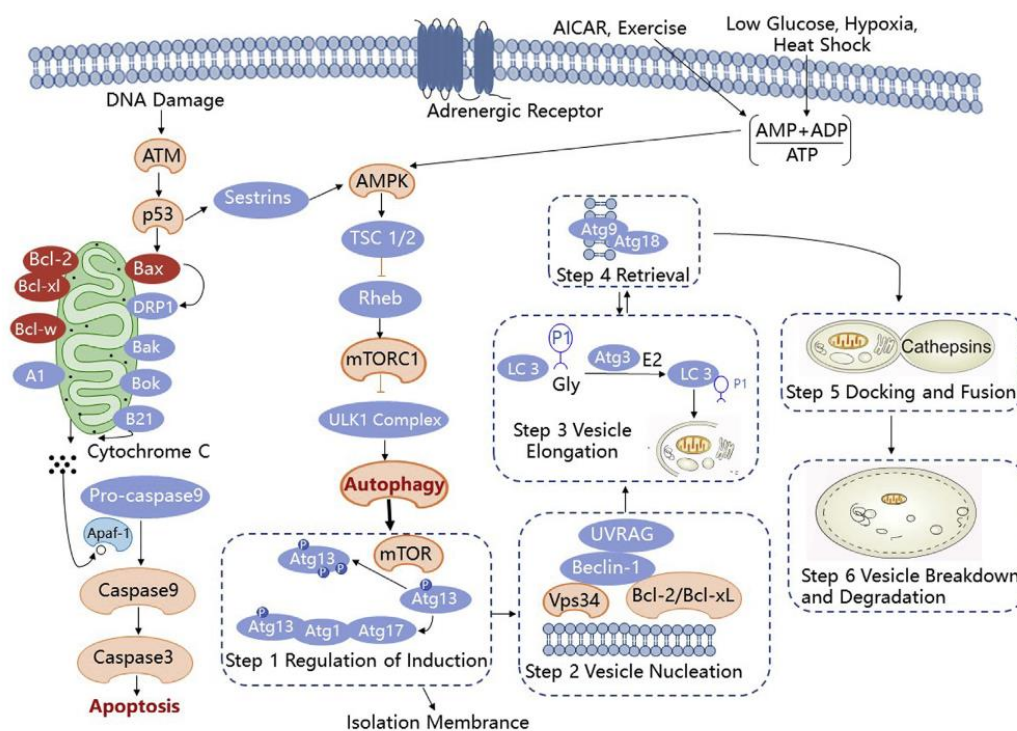


Figure 42. Crosstalk among signal transduction pathways in which Ganoderic acids participates in autophagy and apoptosis. Ganoderic acid induces cell cycle arrest (G1 phase) by activating p53. Simultaneously, autophagy was induced by Ganoderic acid via p53 and the downstream AMPK pathway. Source: (Liang et al., 2019)

The peptide α -amanitin obtained from *Amanita phalloides* has been proposed as a potential new targeted therapy in chemo resistant colorectal cancer. The mechanism consists of the conjugation of α -amanitin with an epithelial cell adhesion molecule (EpCAM) antibody. This fact reduces the original toxicity of α -amanitin and allows it to target specifically p53 deficient CRC cells where the α -amanitin will inhibit the catalytic subunit of RNA polymerase II complex (POLR2A) leading to cell death (**Figure 43**). Treatment with these α -amanitin conjugates led to complete tumour regression in

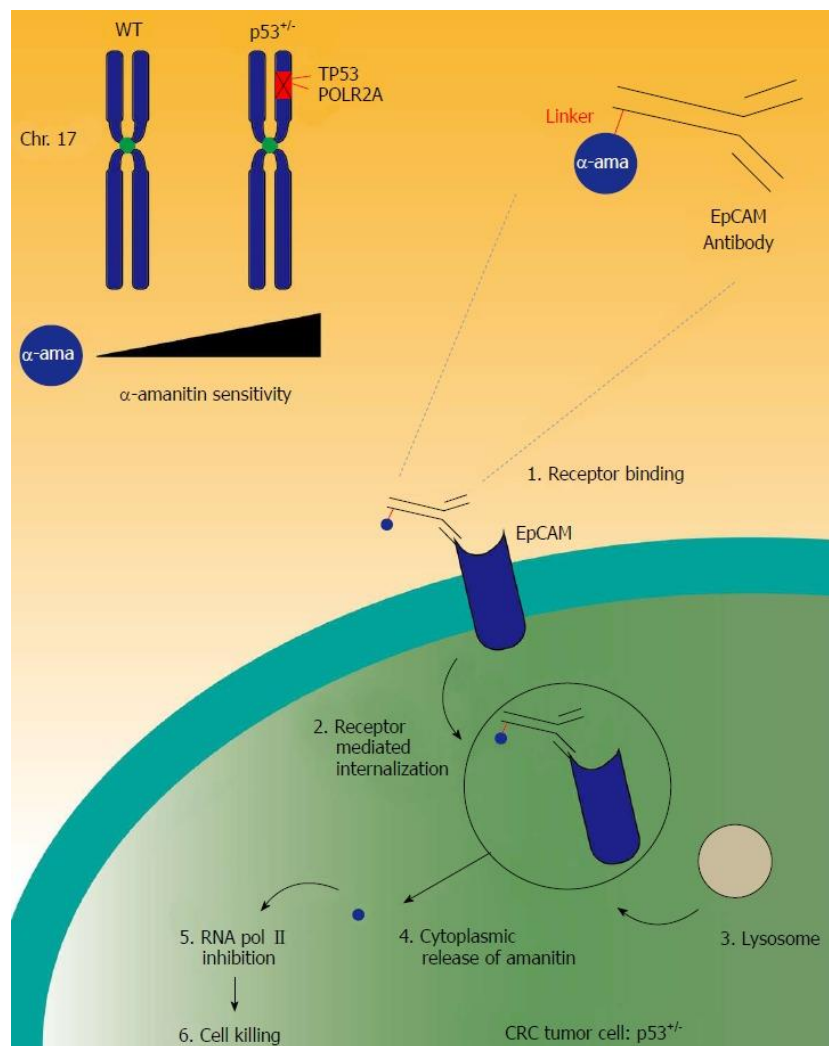


Figure 43. Working model of α -amanitin antibody-drug conjugates. α -amanitin is conjugated with an EpCAM antibody to increase its specificity and reduce global toxicity. Source: (Van Der Jeught et al., 2018)

murine models of human CRC with hemizygous deletion of POLR2A (Van Der Jeught et al., 2018). The coenzyme Q0 (COQ0), from *Antrodia cinnamomea*, is effective in reducing

the viability of the A549, HepG2, and SW480 cancer cell lines, as a function of dose and time, by inducing apoptosis (Chung et al., 2014). The terpenoid Erinacine A obtained from an ethanol extract of *Hericium erinaceus* was able to promote the inhibition of cell migration and proliferation as well as the induction of apoptosis through the up-regulation of the PI3K/mTOR/p70S6K pathway and the production of ROS in colorectal cell lines DLD-1 and HCT-116 (Lee et al., 2017). These effects were also visible *in vivo* over HCT-116 cells injected in nude mice.

Therefore, there is no doubt that fungi and the products derived from them, have a very great potential for cancer treatment. In fact, several pharmaceutical companies are already engaged in the production of anti-cancer drugs, as well as formulas and supplements for their prevention.

5. Antitumoral activity of the Basidiomycetes: *T. versicolor* and *G. frondosa*

The Basidiomycota division or "phylum" comprises three main groups or subdivisions: *Agaricomycotina*, *Ustilaginomycotina* and *Pucciniomycotina* (Moore et al., 2000).

- *Agaricomycotina*: This subdivision includes gelatinous fungi, basidiomycetic yeasts, including wood and mulch decomposers, and mycorrhizal species, along with a small number of plant or human pathogens.
- *Pucciniomycotina*: Approximately 90% of the subdivision is made up of rusts, obligate plant pathogens, but also includes parasites of insects and other fungi.
- *Ustilaginomycotina*: Includes parasitic species of plants.

Regarding its structure, basidiomycetes have two fundamental parts, the thallus or vegetative body and the carpophore or fruiting body.

- The thallus or vegetative body is made up of microscopic hyphae and their set is called the mycelium. These hyphae are covered by a cell wall composed mainly of a polysaccharide, chitin (although some groups have cellulose or other polysaccharides).
- The carpophore or fruiting body is what is commonly known as a "mushroom". It originates as a consequence of the differentiating growth and intertwining of

hyphae together with their rapid expansion caused by the absorption of water. Its purpose is to produce and disseminate spores, thus ensuring the survival of the fungus.

In the present study, we will be focusing in two fungal species belonging to the subdivision *Agaricomycotina*, *Trametes versicolor* from the order *Polyporales* and the family *Polyporaceae*, and *Grifola frondosa* from the order *Polyporales* and the family *Meripilaceae*.

5.1. *Trametes versicolor*

Trametes versicolor (Figure 44), belongs to the *Basidiomycetes* class and contains multiple bioactive substances such as polysaccharides, proteins, peptides, amino acids, glitter, terpenes, among others. Some of the pharmacologically active molecules are secondary metabolites belonging to small molecular weight compounds like flavonoid (flavones, flavonols, flavanone, flavanols, biflavonoids, isoflavonoids) and hydroxy cinnamic acids.



Figure 44. Picture of *Trametes versicolor*. Source: https://www.lifeder.com/wp-content/uploads/2019/08/Figura_1_Trametes_versicolor_a1_5.jpg

The main bioactive components of *Trametes versicolor* are polysaccharopeptides (PSPs). Of all of them, Polysaccharide Peptide (PSP) and Krestin or Polysaccharide-K (PSK) are the most biologically active components. The PSP polysaccharide is a β -glucan with a β - (1-3) -glucose structure with (1-6) - β -glucose branches. For its part, PSK is formed

by a main chain of beta-glucan β -1,4 with side chains of β -1,3 and β -1,6. D-glucose is the main monosaccharide, while arabinose and rhamnose are also present in its structure to a lesser extent (H. X. Wang et al., 1996). Interestingly, the molecular weight and the structures of PSK and PSP are different depending on the strain and are variable in different culture conditions (Santos Arteiro et al., 2012).

Important evidence highlights the effect of *Trametes versicolor* extracts over carcinogenesis.

From an immunomodulatory perspective, PSK acts as an agonist of Toll-like receptors, it specifically interacts with TLR2 and TLR4 mediated signalling pathways. For its part, PSP stimulates TLR4 expression and TRAF6, its downstream signalling molecule. PSP also increases the phosphorylation of the transcription factors NF- κ B p65 and c-Jun (Z. Wang et al., 2015). All these elements are related with the activation of the immune system and inducing the production of inflammatory cytokines, necessary for the activation of T lymphocytes by dendritic cells and macrophages.

PSP and PSK have also proven to induce proliferative response on blood lymphocytes, as well as an increase in mRNA expression of the proinflammatory cytokines TNF- α , IL-1 β and IL-6. (Pawlikowska et al., 2016). Other studies has also shown similar results about PSP and PSK treatment like the upregulation of MHC (class II and CD86) expression, the increase in monocytes counts (CD14+/CD16-) and the activation of NK cells to produce IFN- γ (Koido et al., 2013; H. Lu, Yang, Gad, Inatsuka, et al., 2011; Sekhon et al., 2013).

Besides its multiple effects on the immune system, these polysaccharopeptides have also been proven to exert their effect through direct toxicity to cancer cells. This cytotoxicity has been proven in various studies. For example, PSK is able to promote apoptosis by activation of caspase-3 and produce the phosphorylation of p38 MAPK, which participates in a signalling cascade involved in apoptosis and autophagy (Hirahara et al., 2013). Moreover, molecular characterization of PSP showed that it induces apoptosis mediating the upregulation of early transcription factors as AP-1, EGR1, IER2 and IER5 by phosphorylation and the downregulation of the cancer modulator pathway NF- κ B. This molecular characterization of PSP also proved that several apoptotic and

anti-proliferative genes such as GADD45A/B and TUSC2 had increased expression in HL-60 cells treated with PSP extracts, as well as affect the expression of carcinogenesis-related gene transcripts (SAT, DCT, Melan-A, uPA and cyclin E1) (Zeng et al., 2005). Other mechanisms described for the anticancer effect through direct toxicity include disruption of cell cycle progression and arrest at G0, G0/G1, G1/S and G2/M phases as well as inhibition of cell migration and invasion via inhibition of key angiogenic enzymes such as matrix metalloproteases (Luo et al., 2014; Ricciardi et al., 2017).

The effects of PSP and PSK from *Trametes versicolor* has been tested also in different animal models, showing promising effects. Apart from its antitumor effect by inhibition of tumour growth and spreading of the tumour (Chang et al., 2017)(Ko et al., 2017), PSP also showed to suppress angiogenesis through the downregulation of vascular endothelial cell growth factor (VEGF) expression (J. C. K. Ho et al., 2004).

Regarding the effect of the extracts over the immune system of animal models, PSP and PSK extracts from *Trametes versicolor* affect numerous signalling pathways involved in the activation of the immune system. For instance, PSK treatment increased number of activated dendritic cells (DC) in the lymph nodes and stimulated the proliferation of T-cells and their production of multiple cytokines (IFN- γ , IL-2, and TNF- α) (Engel et al., 2013). PSP was also responsible for the increase in natural killer cell, lymphocyte and granulocyte counts in blood and spleen from nude mice with glioma (X. W. Mao et al., 2001). Treatment with PSK increased docetaxel-induced suppression and apoptosis in prostate cancer tumours from a mice model, along with higher count of tumour-infiltrating CD4+ and CD8+ T cells and enhanced mRNA expression of IFN- γ (Wenner et al., 2012). The mechanism under this activation of the immune response in animal models could be mediated by the TLR4 and TLR2 pathways, inducing TNF α and IL-6 secretion (**Figure 45**) (H. Lu, Yang, Gad, Wenner, et al., 2011; Price et al., 2010).

Other *Trametes versicolor* extracts different from PSP and PSK, were also immunomodulatory active agents in animal models increasing IL-6 levels and inducing greater activation of NF- κ B signalling pathway. This fact led to higher production of pro-inflammatory cytokines and to consider these extracts as potential immunostimulant agents (Jędrzejewski et al., 2019).

Trametes versicolor extracts also showed to suppress cell proliferation by downregulating the phosphorylation of tumour suppressor protein Retinoblastoma (Rb), involved in cell cycle control, and increase Poly (ADP-ribose) polymerase (PARP) cleavage, a process of vital importance for apoptosis (Tze Chen Hsieh & Wu, 2013). In the same way, *Trametes versicolor* extracts were able to inhibit cell migration and invasion by suppressing the activity and expression of MMP-9 metalloproteinase (Luo et al., 2014). Other studies, proved that TV is able to upregulate the levels of transcription factors STAT1 and STAT3, mediators in the expression of various genes in response to certain cellular stimuli and thus plays an important role in a multitude of cellular processes such as cell proliferation and apoptosis (T. C. Hsieh & Wu, 2001).

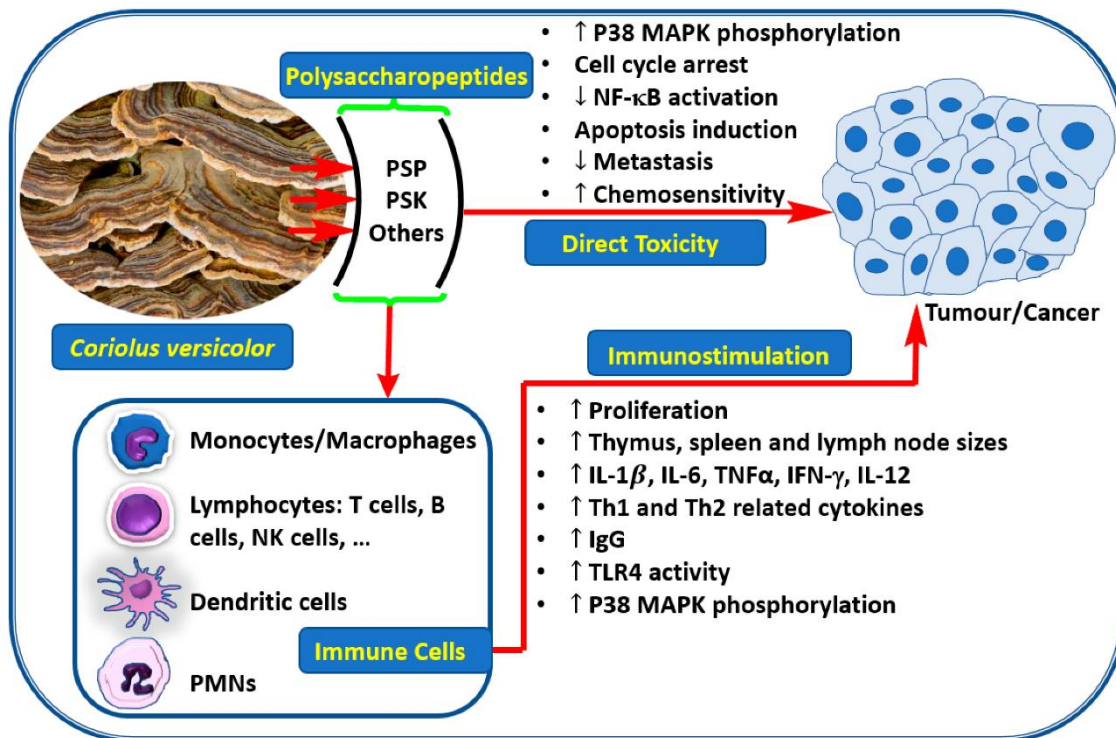


Figure 45. Antitumoral molecular mechanisms of PSP, PSK and other extracts from *Trametes versicolor*. Polysaccharopeptides as PSP and PSK exert its antitumoral effect through both direct toxicity over cancer cells and stimulation of the immune system. Source: (Habtemariam, 2020)

In breast cancer, *Trametes versicolor* extract inhibited cell proliferation through β -estradiol degradation and cell apoptosis. The mRNA levels of anti-apoptotic genes BCL-2 and NF- κ β were decreased while an increase in the mRNA levels of proapoptotic gene p53 was detected (Chauhan et al., 2019). These results are in line with the ones

obtained using an orthotopic animal model of triple-negative human breast cancer, where other extracts from *Trametes versicolor* had the potential to downregulate the expression of PLAU - urokinase-type plasminogen activator (uPA protein), a protein that plays a major role in tumour progression and metastasis as its activation initiates a series of proteolytic cascade to degrade the components of the extracellular matrix; and CXCR4 a receptor that through multiple pathways regulates cell adhesion, survival, and proliferation (J. Jiang et al., 2012).

Many efforts have been made to bring all these promising results into treating real patients. A significant number of studies have reached this goal. Some of them are included in the systematic review and meta-analysis of Eliza et al. (Eliza et al., 2012) where they evaluated the survival rates in cancer patients from 13 different clinical trials on *Trametes versicolor*. They reported strong results showing a significant increase in survival rates when compared with conventional anti-cancer agents alone. Specifically, a reduction of 9% in 5-year mortality was notified, which means one additional patient alive for every 11 patients treated. This improvement in the 5-year survival rate in patients receiving combination treatment was documented in cases of breast cancer, gastric cancer, and colorectal cancer. Another systematic review and meta-analysis of randomized controlled trials from Zhong et al. (Zhong et al., 2019) proved that *Trametes versicolor* extracts were significantly associated with a lower risk of mortality and had a positive impact elevating levels of CD3 and CD4. The effect of *Trametes versicolor* extracts over the immune system observed *in vitro* and in animal models was also observed in patients. Peripheral blood mononuclear cells (PBMCs) isolated from breast cancer patients treated with PSP showed upregulation of the TLR4-TIRAP/MAL-MyD88 pathway genes and proteins as well as higher levels of IL-12, IL-6, and TNF- α levels (J. Wang et al., 2013). Finally, a comprehensive study of gastric cancer involving 349 patients reported that the use of PSK as adjuvant immunotherapy greatly improved the 3-year recurrence-free survival (RFS) rates in MHC class I-negative patients (G. Ito et al., 2012).

At the moment, according to database ClinicalTrials.gov there is two completed clinical trials on the effects of *Trametes versicolor*, one for unresectable hepatocellular carcinoma in phase II with 20 patients and another one for stage I, II, or III breast cancer

in phase I with 11 participants. Results from both studies remain unpublished. (Habtemariam, 2020).

5.2. *Grifola frondosa*

Grifola frondosa contains a deep variety of bioactive substances like polysaccharides, peptides, amino acids, fatty acids, vitamins, terpenes, triterpenes and low molecular weight (LMW) molecules (sesquiterpenes, triacylglycerols, isoflavones, etc.). From all of them, increasing evidence show that polysaccharides, specifically β -glucans have direct actions on tumour cells. β -glucans are formed by a backbone of β -1,3-linked β -D-glucopyranosyl units with β -1,6-linked side chains with a variety of distributions and lengths.

Regarding their immunomodulatory properties, orally administration of β -glucans from *Grifola frondosa* activated macrophages and Dendritic Cells (DCs), functionally defective in tumour-bearing patients, which induced T helper (Th) cells and cytotoxic T cells to inhibit tumour cell growth (Masuda et al., 2013). In this line, a phase I/II trial of a polysaccharide extract from *Grifola frondosa* in breast cancer patients also showed higher production of proinflammatory cytokines including IL-2, IL-10, TNF- α , and IFN- γ by subsets of T cells (Rossi et al., 2018).

The activation of macrophages was further described by Hou et al., who showed that this activation by *Grifola frondosa* extracts was due to its effect over TLR4, an upstream regulator of MyD88-IKK β -NF- κ B p65 pathway (Hou et al., 2017). *Grifola frondosa* extracts upregulated TLR4 expression, resulting in nuclear translocation of NF- κ B p65 subunit increasing nitric oxide and cytokine production.

Other mechanism of action described for β -glucans from *Grifola frondosa* is their anticancer functions through the regulation of different tumoral pathways. For example, it has been described that extracts from *Grifola frondosa* are able to induce apoptosis in breast cancer cells by activation of pro-apoptotic genes like BAK1, BCLAF1, RASSF2, FADD, SPARC, and BCL2L13 (Soares et al., 2011). The same authors also documented the downregulation of PI3K-AKT signalling pathway under treatment with the same extract (Figure 46). Other studies report similar results and prove that the effects over cell

growth arrest, cell differentiation, and apoptotic pathways are caused by an increased expression of p27 (Alonso et al., 2013).

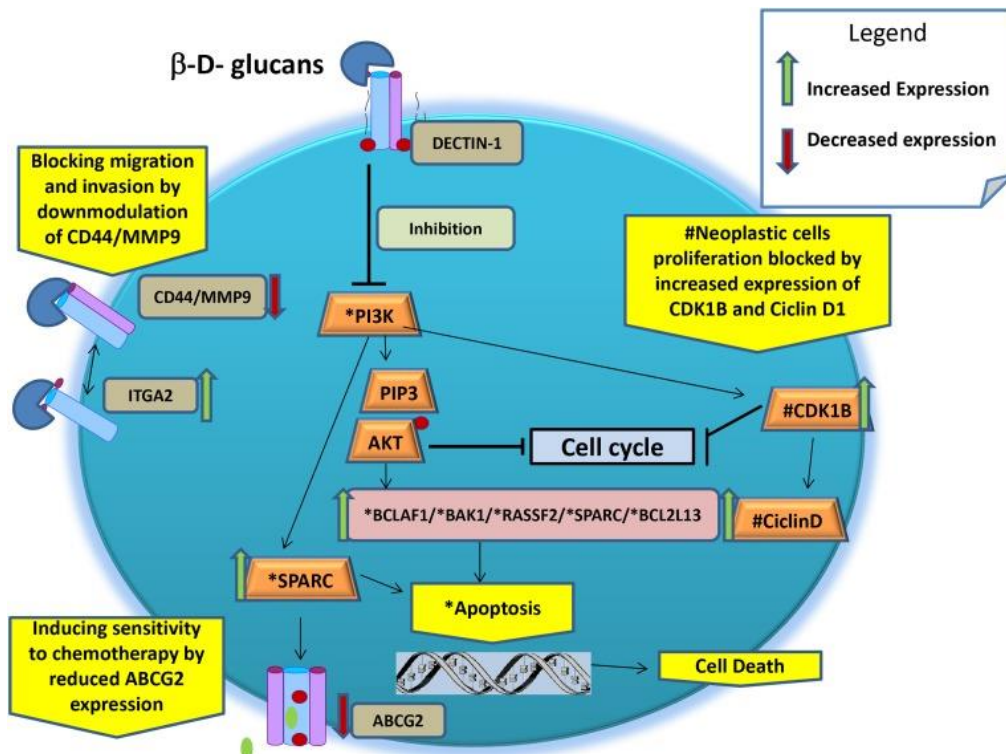


Figure 46. Antitumoral molecular mechanisms of β -glucans from *Grifola frondosa*. Cell death through apoptosis is favoured by β -glucans via PI3K-AKT inhibition and cell cycle arrest. Source: (Rossi et al., 2018)

The anticancer effects of *Grifola frondosa* extracts were also associated with the regulation of cell viability and the apoptotic rate by overexpression of Bax, cleaved caspase-3 and caspase-8 along with lower levels of B-cell lymphoma 2 (Bcl-2) and Bcl-extra large (Bcl-xL) in MCF-7 cells (Y. Zhang et al., 2017). These results were further confirmed in an MCF-7 tumour xenograft model, suggesting the use of *Grifola frondosa* as a potential treatment for breast cancer.

Besides these effects of direct toxicity over cancer cells, *Grifola frondosa* extracts exhibited a marked effect over different mechanisms implicated in metastases. Treatment of breast cancer cells with the extracts decreased their migratory and invasive capabilities by increasing cell adhesion, measured by increased expression of epithelial marker E-Cadherin, and decreasing the number of filopodia and lamellipodia.

These effects were also supported by a downregulation of MMP-2 activity and a reduction of tumour burden and lung metastases in a murine model (Alonso et al., 2017).

Other types of cancer also seem to respond to treatment with β -glucan rich extracts from *Grifola frondosa*. Over Hepatocellular carcinoma (HCC), extracts showed to affect autophagy and apoptosis both *in vitro* and *in vivo*. Results revealed that autophagy was induced by the inhibition of phosphatidylinositol 3-kinase (PI3K) signalling pathway and the stimulation of c-Jun N-terminal kinase (JNK). In the case of apoptosis, extracts promoted cleavage of caspase-3 and -9 and increased the number of cells arrested in S phase (Lin et al., 2016).

The combined treatment of *Grifola frondosa* extracts together with anticancer drugs such as cisplatin or 5-fluoracil (5-Fu) has also reported beneficial effects. Among them, the ability of a *Grifola frondosa* polysaccharide extract to increase the antitumor effect of 5-Fu while improving the immune function of patients was described. A similar effect was observed when performing adjuvant therapy of cisplatin with a purified extract of glucans obtained from *Grifola frondosa*, which not only enhanced antitumor and antimetastatic activity, but also reduced cisplatin-induced myelotoxicity and nephrotoxicity (G. H. Mao et al., 2019; Masuda et al., 2009).

The transfer of all these scientific evidence on *Grifola frondosa* has not been carried out to the clinical practice to the same extent as in the case of *Trametes versicolor*, but some studies have been carried out with patients in phases I and II. A phase I/II study over 34 patients with breast cancer treated with a polysaccharide extract from *Grifola frondosa* reported an immunologically stimulatory effect in peripheral blood from patients (Deng et al., 2009). Another study with lung, liver, and breast tumours in cancer patients concluded that *Grifola frondosa* extracts repress cancer progression and primarily exerts its effect through stimulation of NK cell activity, they also reported the downregulation of tumoral markers expression and lower number of metastases (Kodama et al., 2003).

Regarding clinical trials using *Grifola frondosa* extracts, according to ClinicalTrials.gov there is one completed study with 480 patients suffering from lung and

breast carcinomas in which they monitored T-lymphocyte cell subsets concentrations after treatment with a *Grifola frondosa* extract; one recruiting study in colorectal cancer that estimates to enrol 144 participants and that will end in 2022 where among, other parameters, levels of TNF-alpha and interleukin-6 (IL-6) will be studied. Finally, although it's not a cancer-related clinical trial, there is another Israeli study, still recruiting, that will work with 100 patients to determine if extracts from *Grifola frondosa* could have an impact over different factors: clinical response and remission rates, quality of life, inflammatory markers or faecal microbiome composition and diversity.

Hypothesis and Objectives: Chapter II

As previously mentioned, fungal extracts represent a very important source of potential compounds with antitumor activity. On the other hand, despite the available studies, the mechanism by which fungal extracts exert their antitumoral effect is poorly understood. In particular, it is not well known how fungal extracts may affect the EMT process. The general hypothesis for this work would be:

- Fungal extracts from different autochthonous species from Galicia might have antitumor effect in CRC cells. This antitumoral effect could be exerted through EMT regulation, a key element for tumour progression and metastasis.

In order to investigate this hypothesis, in this study we set out to analyse the antitumoral potential of different species of autochthonous fungi from Galicia. For this purpose, the following specific objectives are proposed.

- **Objective 1-** To analyze the effect of different fungal extracts on colon cancer cell viability and proliferation.
- **Objective 2** – To select the most promising extracts for further studies.
- **Objective 3-** To determine the effect of selected extracts on the reversion of the EMT process, migration and invasion of colon cancer cells.
- **Objective 4-** To study the possible synergistic effect between the most clinical used agents for colorectal cancer, 5-fluorouracil, in combination with selected fungal extracts.

Materials and Methods: Chapter II

1. Material

Fruiting bodies from *Grifola frondosa* and *Trametes versicolor* were produced at Hifas da Terra S.L. plant and ground using industrial blenders. The resulting material was extracted with distilled water at a ratio of 1:12 (w/v) for *Grifola frondosa* and 1:10 (w/v) for *Trametes versicolor* at 80°C for 30 minutes and filtrated with Whatman No. 1 filter paper. The obtained residue was again extracted applying the same procedure and both filtrates where combined and lyophilized. *Grifola frondosa* extract presented a total Glucan content of 45 % (w/w), representing 10.20 % and 34.80 % of α -Glucans and β -glucans, respectively (w/w; β -Glucan Assay Kit Yeast & Mushroom, Megazyme). *Grifola frondosa* extract is present in several MicoSalud® products of Hifas da Terra S.L. *Trametes versicolor* extract presented a total Glucan content of 74.30 % (w/w); where α -Glucans and β -glucans represented 8.7 % and 65.60 % (w/w), respectively. *Trametes versicolor* extract is present in several MicoSalud® products of Hifas da Terra S.L., including Mico-Corio PSK®. Stock solutions of both extracts were re-suspended in distilled water at 50 mg/ml and stored at -20°C.

To determine which solvent and concentration were more suitable for storing and using these extracts we performed initial dilutions of the extracts in different compounds: Ethanol, Dimethyl sulfoxide (DMSO) and distilled water. Once we saw that the extracts could be dissolved in the 3 solvents that we tested we finally choose distilled water as it would be the less cytotoxic for its use in cell culture.

Then we went on to determine the best concentration to make the stock solutions for storage. We performed serial dilutions from 1 mg/ml to 100 mg/ml (1, 2, 5, 10, 20, 50, 75, 100 mg/ml) in order to find a concentration proximal to the saturated solution. We made this for two reasons, the first one because the more concentrated is the solution the best is going to maintain its properties when frozen. The second reason is that making a high concentrated stock solution would mean using less volume when treating the cells in culture and that would affect less the composition of the culture

media. We also made small aliquots of the stock solutions in order to avoid to many cycles of freeze-thawing cycles that could affect the effect of the extracts.

The extracts were received as lyophilized powder. Some of this powder was used to make the stock solutions as we previously described, and some part was kept in a dry atmosphere at room temperature to have some stock of the original extract in case the dilutions were less stable for long time storage.

Other extracts tested also included different fungal species like, *Pleorotus ostreatus*, *Ganoderma lucidum* and *Polypurus umbellatus*. These extracts were also produced by Hifas da Terra S.L. and stored as stock solutions at 50 mg/ml and kept at -20°C. A total of 8 extracts from 5 different fungal species were analysed in the first place and are indicated in (Table 11).

Table 11. List of species from which each extract was obtained.

Extract	Species
Extract 1	<i>Pleorotus ostreatus</i>
Extract 2	<i>Ganoderma lucidum</i>
Extract 3	<i>Ganoderma lucidum</i>
Extract 4	<i>Trametes versicolor</i>
Extract 5	<i>Ganoderma lucidum</i>
Extract 6	<i>Grifola frondosa</i>
Extract 7	<i>Ganoderma lucidum</i>
Extract 8	<i>Polypurus umbellatus</i>

The extracts with the codes: GL001H, GL001R, GL001S, GL001B, GL001M, GL001C, Extract A, Extract B, Extract C, Extract D, Extract E, HE 20-10, HE 20-20, HE 20-30, HE 100-10, HE 100-2.5 c, HE 00-0, HE 100-25 Q, HE 001-BR, CVA20 t05, CVA20 t10, CVA20 t20, CVA100 t01, CVA100 t03, CVA100 t05-25, CVA100 t05-6-RLS 6 and CVA00 t00, are all modifications of the original 8 extracts made by Hifas da Terra S.L. in order to test different parameters of their interest like the type of extraction, filtration, etc. We were not aware of the differences between each extract, and the specific

information about them was kept by the company. 5-Fluorouracil (5-Fu) was purchased from Sigma-Aldrich.

2. Cell lines

Human colon carcinoma LoVo and HT-29 cells from the American Type Culture Collection (ATCC) were grown with F-12K Medium (Kaighn's Modification of Ham's F-12 Medium) and McCoy's 5a Medium Modified, respectively. Madin-Darby Canine Kidney (MDCK) cells from ATCC were cultured in Dulbecco's Modified Eagle Medium (DMEM). Cells were supplemented with penicillin/streptomycin (50U/ml) (Thermo Fischer) and 10% heat-inactivated fetal bovine serum (FBS) (Thermo Fischer) and were grown in a humidified incubator at 37°C with 5% CO₂. All mediums were obtained from Thermo Fischer. Cells were authenticated with the StemElite ID system (Promega) and monthly tested for mycoplasma to ensure free-contamination cultures. Stock of viable cells was kept and restored in liquid nitrogen.

3. Mycoplasma test

Culture medium (1 mL) from 2-3 days was collected in a 1,5 mL tube (Eppendorf) from the plates to be tested. The tube was centrifuged for 5 minutes at 13000 g. Supernatant was removed and the pellet resuspended in 150 µl of 10 % Chelex 100 (Bio-Rad), a chelating material. Samples were then heated at 95°C in a thermoblock for 10 minutes and then cool down at room temperature for 15 minutes. A short spin should be given after this step to collect all condensation drops back to the bottom of the tube. After that the product is ready to be use for Polymerase chain reaction (PCR) as template DNA.

The PCR allows us to detect minimal amounts of a DNA fragment in a sample by using a specific DNA polymerase and primers against that fragment. These will act, under the right conditions, amplifying the number of copies of that fragment facilitating its detection in case it is found in the sample.

For PCR we used Taq DNA Polymerase Kit (Thermo Fischer). The mix prepared was indicated in **(Table 12)**

Table 12. List of components included in the mix for PCR.

10X Reaction Buffer	2.5 μ l
dNTP Mix, 2 mM	0.2 μ l
Forward primer 10 mM	1.25 μ l
Reverse primer 10 mM	1.25 μ l
25 mM MgCl₂	1.5 μ l
Template DNA	1.5 μ l
Taq DNA Polymerase	0.125 μ l
Nuclease free water	16.675 μ l

The sequences of the primers were:

- Forward primer (5'-3'): CGCCTGAGTAGTACGTTTCGC
- Reverse primer (5'-3'): GCGGTGTGTACAAGACCCGA

As positive control, a sample with positive PCR in a previous experiment was used. The negative control was H₂O.

The PCR program used is indicated as follow:

- Initial denaturation: 94 °C for 5 minutes
- Amplification (30 Cycles):
 - Denaturation: 94°C for 20s
 - Annealing: 58°C for 30s
 - Extension: 72°C for 60s
- Final extension: 72°C for 5 minutes

The final product of the PCR (10 μ l) was mixed with DNA loading buffer and finally loaded in a 1% agarose gel with SyBR Safe (Invitrogen). SyBR Safe is nucleic acid stain for visualization of DNA in agarose gels that emits green light (λ_{max} = 524 nm). The gel was run in an electrophoresis cuvette (Bio-Rad) for 30 min at 90V and then viewed using an imager (Amersham Imager 600, GE Healthcare). Presence of bands of 400 bp would mean a positive contamination with mycoplasma in the sample.

4. Cytotoxicity assay

For cytotoxicity assays, cells were trypsinized with 2X Trypsin (Thermo Fischer), counted by Neubauer Hemocytometry in a Neubauer chamber (Thermo Fischer) and 1×10^4 of them were plated per well into a 96-well plate and cultured during 24 h with normal growth medium. Then, cells were treated with 10, 50, 100, 250 or 1000 $\mu\text{g/ml}$ of the extracts from *Trametes versicolor* or *Grifola frondosa* for 24, 48 or 72 h, one plate for each time of study. The dilutions of the different treatments were made from the stock solutions in normal growth medium in 15mL High Clarity Polypropylene Centrifuge Tubes (Falcon). As the vehicle of the dilution was distilled water, no vehicle was added to the control wells as distilled water will not affect cell viability. Also, the low volume of treatment (20 μl of dilution per 1 ml of growth medium) added to the medium would have a negligible effect over its composition.

Once the dilutions were made, as the extracts were not prepared in sterile conditions, we filtrated them prior their use in cell culture to avoid contaminations. For that each dilution in 15mL Tube was transferred to a 10 mL syringe (BD) attached to a Millex-GP Filter, 0.22 μm (Millipore) and filtered into a new 15mL Tube.

Viability was measured by using an MTT [3-(4, 5-dimethylthiazol-2-yl)-2, 5-diphenyltetrazolium bromide] colorimetric cell viability assay kit (Sigma Aldrich, St Louis, MO). The MTT assay is a colorimetric assay for determining cell metabolic activity. The assay bases its function in the activity of the NAD(P)H-dependent cellular oxidoreductase enzymes that are able to reduce the tetrazolium dye MTT into a purple chromogenic insoluble product, formazan. This reaction takes place inside the mitochondria of the cells and the enzymes are only active in living cells. That is the reason why we can correlate the quantity of formazan generated in one well with the viability of its cells.

After each time of treatment cells were treated with 0.5 mg/ml of MTT for 3 hours. Then, medium was removed and 100 μl of Dimethyl sulfoxide (DMSO) was added to each well and shacked for 10-15 min. DMSO lysates the cells and dissolve the formazan salt into a uniform colour solution.

Absorbance was measured at 570 and 630 nm using a Multiskan Plus Reader (Thermo Fisher, MA, USA). Experiments were repeated at least three times and 6 wells were used for each treatment as replicates. The half-maximal inhibitory concentration (IC50) reflects the drug concentration that is needed for 50% inhibition in vitro. These values were calculated from dose-response curves constructed using GraphPad Prism software starting from the viability data obtained by the MTT assay. Specifically, a non-linear regression of dose-response (inhibition) was used for the adjustment of the values:

$$Y = 100 / (1 + 10^{((\text{LogIC50} - X) * \text{HillSlope}))})$$

Results are expressed as mean \pm S.D and as fold change compared to untreated cells.

Cytotoxicity assays were also used to study the effect of the fungal extracts in combination with other drugs like 5-fluorouracil (5-Fu). The combination of cytotoxic agents is nowadays a concept that seems unquestionable and necessary in the treatment of cancer, if we want to obtain a greater antitumor capacity with the minimum toxicity and avoid as far as possible the formation of resistance. 5-fluorouracil is an anticancer chemotherapy drug that works by inhibiting DNA synthesis. It is the cytostatic of choice in the first line of treatment in advanced colorectal cancer.

To study the effect of the combination of fungal extracts with 5-fluorouracil (5-Fu), cells were treated with different concentrations of 5-Fu (5, 10, 100 and 1000ng/ml), dissolved in fresh medium, and then mixed in combination with 250 μ g/ml of fungal extracts. After 72 h of incubation with extracts and 5-Fu, cells were treated with 0.5 mg/ml of MTT for 3 hours and cell viability was calculated as previously mentioned.

5. Sonication

For some fungal extracts with low solubility, sonication was needed to achieve the desired concentration. Sonication consists of the application of ultrasonic frequencies for different processes like dissolve or dilute compounds with low solubility.

In our case, water dilutions of the extracts were prepared previously to the processing with a probe sonicator for 30 minutes. After that, samples were freeze and stored as the rest of the samples.

6. Phase contrast microscopy

For phase-contrast images, 1×10^5 LoVo cells were plated per well in a 12-well plate and cultured for 24 h before treatment with 10 or 100 $\mu\text{g}/\text{ml}$ of *Trametes versicolor* or *Grifola frondosa* extracts for 48 h. Then, cells were fixed with 4% paraformaldehyde in phosphate-buffered saline (PBS) for 20 min. Phase-contrast images were acquired using Nikon Eclipse-Ti microscope with (100x) magnification.

7. Proliferation Assay

To study the regulation of the cell proliferation over fungal extract treatment we performed 5-bromo-2'-deoxyuridine (BrdU). BrdU assay is based on the incorporation of Bromodeoxyuridine, a synthetic nucleoside analogue of thymidine, this compound acts as a label that can be quantified by immunoassay using specific probes. BrdU incorporation into newly synthesized DNA was measured using a cell proliferation colorimetric immunoassay kit (Roche) according to the manufacturer's instructions.

For proliferation assays, 1×10^4 LoVo cells were counted and plated per well into a 96-well plate and after 24 h cells were treated with 10 or 100 $\mu\text{g}/\text{ml}$ of different fungal extracts during 48 h. Then, cells were treated with 10 mM Bromodeoxyuridine (BrdU) for 2 h in an incubator at 37°C, with 5% CO₂ and humidity to saturation.

After 2 h incubation medium was removed by suction. Then cells were fixated, and cellular DNA was denatured in one single step with 200 $\mu\text{l}/\text{well}$ of FixDenat reagent (Roche) for a 30 min incubation at room temperature. The FixDenat solution was then removed and 100 $\mu\text{l}/\text{well}$ anti-BrdU-POD (antibody anti-BrdU conjugated with peroxidase) was added to each well and incubated for 90 min at room temperature. When the incubation was finished the wells were washed 3 times with the washing solution. After removing the last washing step 100 $\mu\text{l}/\text{well}$ of 3,3',5,5'-

Tetramethylbenzidine (TMB) were added. TMB is the chromogenic substrate for the conjugated peroxidase of the antibody and the reaction could take between 5 and 30 min, the reaction should take place at room temperature until the colour development is sufficient for photometric detection. BrdU incorporation into DNA was finally measured using a plate reader Nano Quant Infinite M200 (Tecan) at 370 nm (reference wavelength: approx. 492 nm). Results are expressed as mean \pm S.D and fold change is represented compared to untreated cells.

8. Soft agar anchorage-independent cell growth

Soft agar colony formation assay is a method for assessing this capability *in vitro* and is one of the best tests for characterizing malignant transformation in cells. Anchorage-independent growth is the potential of tumoral cells to grow with independence of solid attachment, a hallmark of carcinogenesis. That is why in this assay we evaluate the ability of cells to grow in the absence of solid surface, seeding them in an agarose layer. Only cells with high oncogenic potential would be able to form colonies in these conditions. With this assay we wanted to evaluate the ability of the fungal extracts to reduce the oncogenic potential of colorectal cancer cell LoVo.

Previously to the initiation of the assay, we prepared the dilutions of the extracts in growth medium 10% FBS and filtered them as previously described. The dilutions were prepared 4X compared to the concentrations we wanted to evaluate as it would be needed for the development of the assay. It was also needed to make an aliquot of growth medium with 20% of FBS. For the agar preparation, a 1% agarose (Sigma Aldrich, St Louis, MO) dilution in distilled water was prepared and then autoclaved to maintain the sterility conditions required for its use posterior in cell culture.

The first day of the assay, agar 1% was warmed up until boiling in a microwave. Then this agar was mixed in a 1:1 dilution with growth medium 20% of FBS, and from that mixture 500 μ l were putted in each well of a 12-well plate. The plate was then left at room temperature in a laminar flow cabinet to cool down for 30 minutes in order to solidify the agar and form a layer over which we will seed the experiment. The remains

of the 1:1 mixture of agar and medium 20% FBS should be kept in a 37°C bath in order to maintain the mixture in a liquid state for its use later.

In this 30-minute gap, 5×10^3 LoVo were counted for each well and centrifuged for 5 min at 1500 g. Then, cells were diluted in 500 µl of a new mix containing 125 µl of the dilution with the correspondent extract and 375 µl of the 1:1 dilution of agar 1% and growth medium with 20% of FBS that we previously prepared. This 500 µl mix is a ¼ dilution of our extract dilution which was prepared at 4X for this reason. Cells were pipetted up and down several times, making sure all cells are well detached one from another so the colonies that may grow inside the agar are formed from solitary cells.

This final mix of 500 µl containing 0.375% low-melting agarose was layered over the 0.5% agarose layer we previously created in each well.

Finally, each well was allowed to solidify for another 30 minutes and subsequently covered with 150 µl culture media in presence or absence of the indicated fungal extracts (10, 100 or 250 µg/ml). Then the plate was transferred to the cell culture incubator. Fungal extracts were refreshed every 3 days. After 21 days, cells were fixed and stained with 0.2% crystal violet. Colonies were counted in Olympus microscope (magnification 40x), and whole wells were photographed. Experiments were repeated two times plated in triplicates. Results are expressed as mean \pm SD and fold change is represented compared to untreated cells.

9. Wound healing assay

The wound healing assay is a technique to study cell migration capacity. It is based on the observation of the behaviour of a confluent monolayer of cells that has previously had a gap or "wound". Cells at the edge of the gap will move into the opening to establish new cell-cell contacts, thus closing the "wound". Usually, this assay is made by performing a scratch on the cell monolayer and controlling its closure at different times. In our case we used a commercial Culture-Inserts Kit (Ibidi), which allowed us to perform this assay with more homogeneous and comparable conditions. The kit contains several silicone inserts with a defined cell-free gap and two spaces on each side to seed the cells.

Before starting with the experiment, it is necessary to determine which would be the ideal number of cells to be seeded cause is important that the cell confluence in the insert is very high to guaranty the good development of the assay. In this line, we prepared 3 inserts and seed them with 3 different numbers of cells (2.5×10^5 cells/ml, 5×10^5 cells/ml and 1×10^6 cells/ml) and confluence was checked after 24h under the microscope.

After we seeded the cells in the inserts the first day, we waited until the next day to detach the inserts from the wells. After that we monitored the closure of the gap different times to evaluate the migration capacity of the cells

Cells were seeded at a high density (7×10^5 cells/ml) in 24-well plates containing Culture-Inserts (Ibidi) and allowed to adhere overnight, the volume of medium inside each side of the insert was 70 μ l. Then, cells were treated for 2 h with 10 μ g/ml of mitomycin C and inserts were removed. The treatment with mitomycin C is needed in order to inhibit the proliferation of the cells and in that way, we assure that the closure of the gap is due to the migration of the cells and not because of its proliferation. Mitomycin C inhibits cell proliferation by producing the crosslinking of DNA, this is the formation of a covalent linking between two nucleotides of the same strand or from the opposite strand. These covalent bonds affect cellular metabolism, including DNA replication and transcription, blocking as a result the cell proliferation.

Cells were treated with 10 or 100 μ g/ml of fungal extracts and wound healing was maintained during 24, 48 and 72 h. Photographs were taken in Nikon Eclipse-Ti microscope (magnification 40x) at the indicated times. Quantification of the distance after cell migration was determined by using ImageJ program, using the MRI Wound Healing Tool (**Figure 47**) (*Wound Healing Tool - ImageJ-macros - MRI's Redmine.pdf*, n.d.). This software measures the free area of a wound in a cellular monolayer on a stack of pictures representing a time-series by automatically identifying the limit between the cell culture front and the plate. As many times the closure of the wound is not uniform all along the space, measure the space in between was not always exact when using traditional methods and was also very laborious. After learning how to use this software the process of quantifying the experiments was definitely much easier and faster and the accuracy of all the measurements was improved.

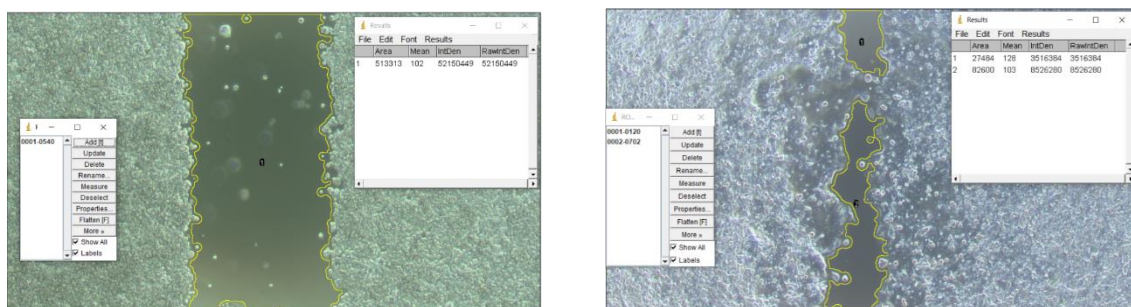


Figure 47. Representative image of how the Image J software automatically recognises the wound area. Experiments were repeated at least two times in replicates and results are expressed as mean \pm S.D and fold change is represented compared to untreated cells.

10. Invasion assay

Cell invasion is a process related to cell migration and it is defined by the capacity of cells to move through the extracellular matrix and degrade it. For evaluating this capacity that is characteristic of tumoral cells the QCMTM ECMatrix Cell Invasion Assay (Millipore) was used.

The bases of this technique are related to the Boyden chamber assay. This approach is based in the Chemotaxis, a process by which cells always move in favour to a concentration gradient of a chemo-attractant.

The kit uses plastic inserts designed to fit in the well of the plates, each insert has a polycarbonate membrane with a pore size of 8 μ m and a structure analogous to the extracellular matrix present in tissues in vivo (85% type I and 15% type III collagen). Only those cells with the ability to invade, will be able to pass through this membrane by degrading its structure. In order to encourage the cells to pass through this membrane a Fetal Bovine Serum (FBS) gradient was created between the upper part of the insert, where 1% FBS DMEM medium was used, and the lower part, where 30% DMEM was used, to favour cellular chemo-attraction.

For invasion assays, cells were cultured in DMEM medium with FBS 1% with the fungal extracts (10 or 100 μ g/ml) for 48 h. Then, LoVo cells were trypsinized, counted (3×10^5 cells/well) and seeded in a cell invasion chamber in a 24-well plate containing 8- μ m pore size polycarbonate membrane covered with a thin layer of extracellular matrix. Previously, the membrane of the insert was rehydrated with 300 μ l of prewarmed serum

free medium, that after 15 min was removed. In the bottom of the well 500 µl Ham's F-12K medium with FBS 30 % were added. Finally, the plate was covered and incubated at 37°C in a CO2 incubator.

After 72 h, medium was removed from the top of the insert by pipetting, and filters were fixed with ethanol 70% and stained with 0.1% Crystal violet solution for 20 min following the manufacturer's specifications. Finally, excess of Crystal violet was washed with PBS and inserts were dried for 30 min before mounting them in the slides for the microscope.

Cells were counted by photographing five-fields in an Olympus microscope (magnification 200x). Experiments were performed in triplicates for each condition and repeated at least two times. Results are expressed as mean ± S.D and fold induction is represented compared to untreated cells.

11. Western Blot, Immunofluorescence and RT-qPCR

Western blot assays, Immunofluorescence and RT-qPCR were performed as described in the first chapter of Material and Methods. For Western blot and Immunofluorescence, the corresponding antibodies are included in (**Table 13**). Primers used (Sigma) for RT-qPCR were designed for human as indicated in the following (**Table 14**). The cell line used for Western blot and Immunofluorescence was LoVo.

Table 13. List of references of all the antibodies used.

Antibody	Reference
E-cadherin	BD 610182
GAPDH	Invitrogen, 39-8600
N-cadherin	Abcam ab18203
Vimentin	Abcam ab137321
Cytokeratin 18	Santa Cruz sc-32329
p21	Santa Cruz sc-6246
Cdk2	Santa Cruz sc-6248
Tubulin	Sigma-Aldrich T9026
pRb	Santa Cruz sc-377528

Table 14. List of primers used for PCR and their sequences.

Gene	Forward primer (5'-3')	Reverse primer (5'-3')
MMP2	AGCGAGTGGATGCCGCCTTTAA	CATTCCAGGCATCTGCGATGAG
MMP9	GCCACTACTGTGCCTTTGAGTC	CCCTCAGAGAATCGCCAGTACT
ZEB1	GCACCTGAAGAGGACCAGAG	TGCATCTGGTGTTCATTTT
Snail	GGCGCACCTGCTCGGGGAGT	GCCGATTTCGCGCAGCA
Twist2	GGAGTCCGCAGTCTTACGA	TCTGGAGGACCTGGTAGAG
E-Cadherin	GCTGAGCTGGACAGGGAGGA	ATGGGGGCGTTGTCATTAC
HPRT	CATTATGCTGAGGATTTGGAAAGG	CTTGAGCACACAGAGGGCTACA
RPLP0	TGGTCATCCAGCAGGTGTTCTGA	ACAGACACTGGCAACATTGCGG

12. Gelatine zymography

Zymography is an electrophoretic technique that allow to observe the activity of hydrolytic enzymes. It is based in the capacity of the enzymes to degrade a certain substrate. This substrate would be included in the composition of the gel where the hydrolytic enzymes will be loaded. After that, the substrate would be degraded by the enzymes proportionally to its abundance. When the gel is stained for the original substrate, the areas of degradation would be visible as clear bands against the stained background.

Zymogram technique was used to detect matrix metalloproteinase 2 and 9 (MMP-2 and MMP-9) activity, by using gelatine as a substrate. 8×10^5 LoVo cells were seeded in 60 mm dishes and incubated with 100 or 250 $\mu\text{g}/\text{ml}$ of fungal extracts diluted in growth medium for 72h. The last 24 h, cells were grown in 1 ml of serum-free medium for starvation. Starvation of the cells is performed to synchronize all the cells to the same cell cycle phase removing therefore the impact that cell cycle will have on the cell's response to treatment.

Subsequently, medium was collected, centrifuged for 5 minutes at 2000 g and used for sample preparation, using cell number for normalization. Samples were prepared under non-reducing conditions, using loading buffer without β -

mercaptoethanol and without boiling. Non reducing agent or boiling are important conditions since these would interfere with refolding of the enzyme and therefore with its activity.

Samples were run at 60 V in a 10% SDS polyacrylamide gels containing gelatin (0.05%) and the composition is indicated as shown in (Table 15). The low voltage used for running the gel is in line with the use of non-reducing conditions, the reason for this is to prevent losing the three-dimensional structure of the enzyme and being able to recover its activity after the experiment.

Table 15. List of components used for the zymography gels and their volumes.

Reactive	Resolving gel 10%	Stacking gel
0.5M Tris-HCl pH 6.8	-	1.2 ml
1.5M Tris-HCl pH 8.8	5 ml	-
40% acrilamida/bisacrilamida (29:1)	4 ml	625 µl
10% SDS	200 µl	50 µl
Tetramethylethylenediamine (TEMED)	20 µl	5 µl
Ammonium persulfate (APS)	200 µl	50 µl
Gelatine 2%	300 µl	-
H ₂ O	10.5 ml	3.6 ml

After electrophoresis, SDS was removed from the gel by extensively washing in 2.5% Triton X-100. Two 30-minute washes were performed in agitation and a final wash in distilled H₂O was done. Metalloproteinase activity was reactivated by incubating the gel in a buffer containing 400 mM Tris-HCl pH 7,5; 0,1 M benzamidine (SIGMA) and 10 mM CaCl₂, for 72 h. The gel was stained with Coomassie Blue R250 in a 10% acetic acid, 50% methanol solution overnight, and then, distained in 10% acetic acid, 50% methanol, until bands were clearly visible. Protease activity appeared as clear bands against a blue background where MMP-2 or MMP-9 has digested gelatine substrate. Gels were photographed and quantified with Amersham Imager 600 equipment. Experiment was repeated three times and quantification is expressed as mean ± SD.

13. Statistical analysis

Statistical significance was determined with GraphPad Prism software applying ANOVA or Kruskal-Wallis test. Shapiro-Wilk test was used to check a normal distribution and Levene test to determine the equality of variances. Results are expressed as means \pm SD. Significance of the Student t-test among the experimental groups indicated in the figures is shown as * $p < 0.05$, ** $p < 0.01$ and *** $p < 0.001$.

Results: Chapter II

1. Screening of different fungal extracts from different species on the effect over viability of colorectal cancer cells

The fungal extracts evaluated in this study belong to five different fungal species, *Grifola frondosa* (GF), *Trametes versicolor* (TV), *Pleorotus ostreatus* (PO), *Ganoderma lucidum* (GL) and *Polypurus umbellatus* (PU). These extracts are rich in polysaccharides and could be an effective source of compounds with antitumoral activity as it has been described for fungal extracts from other species (Min et al., 2018) (Shnyreva et al., 2018). To evaluate the possible anticancer effect of these extracts we started by performing viability assays in colorectal cancer cell line LoVo. LoVo cell line was established from a metastasis derived from a stage IV colorectal adenocarcinoma.

MTT assay was used for the determination of the cytotoxic effect of the fungal extracts with the idea of making an initial screening of all the extracts and select those candidates with more potential for further molecular studies. For the first 8 extracts tested, different concentrations of the extracts (10, 50, 100, 250 µg/ml) and different times of treatment (24, 48 and 72 h) were evaluated.

In the graphs corresponding to a treatment time of 24 h (**Figure 48**), a visible effect of reducing cell viability can be seen in the case of two different extracts from *Ganoderma lucidum* (extracts 2 and 3) of up to 20- 25% at the point of highest concentration 250 µg/ml, although differences were not statistically significant. Other extracts such as *Pleorotus ostreatus* and *Trametes versicolor* (extracts 1 and 4) did not appear to have an appreciable effect after the first 24 hours of treatment.

After 48 h of treatment (**Figure 49**) all the extracts show some effect, either to a greater or lesser extent, on the viability of the tumour cells, in ranges that vary between 10 and 50% reduction in viability for the highest concentration points but still without reaching significance level. The pattern observed in the 24 h graphs with respect to the potency of each extract is also visible in the graphs obtained for the second period.

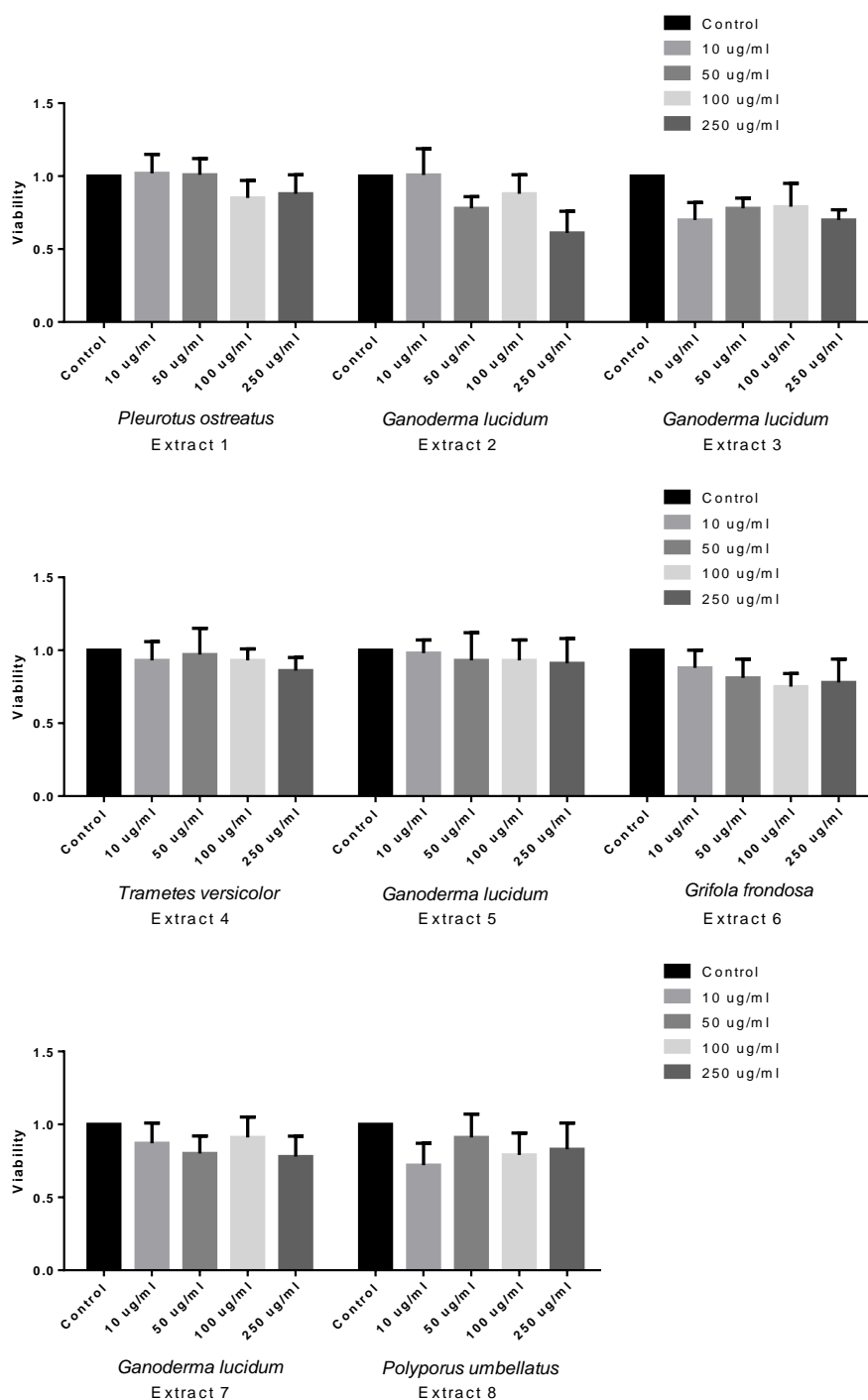


Figure 48. Effect of different fungal extracts over cell viability of colorectal cancer cells after 24 h of treatment. LoVo cells were treated with 10, 50, 100 and 250 µg/ml for 24 h. Viability of cell was represented on the X axis and the concentration of the treatment was represented on the Y axis. Data are the means \pm SD of three independent experiments (* $p < 0.05$, ** $p < 0.01$ *** $p < 0.001$)

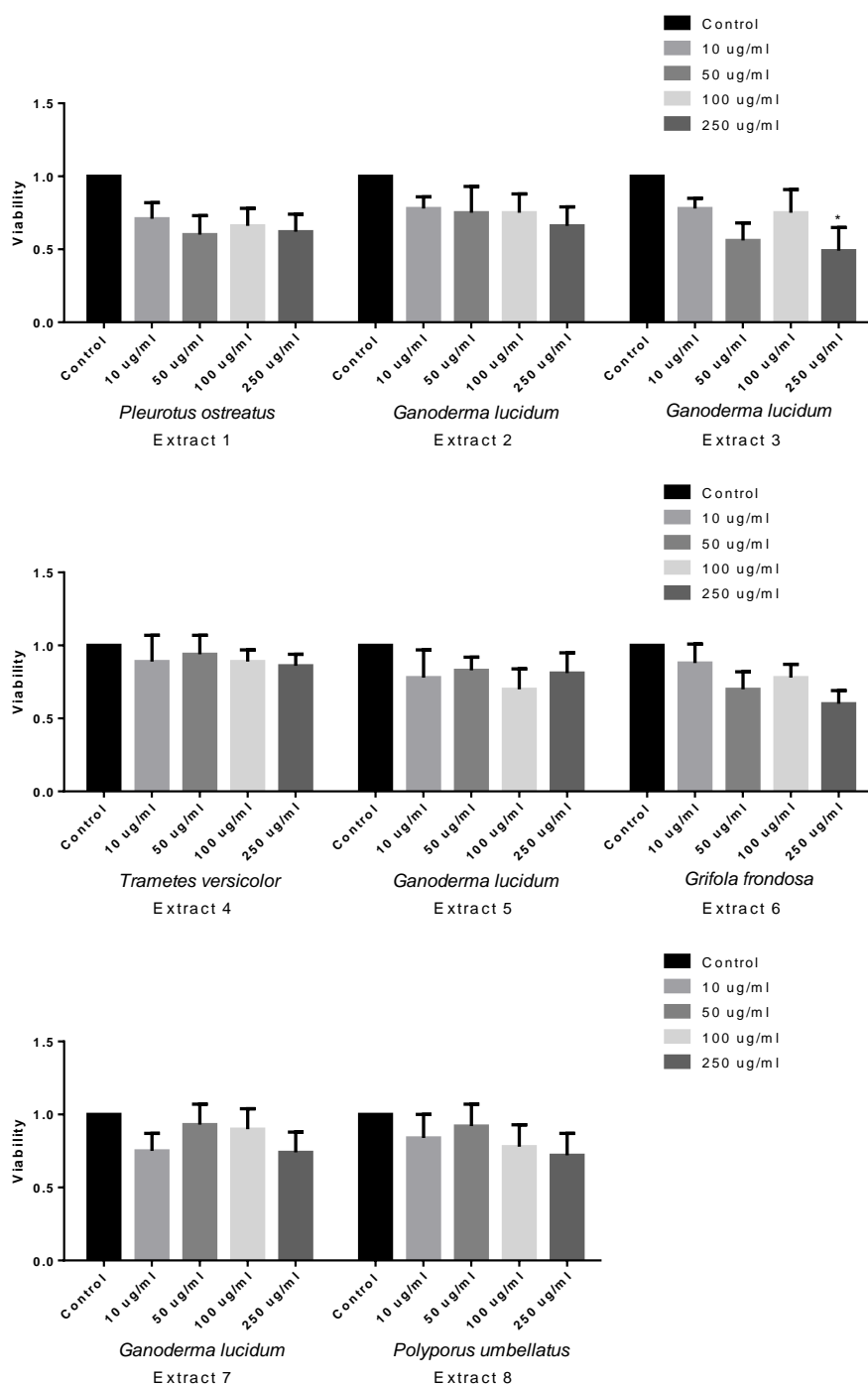


Figure 49. Effect of different fungal extracts over cell viability of colorectal cancer cells after 48 h of treatment. LoVo cells were treated with 10, 50, 100 and 250 µg/ml for 48 h. Viability of cell was represented on the X axis and the concentration of the treatment was represented on the Y axis. Data are the means ± SD of three independent experiments (*p<0.05, **p<0.01 **p<0.001)

Finally, the graphs corresponding to the treatment with the extracts 72 h (**Figure 50**), reveal a marked effect of these on the viability with values that for 7 of the 8 extracts evaluated, that is to say in 87.5 % of cases, reach values greater than 50% reduction in cell viability.

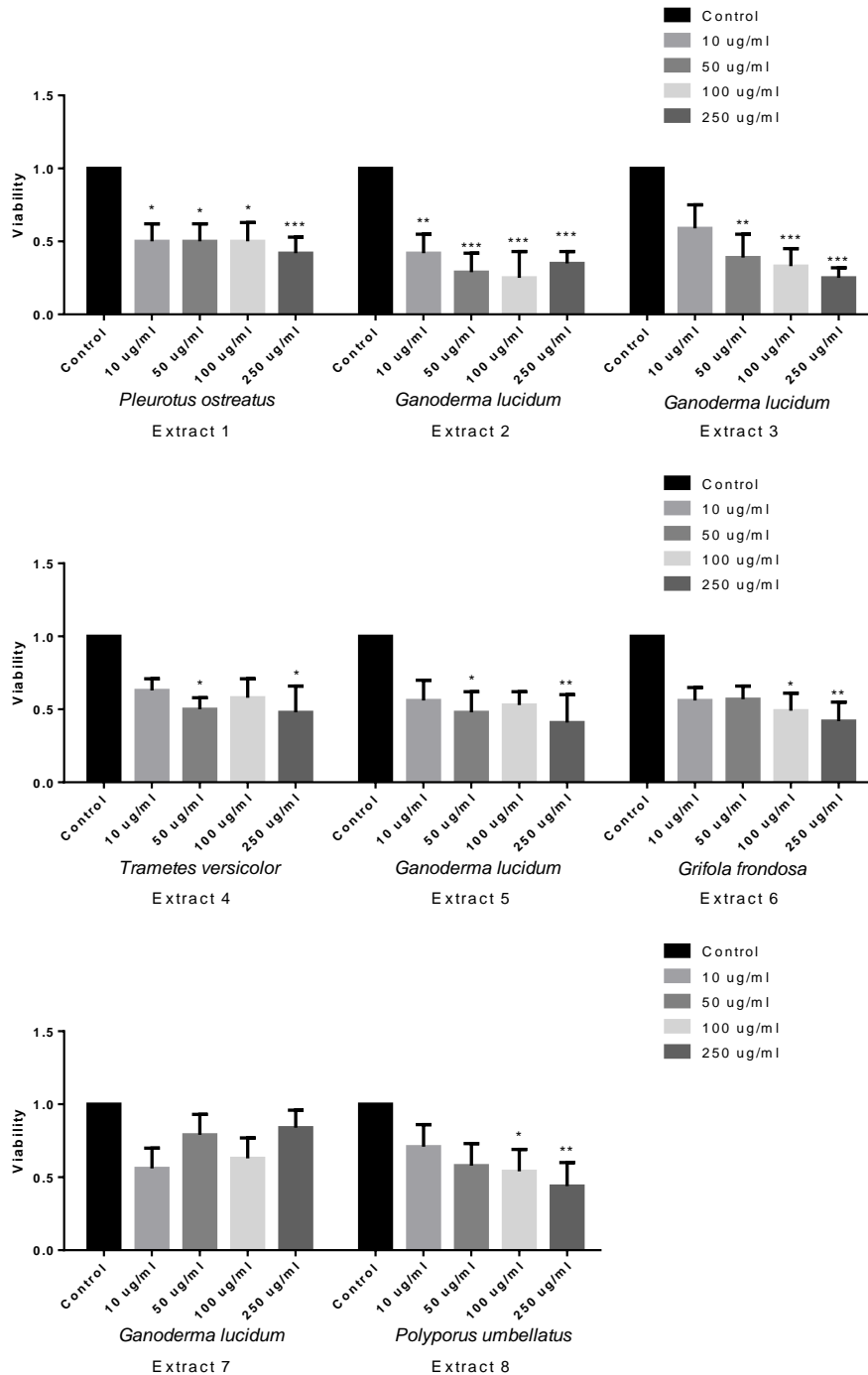


Figure 50. Effect of different fungal extracts over cell viability of colorectal cancer cells after 72 h of treatment. LoVo cells were treated with 10, 50, 100 and 250 µg/ml for 72 h. Viability of cell was represented on the X axis and the concentration of the treatment was represented on

the Y axis. Data are the means \pm SD of three independent experiments (* $p < 0.05$, ** $p < 0.01$, *** $p < 0.001$)

In other words, after 72 h of treatment all the extracts except extract 7 were able to reduce the cell viability of colorectal cancer cells to less than half compared to control cells, without any treatment. This reduction in viability turned out to be statistically significant once the results of each experimental replica were subjected to the corresponding statistical treatment.

As previously commented, the extracts that presented an effect after 24 h, as in the case of both extracts from *Ganoderma lucidum* (extracts 2 and 3) were also those that presented the highest level of reduction in viability. Specifically, the extracts of *Ganoderma lucidum* 2 and 3 reached a level of reduction of cell viability of 75% for the point of highest concentration with respect to control cells after 72 h of treatment. Interestingly, extract 7, also belonging to *Ganoderma lucidum*, was the one that produced the lowest effect, failing to reach the 50% reduction necessary to calculate the IC50. This value defined as the half maximal inhibitory concentration, is a way of measuring the potency of a given substance over one biological function, in this case the concentration of fungal extract needed to achieve a reduction on cell viability of 50%.

The IC50 gives us an idea of inhibitory potency of each substance, and a criterion in order to select the best candidates for further analysis. From the values of cell viability obtained after 72 h of treatment, a graphic representation of the viability was prepared for each extract and concentration and the IC50 value was extrapolated from the graph by logistic regression (**Figure 51**).

All IC50 values (**Table 16**) were found in a range between 9,59 $\mu\text{g/ml}$ and 277,8 $\mu\text{g/ml}$ with the exception of extract 7. This result helped to determine the most appropriate concentration for the extracts and were taken into account for the following experiments.

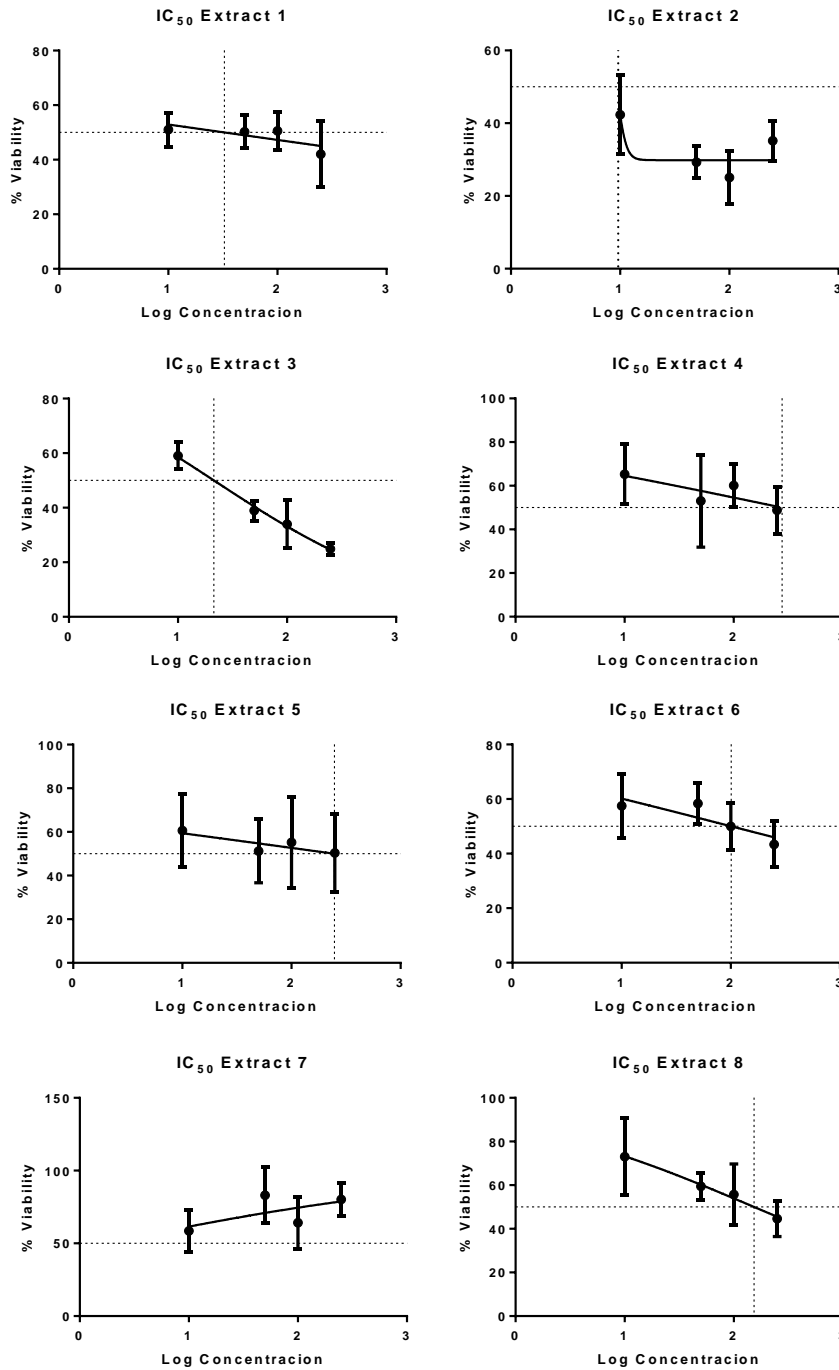


Figure 51. IC₅₀ determination from the dose-response graphs of the extracts over cell viability. Graphs created for determination of the IC₅₀ value. Viability of cells was represented on the X axis and the logarithmic concentration of the treatment was represented on the Y axis, IC₅₀ value was obtained by logistic regression. Data are the means \pm SD of three independent experiments.

Table 16. IC50 values in LoVo cells with each extract for 72 h treatment. Data is expressed in $\mu\text{g/ml}$

72 h	IC ₅₀ ($\mu\text{g/ml}$)
Muestra 1: <i>Pleurotus ostreatus</i>	10,97
Muestra 2: <i>Ganoderma lucidum</i>	6,9
Muestra 3: <i>Ganoderma lucidum</i>	20,09
Muestra 4: <i>Trametes versicolor</i>	224,02
Muestra 5: <i>Ganoderma lucidum</i>	208,46
Muestra 6: <i>Grifola frondosa</i>	127,12
Muestra 7: <i>Ganoderma lucidum</i>	-
Muestra 8: <i>Polyporus umbellatus</i>	174,24

2. Evaluation of specific modifications in the extraction, composition and/or processing of fungal extracts

Apart from the initial eight first extracts evaluated, another four sets of extracts (Modified set 1 of 6 extracts GL001H, GL001B, GL001R, GL001M, GL001S, GL001C, Modified set 2 of 5 extracts A,B,C,D, E, Modified set 3 of 8 extracts HE 00-0, HE 20-10, HE 20-20, HE 20-30, HE 001-BR, HE 100-10, HE 100-2.5C HE 100-25Q and Modified set 4 CVA00 T00, CVA20 T20, CVA20 T05, CVA 100 T01, CVA20 T10, CVA100 T03, CVA100 T05-6-RLS6, CVA100 T05-25) were tested for their cytotoxic potential. All these other extracts are derived from the initial 8 extracts and its described species. They consist in different modifications on the composition of the first extracts due to alternative processing. Given that the extracts were provided by the biotechnological companies Hifas da Terra S.L. and/or CZ Vaccines, most of the information was confidential therefore we did not know specifically what modifications were performed.

For the first eight extracts, we also performed MTT assays in LoVo colorectal cancer cell line for the evaluation of the effect of the extracts over cell viability. In this case the concentrations varied from one set of extracts to another depending on the potency of each set of extracts. In fact, we had to increase the concentration of the treatment up to 5000 $\mu\text{g/ml}$ due to the poor detected effect of the new sets of extracts.

For the next set of six extracts (Modified set 1), the concentrations tested went from 1000 $\mu\text{g/ml}$ to 5000 $\mu\text{g/ml}$. This increase in the range of concentrations was done after the observation that the treatment with the original range did not substantially

affect cell viability. At the same time for these extracts and for the following ones evaluated, we reduced the times of treatment from the original three (24, 48 and 72h) to only one, the one we saw best the cytotoxic effect of the extracts (72h).

The effect showed by the extracts was variable although all of them were able to significantly reduce cell viability at the highest concentrations tested (**Figure 52**).

Extracts GL001S and GL001R

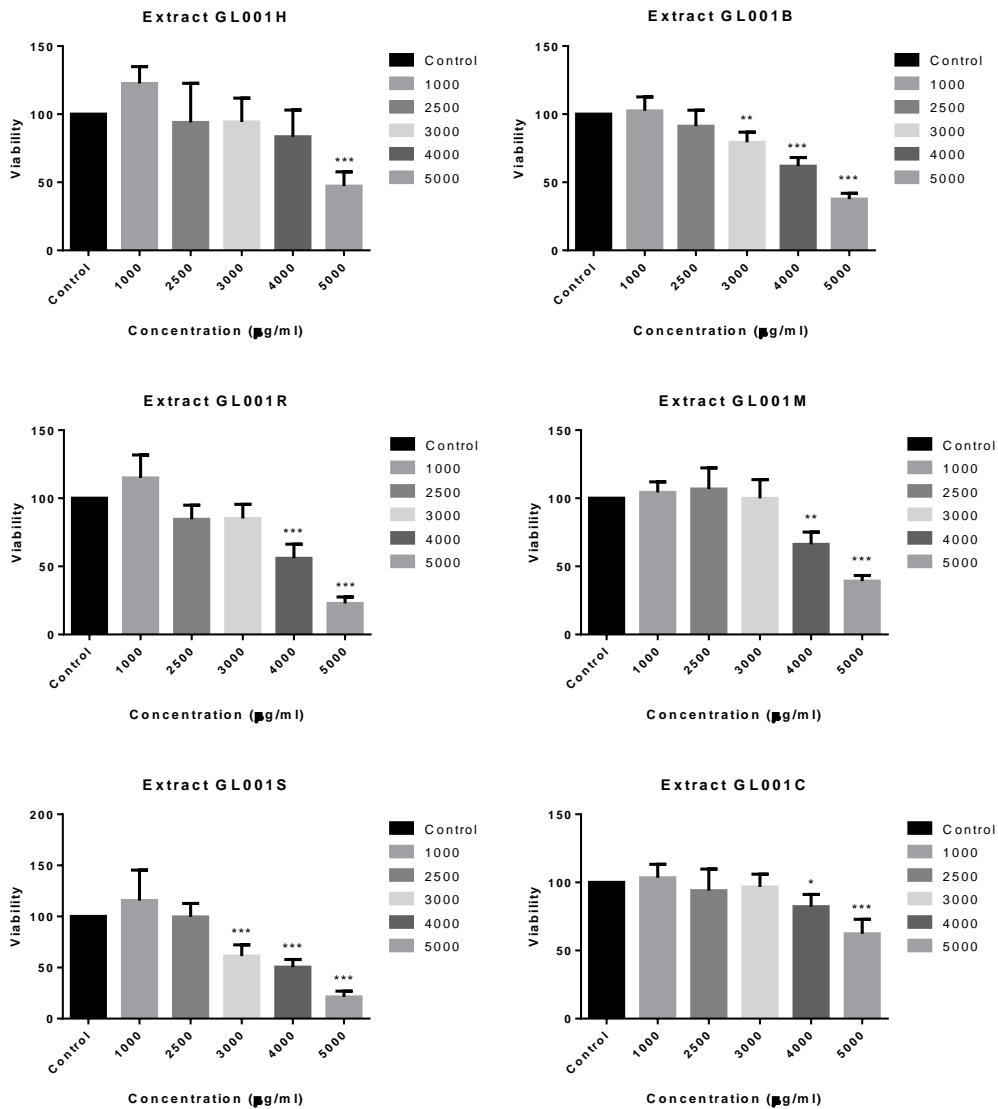


Figure 52. Effect of different fungal extracts over cell viability of colorectal cancer cells after 72 h of treatment. LoVo cells were treated with 1000, 2500, 3000, 4000 and 5000 µg/ml for 72 h. Viability of cell was represented on the X axis and the concentration of the treatment was represented on the Y axis. Data are the means ± SD of three independent experiments (*p<0.05, **p<0.01, ***p<0.001)

were able to reduce LoVo cells viability to just a 20% compared to the control while other extracts such as GL001H, GL001B and GL001M were moderately less effective achieving values of inhibition of cell viability slightly above 50%. GL001C, was the less effective extract and was unable to reduce cell viability below the 50%. However, the effect of this extracts with additional modifications was clearly lower than the initial extracts as it can be clear by observing the IC₅₀ value obtained (**Table 17**) from the logarithmic representation of this results and the posterior logistic regression (**Figure 53**).

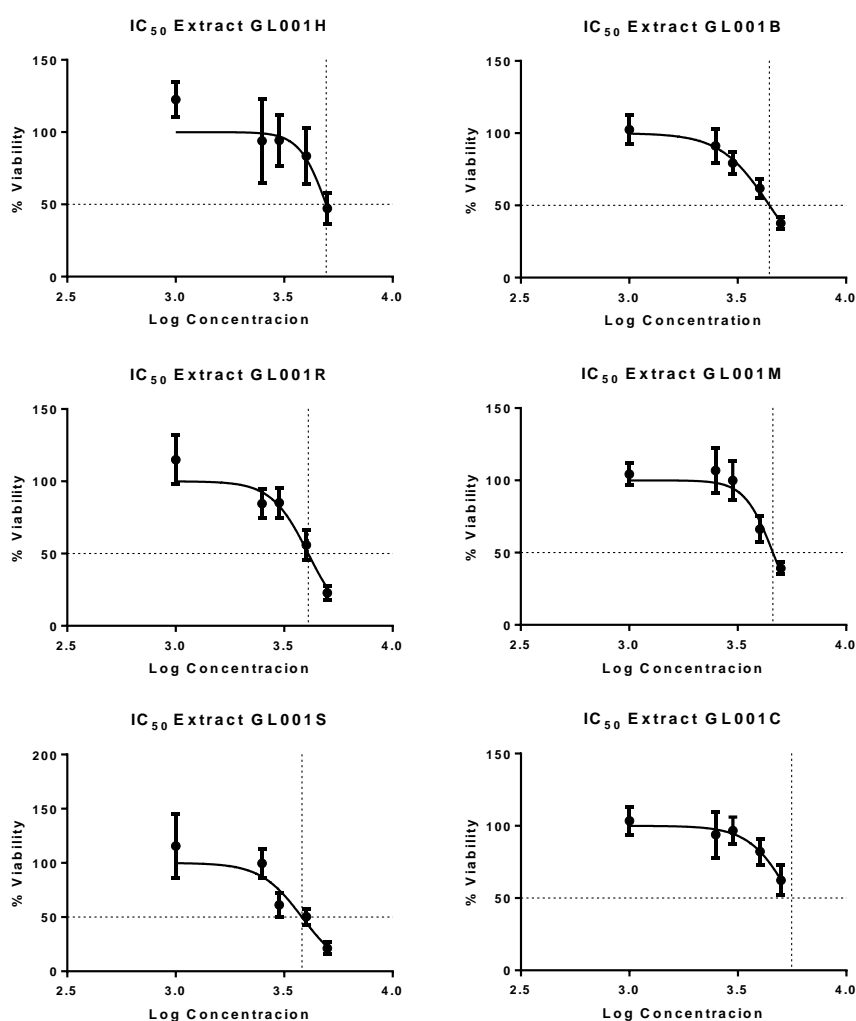


Figure 53. IC₅₀ determination from the dose-response graphs of the extracts over cell viability. Graphs created for determination of the IC₅₀ value. Viability of cells was represented on the X axis and the logarithmic concentration of the treatment was represented on the Y axis. Data are the means ± SD of three independent experiments.

Table 17. IC50 values in LoVo cells with each extract for 72 h treatment. Data is expressed in $\mu\text{g/ml}$

Extract	IC ₅₀ ($\mu\text{g/ml}$)
GL001H	4940
GL001R	4082
GL001S	3817
GL001B	4433
GL001M	4596
GL001C	5593

The IC50 values for this second set of extracts varied from 3817 and 5593 $\mu\text{g/ml}$. This range is approximately 20 times higher than the initial extracts, which means we need 20 times more extract for achieving the same level of cell viability inhibition in colon cancer cells. Due to this change in the effect of the extracts, we discarded them for future experiments.

Another two sets of modified extracts (Modified sets 2 and 3) were received for its testing, all of them resulted in lower cytotoxic effect on cancer colon cells compared to the effect of the initial eight extracts (**Figures 54 and 55**). In fact, none of the new extracts were able to achieve levels of inhibition above 50%, necessary requirement for the determination of the IC50 values. The cytotoxic effect of the last three sets of extracts evaluated by MTT, was determined by treating the cells with concentrations between 10 $\mu\text{g/ml}$ and 1000 $\mu\text{g/ml}$ this time for 72h. We reduced the higher concentration of treatment from 5000 to 1000 $\mu\text{g/ml}$, because we will only consider including the extracts in further studies if the IC50 value would be in that range as it is the case of the original set of extracts.

With the last set of extracts (Modified set 3), we had to implement a new method for the preparation of the stock dilutions. Apart from the initial study of the best solvent for the extracts mentioned in Materials and Methods, we had to improve the method. Instead of simply diluting the lyophilized extract in distilled water, we had to add a new step to the process, the sonication, to mix samples by ultrasounds and achieve a homogenized solution. Given that this process may affect the stability of the extracts

and therefore their effect over the cells, so we performed a previous experiment to test if the cytotoxic effect of the extracts could be altered by this new processing.

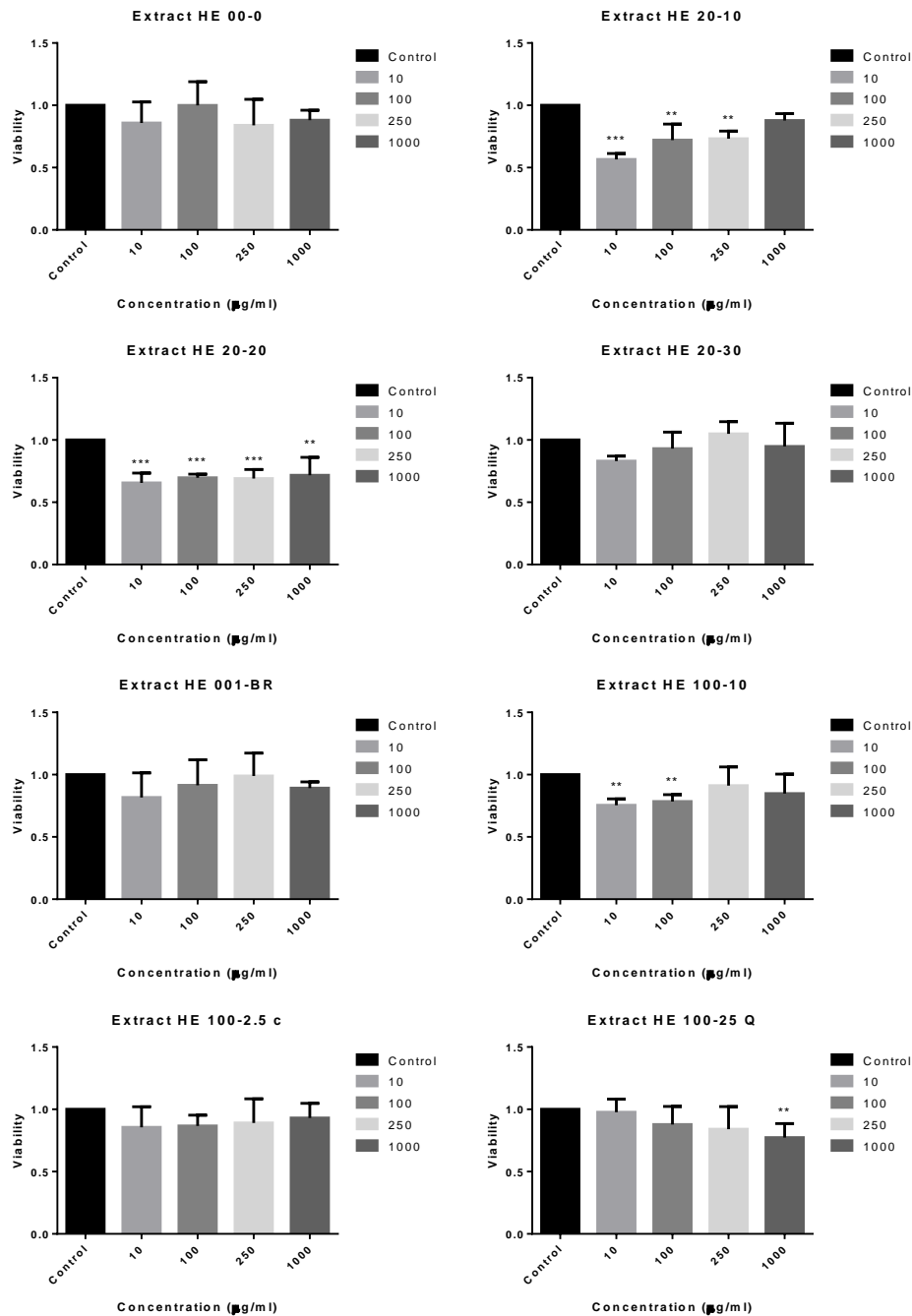


Figure 54. Effect of different fungal extracts on cell viability of colorectal cancer cells after 72 h of treatment. LoVo cells were treated with 10, 100, 250, and 1000 µg/ml for 72 h. Viability of cell was represented on the X axis and the concentration of the treatment was represented on the Y axis. Data are the means ± SD of three independent experiments (*p<0.05, **p<0.01, ***p<0.001)

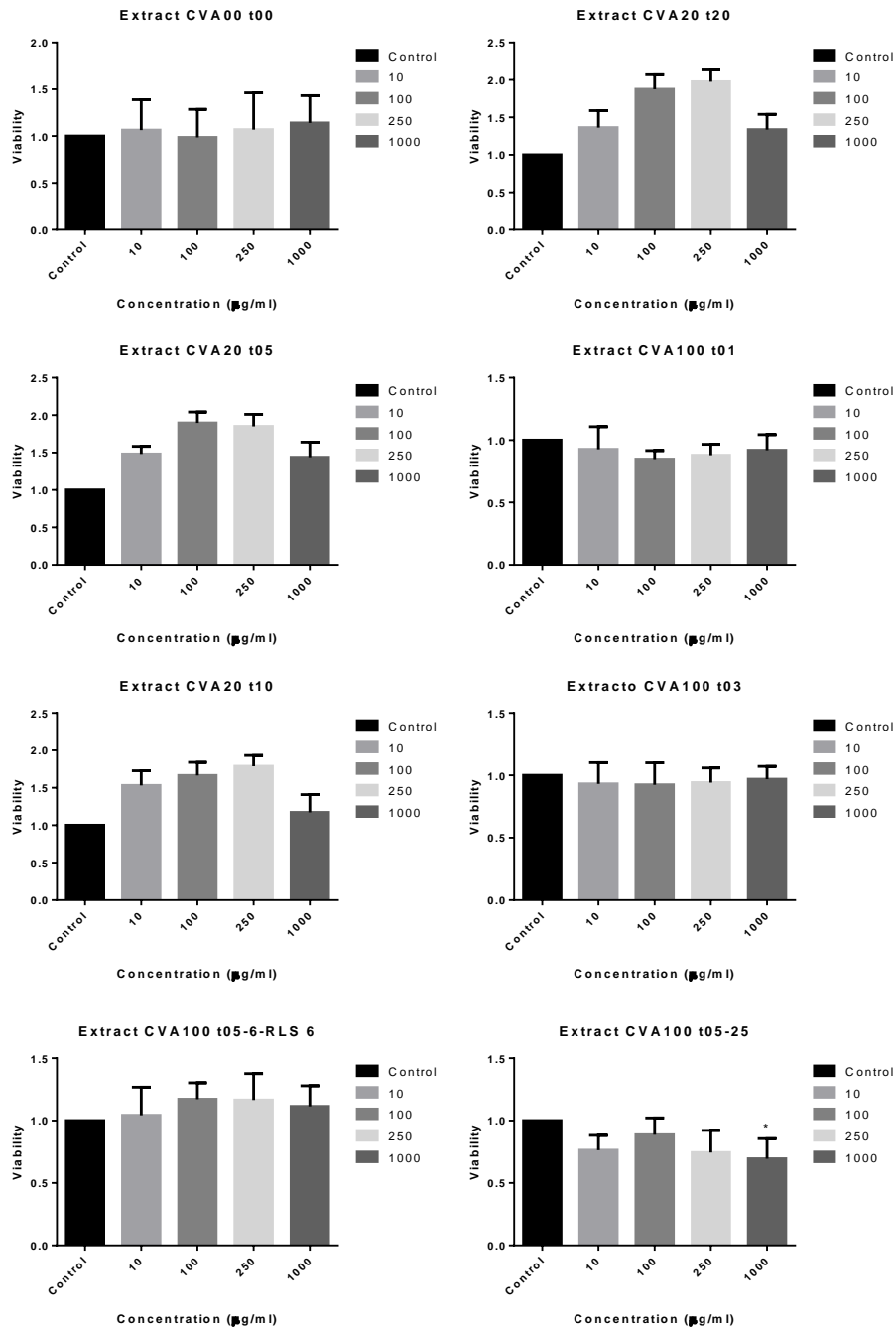


Figure 55. Effect of different fungal extracts on cell viability of colorectal cancer cells after 72 h of treatment. LoVo cells were treated with 10, 100, 250, and 1000 µg/ml for 72 h. Viability of cell was represented on the X axis and the concentration of the treatment was represented on the Y axis. Data are the means ± SD of three independent experiments (*p<0.05, **p<0.01, ***p<0.001)

The result of the experiment showed that sonication did not affect the effect of the extract on cell viability (**Figure 56**).

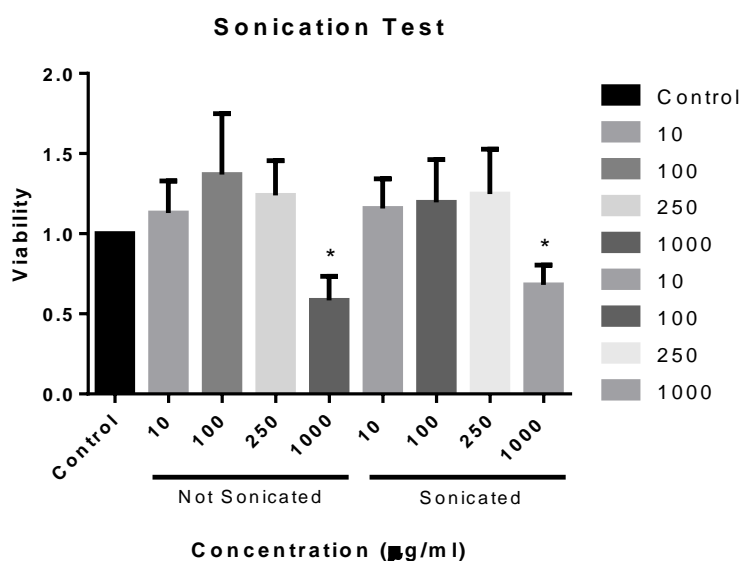


Figure 56. Effect of sonication on fungal extract effectivity in colorectal cancer cells. LoVo cells were treated with 10, 100, 250, and 1000 µg/ml of sonicated and not sonicated extracts for 72 h. Viability of cell was represented on the X axis and the concentration and processing of the treatment was represented on the Y axis. Data are the means ± SD of three independent experiments (*p<0.05, **p<0.01 **p<0.001)

The results obtained from this last set of extracts were again in the line of all the new set tested, with lower effect over the cell viability of colorectal cancer cells (**Figure 57**). Only extracts D and E seemed to have a noticeable effect at high concentrations. The case of the extract E is special, it was the only extract not provided as a lyophilized powder, instead it was in liquid form, so we tested prefiltered dilutions of it in the culture medium.

Our results indicate that all these modified versions of the extracts have lower inhibition effect on colorectal cells than the original set of extracts tested. Given the restricted information provided about the implemented modifications to the initial extracts, the conclusions are limited. However, we further continue to analyse the possible molecular mechanism involved using those with more promising cytotoxicity activity.

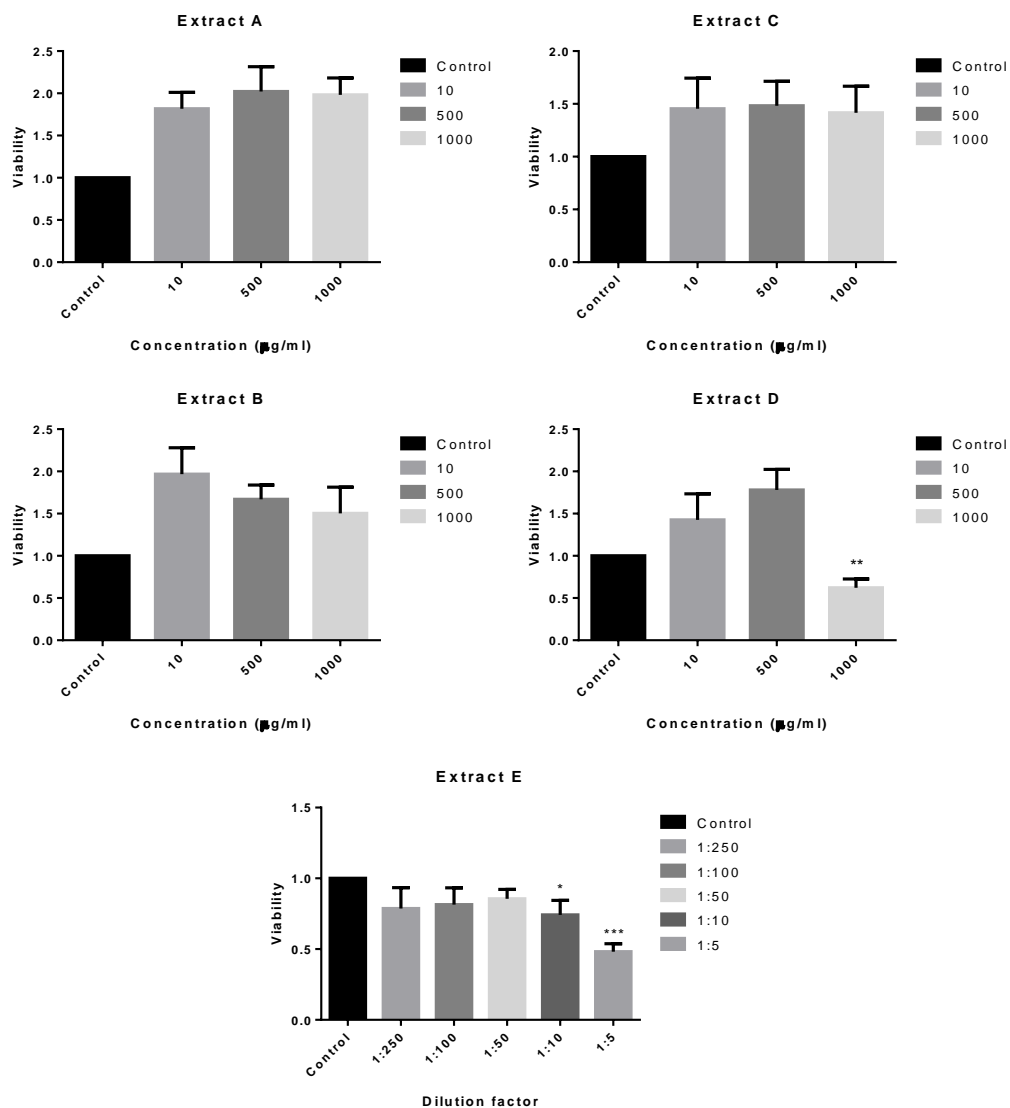


Figure 57. Effect of different fungal extracts on cell viability of colorectal cancer cells after 72 h of treatment. LoVo cells were treated with 10, 500, and 1000 µg/ml or 1:250, 1:100, 1:50, 1:10 and 1:5 for 72 h. Viability of cell was represented on the X axis and the concentration of the treatment was represented on the Y axis. Data are the means ± SD of three independent experiments (*p<0.05, **p<0.01 ***p<0.001)

3. Screening of different fungal extracts from different species on the effect on the cell phenotype of colorectal cancer cells

After the initial screening on the effect of the extracts on cell viability, the first eight extracts (Extracts 1-8) from the species *Grifola frondosa*, *Trametes versicolor*, *Pleurotus ostreatus*, *Ganoderma lucidum* and *Polyporus umbellatus*, were selected for a second screening. In this case, we wanted to analyze the effect of the extracts on the phenotype of the LoVo cells.

Under control conditions, the colorectal cancer cell line LoVo has a mesenchymal phenotype characterized by weak cell-cell contacts and the presence of protrusions on the cell membrane. This characteristic tumor cell phenotype contrasts with the phenotype of non-transformed epithelial cells characterized by the presence of apico-basal polarity and tight cell-cell junctions.

The objective of our trial was to analyze whether the treatment with the extracts was capable of reversing the mesenchymal phenotype of colorectal cancer cells into a more epithelial one. For that, cells were treated with different concentrations of the extracts (10 and 100 $\mu\text{g}/\text{ml}$) for 72 h and the analysis was carried out by phase contrast microscopy images (**Figures 58 and 59**).

The images obtained, showed that some extracts were able to induce tighter cell-cell contacts, specially this can be seen in the images shown in cell treated by the extracts 4 and 6 (*Trametes versicolor* and *Grifola frondosa*) at a concentration of 100 $\mu\text{g}/\text{ml}$.

In control cultured cells, without treatment, a scattered phenotype without close cell-cell contacts is observed. Interestingly, the treatment with extracts 4 and 6, led cells to a more compact colony structure with closely contacts between them. The same tendency is noticeable with the extracts 1, 3 and 7 (*Pleurotus ostreatus* and *Ganoderma lucidum*) but to a minor degree. The rest of extracts did not seem to affect the mesenchymal like phenotype of the cells.

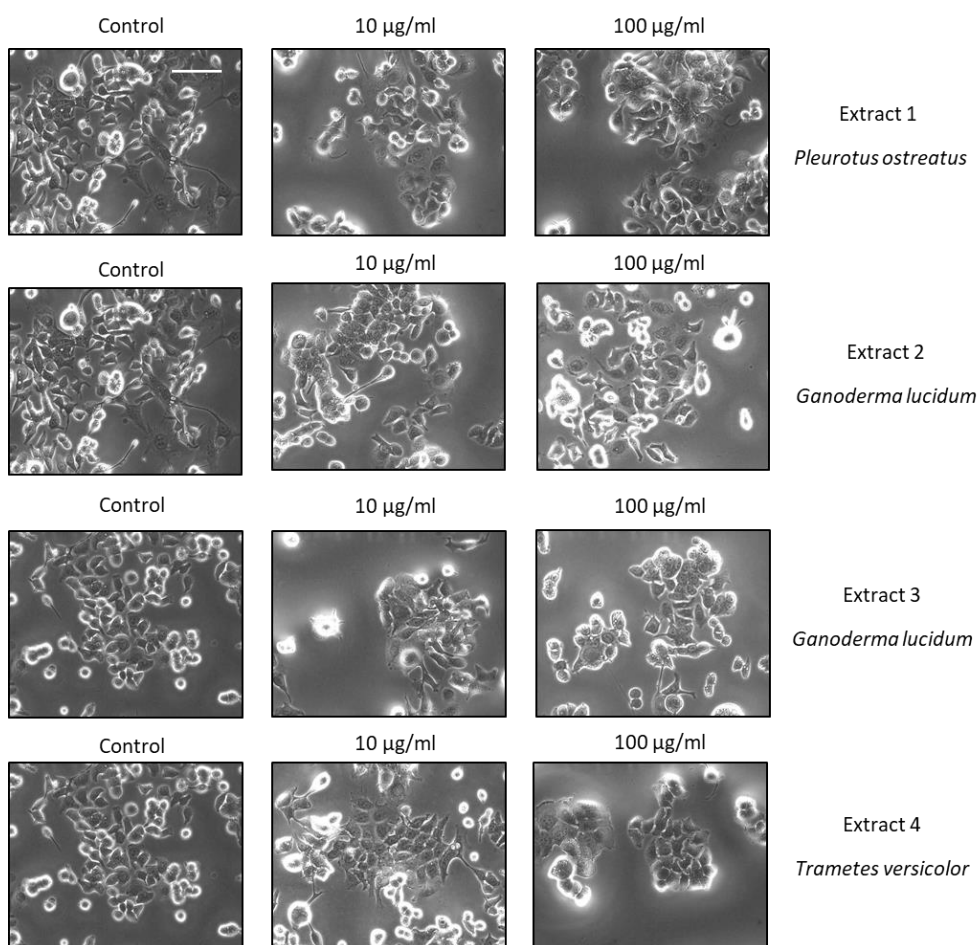


Figure 58. Effect of different fungal extracts on the cell phenotype of colorectal cancer cell line. LoVo cells were treated with 10 and 100 $\mu\text{g/ml}$ of each extract for 72 h and images were taken by microscopy at 10X magnification. Scale bar 100 μm .

Altogether, the results obtained from both screening studies lead to the selection of the two most promising extracts with the aim of continuing our study. Extracts 4 and 6 (*Trametes versicolor* and *Grifola frondosa*, respectively) were chosen as it was observed an important effect in the cell phenotype and cell cytotoxicity. These selected extracts were used for further analysis of the possible molecular mechanism implicated in their effect.

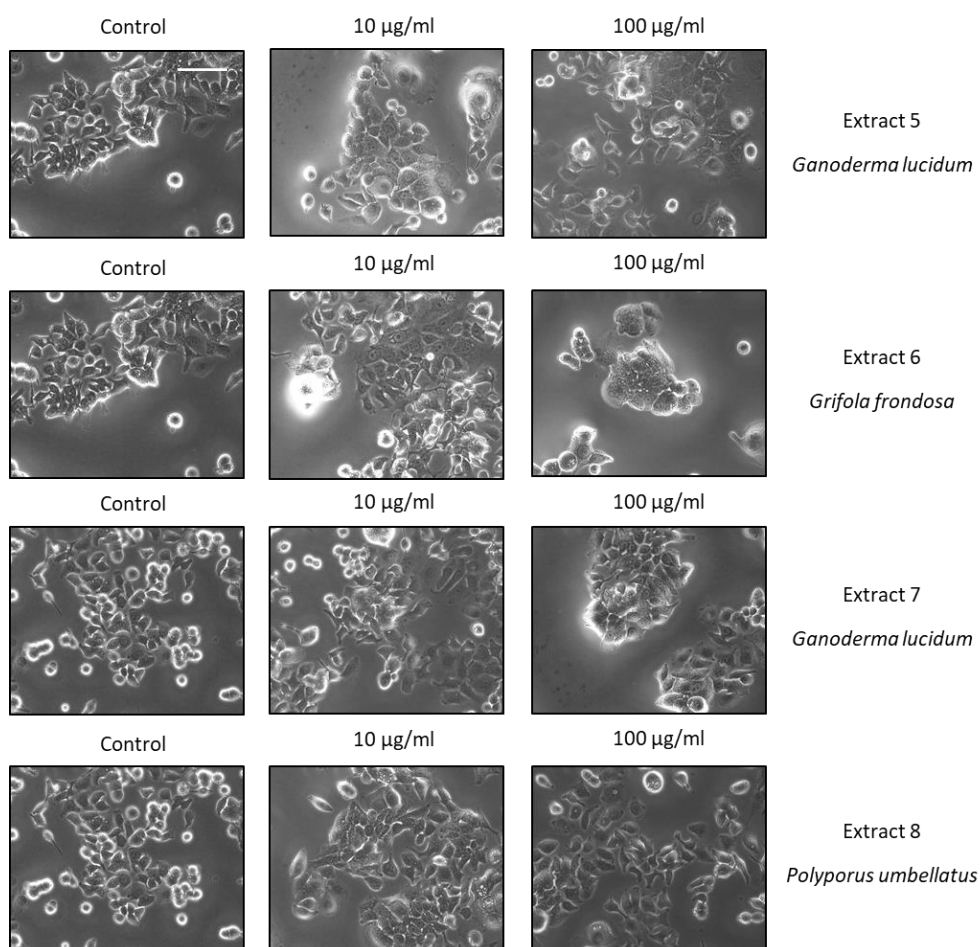


Figure 59. Effect of different fungal extracts on the cell phenotype of colorectal cancer cell line. LoVo cells were treated with 10 and 100 µg/ml of each extract for 72 h and images were taken by microscopy at 10X magnification. Scale bar 100 µm.

4. Effect of *Trametes versicolor* and *Grifola frondosa* extracts on viability and proliferation of colon cancer cells

Before starting with new experiments to explore the functional effects of the extracts *Trametes versicolor* (TV) and *Grifola frondosa* (GF) in different cellular processes, we extended the analyses of cell viability by MTT, using another colorectal cell line, HT-29, with a more epithelial morphology compared to LoVo cells. Cells were treated for 24, 48 and 72h with concentrations ranging from 10 µg/ml to 250 µg/ml. No significant effect was detected during treatment of HT-29 cells with TV extracts after 24 h, 48 h and 72 h (**Figure 60**). Treatment with GF extract on HT-29 cells was more effective compared to

the effect in LoVo cells. In these cells, at a low concentration of 50 µg/ml, a strong decrease in cell viability after 24 h, 48 and 72 h were observed. This inhibitory effect was up to 60-70% of reduction after 72 h of treatment with GF with a concentration of 100 µg/ml, and similar results were obtained with the concentration of 250 µg/ml at all 24 h, 48 h and 72 h.

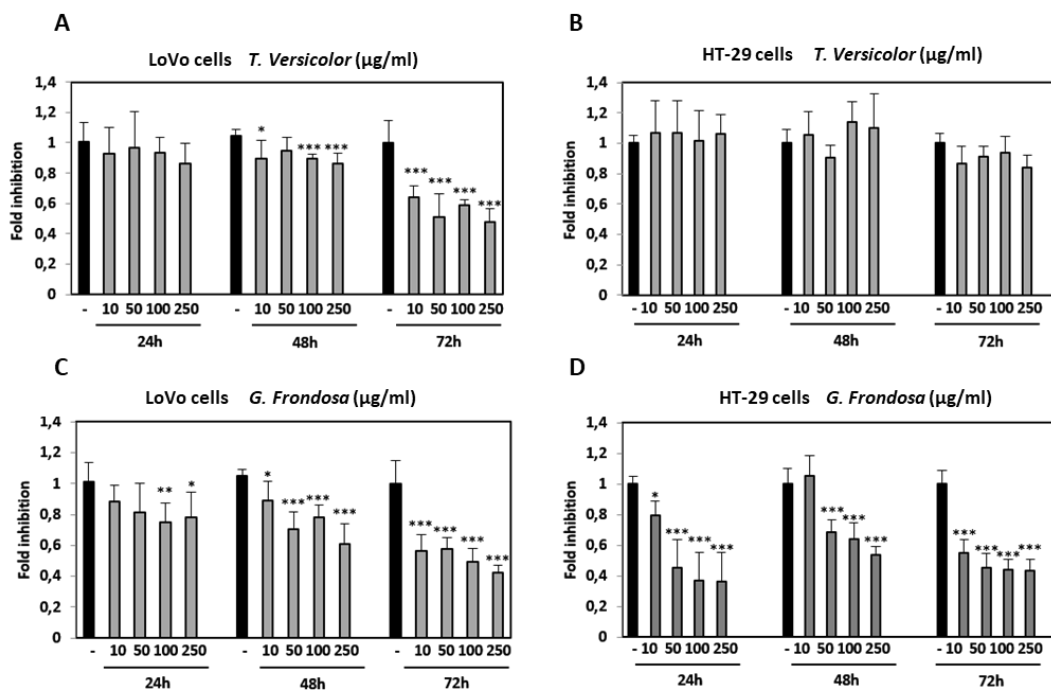


Figure 60. Effect of TV and GF extracts on cell viability of LoVo and HT-29 cells. LoVo and HT-29 cells were treated with TV and GF at 10, 50, 100 and 250 µg/ml for 24, 48 and 72 h. Fold inhibition of viability was represented on the X axis and the concentration and time of the treatment was represented on the Y axis. Data are the means ± SD of three independent experiments (*p<0.05, **p<0.01, ***p<0.001)

IC50 values were calculated for each cell line resulting in a range from 127,12 and 224,02 µg/ml for LoVo cells and of 21,07 for HT-29 in the case of the GF extract both at a time of 72 h as shown in (Table 18). TV extract did not produce a reduction on cell viability higher than 50% in HT-29 cells, so it was not possible to determine the IC50 value. IC50 values were also calculated for the time of 24h, at this time of treatment only GF extract was able to reduce cell viability over the level of 50% for both cell lines while for TV extract this limit was not achieved.

Table 18. IC50 values for TV and GF for each time of treatment. Data is expressed in µg/ml.

	IC ₅₀ (µg/ml)	
	24h	72h
LoVo		
<i>Trametes versicolor</i>	-	224,02
<i>Grifola frondosa</i>	934,82	127,12
HT-29		
<i>Trametes versicolor</i>	-	-
<i>Grifola frondosa</i>	44,09	21,07

Additionally, effect of TV and GF extracts on cell proliferation were analyzed by BrdU assay. After treatment of LoVo cells for 48 h with 10 and 100 µg/ml of each extract, proliferation rate was measured by incorporation of BrdU. Quantification of BrdU incorporation by cells showed that exposure even at low concentrations such as 10 µg/ml of TV extract caused significant inhibition, up to 45% compared to untreated cells (**Figure 61**). In the case of GF, treatment with 10 µg/ml caused an inhibition of between 50 and 60%, while for the highest concentration of 100 µg/ml, reached 80%. It should be noted that the extracts seem to have a more marked effect on cell proliferation than on cell viability, therefore more pronounced growth inhibition with low concentrations are detected, avoiding cytotoxic effect.

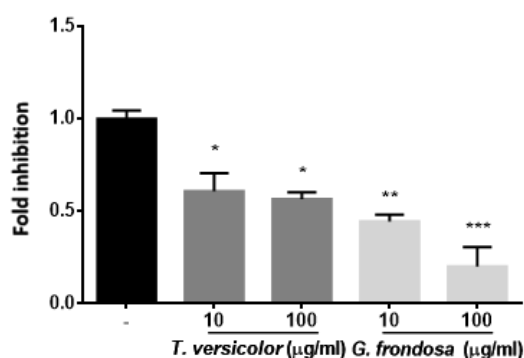


Figure 61. Effect of TV and GF extracts on cell proliferation in LoVo and HT-29 cells. LoVo and HT-29 cells were treated with 10 and 100 µg/ml for 48 h. Fold inhibition of proliferation was represented on the X axis and the concentration was represented on the Y axis. Data are the means ± SD of three independent experiments (*p<0.05, **p<0.01, ***p<0.001)

5. Effect of *Trametes versicolor* and *Grifola frondosa* extracts on the anchorage-independent cell growth of LoVo cells

The next step was analyzing the possible effect of the extracts on the oncogenic potential of colorectal cancer cells. Tumor cells are characterized by being able to survive and grow in the absence of a solid substrate, which is characteristic of tumor cells.

To study if the treatment with TV and GF extracts is able to affect this cellular process, an anchorage-independent cell growth assay was performed. Cells were treated with 10, 100 and 250 µg/ml of each extract for up to 21 days in soft agar. After that time colony formation was evaluated by manual counting and pictures were taken by microscopy.

As shown in **Figure 62**, both extracts were able to significantly reduce colony formation on soft agar even at very low concentrations of 10 µg/ml. The level of inhibition of colony formation reached up to more than 50% and with very low dose-dependent effect with almost the same level of inhibition with the lower concentration (10 µg/ml) that with the highest one (250 µg/ml). We can therefore say that the extracts of *Trametes versicolor* and *Grifola frondosa* are able to reduce the oncogenic potential of colorectal cancer cells.

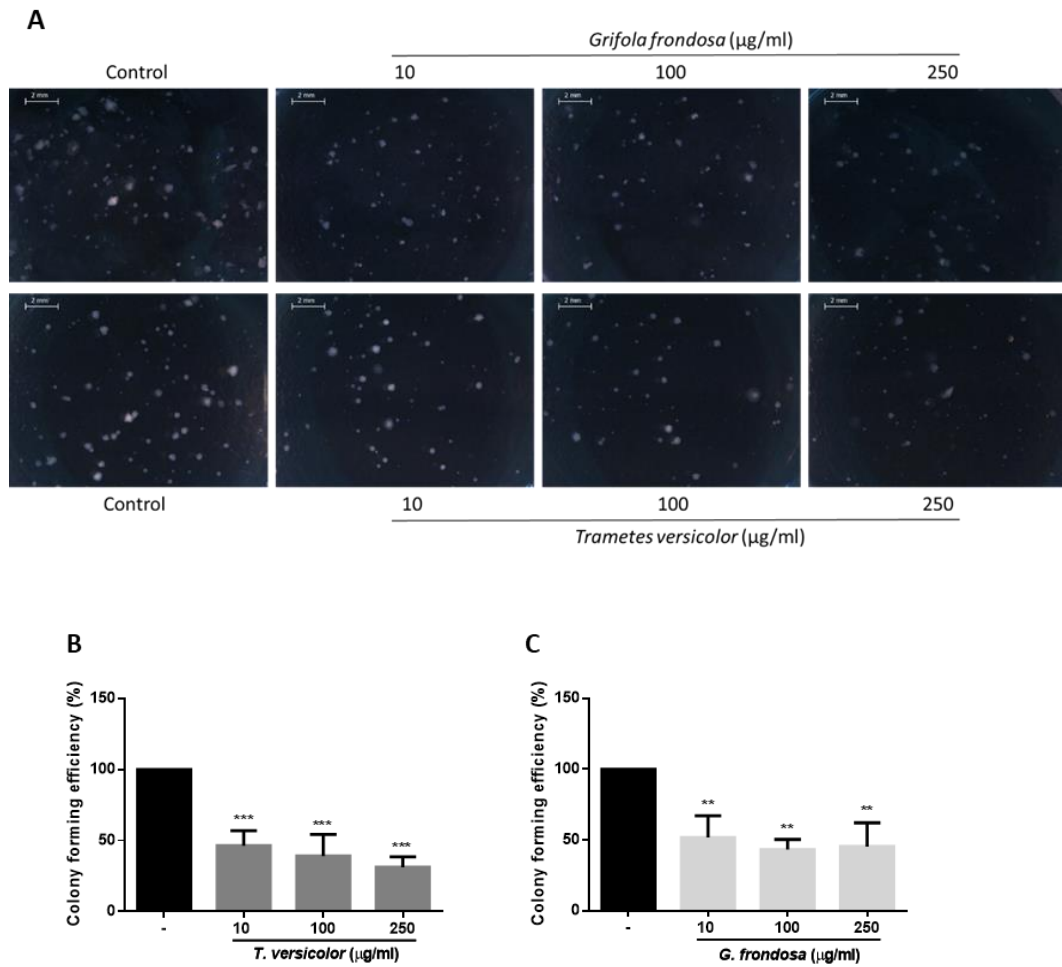


Figure 62. Effect of TV and GF extracts over anchorage-independent growth of LoVo cells. LoVo cells were treated with 10, 100 and 250 $\mu\text{g/ml}$ for 21 days. Images were taken by microscopy at 4X magnification. **A**, Microscope images of LoVo cells colonies grown in agar under 10x magnifying glass. **B**, Quantification of colony forming efficiency (%) was represented on the X axis and the concentration of TV versicolor extract was represented on the Y axis. **C**, Quantification of colony forming efficiency (%) was represented on the X axis and the concentration of GF versicolor extract was represented on the Y axis. Data are the means \pm SD of three independent experiments (* $p < 0.05$, ** $p < 0.01$ *** $p < 0.001$)

6. Effect of *Trametes versicolor* and *Grifola frondosa* extracts on cell migration in LoVo colon cancer cells

Based on the observation of the effect of the extracts in cell invasion, we thought it was reasonable to study if cell migration could also be affected by the activity of the extracts. One of the pivotal steps of the tumoral and metastatic process is the ability of cells to migrate, to be able to escape from the primary tumour. Therefore, we performed wound-healing assays in LoVo cells to determine cell migration capability.

Cells were seeded in special inserts trying to simulate a wound in the cell monolayer, the cells were treated with two different concentrations of TV and GF extracts, 10 and 100 µg/ml and photographs were taken at 24, 48 and 72 hours. The closure of the artificially created gap was monitored with the images and then quantified by a special plugin of the Image J software (MRI Wound healing tool).

Concentrations of 10 and 100 µg/ml of TV extracts were able to reduce about 50% of wound closure after 48 h (**Figure 63**). TV extract was not so effective when treating for 72 h reaching a level of inhibition of migration not higher than 20%. Similar results were obtained after treatment with GF for 48 h with a concentration of 10 µg/mg. The results also showed a 40% and 20% of reduction in wound closure in LoVo cells after treatment with 100 µg/ml of GF extracts for 48 and 72 h, respectively.

We can conclude by these results that TV and GF have a significative effect on the reduction of the migrative potential of LoVo colorectal cancer cells *in vitro*.

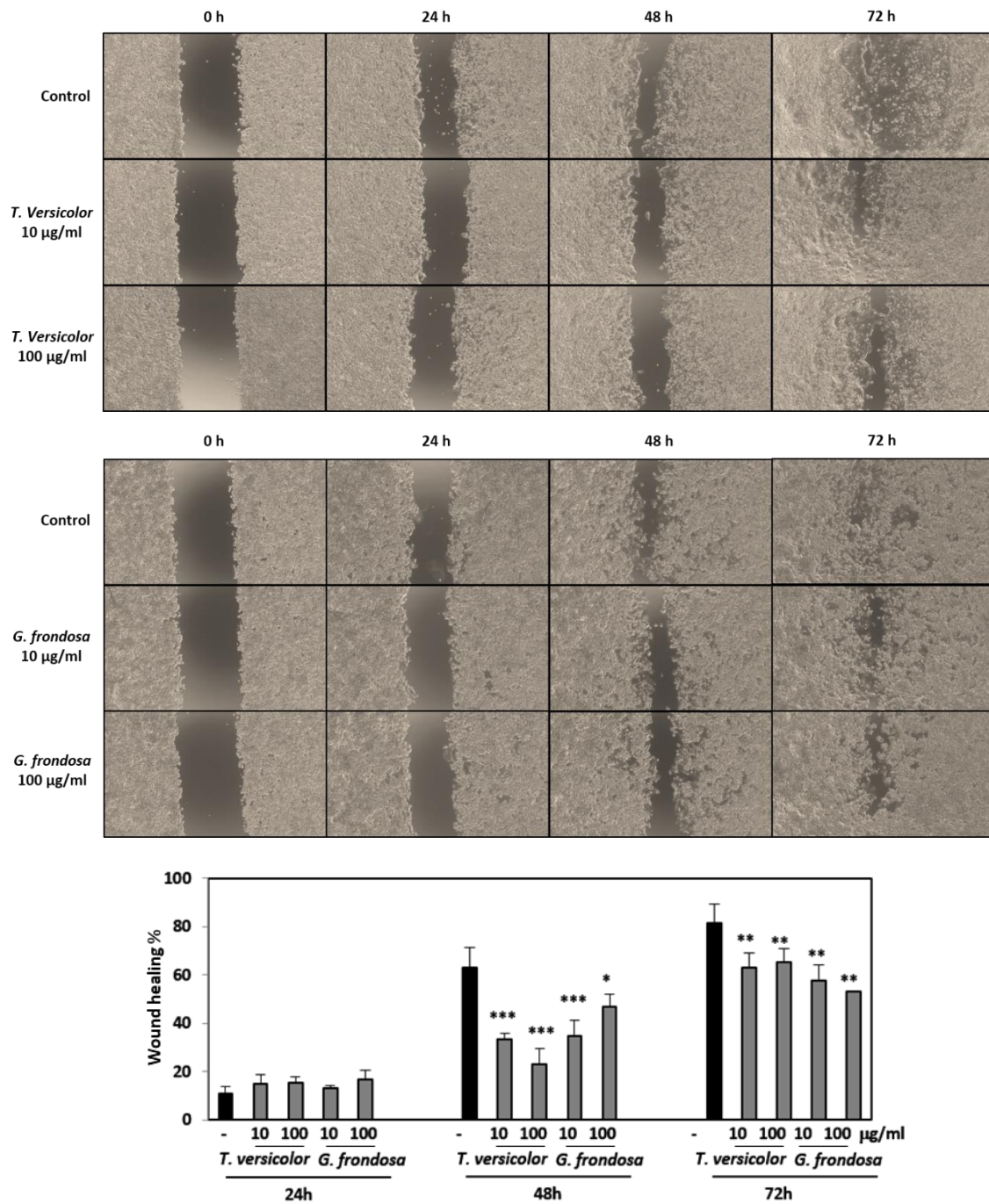


Figure 63. Effect of TV and GF extracts in cell migration of LoVo cells. LoVo cells were treated with 10 and 100 µg/ml for 72 h. Upper panel shows the gap closure of the wound by cell migration, lower panel shows the quantification of wound closure. Inhibition of wound healing was represented on the X axis and the concentration was represented on the Y axis. Data are the means ± SD of three independent experiments (*p<0.05, **p<0.01 **p<0.001)

7. Effect of *Trametes versicolor* and *Grifola frondosa* extracts on cell invasion in LoVo colon cancer cells

Given the observed effect of the extracts on the oncogenic potential of colorectal cancer cells, we wondered if they may also have a role in cell invasion as is one of the most important characteristics to allow cells to disseminate to secondary sites to form metastasis. Invasion allows cells to degrade the extracellular matrix and to invade other tissues and organs.

To analyse if our extracts are able to alter the invasive capabilities of tumoral cells, an invasion assay was performed in LoVo cells. Cells were treated with 10 and 100 µg/ml of each extract for 72 h in cell invasion chambers, covered by artificial extracellular matrix. After that period of time, invasive cells that were able to go across the membrane including a layer of extracellular matrix were stained and counted. The results showed that the treatment with the extracts was able to attenuate the invasion potential of LoVo cells (**Figure 64**). TV extracts appear to have a stronger effect compared with GF in this case, but both of the extracts are able to exert their effect even at low concentrations.

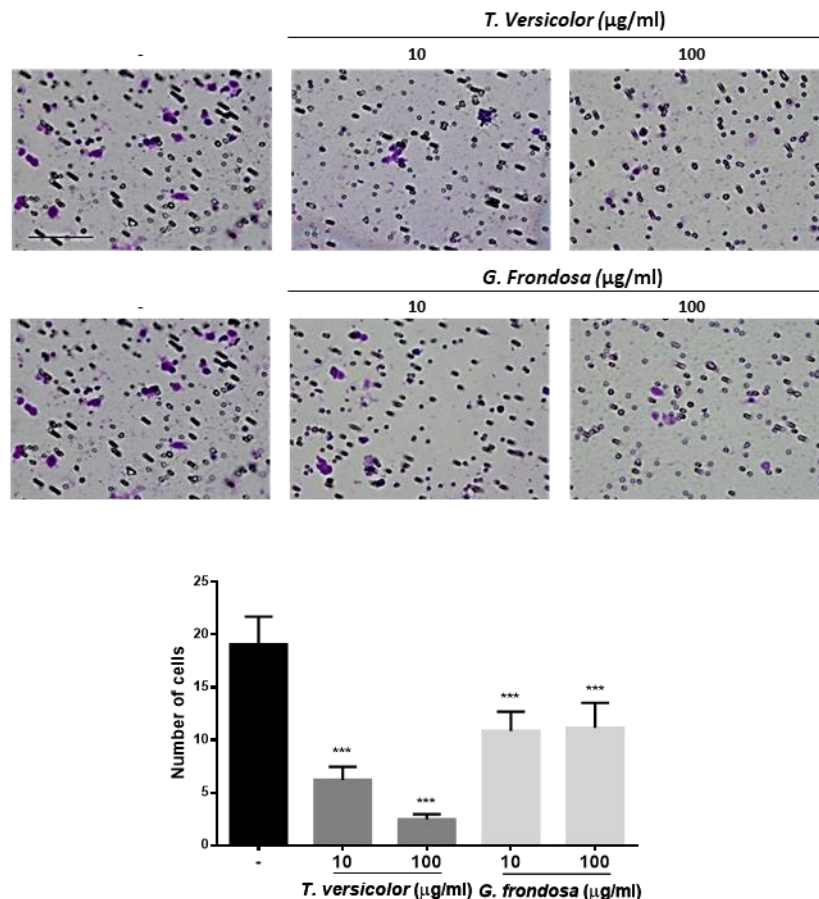


Figure 64. Effect of TV and GF extracts over cell invasion of LoVo cells. LoVo cells were treated with 10 and 100 µg/ml for 72 h. Number of invasive cells was represented on the X axis and the concentration was represented on the Y axis. Upper panel show invasive cells in the wells, lower panel corresponds to the quantification of those cells. Data are the means ± SD of three independent experiments (*p<0.05, **p<0.01 ***p<0.001)

8. Effect of TV and GF extracts on E-cadherin and mesenchymal markers protein expression

In order to deeply understand the possible mechanism that could be responsible for the functional effects observed on colorectal cancer cells, we analysed the levels of protein expression of epithelial and mesenchymal markers. As many of the results gathered were pointing to a role of the extracts in cells motility and phenotype, we thought that testing the expression of proteins involved in cell structure and cell contacts could lead to start giving a molecular explanation to the results we were observing.

Epithelial cells express E-cadherin, which is a classic protein, key in cell-cell adhesion and its loss has been linked to cell invasion. Together with this epithelial marker Citokeratin-18 is also considered an important marker for the epithelial phenotype. Citokeratin-18 is a protein related with the filament family of proteins. Vimentin and N-cadherin are mesenchymal protein characteristic of the mesenchymal phenotype. Vimentin is also a protein related with the filament family and N-cadherin is also a protein involved in cell-cell contacts and its overexpression have been linked to the acquisition of a mesenchymal phenotype.

The expression of these four proteins was assayed by Western blot after the treatment with different concentrations of TV and GF extracts. Cells were treated for 72 h with 100 and 250 µg/mg of each extract and then collected and lysed for protein extraction. A statistically significant increase of E-cadherin was detected when LoVo cells were treated with both fungal extracts as shown in (**Figure 65A**). Vimentin expression was not detected neither in the treated or the untreated conditions (**Figure 65B**). Not statistically significant differences were detected with N-cadherin and Citokeratin-18 analysis.

N-cadherin seemed to be slightly down regulated specially under treatment with the TV extract and with the highest concentration of the GF extract (**Figure 65C**). However, these differences were not statistically significant. Citokeratin-18 did not seem to be affected by fungal extract treatment although some upregulation could be detected when treating with the highest concentration of TV (**Figure 65D**). E-cadherin expression was also checked by immunofluorescence but the recovery of its expression at cell-cell contacts after the treatment with the extracts was that evident as detected with the Western-blot (**Figure 66**).

Taking into consideration all these results show that the tumour suppressor E-cadherin expression is recovered under TV and GF treatment in LoVo cell line.

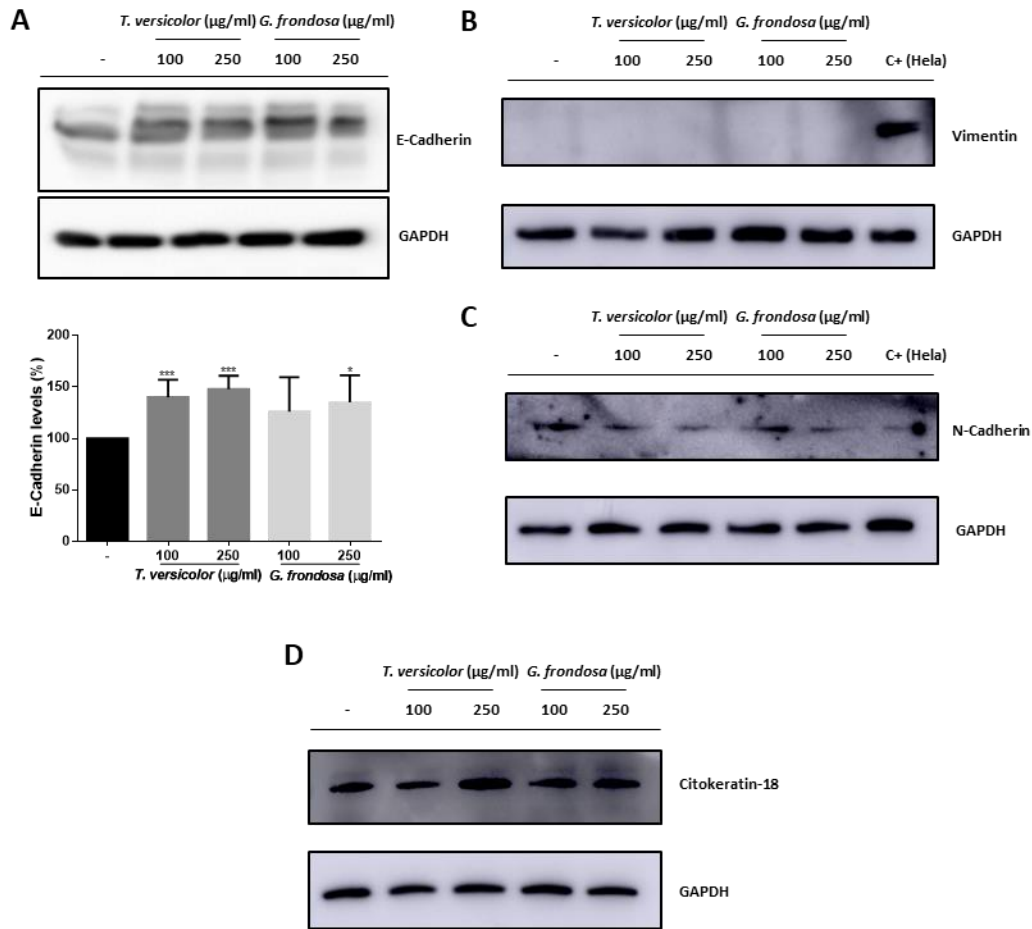


Figure 65. Effect of TV and GF extracts in protein expression of epithelial and mesenchymal markers measured by Western blot. LoVo cells were treated with 100 and 250 µg/ml for 72 h and then lysed for protein extraction. **A**, Effect of TV and GF extracts in protein expression of E-Cadherin. **B**, Effect of TV and GF extracts in protein expression of Vimentin (Hela cell line was used as positive control). **C**, Effect of TV and GF extracts in protein expression of N-Cadherin. **D**, Effect of TV and GF extracts in protein expression of Citokeratin-18. Data are the means ± SD of three independent experiments (*p<0.05, **p<0.01, ***p<0.001)

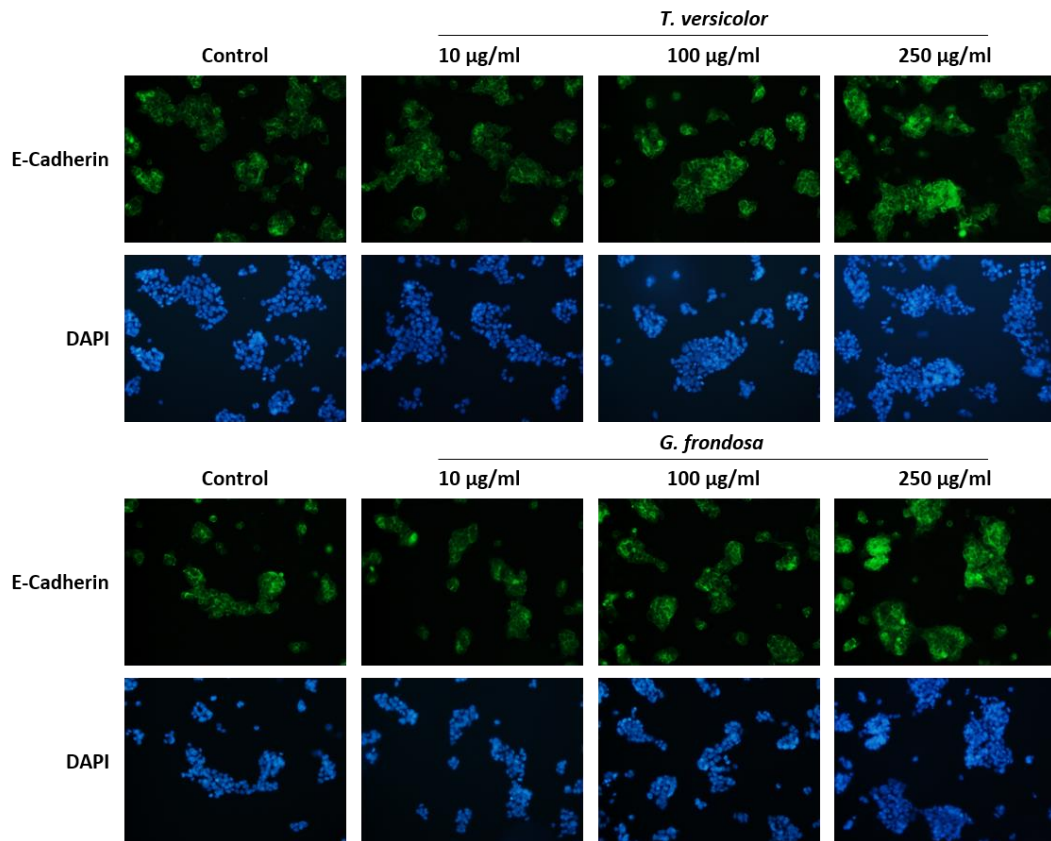


Figure 66. Effect of TV and GF extracts on protein expression of E-Cadherin measured by Immunofluorescence. LoVo cells were treated with 10, 100 and 250 µg/ml for 72 h and then fixed before staining with primary and fluorophore-labelled secondary antibody. Nuclear staining with DAPI.

9. Effect of TV and GF extracts on mRNA expression of E-cadherin and their transcription repressors

The regulation of E-Cadherin, in addition to the protein level, can be regulated at a genetic and epigenetic level, with epigenetic mechanisms being much more common. Among these, the transcription factors Snail, Twist and Zeb stand out, they are capable of coordinating the repression of epithelial genes, such as E-Cadherin and the induction of mesenchymal genes.

Due to the effect saw over E-cadherin expression in LoVo cells under treatment with the extracts, we wanted to know if this regulation was at a transcriptional, post-

transcriptional or a post-translational level. For that we analysed the levels of expression of E-Cadherin mRNA by RT-qPCR.

We also analysed the expression of another three genes, +. These genes are transcriptional factors that regulate E-cadherin at a transcriptional level. Cells were treated for 48 h with different concentrations of the extracts 100 and 250 µg/ml and then they were collected and lysed for RNA extraction and purification. RNA was used for reverse transcription and transformed into cDNA.

Results show no marked effect of the extracts on E-Cadherin mRNA expression, only a slight reduction under *G. frondosa* treatment suggesting no apparent regulation of the extracts on E-cadherin at a transcriptional level. However, the analysis of E-cadherin transcriptional repressors, Twist2, Zeb1 and Snail1, showed an upregulation of them under treatment with the fungal extracts (**Figure 67**).

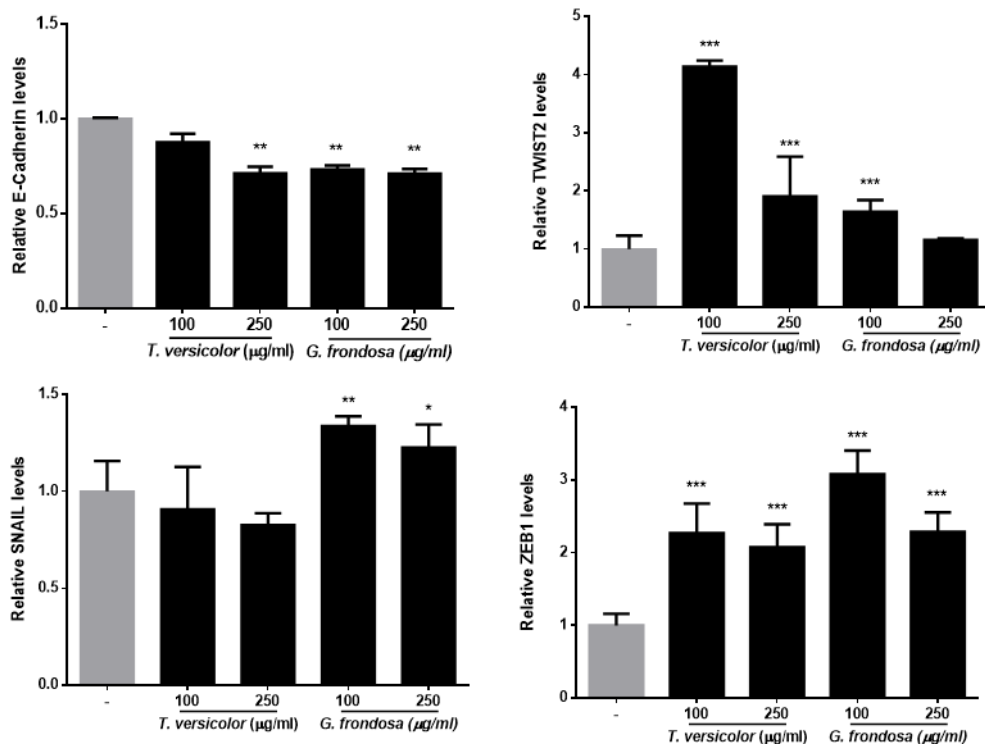


Figure 67. Effect of TV and GF extracts in mRNA expression of E-Cadherin and transcriptional factors measured by RT-qPCR. LoVo cells were treated with 100 and 250 µg/ml for 48 h and then cells were lysed for ARN extraction and purification. ARN expression was measured by RT-qPCR and data was processed with qbase software. Data are the means ± SD of three independent experiments (*p<0.05, **p<0.01 **p<0.001).

10. Effect of TV and GF extracts on the expression of cell cycle regulators pRb, p21 and CDK2

As the extracts had shown a significative effect over cell proliferation and viability as well as in the oncogenic potential of colorectal cancer cells, we hypothesized that some cell cycle regulator proteins may be regulated by these extracts and may be the responsible for the effect we detected.

We focused our scope in well described proteins with an important role in cell cycle control and that had been described as tumour suppressors or related with tumoral progression. Phosphorylated retinoblastoma protein (pRb) is a tumour suppressor protein altered in many types of cancer, normally prevents cell proliferation, blocking the progression of the cell cycle. P21 is regulated by the tumour suppressor gene p53, and it also acts by regulating G0/G1 cell cycle arrest. Finally, CDK2 is essential for the G1/S transition in the cell cycle. We analysed the expression of these three proteins by western blotting after treating the cells with different concentrations of the extracts. LoVo cells were treated for 72 h with 100 and 250 $\mu\text{g}/\text{mg}$ of TV and GF extracts and then collected and lysed for protein extraction.

Images obtained show an upregulation of p21 and pRb expression when treating with TV and GF extracts (**Figure 68**). This upregulation is seen with both concentrations used 100 and 250 $\mu\text{g}/\text{mg}$, although it was not statistically significative. However, CDK2 results did not show significant regulation one way or another by the treatment.

These results suggest that the antiproliferative and antitumoral effect showed by the extracts may be explained by the regulation of p21 and pRb.

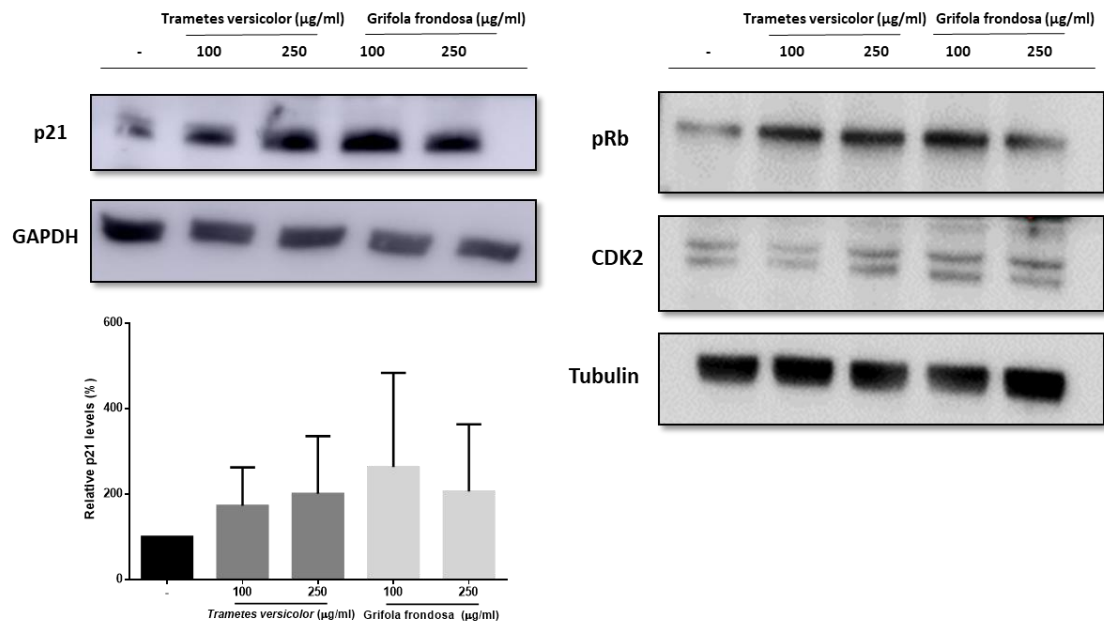


Figure 68. Effect of TV and GF extracts in protein expression of p21, pRb and CDK2 by Western blot. LoVo cells were treated with 100 and 250 µg/ml for 72 h and then lysed for protein extraction. Data are the means \pm SD of three independent experiments (* $p < 0.05$, ** $p < 0.01$, *** $p < 0.001$)

11. Effect of TV and GF extracts on metalloproteinase activity and mRNA expression

Continuing with our major objective of uncovering the mechanism that explained the effect of the extracts in colorectal cancer cells, we focussed our attention on the proteins involved in invasive process.

The degradation of the extracellular matrix (ECM) is known to be a crucial event in tumour "malignancy" and during tumour invasion and metastasis. Faced with the growth of the tumour mass, the degradative action of MMPs on the ECM is very important because it is capable of altering the cell-ECM and cell-cell junctions, favouring tissue invasion. In general, what MMPs do is create a favourable environment for tumour development, a microenvironment that promotes "malignancy." The expression of metalloproteinases is found at increased levels in human tumours and associated with their metastasis, and for this reason they are a target increasingly studied in antineoplastic therapies. MMP-2 and MMP-9 gelatinases are the two most members of

the MMP family and have been widely studied because of their constant association with tumour invasion and metastasis. For its study we performed two approaches by analysing on one hand the mRNA expression of MMP-2 and MMP-9 by RT-qPCR and on the other hand we performed a zymogram assay for evaluating enzyme activity. Zymography is an electrophoretic technique developed under non-reducing conditions with the objective of protecting enzyme structure and evaluate their proteolytic activity.

For zymography, culture medium was collected from LoVo cells after treatment with both fungal extracts at different concentrations 100 and 250 $\mu\text{g}/\text{mg}$ for 72 h. Samples were prepared for its loading in a special polyacrylamide gel containing gelatine. Decreased MMP-2 activity was detected after treatment with both fungal extracts (**Figure 69A**). Although both fungal extracts were able to induce a strong reduction in MMP-2 activity, this reduction was more prominent using the GF extract, achieving up to a 60% decrease in MMP-2 activity with concentration lowest tested at 100 $\mu\text{g}/\text{mg}$. MMP-9 activity was also regulated, but its detection was clearly lower than with MMP-2. Both extracts downregulated MMP-9 activity even though control cells MMP-9 activity was already very low. In fact, for the cells treated with the highest concentration of GF, MMP-9 completely disappeared.

For RT-qPCR cells were treated for 48 h with different concentrations of the extracts (100 and 250 $\mu\text{g}/\text{ml}$) and then they were collected and lysed for RNA extraction and purification. RNA was used for reverse transcription to convert it into cDNA. The results showed a significant increased expression of MMP-9 for both treatments and concentrations with the extracts but specially with the TV extract. MMP-2 mRNA expression was only increased under the treatment with GF extract at 250 $\mu\text{g}/\text{ml}$ (**Figure 69A, B**).

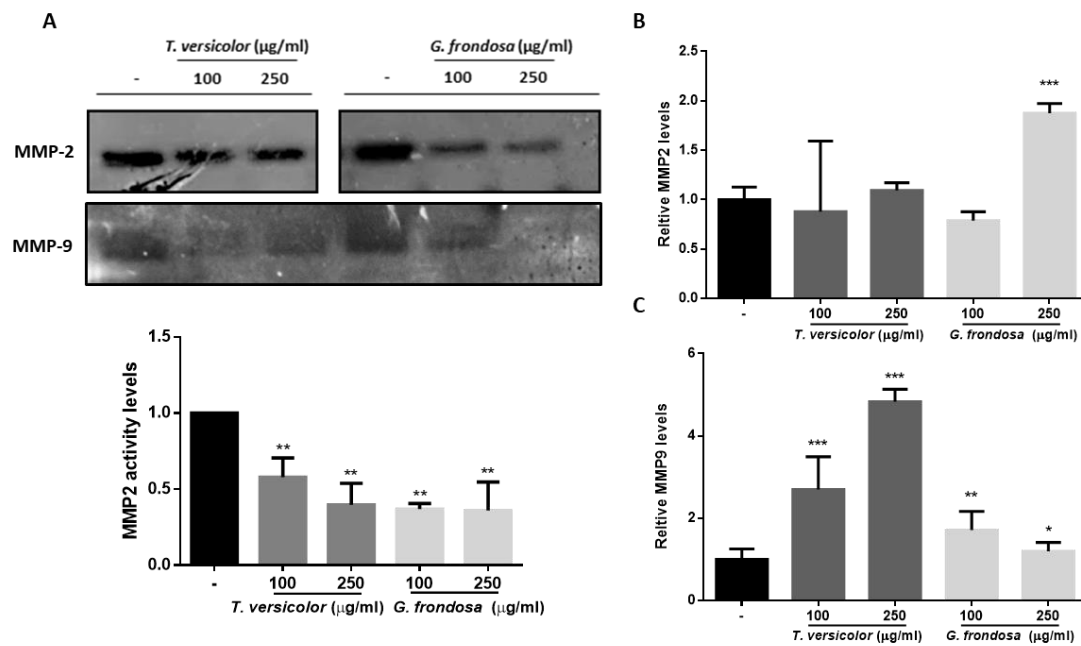


Figure 69. Effect of TV and GF extracts in metalloproteinase activity and mRNA expression. LoVo cells were treated with 100 and 250 µg/ml for 72 h and then culture medium was collected from these cells and processed for its analysis. **A**, Effect of TV and GF extracts in the MMP-2 and MMP-9 activity was measured by zymography. **B**, Effect of TV and GF extracts in mRNA expression of MMP-9. **C**, Effect of TV and GF extracts in mRNA expression of MMP-2. Data are the means ± SD of three independent experiments (*p<0.05, **p<0.01 ***p<0.001)

12. TV and GF extracts increases the effect of the chemotherapy drug 5-fluorouracil

Despite all the anti-tumoral effects that the extracts show in colorectal cancer cells we wanted to analyse whether TV and GF could be used in combination of established drug treatments commonly used in the treatment of colorectal cancer patients.

The combination of chemotherapy with other agents, such as natural products, has been widely studied (Herranz-López et al., 2018). However, the optimal combination regimen has not been determined. 5-fluorouracil (5-Fu) is a cytotoxic agent commonly used to treat patients with colon cancer in clinics. To see if the combination of TV and GF extracts with 5-Fu could be beneficial for the therapeutic output of colorectal cancer

cells we examined the cytotoxic effect of 250 µg/ml treatment with GF and TV extracts in combination with increasing concentrations of 5-Fu.

For that, LoVo cells were treated for 72h with increasing concentrations of 5-Fu (0.005, 0.01, 0.1 and 1 µg/ml) alone or in combination with a 250 µg/ml treatment of each extract. After that cell were assayed for MTT assay and cell viability was determined.

Results showed that at lower combination of 5-Fu concentrations (0.005 µg/ml) with the extracts significantly increases the cytotoxic effect of the cytotoxic agent (**Figure 70A, B**). Indeed, TV was the extract that produced the highest combination effect of the two extracts with an increase of about 20% in the reduction of colorectal cancer cell viability.

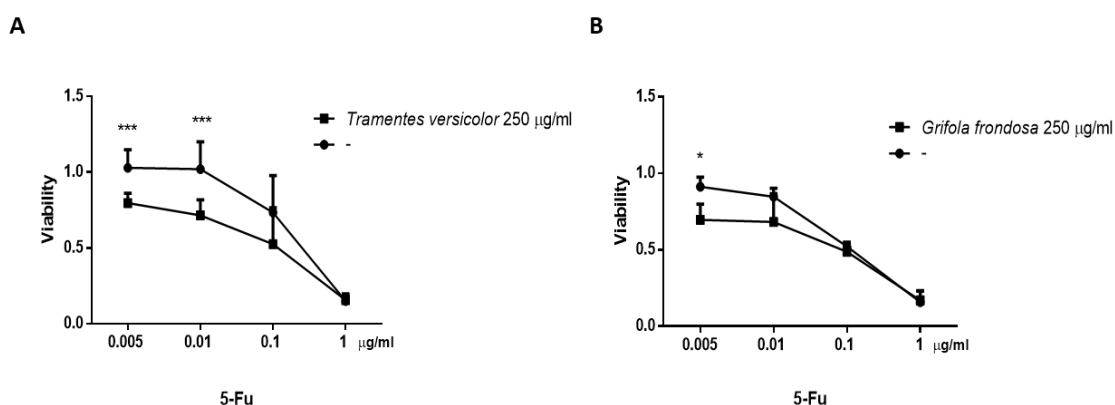


Figure 70. Effect of the combined treatment of TV and GF extracts in combination with 5-Fluorouracil on in colorectal cancer cell viability. LoVo cells were treated with increasing concentrations of 5-Fu (0.005, 0.01, 0.1 and 1 µg/ml) alone or in combination with a 250 µg/ml treatment of each extract for 72 h and then viability was measured by MTT assay. **A**, Effect of TV extract in cell viability in combination with different concentrations of 5-Fu. **B**, Effect of GF extract in cell viability in combination with different concentrations of 5-Fu. Data are the means ± SD of three independent experiments (*p<0.05, **p<0.01 ***p<0.001).

At the same time and despite the fact these extracts are obtained from edible fungal species that does not show any cell toxicity, we wanted to study if this cytotoxic effect was specific in cancer cells. For that, we carried out MTT assays using the same concentrations of the extracts used in the experiments but in this case using a normal

non-transformed epithelial cell line, Madin-Darby Canine Kidney (MDCK) cell line. MTT assay was performed with the same concentrations and time of treatment with each extract and the results showed no impact of any of the extracts at all the concentrations tested in cell viability (**Figure 71A**).

We also repeated the experiment in combination with 5-Fu to determine whether the combination of the extracts with the cytotoxic agent was specific in cancer cells and in non-tumour epithelial cells. The results of this experiment also show that the levels of cytotoxicity were not modified in non-tumour cells by the addition of TV and GF extracts (**Figure 71B, C**). This result suggests that the cytotoxic effect of the extracts is specific of tumoral cells and that at the concentrations tested are safe for healthy human cells.

Taken together, all the results indicate the *in vitro* anti-proliferative and anti-invasive effect of TV and GF extracts in colorectal cancer cells. The extracts exert this effect, at least in part, due to the upregulation of E-cadherin expression, the upregulation of cell cycle control proteins p21 and pRb and a reduction of MMP-9 and MMP-2 activity. Moreover, the extracts have the potential to improve their antitumor action when combined with 5-fluoracil, specially at a low dose.

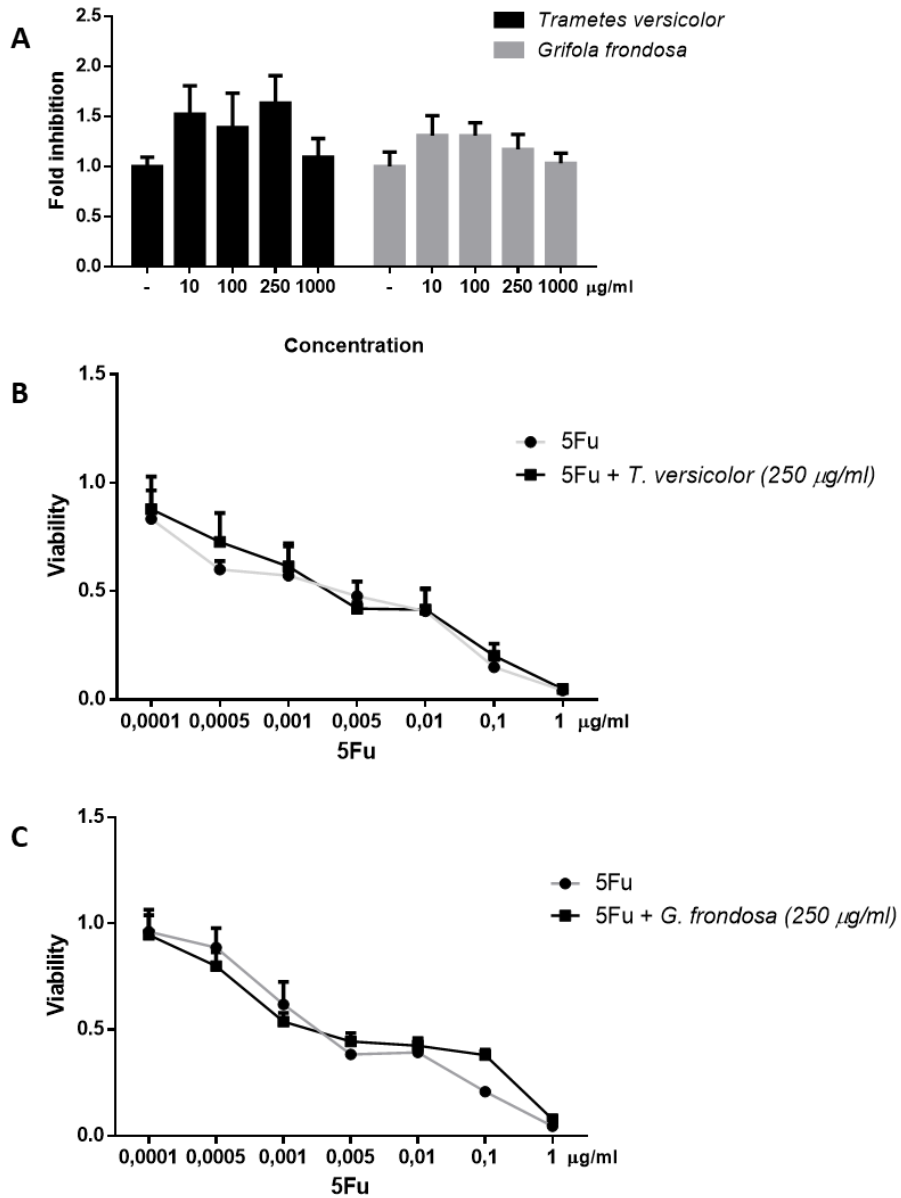


Figure 71. Effect of TV and GF extracts in non-transformed epithelial cells viability and in combination with 5-Fluorouracil. A, Effect of TV and GF extracts in MDCK cell viability when treated with 10, 100, 250 and 1000 µg/ml measured by MTT assay. **B,** Effect of TV extract in MDCK cell viability in combination with different concentrations of 5-Fu (0.0001, 0.0005, 0.001, 0.005, 0.01, 0.1 and 1 µg/ml). **C,** Effect of GF extract in MDCK cell viability in combination with different concentrations of 5-Fu (0.0001, 0.0005, 0.001, 0.005, 0.01, 0.1 and 1 µg/ml). Data are the means ± SD of three independent experiments (*p<0.05, **p<0.01 ***p<0.001)

Discussion: Chapter II

Fungal extracts have been shown to be a valuable source of natural bioactive compounds with potential pharmacological effects due to their proven antimicrobial, antiviral, antitumor, and antioxidant activities. Most of the pharmacological properties of fungi are due to the presence of polysaccharides and their derivatives in their composition (Moradali et al., 2007). The biological activity of polysaccharides as immunomodulators and antitumor agents has made that certain species of fungi have a special importance in the treatment of cancer (Hou et al., 2017; Saleh et al., 2017; Wenner et al., 2012). This importance is also due not only to the direct anticancer effect, but to its potential as adjuvants to classic treatments such as chemotherapy, radiotherapy, or immunotherapy (Rossi et al., 2018; H. Wang et al., 2017). In this work, we focus on the study of a series of fungal polysaccharide-rich extracts, obtained from autochthonous fungi of Galicia. Specifically, in its possible antitumor effect on colorectal cancer cells.

We started this study by evaluating the effect of all the extracts over the viability and the cell phenotype of colorectal cancer cells. From the initial 35 fungal extracts evaluated in the preliminary screening, only 2 of them were selected for further in-depth study given their cytotoxic effect and on the cell phenotype. The characterization of these two fungal extracts, belonging to the species *Grifola frondosa* and *Trametes versicolor*, included the analysis of their effect on multiple tumour characteristics, mainly those related to the EMT process. Some of these characteristics studied were cell proliferation, cell migration and invasion, or anchor-independent growth. In addition, the possible regulation of the main markers of EMT was studied when treated with both extracts, as well as their effect in combination with clinical reference chemotherapy drugs.

Our results suggest that these polysaccharide-rich extracts obtained from autochthonous strains of *Trametes versicolor* (TV) and *Grifola frondosa* (GF) may have a potential antitumor effect in human colon cancer cells lines. This antitumour effect was not only responsible for the inhibition of tumour cell proliferation but also in different EMT related mechanisms such as anchorage-independent cell growth, cell migration and

invasion that facilitate the metastatic process in multiple carcinoma types (Aparicio et al., 2015).

Although fungi exert their pharmacological actions through multiple pathways, one of the most studied is their direct cytotoxic action through the inhibition of cell proliferation (Evidente et al., 2014). In the initial screening that we conducted in the first phase of this work, it was observed that TV and GF extracts were capable of reducing the viability of colorectal cancer cells in values greater than 50% in concentration ranges that varied between 50 and 250 µg/ml at 72 h of treatment. In addition, in the specific case of TV and GF extracts, their effect on cell proliferation was also evaluated by BrdU, this effect being even more marked, reaching up to 80% reduction in proliferation even at low concentrations. This makes the extracts have a high potential inhibiting tumour growth while avoiding cytotoxic concentrations. These results are in line with the ones obtained in other studies with similar characteristics in which the antiproliferative effect of fungal extracts on various tumour cell lines (Hela, HEK293, SW1573) was confirmed (Couttolenc et al., 2016; Kumari et al., 2018; Queiroz et al., 2015). Some of these studies show an earlier effect in some of its extracts, with significant effects after 24 h of treatment. In our case, the effects on cell viability are not remarkable until after 72 h in the presence of the extract, even though it is already possible to appreciate a modest effect at earlier times (24 and 48 h). These observed differences between the effect of the extracts at early times do not seem to be linked to different mechanisms of action, but rather to a cytotoxic effect, since these extracts have also greater global cytotoxicity.

In our attempt to determine the molecular mechanism by which the extracts were capable of having a significant effect on the viability and proliferation of colorectal cancer cells, we confirmed the hypothesis that some cell cycle regulatory proteins were being affected by the extracts. Previous studies in other fungal extracts, and specifically in TV and GF, had already described that one of the mechanisms by which this type of extracts were capable of reducing cell viability and proliferation was by controlling proteins involved in regulating the cycle (Harhaji et al., 2008; Jiménez-Medina et al., 2008; Wan et al., 2010). Among the proteins identified as regulated by TV and GF extracts we could find Rb, p53 or p27 (C. Y. Ho et al., 2005; Tze Chen Hsieh & Wu, 2013; Rossi et al., 2018). Our results revealed that the treatment of LoVo cells with extracts

from TV and GF was able to upregulate the levels of protein expression of the proteins pRb and p21. These proteins are involved in the regulation of the cell cycle and control its progress in the G1/S and G2/M phases, in fact, mechanisms including disruption of cell cycle progression and arrest at G0, G0/G1, G1/S and G2/M phases has also been described (Ricciardi et al., 2017). However, other proteins such as CDK2 did not have significant regulation. These results suggest that the antiproliferative and antitumoral effect showed by the extracts may be explained by the regulation of p21 and pRb. This regulation in pRb expression after treatment with TV and GF extracts has also been observed in other types of cancer such as leukaemia and breast cancer (Tze Chen Hsieh & Wu, 2013; Rossi et al., 2018). However, other studies in which TV or GF extracts are used did not find p21 to be regulated (J. Jiang et al., 2012; Shomori et al., 2009). These studies, on the other hand, have used different extraction methods for the extracts and are focused on the study of gastric and breast cancer, not in colorectal cancer, so the results cannot be fully extrapolated.

Part of the 35 extracts analysed consisted of extracts of the same species obtained using different extraction methods. This had the objective of determining which of them could give rise to an extract with the greatest effect. The extraction method is vital to obtain the greatest possible amount of bioactive compounds and historically it has represented a bottleneck when using natural products in drug development (Q. W. Zhang et al., 2018). In our study, the attempts to improve the effectiveness of the initial 8 extracts by modifications to the extraction process were unsuccessful and their effectiveness was dramatically reduced. Moreover, these differences in the effectiveness of the extracts as a function of factors related to the extraction process such as time, temperature or the type of compound used for the extraction, were observable even among the 8 initial extracts themselves, in which the effectiveness of extracts belonging to the same species varied significantly.

Although the ability to sustain chronic proliferation is one of the characteristic features of cancer cells, it is not the only one. In fact, up to 8 hallmarks of cancer have been described (Hanahan & Weinberg, 2011). Among them, one stands out for its importance in the acquisition of malignancy by neoplastic cells, the activation of invasion and metastasis. In order for tumour cells to be able to progress to higher pathological

degrees of malignancy, they must acquire a series of key characteristics such as changes at the morphological level, the ability to migrate and invade adjacent tissues or independent growth of the extracellular matrix. Throughout our research, we were interested in determining whether TV and GF extracts could have some effect on these characteristics and therefore have an antitumor effect through this route. The properties of both GF and TV in the treatment of cancer have already been widely described. Among the antitumor properties that has been demonstrated from GF extracts would be, the induction of apoptosis by downregulation of Pi3k-Akt signalling (Soares et al., 2011), the blockade of neoplastic proliferation through the overexpression of P27 and PTEN (Rossi et al., 2018), the decrease in migratory and invasive capacity due to the increase of integrins $\alpha 2$ expression and the downmodulation of MMP-9 metalloproteinase (Alonso et al., 2013), and finally the induction of chemotherapy sensitivity (Rahman et al., 2011). From an immunomodulatory point of view, GF extracts rich in B-glucans demonstrated the inhibition of tumour growth through the activation of macrophages and dendritic cells responsible for the induction of helper and cytotoxic T cells (Masuda et al., 2013). This activation of macrophages was further described by Hou et al., who showed that this activation by *Grifola frondosa* extracts was due to its effect over TLR4, an upstream regulator of MyD88-IKK β -NF- κ B p65 pathway (Hou et al., 2017).

For TV there is also important evidence of the effects of its extracts over carcinogenesis. As well as GF it has immunomodulatory properties mainly linked to the induction of pro-inflammatory cytokines necessary for the activation of T lymphocytes (Pawlikowska et al., 2016). Among the molecular mechanisms involved in this induction would be the activation of Toll-like receptors TLR2 and TLR4 or the phosphorylation of transcription factors NF- κ B p65 and c-Jun (Z. Wang et al., 2015). TV extracts also proved to have direct toxicity over cancer cells through various mechanisms. It has been described that polysaccharopeptides from TV, promotes apoptosis via activation of caspase-3 and p38 MAPK (Hirahara et al., 2013). Other studies has shown the potential of these extracts as inhibitors of cell migration and invasion due to their effect as inhibitors of key angiogenic enzymes such as matrix metalloproteases (Luo et al., 2014) and down regulators of vascular endothelial cell growth factor (VEGF) expression (J. C. K. Ho et al., 2004).

In our study, the treatment with both GF and TV was able to significantly reduce the oncogenic potential of colorectal cancer cells as well as reduce their migratory and invasive capacities. The possible mechanism for these observed effects may be, at least in part, due to the recovery of the expression levels of the epithelial marker E-Cadherin in cells treated with these extracts. This fact is also supported by a clear phenotypic change in LoVo cells in the presence of both extracts. Tumour cells with a markedly mesenchymal phenotype revert to a much more epithelial phenotype with much closer cell-cell contacts. This type of phenotypic plasticity is, let us remember, one of the key elements of the EMT process, which is primarily responsible for the activation of tumour invasive and migrative capacities (Kalluri & Weinberg, 2009). More specifically, loss of E-cadherin during the acquisition of invasive characteristics has been linked to the metastatic process of colon tumour cells (Nieto, 2013; Ye & Weinberg, 2015). There are not many previous studies regarding the effect of fungal extracts on key epithelial markers in the EMT process. However, very recently, a study has been published in which a compound of fungal origin is capable of reversing EMT-imparted cancer stem cell features, at the same time that it inhibits the growth of breast tumour cells (Reisenauer et al., 2021). Specifically, this study describes how said fungal compound, ophiobolin A, has a greater effect on those cells that have undergone EMT and acts by altering cellular phenotypes, increasing sensitivity to chemotherapy, and suppressing growth of mammary cell tumours with exogenous TWIST-expression. Similar results have been reported in natural extracts obtained in this case from plants. Specifically, it has been observed that some of these extracts are capable of inhibiting EMT transcription factors such as SNAIL, TWIST and ZEB, regulators of E-Cadherin expression (Avila-Carrasco et al., 2019). Other authors demonstrated the ability to block the enhancement of cell migration by TGF- β 1 – induced EMT through recovering the loss of E-cadherin (Jo et al., 2015). Further investigations are needed to deepen the knowledge of the mechanisms that lead these extracts to be able to regulate the expression of E-cadherin. In any case, the analysis of the mRNA expression of both E-Cadherin and its transcription factors Twist, Zeb, and Snail, did not show a marked effect, suggesting that the extracts are not exerting a regulation at the transcriptional level.

Another possible mechanisms responsible for the effect of these extracts, particularly for the reduction in the invasive capacity of the cells, is the downregulation of the activity of the metalloproteinases MMP-2 and MMP-9. Metalloproteinases are responsible for degrading extracellular matrix and promote cell growth and invasion in colorectal cancer, also, low levels of MMP-2 have been associated with survival in breast carcinoma (Dong et al., 2011; López-Otín & Matrisian, 2007; Talvensaari-Mattila et al., 2003). We were able to analyse the effect of the extracts on the activity of these enzymes by zymography and we also evaluated their expression levels at the mRNA level. We observed by these means, a significant reduction in the enzymatic activity of both MMP-9 and MMP-2 in the presence of both extracts. However, this down-regulation did not take place at the level of mRNA expression. Taken together, the results suggest that TV and GF extracts directly or indirectly modulate the activity of these key enzymes in the invasive process (Radisky & Radisky, 2010) without modifying their overall protein expression in the cell. Some previous studies had already observed an effect of TV on metalloproteinases (Habtemariam, 2020; Saleh et al., 2017), but only describing their potential of reducing their expression at the protein level (Jędrzejewski et al., 2020). Others have reported effects of TV fungal extracts on the enzymatic activity of MMP-9 and MMP-2 in mouse mammary carcinoma and human pancreatic and gastric cancer cell lines (Luo et al., 2014; H. Zhang et al., 2000). Interestingly, in both studies it is shown that anti-migratory activity was not linked to anti-proliferative activity. Contrary we observed that GF and TV showed both anti-proliferative and anti-migratory action in human colon cancer cells. In our case, the results show that the treatment with the extracts also affects the activity of these enzymes. It has been reported that MMPs activity may be regulated at different levels such as transcription, mRNA half-life, secretion, localization, regulation by proteolytic cleavage, proteinase inhibitors or post-translational modification (such as phosphorylation, or acetylation) (Hadler-Olsen et al., 2011). However, further studies are needed to determine the potential mechanism by which metalloproteinase activity is regulated by these two TV and GF extracts.

Given the positive results obtained by the extracts in terms of their antitumor activity, it was proposed to evaluate their potential in combination with reference chemotherapeutic agents used in the clinical treatment of colorectal cancer. The

adjuvant treatment of chemotherapeutic agents together with other agents, such as compounds of natural origin, has been deeply studied (Herranz-López et al., 2018). As chemotherapeutic agent we used 5-Fluorouracil (5-FU) which is considered an essential component of systemic chemotherapy for colorectal cancer (CRC) in the palliative and adjuvant settings (Vodenkova et al., 2020). In this work, we showed that the combination of 5-FU treatment with TV and GF extracts significantly increases the cytotoxic effect of the chemotherapeutic agent, being this effect specific to tumour cells. Previous results of studies that have used TV and GF extracts for the treatment of cancer patients in conjunction with or in addition to other treatments, have already demonstrated the positive and synergistic effects of this combination. Specifically, a meta-study on TV involving 4,246 cancer patients show that it might have potential benefits on the overall survival and quality of life in cancer patients (Zhong et al., 2019). Another study in cancer patients using GF extract in combination with chemotherapy, demonstrated its ability to decrease the size of lung, liver, and breast tumours in cancer patients through the activation of NK cells (Kodama et al., 2003). Other studies have also documented synergistic effects while treating chemotherapeutic agents with TV and GF extracts. Specifically, the combination of 5-FU with GF extracts has been shown to increase the antitumor activity of 5-Fu in a mouse tumour model (G. Mao et al., 2018) as well as to accelerate the anticancer activity of 5-FU in human gastric carcinoma cells (B. J. Shi et al., 2007). Therefore, our results point out to a potential role of these extracts as adjuvants in the treatment of colorectal cancer with 5-FU. However, the potential antitumor effect of the polysaccharide-rich GF and TV extracts in other human cancer cells and in vivo model systems awaits to be elucidated. Future clinical trials will be needed to further evaluate safety and efficacy of these two newly developed GF and TV extracts.

Conclusions: Chapter II

1. Fungal extracts exerted different levels of inhibition on cell viability and proliferation in colon cancer cells.
2. *Extracts from Trametes versicolor (TV) and Grifola frondosa (GF) were selected given their effect on cell cytotoxicity and on a more epithelial cell-type phenotype.*
3. TV and GF extracts significantly inhibited oncogenic potential, cell migration and invasion in colon cancer cells.
4. TV and GF extracts increased expression of the E-cadherin epithelial marker and downregulated MMP-2 activity.
5. Combination of TV and GF extracts with the chemotherapy agent, 5-fluorouracil, increases cell cytotoxicity.

Bibliography

- Aamann, L., Vestergaard, E. M., & Grønbaek, H. (2014). Trefoil factors in inflammatory bowel disease. *World Journal of Gastroenterology*, *20*(12), 3223–3230.
<https://doi.org/10.3748/wjg.v20.i12.3223>
- Abdel-Azeem, A. M. (2010). The history, fungal biodiversity, conservation, and future perspectives for mycology in Egypt. *IMA Fungus*, *1*(2), 123–142.
<https://doi.org/10.5598/imafungus.2010.01.02.04>
- Abella, V., Valladares, M., Rodriguez, T., Haz, M., Blanco, M., Tarrío, N., Iglesias, P., Aparicio, L. A., & Figueroa, A. (2012). miR-203 Regulates Cell Proliferation through Its Influence on Hakai Expression. *PLoS ONE*, *7*(12).
<https://doi.org/10.1371/journal.pone.0052568>
- Alix-Panabières, C. (2020). The future of liquid biopsy. In *Nature* (Vol. 579, Issue 7800, p. S9). NLM (Medline). <https://doi.org/10.1038/d41586-020-00844-5>
- Alonso, E. N., Ferronato, M. J., Gandini, N. A., Fermento, M. E., Obiol, D. J., López Romero, A., Arévalo, J., Villegas, M. E., Facchinetti, M. M., & Curino, A. C. (2017). Antitumoral Effects of D-Fraction from *Grifola Frondosa* (Maitake) Mushroom in Breast Cancer. *Nutrition and Cancer*, *69*(1), 29–43.
<https://doi.org/10.1080/01635581.2017.1247891>
- Alonso, E. N., Orozco, M., Nieto, A. E., & Balogh, G. A. (2013). Genes related to suppression of malignant phenotype induced by maitake D-fraction in breast cancer cells. *Journal of Medicinal Food*, *16*(7), 602–617.
<https://doi.org/10.1089/jmf.2012.0222>
- Amin, M. B. et al. (2016). *AJCC Cancer Staging Manual 8th Edition*. Springer International Publishing.
- Aparicio, L. A., Abella, V., Valladares, M., & Figueroa, A. (2013). Posttranscriptional regulation by RNA-binding proteins during epithelial-to-mesenchymal transition. In *Cellular and Molecular Life Sciences* (Vol. 70, Issue 23, pp. 4463–4477).

<https://doi.org/10.1007/s00018-013-1379-0>

Aparicio, L. A., Blanco, M., Castosa, R., Concha, Á., Valladares, M., Calvo, L., & Figueroa, A. (2015). Clinical implications of epithelial cell plasticity in cancer progression. In *Cancer Letters* (Vol. 366, Issue 1, pp. 1–10). Elsevier Ireland Ltd.

<https://doi.org/10.1016/j.canlet.2015.06.007>

Aparicio, L. A., Valladares, M., Blanco, M., Alonso, G., & Figueroa, A. (2012). Biological influence of Hakai in cancer: A 10-year review. In *Cancer and Metastasis Reviews* (Vol. 31, Issues 1–2, pp. 375–386). Cancer Metastasis Rev.

<https://doi.org/10.1007/s10555-012-9348-x>

Avila-Carrasco, L., Majano, P., Sánchez-Tomé, J. A., Selgas, R., López-Cabrera, M., Aguilera, A., & González Mateo, G. (2019). Natural Plants Compounds as Modulators of Epithelial-to-Mesenchymal Transition. *Frontiers in Pharmacology*, 10. <https://doi.org/10.3389/fphar.2019.00715>

Bahman, A. A., Abaza, M. S. I., Khoushiash, S. I., & Al-Attiyah, R. J. (2018). Sequence-dependent effect of sorafenib in combination with natural phenolic compounds on hepatic cancer cells and the possible mechanism of action. *International Journal of Molecular Medicine*, 42(3), 1695–1715.

<https://doi.org/10.3892/ijmm.2018.3725>

Bakhoun, S. F., Silkworth, W. T., Nardi, I. K., Nicholson, J. M., Compton, D. A., & Cimini, D. (2014). The mitotic origin of chromosomal instability. In *Current Biology* (Vol. 24, Issue 4). Curr Biol. <https://doi.org/10.1016/j.cub.2014.01.019>

Bartlett, K., & Eaton, S. (2004). Mitochondrial β -oxidation. In *European Journal of Biochemistry* (Vol. 271, Issue 3, pp. 462–469). Eur J Biochem.

<https://doi.org/10.1046/j.1432-1033.2003.03947.x>

Bawankar, P., Lence, T., Paolantoni, C., Hausmann, I. U., Kazlauskiene, M., Jacob, D., Heidelberger, J. B., Richter, F. M., Nallasivan, M. P., Morin, V., Kreim, N., Beli, P., Helm, M., Jinek, M., Soller, M., & Roignant, J. Y. (2021). Hakai is required for stabilization of core components of the m6A mRNA methylation machinery. *Nature Communications*, 12(1), 1–15. <https://doi.org/10.1038/s41467-021-23892->

- Benjamin, J. L., Sumpter, R., Levine, B., & Hooper, L. V. (2013). Intestinal epithelial autophagy is essential for host defense against invasive bacteria. *Cell Host and Microbe*, *13*(6), 723–734. <https://doi.org/10.1016/j.chom.2013.05.004>
- Bennike, T. B., Carlsen, T. G., Ellingsen, T., Bonderup, O. K., Glerup, H., Bøgsted, M., Christiansen, G., Birkelund, S., Stensballe, A., & Andersen, V. (2015). Neutrophil extracellular traps in ulcerative colitis: A proteome analysis of intestinal biopsies. *Inflammatory Bowel Diseases*, *21*(9), 2052–2067. <https://doi.org/10.1097/MIB.0000000000000460>
- Berkhout, M., Gosens, M. J. E. M., Brouwer, K. M., Peters, W. H. M., Nagengast, F. M., van Krieken, J. H. J. M., & Nagtegaal, I. D. (2006). Loss of extracellular E-cadherin in the normal mucosa of duodenum and colon of patients with familial adenomatous polyposis. *Human Pathology*, *37*(11), 1389–1399. <https://doi.org/10.1016/j.humpath.2006.05.018>
- Bernardo, D., Marin, A. C., Fernández-Tomé, S., Montalban-Arques, A., Carrasco, A., Tristán, E., Ortega-Moreno, L., Mora-Gutiérrez, I., Díaz-Guerra, A., Caminero-Fernández, R., Miranda, P., Casals, F., Caldas, M., Jiménez, M., Casabona, S., De La Morena, F., Esteve, M., Santander, C., Chaparro, M., & Gisbert, J. P. (2018). Human intestinal pro-inflammatory CD11c^{high}CCR2⁺CX3CR1⁺ macrophages, but not their tolerogenic CD11c⁻CCR2⁻CX3CR1⁻ counterparts, are expanded in inflammatory bowel disease article. *Mucosal Immunology*, *11*(4), 1114–1126. <https://doi.org/10.1038/s41385-018-0030-7>
- Blagodatski, A., Yatsunskaya, M., Mikhailova, V., Tiasto, V., Kagansky, A., & Katanaev, V. L. (2018). Medicinal mushrooms as an attractive new source of natural compounds for future cancer therapy. *Oncotarget*, *9*(49), 29259–29274. <https://doi.org/10.18632/oncotarget.25660>
- Boltin, D., Perets, T. T., Vilkin, A., & Niv, Y. (2013). Mucin function in inflammatory bowel disease: An update. In *Journal of Clinical Gastroenterology* (Vol. 47, Issue 2, pp. 106–111). J Clin Gastroenterol. <https://doi.org/10.1097/MCG.0b013e3182688e73>

- Borren, N. Z., Conway, G., Garber, J. J., Khalili, H., Budree, S., Mallick, H., Yajnik, V., Xavier, R. J., & Ananthakrishnan, A. N. (2018). Differences in clinical course, genetics, and the microbiome between familial and sporadic inflammatory bowel diseases. *Journal of Crohn's and Colitis*, *12*(5), 525–531.
<https://doi.org/10.1093/ecco-jcc/jjx154>
- Botaille, F., Rohrmeier, C., Bates, R., Weber, A., Reider, F., Brenmoehl, J., Strauch, U., Farkas, S., Fürst, A., Hofstätter, F., Schölmerich, J., Herfarth, H., & Rogler, G. (2008). Evidence for a role of epithelial mesenchymal transition during pathogenesis of fistulae in Crohn's disease. *Inflammatory Bowel Diseases*, *14*(11), 1514–1527. <https://doi.org/10.1002/ibd.20590>
- Botteri, E., Iodice, S., Bagnardi, V., Raimondi, S., Lowenfels, A. B., & Maisonneuve, P. (2008). Smoking and colorectal cancer: A meta-analysis. In *JAMA - Journal of the American Medical Association* (Vol. 300, Issue 23, pp. 2765–2778). JAMA.
<https://doi.org/10.1001/jama.2008.839>
- Bray, F., Ferlay, J., Soerjomataram, I., Siegel, R. L., Torre, L. A., & Jemal, A. (2018). Global cancer statistics 2018: GLOBOCAN estimates of incidence and mortality worldwide for 36 cancers in 185 countries. *CA: A Cancer Journal for Clinicians*, *68*(6), 394–424. <https://doi.org/10.3322/caac.21492>
- Breese, E. J., Michie, C. A., Nicholls, S. W., Murch, S. H., Williams, C. B., Domizio, P., Walker-Smith, J. A., & Macdonald, T. T. (1994). Tumor necrosis factor α -producing cells in the intestinal mucosa of children with inflammatory bowel disease. *Gastroenterology*, *106*(6), 1455–1466. [https://doi.org/10.1016/0016-5085\(94\)90398-0](https://doi.org/10.1016/0016-5085(94)90398-0)
- Buckley, D., Duke, G., Heuer, T. S., O'Farrell, M., Wagman, A. S., McCulloch, W., & Kemble, G. (2017). Fatty acid synthase – Modern tumor cell biology insights into a classical oncology target. In *Pharmacology and Therapeutics* (Vol. 177, pp. 23–31). Elsevier Inc. <https://doi.org/10.1016/j.pharmthera.2017.02.021>
- BYERRUM, R. U., CLARKE, D. A., LUCAS, E. H., RINGLER, R. L., STEVENS, J. A., & STOCK, C. C. (1957). Tumor inhibitors in *Boletus edulis* and other *Holobasidiomycetes*. *Antibiotics & Chemotherapy (Northfield, Ill.)*, *7*(1), 1–4.

- Cabrera, O., Berman, D. M., Kenyon, N. S., Ricordi, C., Berggren, P. O., & Caicedo, A. (2006). The unique cytoarchitecture of human pancreatic islets has implications for islet cell function. *Proceedings of the National Academy of Sciences of the United States of America*, *103*(7), 2334–2339.
<https://doi.org/10.1073/pnas.0510790103>
- Camoglio, L., Te Velde, A. A., Tigges, A. J., Das, P. K., & Van Deventer, S. J. H. (1998). Altered Expression of Interferon- γ and Interleukin-4 in Inflammatory Bowel Disease. *Inflammatory Bowel Diseases*, *4*(4), 285–290.
<https://doi.org/10.1097/00054725-199811000-00005>
- Canavan, C., Abrams, K. R., & Mayberry, J. (2006). Meta-analysis: Colorectal and small bowel cancer risk in patients with Crohn's disease. *Alimentary Pharmacology and Therapeutics*, *23*(8), 1097–1104. <https://doi.org/10.1111/j.1365-2036.2006.02854.x>
- Cancer Today*. (n.d.). Retrieved May 28, 2020, from https://gco.iarc.fr/today/online-analysis-multi-bars?v=2018&mode=cancer&mode_population=countries&population=900&populations=900&key=asr&sex=0&cancer=39&type=0&statistic=5&prevalence=0&population_group=0&ages_group%5B%5D=0&ages_group%5B%5D=17&nb_items=10&group_cancer=1&include_nmsc=1&include_nmsc_other=1&type_multiple=%257B%2522inc%2522%253Atrue%252C%2522mort%2522%253Afalse%252C%2522prev%2522%253Afalse%257D&orientation=horizontal&type_sort=0&type_nb_items=%257B%2522top%2522%253Atrue%252C%2522bottom%2522%253Afalse%257D&population_group_globocan_id=
- Cao, Y., Xu, X., Liu, S., Huang, L., & Gu, J. (2018). Ganoderma: A cancer immunotherapy review. *Frontiers in Pharmacology*, *9*(OCT).
<https://doi.org/10.3389/fphar.2018.01217>
- Castosa, R., Martinez-Iglesias, O., Roca-Lema, D., Casas-Pais, A., Díaz-Díaz, A., Iglesias, P., Santamarina, I., Grana, B., Calvo, L., Valladares-Ayerbes, M., Concha, Á., & Figueroa, A. (2018). Hakai overexpression effectively induces tumour progression and metastasis in vivo. *Scientific Reports*, *8*(1). <https://doi.org/10.1038/s41598->

- Cenac, N., Andrews, C. N., Holzhausen, M., Chapman, K., Cottrell, G., Andrade-Gordon, P., Steinhoff, M., Barbara, G., Beck, P., Bunnett, N. W., Sharkey, K. A., Ferraz, J. G. P., Shaffer, E., & Vergnolle, N. (2007). Role for protease activity in visceral pain in irritable bowel syndrome. *Journal of Clinical Investigation*, *117*(3), 636–647. <https://doi.org/10.1172/JCI29255>
- Chang, Y., Zhang, M., Jiang, Y., Liu, Y., Luo, H., Hao, C., Zeng, P., & Zhang, L. (2017). Preclinical and clinical studies of coriolus versicolor polysaccharopeptide as an immunotherapeutic in China. *Discovery Medicine*, *23*(127).
- Chassaing, B., Aitken, J. D., Malleshappa, M., & Vijay-Kumar, M. (2014). Dextran sulfate sodium (DSS)-induced colitis in mice. *Current Protocols in Immunology*, *104*(SUPPL.104), Unit. <https://doi.org/10.1002/0471142735.im1525s104>
- Chassaing, B., Koren, O., Goodrich, J. K., Poole, A. C., Srinivasan, S., Ley, R. E., & Gewirtz, A. T. (2015). Dietary emulsifiers impact the mouse gut microbiota promoting colitis and metabolic syndrome. *Nature*, *519*(7541), 92–96. <https://doi.org/10.1038/nature14232>
- Chaturvedi, V. K., Agarwal, S., Gupta, K. K., Ramteke, P. W., & Singh, M. P. (2018). Medicinal mushroom: boon for therapeutic applications. In *3 Biotech* (Vol. 8, Issue 8). Springer Verlag. <https://doi.org/10.1007/s13205-018-1358-0>
- Chauhan, P. S., Kumarasamy, M., Sosnik, A., & Danino, D. (2019). Enhanced Thermostability and Anticancer Activity in Breast Cancer Cells of Laccase Immobilized on Pluronic-Stabilized Nanoparticles. *ACS Applied Materials and Interfaces*, *11*(43), 39436–39448. <https://doi.org/10.1021/acsami.9b11877>
- Chen, D., Frezza, M., Schmitt, S., Kanwar, J., & P. Dou, Q. (2011). Bortezomib as the First Proteasome Inhibitor Anticancer Drug: Current Status and Future Perspectives. *Current Cancer Drug Targets*, *11*(3), 239–253. <https://doi.org/10.2174/156800911794519752>
- Chen, Shaodan, Yong, T., Zhang, Y., Su, J., Jiao, C., & Xie, Y. (2017). Anti-tumor and Anti-angiogenic Ergosterols from *Ganoderma lucidum*. *Frontiers in Chemistry*, *5*.

<https://doi.org/10.3389/fchem.2017.00085>

- Chen, Shuping, Liu, C., Huang, X., Hu, L., Huang, Y., Chen, H., Fang, Q., Dong, N., Li, M., Tang, W., & Nie, S. (2020). Comparison of immunomodulatory effects of three polysaccharide fractions from *Lentinula edodes* water extracts. *Journal of Functional Foods*, *66*, 103791. <https://doi.org/10.1016/j.jff.2020.103791>
- Chen, W., Tan, H., Liu, Q., Zheng, X., Zhang, H., Liu, Y., & Xu, L. (2019). A review: The bioactivities and pharmacological applications of *phellinus linteus*. In *Molecules* (Vol. 24, Issue 10). MDPI AG. <https://doi.org/10.3390/molecules24101888>
- Chen, W. Y., Chang, C. Y., Li, J. R., Wang, J. Der, Wu, C. C., Kuan, Y. H., Liao, S. L., Wang, W. Y., & Chen, C. J. (2018). Anti-inflammatory and neuroprotective effects of fungal immunomodulatory protein involving microglial inhibition. *International Journal of Molecular Sciences*, *19*(11). <https://doi.org/10.3390/ijms19113678>
- Chen, Y., Yang, B., Ross, R. P., Jin, Y., Stanton, C., Zhao, J., Zhang, H., & Chen, W. (2019). Orally Administered CLA Ameliorates DSS-Induced Colitis in Mice via Intestinal Barrier Improvement, Oxidative Stress Reduction, and Inflammatory Cytokine and Gut Microbiota Modulation. *Journal of Agricultural and Food Chemistry*, *67*(48), 13282–13298. <https://doi.org/10.1021/acs.jafc.9b05744>
- Chihara, G., Hamuro, J., Maeda, Y. Y., Arai, Y., & Fukuoka, F. (1970). Fractionation and Purification of the Polysaccharides with Marked Antitumor Activity, Especially Lentinan, from *Lentinus edodes* (Berk.) Sing. (an Edible Mushroom). *Cancer Research*, *30*(11), 2776–2781.
- Christou, N., Perraud, A., Blondy, S., Jauberteau, M. O., Battu, S., & Mathonnet, M. (2017). E-cadherin: A potential biomarker of colorectal cancer prognosis. In *Oncology Letters* (Vol. 13, Issue 6, pp. 4571–4576). Spandidos Publications. <https://doi.org/10.3892/ol.2017.6063>
- Chung, C.-H., Yeh, S.-C., Chen, C.-J., & Lee, K.-T. (2014). Coenzyme Q0 from *Antrodia cinnamomea* in Submerged Cultures Induces Reactive Oxygen Species-Mediated Apoptosis in A549 Human Lung Cancer Cells. *Evidence-Based Complementary and Alternative Medicine : ECAM*, *2014*. <https://doi.org/10.1155/2014/246748>

- Cleynen, I., Vazeille, E., Artieda, M., Verspaget, H. W., Szczypiorska, M., Bringer, M. A., Lakatos, P. L., Seibold, F., Parnell, K., Weersma, R. K., Mahachie John, J. M., Morgan-Walsh, R., Staelens, D., Arijs, I., De Hertogh, G., Müller, S., Tordai, A., Hommes, D. W., Ahmad, T., ... Darfeuille-Michaud, A. (2014). Genetic and microbial factors modulating the ubiquitin proteasome system in inflammatory bowel disease. In *Gut* (Vol. 63, Issue 8, pp. 1265–1274). BMJ Publishing Group. <https://doi.org/10.1136/gutjnl-2012-303205>
- Coelho, L. C. B. B., Silva, P. M. D. S., Lima, V. L. de M., Pontual, E. V., Paiva, P. M. G., Napoleão, T. H., & Correia, M. T. D. S. (2017). Lectins, Interconnecting Proteins with Biotechnological/Pharmacological and Therapeutic Applications. *Evidence-Based Complementary and Alternative Medicine : ECAM*, 2017, 1594074. <https://doi.org/10.1155/2017/1594074>
- COLORECTAL CANCER | *Harrison's Manual of Medicine*. (n.d.). Retrieved May 2, 2021, from https://harrisons.unboundmedicine.com/harrisons/view/Harrisons-Manual-of-Medicine/623689/all/COLORECTAL_CANCER
- Consolazio, A., Alò, P. L., Rivera, M., Iacopini, F., Paoluzi, O. A., Crispino, P., Pica, R., & Paoluzi, P. (2006). Overexpression of fatty acid synthase in ulcerative colitis. *American Journal of Clinical Pathology*, 126(1), 113–118. <https://doi.org/10.1309/PUBVQNDNVQKJVC8M>
- COOK, A. H., & LACEY, M. S. (1945). Production of antibiotics by fungi. *British Journal of Experimental Pathology*, 26(6), 404–409.
- Cottet, V., Jooste, V., Fournel, I., Bouvier, A. M., Faivre, J., & Bonithon-Kopp, C. (2012). Long-term risk of colorectal cancer after adenoma removal: A population-based cohort study. *Gut*, 61(8), 1180–1186. <https://doi.org/10.1136/gutjnl-2011-300295>
- Couttolenc, A., Espinoza, C., Fernández, J. J., Norte, M., Plata, G. B., Padrón, J. M., Shnyreva, A., & Trigoso, Á. (2016). Antiproliferative effect of extract from endophytic fungus *Curvularia trifolii* isolated from the “Veracruz Reef System” in Mexico. *Pharmaceutical Biology*, 54(8), 1392–1397. <https://doi.org/10.3109/13880209.2015.1081254>

- Cunningham, K. G., Manson, W., Spring, F. S., & Hutchinson, S. A. (1950). Cordycepin, a Metabolic Product isolated from Cultures of *Cordyceps militaris* (Linn.) Link. In *Nature* (Vol. 166, Issue 4231, p. 949). Nature Publishing Group.
<https://doi.org/10.1038/166949a0>
- Dara, S. K., Montalva, C., & Barta, M. (2019). Microbial control of invasive forest pests with entomopathogenic fungi: A review of the current situation. In *Insects* (Vol. 10, Issue 10). MDPI AG. <https://doi.org/10.3390/insects10100341>
- Data explorer | ECIS. (n.d.). Retrieved May 28, 2020, from
https://ecis.jrc.ec.europa.eu/explorer.php?%0-0%1-AEE%2-All%4-1,2%3-All%6-0,85%5-2008,2008%7-7%CEstByCancer%X0_8-3%CEstRelativeCanc%X1_8-3%X1_9-AE28
- Daulagala, A. C., Bridges, M. C., & Kourtidis, A. (2019). E-cadherin beyond structure: A signaling hub in colon homeostasis and disease. In *International Journal of Molecular Sciences* (Vol. 20, Issue 11). MDPI AG.
<https://doi.org/10.3390/ijms20112756>
- Davis, M. M. (2008). A Prescription for Human Immunology. In *Immunity* (Vol. 29, Issue 6, pp. 835–838). Immunity. <https://doi.org/10.1016/j.immuni.2008.12.003>
- De Robertis, M., Massi, E., Poeta, M., Carotti, S., Morini, S., Cecchetelli, L., Signori, E., & Fazio, V. (2011). The AOM/DSS murine model for the study of colon carcinogenesis: From pathways to diagnosis and therapy studies. *Journal of Carcinogenesis*, 10. <https://doi.org/10.4103/1477-3163.78279>
- De Souza, H. S. P., & Fiocchi, C. (2016). Immunopathogenesis of IBD: Current state of the art. In *Nature Reviews Gastroenterology and Hepatology* (Vol. 13, Issue 1, pp. 13–27). Nature Publishing Group. <https://doi.org/10.1038/nrgastro.2015.186>
- Decara, J., Rivera, P., López-Gamero, A. J., Serrano, A., Pavón, F. J., Baixeras, E., Rodríguez de Fonseca, F., & Suárez, J. (2020). Peroxisome Proliferator-Activated Receptors: Experimental Targeting for the Treatment of Inflammatory Bowel Diseases. In *Frontiers in Pharmacology* (Vol. 11, p. 730). Frontiers Media S.A. <https://doi.org/10.3389/fphar.2020.00730>

- Dekker, E., Tanis, P. J., Vleugels, J. L. A., Kasi, P. M., & Wallace, M. B. (2019). Colorectal cancer. In *The Lancet* (Vol. 394, Issue 10207, pp. 1467–1480). Lancet Publishing Group. [https://doi.org/10.1016/S0140-6736\(19\)32319-0](https://doi.org/10.1016/S0140-6736(19)32319-0)
- Deng, G., Lin, H., Seidman, A., Fornier, M., D'Andrea, G., Wesa, K., Yeung, S., Cunningham-Rundles, S., Vickers, A. J., & Cassileth, B. (2009). A phase I/II trial of a polysaccharide extract from *Grifola frondosa* (Maitake mushroom) in breast cancer patients: Immunological effects. *Journal of Cancer Research and Clinical Oncology*, *135*(9), 1215–1221. <https://doi.org/10.1007/s00432-009-0562-z>
- Díaz-Díaz, A., Casas-Pais, A., Calamia, V., Castosa, R., Martínez-Iglesias, O., Roca-Lema, D., Santamarina, I., Valladares-Ayerbes, M., Calvo, L., Chantada, V., & Figueroa, A. (2017). Proteomic Analysis of the E3 Ubiquitin-Ligase Hakai Highlights a Role in Plasticity of the Cytoskeleton Dynamics and in the Proteasome System. *Journal of Proteome Research*, *16*(8), 2773–2788. <https://doi.org/10.1021/acs.jproteome.7b00046>
- Díaz-Díaz, A., Roca-Lema, D., Casas-Pais, A., Romay, G., Colombo, G., Concha, Á., Graña, B., & Figueroa, A. (2020). Heat shock protein 90 chaperone regulates the E3 ubiquitin-ligase hakai protein stability. *Cancers*, *12*(1). <https://doi.org/10.3390/cancers12010215>
- Dienstmann, R., Vermeulen, L., Guinney, J., Kopetz, S., Tejpar, S., & Tabernero, J. (2017). Consensus molecular subtypes and the evolution of precision medicine in colorectal cancer. In *Nature Reviews Cancer* (Vol. 17, Issue 2, pp. 79–92). Nature Publishing Group. <https://doi.org/10.1038/nrc.2016.126>
- Dinallo, V., Marafini, I., Fusco, D. Di, Laudisi, F., Franzè, E., Grazia, A. Di, Figliuzzi, M. M., Caprioli, F., Stolfi, C., Monteleone, I., & Monteleone, G. (2019). Neutrophil extracellulartraps sustain inflammatory signals in ulcerative colitis. *Journal of Crohn's and Colitis*, *13*(6), 772–784. <https://doi.org/10.1093/ecco-jcc/jyy215>
- Dong, W., Li, H., Zhang, Y., Yang, H., Guo, M., Li, L., & Liu, T. (2011). Matrix metalloproteinase 2 promotes cell growth and invasion in colorectal cancer. *Acta Biochimica et Biophysica Sinica*, *43*(11), 840–848. <https://doi.org/10.1093/abbs/gmr085>

- Dongre, A., & Weinberg, R. A. (2019). New insights into the mechanisms of epithelial–mesenchymal transition and implications for cancer. In *Nature Reviews Molecular Cell Biology* (Vol. 20, Issue 2, pp. 69–84). Nature Publishing Group.
<https://doi.org/10.1038/s41580-018-0080-4>
- Donnet-Hughes, A., Schiffrin, E. J., & Turini, M. E. (2001). The intestinal mucosa as a target for dietary polyunsaturated fatty acids. *Lipids*, 36(9), 1043–1052.
<https://doi.org/10.1007/s11745-001-0815-4>
- Dubuquoy, L., Rousseaux, C., Thuru, X., Peyrin-Biroulet, L., Romano, O., Chavatte, P., Chamailard, M., & Desreumaux, P. (2006). PPAR γ as a new therapeutic target in inflammatory bowel diseases. In *Gut* (Vol. 55, Issue 9, pp. 1341–1349). BMJ Publishing Group. <https://doi.org/10.1136/gut.2006.093484>
- Dupre-Crochet, S., Figueroa, A., Hogan, C., Ferber, E. C., Bialucha, C. U., Adams, J., Richardson, E. C. N., & Fujita, Y. (2007). Casein Kinase 1 Is a Novel Negative Regulator of E-Cadherin-Based Cell-Cell Contacts. *Molecular and Cellular Biology*, 27(10), 3804–3816. <https://doi.org/10.1128/mcb.01590-06>
- Eaden, J. A., Abrams, K. R., & Mayberry, J. F. (2001). The risk of colorectal cancer in ulcerative colitis: A meta-analysis. *Gut*, 48(4), 526–535.
<https://doi.org/10.1136/gut.48.4.526>
- Eichele, D. D., & Kharbanda, K. K. (2017). Dextran sodium sulfate colitis murine model: An indispensable tool for advancing our understanding of inflammatory bowel diseases pathogenesis. In *World Journal of Gastroenterology* (Vol. 23, Issue 33, pp. 6016–6029). Baishideng Publishing Group Co., Limited.
<https://doi.org/10.3748/wjg.v23.i33.6016>
- Elisashvili, V. (2012). Submerged cultivation of medicinal mushrooms: Bioprocesses and products (review). *International Journal of Medicinal Mushrooms*, 14(3), 211–239. <https://doi.org/10.1615/IntJMedMushr.v14.i3.10>
- Eliza, W. L. Y., Fai, C. K., & Chung, L. P. (2012). Efficacy of Yun Zhi (*Coriolus versicolor*) on survival in cancer patients: systematic review and meta-analysis. *Recent Patents on Inflammation & Allergy Drug Discovery*, 6(1), 78–87.

<https://doi.org/10.2174/187221312798889310>

Elson, C. O., Sartor, R. B., Tennyson, G. S., & Riddell, R. H. (1995). Experimental models of inflammatory bowel disease. *Gastroenterology*, *109*(4), 1344–1367.

[https://doi.org/10.1016/0016-5085\(95\)90599-5](https://doi.org/10.1016/0016-5085(95)90599-5)

Engel, A. L., Sun, G. C., Gad, E., Rastetter, L. R., Strobe, K., Yang, Y., Dang, Y., Disis, M. L., & Lu, H. (2013). Protein-bound polysaccharide activates dendritic cells and enhances OVA-specific T cell response as vaccine adjuvant. *Immunobiology*, *218*(12), 1468–1476. <https://doi.org/10.1016/j.imbio.2013.05.001>

Evidente, A., Kornienko, A., Cimmino, A., Andolfi, A., Lefranc, F., Mathieu, V., & Kiss, R. (2014). Fungal metabolites with anticancer activity. In *Natural Product Reports* (Vol. 31, Issue 5, pp. 617–627). Royal Society of Chemistry.

<https://doi.org/10.1039/c3np70078j>

Fafián-Labora, J., Carpintero-Fernández, P., Jordan, S. J. D., Shikh-Bahaei, T., Abdullah, S. M., Mahenthiran, M., Rodríguez-Navarro, J. A., Niklison-Chirou, M. V., & O’Loughlen, A. (2019). FASN activity is important for the initial stages of the induction of senescence. *Cell Death and Disease*, *10*(4), 1–15.

<https://doi.org/10.1038/s41419-019-1550-0>

Fhu, C. W., & Ali, A. (2020). Fatty Acid Synthase: An Emerging Target in Cancer. In *Molecules* (Vol. 25, Issue 17). MDPI AG.

<https://doi.org/10.3390/molecules25173935>

Fickers, P., Benetti, P. H., Waché, Y., Marty, A., Mauersberger, S., Smit, M. S., & Nicaud, J. M. (2005). Hydrophobic substrate utilisation by the yeast *Yarrowia lipolytica*, and its potential applications. *FEMS Yeast Research*, *5*(6–7), 527–543.

<https://doi.org/10.1016/j.femsyr.2004.09.004>

Figueroa, A., Fujita, Y., & Gorospe, M. (2009). Hacking RNA: Hakai promotes tumorigenesis by enhancing the RNA-binding function of PSF. In *Cell Cycle* (Vol. 8, Issue 22, pp. 3648–3651). Taylor and Francis Inc.

<https://doi.org/10.4161/cc.8.22.9909>

Figueroa, A., Kotani, H., Toda, Y., Mazan-Mamczarz, K., Mueller, E. C., Otto, A., Disch,

- L., Norman, M., Ramdasi, R. M., Keshtgar, M., Gorospe, M., & Fujita, Y. (2009). Novel roles of Hakai in cell proliferation and oncogenesis. *Molecular Biology of the Cell*, *20*(15), 3533–3542. <https://doi.org/10.1091/mbc.E08-08-0845>
- Fischer, A., Zundler, S., Atreya, R., Rath, T., Voskens, C., Hirschmann, S., López-Posadas, R., Watson, A., Becker, C., Schuler, G., Neufert, C., Atreya, I., & Neurath, M. F. (2016). Differential effects of $\alpha 4\beta 7$ and GPR15 on homing of effector and regulatory T cells from patients with UC to the inflamed gut in vivo. *Gut*, *65*(10), 1642–1664. <https://doi.org/10.1136/gutjnl-2015-310022>
- Fleming, A. (1929). ON THE ANTIBACTERIAL ACTION OF CULTURES OF A PENICILLIUM, WITH SPECIAL REFERENCE TO THEIR USE IN THE ISOLATION OF B. INFLUENZÆ. In *British journal of experimental pathology* (Vol. 10, Issue 3). Wiley-Blackwell.
- Franceschini, A., Szklarczyk, D., Frankild, S., Kuhn, M., Simonovic, M., Roth, A., Lin, J., Minguéz, P., Bork, P., Von Mering, C., & Jensen, L. J. (2013). STRING v9.1: Protein-protein interaction networks, with increased coverage and integration. *Nucleic Acids Research*, *41*(D1). <https://doi.org/10.1093/nar/gks1094>
- Fujimoto, K., Kinoshita, M., Tanaka, H., Okuzaki, D., Shimada, Y., Kayama, H., Okumura, R., Furuta, Y., Narazaki, M., Tamura, A., Hatakeyama, S., Ikawa, M., Tsuchiya, K., Watanabe, M., Kumanogoh, A., Tsukita, S., & Takeda, K. (2017). Regulation of intestinal homeostasis by the ulcerative colitis-Associated gene RNF186. *Mucosal Immunology*, *10*(2), 446–459. <https://doi.org/10.1038/mi.2016.58>
- Fujita, Y., Krause, G., Scheffner, M., Zechner, D., Leddy, H. E. M., Behrens, J., Sommer, T., & Birchmeier, W. (2002). Hakai, a c-Cbl-like protein, ubiquitinates and induces endocytosis of the E-cadherin complex. *Nature Cell Biology*, *4*(3), 222–231. <https://doi.org/10.1038/ncb758>
- Fukuda, H., Iritani, N., Sugimoto, T., & Ikeda, H. (1999). Transcriptional regulation of fatty acid synthase gene by insulin/glucose, polyunsaturated fatty acid and leptin in hepatocytes and adipocytes in normal and genetically obese rats. *European Journal of Biochemistry*, *260*(2), 505–511. <https://doi.org/10.1046/j.1432-1327.1999.00183.x>

- Gang, X., Yang, Y., Zhong, J., Jiang, K., Pan, Y., Jeffrey Karnes, R., Zhang, J., Xu, W., Wang, G., & Huang, H. (2016). P300 acetyltransferase regulates fatty acid synthase expression, lipid metabolism and prostate cancer growth. *Oncotarget*, 7(12), 15135–15149. <https://doi.org/10.18632/oncotarget.7715>
- Gansler, T. S., Hardman, W., Hunt, D. A., Schaffel, S., & Hennigar, R. A. (1997). Increased expression of fatty acid synthase (OA-519) in ovarian neoplasms predicts shorter survival. *Human Pathology*, 28(6), 686–692. [https://doi.org/10.1016/S0046-8177\(97\)90177-5](https://doi.org/10.1016/S0046-8177(97)90177-5)
- Geng, X., Biancone, L., Hui Hui Dai, Lin, J. J. C., Yoshizaki, N., Dasgupta, A., Pallone, F., & Das, K. M. (1998). Tropomyosin isoforms in intestinal mucosa: Production of autoantibodies to tropomyosin isoforms in ulcerative colitis. *Gastroenterology*, 114(5), 912–922. [https://doi.org/10.1016/S0016-5085\(98\)70310-5](https://doi.org/10.1016/S0016-5085(98)70310-5)
- Genua, F., Raghunathan, V., Jenab, M., Gallagher, W. M., & Hughes, D. J. (2021). The Role of Gut Barrier Dysfunction and Microbiome Dysbiosis in Colorectal Cancer Development. In *Frontiers in Oncology* (Vol. 11, p. 1016). Frontiers Media S.A. <https://doi.org/10.3389/fonc.2021.626349>
- Geremia, A., & Arancibia-Cárcamo, C. V. (2017). Innate lymphoid cells in intestinal inflammation. In *Frontiers in Immunology* (Vol. 8, Issue OCT). Frontiers Media S.A. <https://doi.org/10.3389/fimmu.2017.01296>
- Gong, E. Y., Park, E., & Lee, K. (2010). Hakai acts as a coregulator of estrogen receptor alpha in breast cancer cells. *Cancer Science*, 101(9), 2019–2025. <https://doi.org/10.1111/j.1349-7006.2010.01636.x>
- Grady, W. M., & Carethers, J. M. (2008). Genomic and Epigenetic Instability in Colorectal Cancer Pathogenesis. In *Gastroenterology* (Vol. 135, Issue 4, pp. 1079–1099). W.B. Saunders. <https://doi.org/10.1053/j.gastro.2008.07.076>
- Guo, Y. J., Deng, G. F., Xu, X. R., Wu, S., Li, S., Xia, E. Q., Li, F., Chen, F., Ling, W. H., & Li, H. Bin. (2012). Antioxidant capacities, phenolic compounds and polysaccharide contents of 49 edible macro-fungi. *Food and Function*, 3(11), 1195–1205. <https://doi.org/10.1039/c2fo30110e>

- Habtemariam, S. (2020). *Trametes versicolor* (Synn. *Coriolus versicolor*) Polysaccharides in Cancer Therapy: Targets and Efficacy. *Biomedicines*, 8(5). <https://doi.org/10.3390/biomedicines8050135>
- Hadler-Olsen, E., Fadnes, B., Sylte, I., Uhlin-Hansen, L., & Winberg, J. O. (2011). Regulation of matrix metalloproteinase activity in health and disease. In *FEBS Journal* (Vol. 278, Issue 1, pp. 28–45). FEBS J. <https://doi.org/10.1111/j.1742-4658.2010.07920.x>
- Halfvarson, J., Brislawn, C. J., Lamendella, R., Vázquez-Baeza, Y., Walters, W. A., Bramer, L. M., D'Amato, M., Bonfiglio, F., McDonald, D., Gonzalez, A., McClure, E. E., Dunkleberger, M. F., Knight, R., & Jansson, J. K. (2017). Dynamics of the human gut microbiome in inflammatory bowel disease. *Nature Microbiology*, 2(5), 1–7. <https://doi.org/10.1038/nmicrobiol.2017.4>
- Hanahan, D., & Weinberg, R. A. (2011). Hallmarks of cancer: The next generation. In *Cell* (Vol. 144, Issue 5, pp. 646–674). Elsevier. <https://doi.org/10.1016/j.cell.2011.02.013>
- Harhaji, L., Mijatović, S., Maksimović-Ivanić, D., Stojanović, I., Momčilović, M., Maksimović, V., Tufegdžić, S., Marjanović, Ž., Mostarica-Stojković, M., Vučinić, Ž., & Stošić-Grujičić, S. (2008). Anti-tumor effect of *Coriolus versicolor* methanol extract against mouse B16 melanoma cells: In vitro and in vivo study. *Food and Chemical Toxicology*, 46(5), 1825–1833. <https://doi.org/10.1016/j.fct.2008.01.027>
- Hawksworth, D. L. (1991). The fungal dimension of biodiversity: magnitude, significance, and conservation. *Mycological Research*, 95(6), 641–655. [https://doi.org/10.1016/S0953-7562\(09\)80810-1](https://doi.org/10.1016/S0953-7562(09)80810-1)
- Hawksworth, David L., & Lücking, R. (2017). Fungal Diversity Revisited: 2.2 to 3.8 Million Species. *Microbiology Spectrum*, 5(4). <https://doi.org/10.1128/microbiolspec.funk-0052-2016>
- Hay, E. D. (1970). *Epithelial-mesenchymal interactions: 18th Hahnemann Symposium*. R. Fleischmajer and R. E. Billingham eds. Williams and Wilkins Co., Baltimore. 326 pp. 1968. 3(1), 100–101. <https://doi.org/10.1002/tera.1420030125>

- Hay, E. D. (1995). An overview of epithelio-mesenchymal transformation Hay, E. D. (1995). An overview of epithelio-mesenchymal transformation. In *Acta Anatomica* (Vol. 154, Issue 1, pp. 8–20). Acta Anat (Basel). <https://doi.org/10.1159/000147748>. In *Acta Anatomica* (Vol. 154, Issue 1, pp. 8–20). Acta Anat (Basel). <https://doi.org/10.1159/000147748>
- Hayday, A. C., & Peakman, M. (2008). The habitual, diverse and surmountable obstacles to human immunology research. In *Nature Immunology* (Vol. 9, Issue 6, pp. 575–580). Nature Publishing Group. <https://doi.org/10.1038/ni0608-575>
- Heerboth, S., Housman, G., Leary, M., Longacre, M., Byler, S., Lapinska, K., Willbanks, A., & Sarkar, S. (2015). EMT and tumor metastasis. *Clinical and Translational Medicine*, 4(1). <https://doi.org/10.1186/s40169-015-0048-3>
- Heimerl, S., Moehle, C., Zahn, A., Boettcher, A., Stremmel, W., Langmann, T., & Schmitz, G. (2006). Alterations in intestinal fatty acid metabolism in inflammatory bowel disease. *Biochimica et Biophysica Acta - Molecular Basis of Disease*, 1762(3), 341–350. <https://doi.org/10.1016/j.bbadis.2005.12.006>
- Henrikson, N. B., Webber, E. M., Goddard, K. A., Scrol, A., Piper, M., Williams, M. S., Zallen, D. T., Calonge, N., Ganiats, T. G., Janssens, A. C. J. W., Zauber, A., Lansdorp-Vogelaar, I., Van Ballegooijen, M., & Whitlock, E. P. (2015). Family history and the natural history of colorectal cancer: Systematic review. In *Genetics in Medicine* (Vol. 17, Issue 9, pp. 702–712). Nature Publishing Group. <https://doi.org/10.1038/gim.2014.188>
- Hensel, K. O., Boland, V., Postberg, J., Zilbauer, M., Heuschkel, R., Vogel, S., Gödde, D., Wirth, S., & Jenke, A. C. (2014). Differential expression of mucosal trefoil factors and mucins in pediatric inflammatory bowel diseases. *Scientific Reports*, 4(1), 1–5. <https://doi.org/10.1038/srep07343>
- Herranz-López, M., Losada-Echeberría, M., & Barrajón-Catalán, E. (2018). The Multitarget Activity of Natural Extracts on Cancer: Synergy and Xenohormesis. *Medicines*, 6(1), 6. <https://doi.org/10.3390/medicines6010006>
- Hershko, A., Ciechanover, A., Heller, H., Haas, A. L., & Rose, I. A. (1980). Proposed role

of ATP in protein breakdown: conjugation of protein with multiple chains of the polypeptide of ATP-dependent proteolysis. *Proceedings of the National Academy of Sciences of the United States of America*, 77(4), 1783–1786.

<https://doi.org/10.1073/pnas.77.4.1783>

Hershko, A., Ciechanover, A., & Rose, I. A. (1979). Resolution of the ATP dependent proteolytic system from reticulocytes: A component that interacts with ATP. *Proceedings of the National Academy of Sciences of the United States of America*, 76(7), 3107–3110. <https://doi.org/10.1073/pnas.76.7.3107>

Hirahara, N., Edamatsu, T., Fujieda, A., Fujioka, M., Wada, T., & Tajima, Y. (2013). Protein-bound polysaccharide-K induces apoptosis via mitochondria and p38 mitogen-activated protein kinase-dependent pathways in HL-60 promyelomonocytic leukemia cells. *Oncology Reports*, 30(1), 99–104. <https://doi.org/10.3892/or.2013.2412>

Ho, C. Y., Kim, C. F., Leung, K. N., Fung, K. P., Tse, T. F., Chan, H., & Lau, C. B. S. (2005). Differential anti-tumor activity of *Coriolus versicolor* (Yunzhi) extract through p53- and/or Bcl-2-dependent apoptotic pathway in human breast cancer cells. *Cancer Biology and Therapy*, 4(6), 638–644. <https://doi.org/10.4161/cbt.4.6.1721>

Ho, J. C. K., Konerding, M. A., Gaumann, A., Groth, M., & Liu, W. K. (2004). Fungal polysaccharopeptide inhibits tumor angiogenesis and tumor growth in mice. *Life Sciences*, 75(11), 1343–1356. <https://doi.org/10.1016/j.lfs.2004.02.021>

Hoeksma, J., Misset, T., Wever, C., Kemmink, J., Kruijtzter, J., Versluis, K., Liskamp, R. M. J., Boons, G. J., Heck, A. J. R., Boekhout, T., & den Hertog, J. (2019). A new perspective on fungal metabolites: identification of bioactive compounds from fungi using zebrafish embryogenesis as read-out. *Scientific Reports*, 9(1), 17546. <https://doi.org/10.1038/s41598-019-54127-9>

Horiuchi, K., Kawamura, T., Iwanari, H., Ohashi, R., Naito, M., Kodama, T., & Hamakubo, T. (2013). Identification of Wilms' tumor 1-associating protein complex and its role in alternative splicing and the cell cycle. *Journal of Biological Chemistry*, 288(46), 33292–33302. <https://doi.org/10.1074/jbc.M113.500397>

- Hou, L., Meng, M., Chen, Y., & Wang, C. (2017). A water-soluble polysaccharide from *Grifola frondosa* induced macrophages activation via TLR4-MyD88-IKK β -NF- κ B p65 pathways. *Oncotarget*, *8*(49), 86604–86614.
<https://doi.org/10.18632/oncotarget.21252>
- Hsieh, T. C., & Wu, J. M. (2001). Cell growth and gene modulatory activities of Yunzhi (Windsor Wunxi) from mushroom *Trametes versicolor* in androgen-dependent and androgen-insensitive human prostate cancer cells. *International Journal of Oncology*, *18*(1), 81–88. <https://doi.org/10.3892/ijo.18.1.81>
- Hsieh, Tze Chen, & Wu, J. M. (2013). Regulation of cell cycle transition and induction of apoptosis in HL-60 leukemia cells by the combination of *Coriolus versicolor* and *Ganoderma lucidum*. *International Journal of Molecular Medicine*, *32*(1), 251–257.
<https://doi.org/10.3892/ijmm.2013.1378>
- Hsu, D. K. W., Donohue, P. J., Alberts, G. F., & Winkles, J. A. (1993). Fibroblast growth factor-1 induces phosphofruktokinase, fatty acid synthase and Ca²⁺-ATPase mRNA expression in NIH 3T3 cells. *Biochemical and Biophysical Research Communications*, *197*(3), 1483–1491. <https://doi.org/10.1006/bbrc.1993.2644>
- Huang, Z., Wu, Y., Zhou, X., Xu, J., Zhu, W., Shu, Y., & Liu, P. (2014). Efficacy of therapy with bortezomib in solid tumors: A review based on 32 clinical trials. In *Future Oncology* (Vol. 10, Issue 10, pp. 1795–1807). Future Medicine Ltd.
<https://doi.org/10.2217/fon.14.30>
- Hwang, B. S., Lee, I. K., & Yun, B. S. (2016). Phenolic compounds from the fungus *Inonotus obliquus* and their antioxidant properties. *Journal of Antibiotics*, *69*(2), 108–110. <https://doi.org/10.1038/ja.2015.83>
- Inamura, K. (2018). Colorectal cancers: An update on their molecular pathology. In *Cancers* (Vol. 10, Issue 1). MDPI AG. <https://doi.org/10.3390/cancers10010026>
- Inoue, S., Nakase, H., Matsuura, M., Mikami, S., Ueno, S., Uza, N., & Chiba, T. (2009). The effect of proteasome inhibitor MG132 on experimental inflammatory bowel disease. *Clinical and Experimental Immunology*, *156*(1), 172–182.
<https://doi.org/10.1111/j.1365-2249.2008.03872.x>

- Ito, G., Tanaka, H., Ohira, M., Yoshii, M., Muguruma, K., Kubo, N., Yashiro, M., Yamada, N., Maeda, K., Sawada, T., & Hirakawa, K. (2012). Correlation between efficacy of PSK postoperative adjuvant immunochemotherapy for gastric cancer and expression of MHC class I. *Experimental and Therapeutic Medicine*, *3*(6), 925–930. <https://doi.org/10.3892/etm.2012.537>
- Ito, R., Shin-Ya, M., Kishida, T., Urano, A., Takada, R., Sakagami, J., Imanishi, J., Kita, M., Ueda, Y., Iwakura, Y., Kataoka, K., Okanoue, T., & Mazda, O. (2006). Interferon-gamma is causatively involved in experimental inflammatory bowel disease in mice. *Clinical and Experimental Immunology*, *146*(2), 330–338. <https://doi.org/10.1111/j.1365-2249.2006.03214.x>
- Itoh, Y., & Nagase, H. (2002). Matrix metalloproteinases in cancer. *Essays in Biochemistry*, *38*, 21–36. <https://doi.org/10.1042/bse0380021>
- Itzkowitz, S. H., & Yio, X. (2004). Inflammation and cancer - IV. Colorectal cancer in inflammatory bowel disease: The role of inflammation. In *American Journal of Physiology - Gastrointestinal and Liver Physiology* (Vol. 287, Issues 1 50-1). Am J Physiol Gastrointest Liver Physiol. <https://doi.org/10.1152/ajpgi.00079.2004>
- Ivashkiv, L. B. (2018). IFN γ : signalling, epigenetics and roles in immunity, metabolism, disease and cancer immunotherapy. In *Nature Reviews Immunology* (Vol. 18, Issue 9, pp. 545–558). Nature Publishing Group. <https://doi.org/10.1038/s41577-018-0029-z>
- Jackson, B. C., Nebert, D. W., & Vasiliou, V. (2010). Update of human and mouse matrix metalloproteinase families. *Human Genomics*, *4*(3), 194–201. <https://doi.org/10.1186/1479-7364-4-3-194>
- Jang, S. H., Park, J., Jang, S. H., Chae, S. W., Jung, S. J., So, B. O., Ha, K. C., Sin, H. S., & Jang, Y. S. (2016). In vitro stimulation of NK cells and lymphocytes using an extract prepared from mycelial culture of *Ophiocordyceps sinensis*. *Immune Network*, *16*(2), 140–145. <https://doi.org/10.4110/in.2016.16.2.140>
- Jankovic, D., Kugler, D. G., & Sher, A. (2010). IL-10 production by CD4⁺ effector T cells: A mechanism for self-regulation. In *Mucosal Immunology* (Vol. 3, Issue 3, pp. 239–

- 246). Nature Publishing Group. <https://doi.org/10.1038/mi.2010.8>
- Jayachandran, M., Xiao, J., & Xu, B. (2017). A critical review on health promoting benefits of edible mushrooms through gut microbiota. In *International Journal of Molecular Sciences* (Vol. 18, Issue 9). MDPI AG.
<https://doi.org/10.3390/ijms18091934>
- Jayachandran, U., Grey, H., & Cook, A. G. (2015). Nuclear factor 90 uses an ADAR2-like binding mode to recognize specific bases in dsRNA. *Nucleic Acids Research*, *44*(4), 1924–1936. <https://doi.org/10.1093/nar/gkv1508>
- Jędrzejewski, T., Piotrowski, J., Pawlikowska, M., Wrotek, S., & Kozak, W. (2019). Extract from *Coriolus versicolor* fungus partially prevents endotoxin tolerance development by maintaining febrile response and increasing IL-6 generation. *Journal of Thermal Biology*, *83*, 69–79.
<https://doi.org/10.1016/j.jtherbio.2019.05.005>
- Jędrzejewski, T., Sobocińska, J., Pawlikowska, M., Działuk, A., & Wrotek, S. (2020). Extract from the *coriolus versicolor* fungus as an anti-inflammatory agent with cytotoxic properties against endothelial cells and breast cancer cells. *International Journal of Molecular Sciences*, *21*(23), 1–17.
<https://doi.org/10.3390/ijms21239063>
- Jess, T., Rungoe, C., & Peyrin-Biroulet, L. (2012). Risk of Colorectal Cancer in Patients With Ulcerative Colitis: A Meta-analysis of Population-Based Cohort Studies. *Clinical Gastroenterology and Hepatology*, *10*(6), 639–645.
<https://doi.org/10.1016/j.cgh.2012.01.010>
- Jiang, H., Shen, J., & Ran, Z. (2018). Epithelial-mesenchymal transition in Crohn's disease. In *Mucosal Immunology* (Vol. 11, Issue 2, pp. 294–303). Nature Publishing Group. <https://doi.org/10.1038/mi.2017.107>
- Jiang, J., Thyagarajan-Sahu, A., Loganathan, J., Eliaz, I., Terry, C., Sandusky, G. E., & Sliva, D. (2012). BreastDefend™ prevents breast-to-lung cancer metastases in an orthotopic animal model of triple-negative human breast cancer. *Oncology Reports*, *28*(4), 1139–1145. <https://doi.org/10.3892/or.2012.1936>

- Jiang, W., Huang, H., Ding, L., Zhu, P., Saiyin, H., Ji, G., Zuo, J., Han, D., Pan, Y., Ding, D., Ma, X., Zhang, Y., Wu, J., Yi, Q., Liu, J. O., Huang, H., Dang, Y., & Yu, L. (2015). Regulation of cell cycle of hepatocellular carcinoma by NF90 through modulation of cyclin E1 mRNA stability. *Oncogene*, *34*(34), 4460–4470. <https://doi.org/10.1038/onc.2014.373>
- Jiao, S., Peters, U., Berndt, S., Brenner, H., Butterbach, K., Caan, B. J., Carlson, C. S., Chan, A. T., Chang-Claude, J., Chanock, S., Curtis, K. R., Duggan, D., Gong, J., Harrison, T. A., Hayes, R. B., Henderson, B. E., Hoffmeister, M., Kolonel, L. N., Le Marchand, L., ... Hsu, L. (2014). Estimating the heritability of colorectal cancer. *Human Molecular Genetics*, *23*(14), 3898–3905. <https://doi.org/10.1093/hmg/ddu087>
- Jiménez-Medina, E., Berruguilla, E., Romero, I., Algarra, I., Collado, A., Garrido, F., & Garcia-Lora, A. (2008). The immunomodulator PSK induces in vitro cytotoxic activity in tumour cell lines via arrest of cell cycle and induction of apoptosis. *BMC Cancer*, *8*, 78. <https://doi.org/10.1186/1471-2407-8-78>
- Jo, E., Park, S. J., Choi, Y. S., Jeon, W. K., & Kim, B. C. (2015). Kaempferol Suppresses Transforming Growth Factor- β 1-Induced Epithelial-to-Mesenchymal Transition and Migration of A549 Lung Cancer Cells by Inhibiting Akt1-Mediated Phosphorylation of Smad3 at Threonine-179. *Neoplasia (United States)*, *17*(7), 525–537. <https://doi.org/10.1016/j.neo.2015.06.004>
- Jodeleit, H., Milchram, L., Soldo, R., Beikircher, G., Schönthaler, S., Al-amodi, O., Wolf, E., Beigel, F., Weinhäusel, A., Siebeck, M., & Gropp, R. (2020). Autoantibodies as diagnostic markers and potential drivers of inflammation in ulcerative colitis. *PLOS ONE*, *15*(2), e0228615. <https://doi.org/10.1371/journal.pone.0228615>
- Jostins, L., Ripke, S., Weersma, R. K., Duerr, R. H., McGovern, D. P., Hui, K. Y., Lee, J. C., Philip Schumm, L., Sharma, Y., Anderson, C. A., Essers, J., Mitrovic, M., Ning, K., Cleynen, I., Theatre, E., Spain, S. L., Raychaudhuri, S., Goyette, P., Wei, Z., ... Whittaker, P. (2012). Host-microbe interactions have shaped the genetic architecture of inflammatory bowel disease. *Nature*, *491*(7422), 119–124. <https://doi.org/10.1038/nature11582>

JP, H., M, C., H, Z., S, L., JP, C., J, B., S, A., C, T., CA, O., M, G., V, B., Y, F., A, C., R, M., P, L.-P., C, G.-R., J, M., JF, C., M, S., & G, T. (2001). Association of NOD2 leucine-rich repeat variants with susceptibility to Crohn's disease. *Nature*, *411*(6837).

<https://doi.org/10.1038/35079107>

Junhee Seok, H. Shaw Warren, Alex, G. C., Michael, N. M., Henry, V. B., Xu, W., Richards, D. R., McDonald-Smith, G. P., Gao, H., Hennessy, L., Finnerty, C. C., López, C. M., Honari, S., Moore, E. E., Minei, J. P., Cuschieri, J., Bankey, P. E., Johnson, J. L., Sperry, J., ... Tompkins, R. G. (2013). Genomic responses in mouse models poorly mimic human inflammatory diseases. *Proceedings of the National Academy of Sciences of the United States of America*, *110*(9), 3507–3512.

<https://doi.org/10.1073/pnas.1222878110>

Kalluri, R., & Weinberg, R. A. (2009). The basics of epithelial-mesenchymal transition. In *Journal of Clinical Investigation* (Vol. 119, Issue 6, pp. 1420–1428). American Society for Clinical Investigation. <https://doi.org/10.1172/JCI39104>

Kang, Y., & Massagué, J. (2004). Epithelial-mesenchymal transitions: Twist in development and metastasis. In *Cell* (Vol. 118, Issue 3, pp. 277–279). Cell Press. <https://doi.org/10.1016/j.cell.2004.07.011>

Kedrin, D., & Gala, M. K. (2015). Genetics of the serrated pathway to colorectal cancer. In *Clinical and Translational Gastroenterology* (Vol. 6, Issue 4). Nature Publishing Group. <https://doi.org/10.1038/ctg.2015.12>

Keum, N. N., & Giovannucci, E. (2019). Global burden of colorectal cancer: emerging trends, risk factors and prevention strategies. In *Nature Reviews Gastroenterology and Hepatology* (Vol. 16, Issue 12, pp. 713–732). Nature Research. <https://doi.org/10.1038/s41575-019-0189-8>

Kiesler, P., Fuss, I. J., & Strober, W. (2001). Experimental models of inflammatory bowel diseases. In *Medicine et Hygiene* (Vol. 59, Issue 2332, pp. 241–248). Cell Mol Gastroenterol Hepatol. <https://doi.org/10.1016/j.jcmgh.2015.01.006>

Ko, C. H., Yue, G. G. L., Gao, S., Luo, K. W., Siu, W. S., Shum, W. T., Shiu, H. T., Lee, J. K. M., Li, G., Leung, P. C., Evdokiou, A., & Lau, C. B. S. (2017). Evaluation of the

- combined use of metronomic zoledronic acid and *Coriolus versicolor* in intratibial breast cancer mouse model. *Journal of Ethnopharmacology*, 204, 77–85.
<https://doi.org/10.1016/j.jep.2017.04.007>
- Kobayashi, T., Siegmund, B., Le Berre, C., Wei, S. C., Ferrante, M., Shen, B., Bernstein, C. N., Danese, S., Peyrin-Biroulet, L., & Hibi, T. (2020). Ulcerative colitis. *Nature Reviews Disease Primers*, 6(1), 1–20. <https://doi.org/10.1038/s41572-020-0205-x>
- Kodama, N., Komuta, K., & Nanba, H. (2003). Effect of Maitake (*Grifola frondosa*) D-Fraction on the Activation of NK Cells in Cancer Patients. *Journal of Medicinal Food*, 6(4), 371–377. <https://doi.org/10.1089/109662003772519949>
- Koido, S., Homma, S., Okamoto, M., Namiki, Y., Takakura, K., Takahara, A., Odahara, S., Tsukinaga, S., Yukawa, T., Mitobe, J., Matsudaira, H., Nagatsuma, K., Uchiyama, K., Kajihara, M., Arihiro, S., Imazu, H., Arakawa, H., Kan, S., Komita, H., ... Tajiri, H. (2013). Combined TLR2/4-Activated Dendritic/Tumor Cell Fusions Induce Augmented Cytotoxic T Lymphocytes. *PLoS ONE*, 8(3).
<https://doi.org/10.1371/journal.pone.0059280>
- Koundouros, N., & Poulgiannis, G. (2020). Reprogramming of fatty acid metabolism in cancer. In *British Journal of Cancer* (Vol. 122, Issue 1, pp. 4–22). Springer Nature.
<https://doi.org/10.1038/s41416-019-0650-z>
- Kuhajda, F. P., Jenner, K., Wood, F. D., Hennigar, R. A., Jacobs, L. B., Dick, J. D., & Pasternack, G. R. (1994). Fatty acid synthesis: A potential selective target for antineoplastic therapy. *Proceedings of the National Academy of Sciences of the United States of America*, 91(14), 6379–6383.
<https://doi.org/10.1073/pnas.91.14.6379>
- Kühn, R., Löhler, J., Rennick, D., Rajewsky, K., & Müller, W. (1993). Interleukin-10-deficient mice develop chronic enterocolitis. *Cell*, 75(2), 263–274.
[https://doi.org/10.1016/0092-8674\(93\)80068-P](https://doi.org/10.1016/0092-8674(93)80068-P)
- Kuipers, E. J., Grady, W. M., Lieberman, D., Seufferlein, T., Sung, J. J., Boelens, P. G., Van De Velde, C. J. H., & Watanabe, T. (2015). Colorectal cancer. *Nature Reviews Disease Primers*, 1(1), 1–25. <https://doi.org/10.1038/nrdp.2015.65>

- Kumari, M., Taritla, S., Sharma, A., & Jayabaskaran, C. (2018). Antiproliferative and antioxidative bioactive compounds in extracts of marine-derived endophytic fungus *Talaromyces purpureogenus*. *Frontiers in Microbiology*, *9*(AUG), 1777. <https://doi.org/10.3389/fmicb.2018.01777>
- Kuriakose, G. C., Lakshmanan M, D., BP, A., RS, H. K., TH, A. K., Ananthaswamy, K., & Jayabhaskaran, C. (2018). Extract of *Penicillium sclerotiorum* an endophytic fungus isolated from *Cassia fistula* L. induces cell cycle arrest leading to apoptosis through mitochondrial membrane depolarization in human cervical cancer cells. *Biomedicine and Pharmacotherapy*, *105*, 1062–1071. <https://doi.org/10.1016/j.biopha.2018.06.094>
- Kyrgiou, M., Kalliala, I., Markozannes, G., Gunter, M. J., Paraskevaidis, E., Gabra, H., Martin-Hirsch, P., & Tsilidis, K. K. (2017). Adiposity and cancer at major anatomical sites: Umbrella review of the literature. In *BMJ (Online)* (Vol. 356). BMJ Publishing Group. <https://doi.org/10.1136/bmj.j477>
- Langer, V., Vivi, E., Regensburger, D., Winkler, T. H., Waldner, M. J., Rath, T., Schmid, B., Skottke, L., Lee, S., Jeon, N. L., Wohlfahrt, T., Kramer, V., Tripal, P., Schumann, M., Kersting, S., Handtrack, C., Geppert, C. I., Suchowski, K., Adams, R. H., ... Stürzl, M. (2019). IFN- γ drives inflammatory bowel disease pathogenesis through VE-cadherin-directed vascular barrier disruption. *Journal of Clinical Investigation*, *129*(11), 4691–4707. <https://doi.org/10.1172/JCI124884>
- Lassen, K. G., & Xavier, R. J. (2017). Genetic control of autophagy underlies pathogenesis of inflammatory bowel disease. *Mucosal Immunology*, *10*(3), 589–597. <https://doi.org/10.1038/mi.2017.18>
- Lee, K.-C., Kuo, H.-C., Shen, C.-H., Lu, C.-C., Huang, W.-S., Hsieh, M.-C., Huang, C.-Y., Kuo, Y.-H., Hsieh, Y.-Y., Teng, C.-C., Lee, L.-Y., & Tung, S.-Y. (2017). A proteomics approach to identifying novel protein targets involved in erinacine A-mediated inhibition of colorectal cancer cells' aggressiveness. *Journal of Cellular and Molecular Medicine*, *21*(3), 588–599. <https://doi.org/10.1111/jcmm.13004>
- Leggett, B., & Whitehall, V. (2010). Role of the Serrated Pathway in Colorectal Cancer Pathogenesis. *Gastroenterology*, *138*(6), 2088–2100.

<https://doi.org/10.1053/j.gastro.2009.12.066>

- Liang, C., Tian, D., Liu, Y., Li, H., Zhu, J., Li, M., Xin, M., & Xia, J. (2019). Review of the molecular mechanisms of *Ganoderma lucidum* triterpenoids: Ganoderic acids A, C2, D, F, DM, X and Y. In *European Journal of Medicinal Chemistry* (Vol. 174, pp. 130–141). Elsevier Masson SAS. <https://doi.org/10.1016/j.ejmech.2019.04.039>
- Libertucci, J., Dutta, U., Kaur, S., Jury, J., Rossi, L., Fontes, M. E., Shajib, M. S., Khan, W. I., Surette, M. G., Verdu, E. F., & Armstrong, D. (2018). Inflammation-related differences in mucosa-associated microbiota and intestinal barrier function in colonic Crohn's disease. *American Journal of Physiology - Gastrointestinal and Liver Physiology*, *315*(3), G420–G431. <https://doi.org/10.1152/ajpgi.00411.2017>
- Lin, C. H., Chang, C. Y., Lee, K. R., Lin, H. J., Lin, W. C., Chen, T. H., & Wan, L. (2016). Cold-water extracts of *Grifola frondosa* and its purified active fraction inhibit hepatocellular carcinoma in vitro and in vivo. *Experimental Biology and Medicine*, *241*(13), 1374–1385. <https://doi.org/10.1177/1535370216640149>
- Lindequist, U., Niedermeyer, T. H. J., & Jülich, W.-D. (2005). The Pharmacological Potential of Mushrooms. *Evidence-Based Complementary and Alternative Medicine*, *2*, 906016. <https://doi.org/10.1093/ecam/neh107>
- Lissner, D., Schumann, M., Batra, A., Kredel, L. I., Köhl, A. A., Erben, U., May, C., Schulzke, J. D., & Siegmund, B. (2015). Monocyte and M1 macrophage-induced barrier defect contributes to chronic intestinal inflammation in IBD. *Inflammatory Bowel Diseases*, *21*(6), 1297–1305. <https://doi.org/10.1097/MIB.0000000000000384>
- Liu, M., Jiang, K., Lin, G., Liu, P., Yan, Y., Ye, T., Yao, G., Barr, M. P., Liang, D., Wang, Y., Gong, P., Meng, S., & Piao, H. (2018). Ajuba inhibits hepatocellular carcinoma cell growth via targeting of β -catenin and YAP signaling and is regulated by E3 ligase Hakai through neddylation. *Journal of Experimental and Clinical Cancer Research*, *37*(1). <https://doi.org/10.1186/s13046-018-0806-3>
- Liu, Y. N., Lee, W. W., Wang, C. Y., Chao, T. H., Chen, Y., & Ji, H. C. (2005). Regulatory mechanisms controlling human E-cadherin gene expression. *Oncogene*, *24*(56),

- 8277–8290. <https://doi.org/10.1038/sj.onc.1208991>
- Liu, Y. Q., Bai, G., Zhang, H., Su, D., Tao, D. C., Yang, Y., Ma, Y. X., & Zhang, S. Z. (2010). Human RING finger protein ZNF645 is a novel testis-specific E3 ubiquitin ligase. *Asian Journal of Andrology*, *12*(5), 658–666. <https://doi.org/10.1038/aja.2010.54>
- Liu, Zhendong, Li, L., & Xue, B. (2018). Effect of ganoderic acid D on colon cancer Warburg effect: Role of SIRT3/cyclophilin D. *European Journal of Pharmacology*, *824*, 72–77. <https://doi.org/10.1016/j.ejphar.2018.01.026>
- Liu, Zi, Wu, Y., Tao, Z., & Ma, L. (2018). E3 ubiquitin ligase Hakai regulates cell growth and invasion, and increases the chemosensitivity to cisplatin in non-small-cell lung cancer cells. *International Journal of Molecular Medicine*, *42*(2), 1145–1151. <https://doi.org/10.3892/ijmm.2018.3683>
- Locke, A., Schneiderhan, J., & Zick, S. M. (2018). Diets for Health: Goals and Guidelines. *American Family Physician*, *97*(11), 721–728.
- Loh, C. Y., Chai, J. Y., Tang, T. F., Wong, W. F., Sethi, G., Shanmugam, M. K., Chong, P. P., & Looi, C. Y. (2019). The E-Cadherin and N-Cadherin Switch in Epithelial-to-Mesenchymal Transition: Signaling, Therapeutic Implications, and Challenges. In *Cells* (Vol. 8, Issue 10). NLM (Medline). <https://doi.org/10.3390/cells8101118>
- López-Otín, C., & Matrisian, L. M. (2007). Emerging roles of proteases in tumour suppression. In *Nature Reviews Cancer* (Vol. 7, Issue 10, pp. 800–808). Nat Rev Cancer. <https://doi.org/10.1038/nrc2228>
- Lovisa, S., Genovese, G., & Danese, S. (2019). Role of Epithelial-to-Mesenchymal Transition in Inflammatory Bowel Disease. In *Journal of Crohn's and Colitis* (Vol. 13, Issue 5, pp. 659–668). Oxford University Press. <https://doi.org/10.1093/ecco-jcc/jjy201>
- Lu, C. C., Hsu, Y. J., Chang, C. J., Lin, C. S., Martel, J., Ojcius, D. M., Ko, Y. F., Lai, H. C., & Young, J. D. (2016). Immunomodulatory properties of medicinal mushrooms: Differential effects of water and ethanol extracts on NK cell-mediated cytotoxicity. *Innate Immunity*, *22*(7), 522–533. <https://doi.org/10.1177/1753425916661402>

- Lu, H., Yang, Y., Gad, E., Inatsuka, C., Wenner, C. A., Disis, M. L., & Standish, L. J. (2011). TLR2 agonist PSK activates human NK cells and enhances the antitumor effect of HER2-targeted monoclonal antibody therapy. *Clinical Cancer Research*, *17*(21), 6742–6753. <https://doi.org/10.1158/1078-0432.CCR-11-1142>
- Lu, H., Yang, Y., Gad, E., Wenner, C. A., Chang, A., Larson, E. R., Dang, Y., Martzen, M., Standish, L. J., & Disis, M. L. (2011). Polysaccharide krestin is a novel TLR2 agonist that mediates inhibition of tumor growth via stimulation of CD8 T cells and NK cells. *Clinical Cancer Research*, *17*(1), 67–76. <https://doi.org/10.1158/1078-0432.CCR-10-1763>
- Luo, K. W., Yue, G. G. L., Ko, C. H., Lee, J. K. M., Gao, S., Li, L. F., Li, G., Fung, K. P., Leung, P. C., & Lau, C. B. S. (2014). In vivo and in vitro anti-tumor and anti-metastasis effects of *Coriolus versicolor* aqueous extract on mouse mammary 4T1 carcinoma. *Phytomedicine*, *21*(8–9), 1078–1087. <https://doi.org/10.1016/j.phymed.2014.04.020>
- Maloy, K. J., & Powrie, F. (2011). Intestinal homeostasis and its breakdown in inflammatory bowel disease. In *Nature* (Vol. 474, Issue 7351, pp. 298–306). Nature. <https://doi.org/10.1038/nature10208>
- Mao, G. H., Zhang, Z. H., Fei, F., Ding, Y. Y., Zhang, W. J., Chen, H., Ali, S. S., Zhao, T., Feng, W. W., Wu, X. Y., & Yang, L. Q. (2019). Effect of *Grifola frondosa* polysaccharide on anti-tumor activity in combination with 5-Fu in Heps-bearing mice. *International Journal of Biological Macromolecules*, *121*, 930–935. <https://doi.org/10.1016/j.ijbiomac.2018.10.073>
- Mao, G., Li, Q., Deng, C., Wang, Y., Ding, Y., Zhang, W., Chen, Y., Zhao, T., Wei, F., Yang, L., & Wu, X. (2018). The synergism and attenuation effect of Selenium (Se)-enriched *Grifola frondosa* (Se)-polysaccharide on 5-Fluorouracil (5-Fu) in Heps-bearing mice. *International Journal of Biological Macromolecules*, *107*(Pt B), 2211–2216. <https://doi.org/10.1016/j.ijbiomac.2017.10.084>
- Mao, X. W., Green, L. M., & Gridley, D. S. (2001). Evaluation of polysaccharopeptide effects against C6 glioma in combination with radiation. *Oncology*, *61*(3), 243–253. <https://doi.org/10.1159/000055381>

- Martinez-Iglesias, O., Casas-Pais, A., Castosa, R., Díaz-Díaz, A., Roca-Lema, D., Concha, Á., Cortés, Á., Gago, F., & Figueroa, A. (2020). Hakin-1, a new specific small-molecule inhibitor for the E3 ubiquitin-ligase Hakai, inhibits carcinoma growth and progression. *Cancers*, *12*(5). <https://doi.org/10.3390/cancers12051340>
- Masuda, Y., Inoue, H., Ohta, H., Miyake, A., Konishi, M., & Nanba, H. (2013). Oral administration of soluble β -glucans extracted from *Grifola frondosa* induces systemic antitumor immune response and decreases immunosuppression in tumor-bearing mice. *International Journal of Cancer*, *133*(1), 108–119. <https://doi.org/10.1002/ijc.27999>
- Masuda, Y., Inoue, M., Miyata, A., Mizuno, S., & Nanba, H. (2009). Maitake β -glucan enhances therapeutic effect and reduces myelosuppression and nephrotoxicity of cisplatin in mice. *International Immunopharmacology*, *9*(5), 620–626. <https://doi.org/10.1016/j.intimp.2009.02.005>
- Matsuo, S., Yang, W. L., Aziz, M., Kameoka, S., & Wang, P. (2014). Fatty acid synthase inhibitor C75 ameliorates experimental colitis. *Molecular Medicine*, *20*(1), 1–9. <https://doi.org/10.2119/molmed.2013.00113>
- Matuszewska, A., Stefaniuk, D., Jaszek, M., Pięt, M., Zajac, A., Matuszewski, Ł., Cios, I., Graż, M., Paduch, R., & Bancercz, R. (2019). Antitumor potential of new low molecular weight antioxidative preparations from the white rot fungus *Cerrena unicolor* against human colon cancer cells. *Scientific Reports*, *9*(1), 1–10. <https://doi.org/10.1038/s41598-018-37947-z>
- Mazouji, O., Ouhajjou, A., Incitti, R., & Mansour, H. (2021). Updates on Clinical Use of Liquid Biopsy in Colorectal Cancer Screening, Diagnosis, Follow-Up, and Treatment Guidance. In *Frontiers in Cell and Developmental Biology* (Vol. 9, p. 962). Frontiers Media S.A. <https://doi.org/10.3389/fcell.2021.660924>
- McGovern, D. P. B., Kugathasan, S., & Cho, J. H. (2015). Genetics of Inflammatory Bowel Diseases. *Gastroenterology*, *149*(5), 1163-1176.e2. <https://doi.org/10.1053/j.gastro.2015.08.001>
- Mehlen, P., & Puisieux, A. (2006). Metastasis: A question of life or death. In *Nature*

- Reviews Cancer* (Vol. 6, Issue 6, pp. 449–458). Nature Publishing Group.
<https://doi.org/10.1038/nrc1886>
- Mestas, J., & Hughes, C. C. W. (2004). Of Mice and Not Men: Differences between Mouse and Human Immunology. *The Journal of Immunology*, *172*(5), 2731–2738.
<https://doi.org/10.4049/jimmunol.172.5.2731>
- Miller, S. (2012). Cellular and Physiological Effects of Short-Chain Fatty Acids. *Mini-Reviews in Medicinal Chemistry*, *4*(8), 839–845.
<https://doi.org/10.2174/1389557043403288>
- Min, K., Jee, S. C., Sung, J. S., & Kadam, A. A. (2018). Anti-proliferative applications of laccase immobilized on super-magnetic chitosan-functionalized halloysite nanotubes. *International Journal of Biological Macromolecules*, *118*(Pt A), 228–237. <https://doi.org/10.1016/j.ijbiomac.2018.06.074>
- Moayyedi, P., Surette, M. G., Kim, P. T., Libertucci, J., Wolfe, M., Onischi, C., Armstrong, D., Marshall, J. K., Kassam, Z., Reinisch, W., & Lee, C. H. (2015). Fecal Microbiota Transplantation Induces Remission in Patients With Active Ulcerative Colitis in a Randomized Controlled Trial. *Gastroenterology*, *149*(1), 102-109.e6.
<https://doi.org/10.1053/j.gastro.2015.04.001>
- Moller, F. T., Andersen, V., Wohlfahrt, J., & Jess, T. (2015). Familial risk of inflammatory bowel disease: A population-based cohort study 1977-2011. *American Journal of Gastroenterology*, *110*(4), 564–571. <https://doi.org/10.1038/ajg.2015.50>
- Moore, D., Robson, G. D., & Trinci, A. P. J. (2000). 21st Century Guidebook to Fungi. In *21st Century Guidebook to Fungi*. Cambridge University Press.
<https://doi.org/10.1017/cbo9780511977022>
- Moradali, M. F., Mostafavi, H., Ghods, S., & Hedjaroude, G. A. (2007). Immunomodulating and anticancer agents in the realm of macromycetes fungi (macrofungi). In *International Immunopharmacology* (Vol. 7, Issue 6, pp. 701–724). Elsevier. <https://doi.org/10.1016/j.intimp.2007.01.008>
- Mosesson, Y., Mills, G. B., & Yarden, Y. (2008). Derailed endocytosis: An emerging feature of cancer. In *Nature Reviews Cancer* (Vol. 8, Issue 11, pp. 835–850). Nat

Rev Cancer. <https://doi.org/10.1038/nrc2521>

Mukherjee, M., Chow, S. Y., Yusoff, P., Seetharaman, J., Ng, C., Sinniah, S., Koh, X. W., Asgar, N. F. M., Li, D., Yim, D., Jackson, R. A., Yew, J., Qian, J., Iyu, A., Lim, Y. P., Zhou, X., Sze, S. K., Guy, G. R., & Sivaraman, J. (2012). Structure of a novel phosphotyrosine-binding domain in Hakai that targets E-cadherin. *EMBO Journal*, *31*(5), 1308–1319. <https://doi.org/10.1038/emboj.2011.496>

Mukherjee, M., Jing-Song, F., Ramachandran, S., Guy, G. R., & Sivaraman, J. (2014). Dimeric switch of Hakai-truncated monomers during substrate recognition: Insights from solution studies and nmr structure. *Journal of Biological Chemistry*, *289*(37), 25611–25623. <https://doi.org/10.1074/jbc.M114.592840>

Muller, A. G., Sarker, S. D., Saleem, I. Y., & Hutcheon, G. A. (2019). Delivery of natural phenolic compounds for the potential treatment of lung cancer. In *DARU, Journal of Pharmaceutical Sciences* (Vol. 27, Issue 1, pp. 433–449). Springer. <https://doi.org/10.1007/s40199-019-00267-2>

Nakatsu, G., Li, X., Zhou, H., Sheng, J., Wong, S. H., Wu, W. K. K., Ng, S. C., Tsoi, H., Dong, Y., Zhang, N., He, Y., Kang, Q., Cao, L., Wang, K., Zhang, J., Liang, Q., Yu, J., & Sung, J. J. Y. (2015). Gut mucosal microbiome across stages of colorectal carcinogenesis. *Nature Communications*, *6*(1), 1–9. <https://doi.org/10.1038/ncomms9727>

Naranjo-Ortiz, M. A., & Gabaldón, T. (2019). Fungal evolution: diversity, taxonomy and phylogeny of the Fungi. *Biological Reviews*, *94*(6), 2101–2137. <https://doi.org/10.1111/brv.12550>

Neurath, M. F. (2014). Cytokines in inflammatory bowel disease. In *Nature Reviews Immunology* (Vol. 14, Issue 5, pp. 329–342). Nature Publishing Group. <https://doi.org/10.1038/nri3661>

Ng, S. C., Shi, H. Y., Hamidi, N., Underwood, F. E., Tang, W., Benchimol, E. I., Panaccione, R., Ghosh, S., Wu, J. C. Y., Chan, F. K. L., Sung, J. J. Y., & Kaplan, G. G. (2017). Worldwide incidence and prevalence of inflammatory bowel disease in the 21st century: a systematic review of population-based studies. *The Lancet*,

390(10114), 2769–2778. [https://doi.org/10.1016/S0140-6736\(17\)32448-0](https://doi.org/10.1016/S0140-6736(17)32448-0)

Nieto, M. A. (2013). Epithelial plasticity: A common theme in embryonic and cancer cells. In *Science* (Vol. 342, Issue 6159). American Association for the Advancement of Science. <https://doi.org/10.1126/science.1234850>

Normand, R., Du, W., Briller, M., Gaujoux, R., Starosvetsky, E., Ziv-Kenet, A., Shalev-Malul, G., Tibshirani, R. J., & Shen-Orr, S. S. (2018). Found In Translation: a machine learning model for mouse-to-human inference. *Nature Methods*, *15*(12), 1067–1073. <https://doi.org/10.1038/s41592-018-0214-9>

Notarnicola, M., Tutino, V., Calvani, M., Lorusso, D., Guerra, V., & Caruso, M. G. (2012). Serum levels of fatty acid synthase in colorectal cancer patients are associated with tumor stage. *Journal of Gastrointestinal Cancer*, *43*(3), 508–511. <https://doi.org/10.1007/s12029-011-9300-2>

Ogino, S., & Goel, A. (2008). Molecular classification and correlates in colorectal cancer. In *Journal of Molecular Diagnostics* (Vol. 10, Issue 1, pp. 13–27). Association of Molecular Pathology. <https://doi.org/10.2353/jmoldx.2008.070082>

Okayasu, I., Ohkusa, T., Kajiura, K., Kanno, J., & Sakamoto, S. (1996). Promotion of colorectal neoplasia in experimental murine ulcerative colitis. *Gut*, *39*(1), 87–92. <https://doi.org/10.1136/gut.39.1.87>

Okayasu, Isao, Hatakeyama, S., Yamada, M., Ohkusa, T., Inagaki, Y., & Nakaya, R. (1990). A novel method in the induction of reliable experimental acute and chronic ulcerative colitis in mice. *Gastroenterology*, *98*(3), 694–702. [https://doi.org/10.1016/0016-5085\(90\)90290-H](https://doi.org/10.1016/0016-5085(90)90290-H)

Palacios, F., Tushir, J. S., Fujita, Y., & D'Souza-Schorey, C. (2005). Lysosomal Targeting of E-Cadherin: a Unique Mechanism for the Down-Regulation of Cell-Cell Adhesion during Epithelial to Mesenchymal Transitions. *Molecular and Cellular Biology*, *25*(1), 389–402. <https://doi.org/10.1128/mcb.25.1.389-402.2005>

Palmela, C., Chevarin, C., Xu, Z., Torres, J., Sevrin, G., Hirten, R., Barnich, N., Ng, S. C., & Colombel, J. F. (2018). Adherent-invasive *Escherichia coli* in inflammatory bowel disease. In *Gut* (Vol. 67, Issue 3, pp. 574–587). BMJ Publishing Group.

<https://doi.org/10.1136/gutjnl-2017-314903>

Pan, Q., Lou, X., Zhang, J., Zhu, Y., Li, F., Shan, Q., Chen, X., Xie, Y., Su, S., Wei, H., Lin, L., Wu, L., & Liu, S. (2017). Genomic variants in mouse model induced by azoxymethane and dextran sodium sulfate improperly mimic human colorectal cancer. *Scientific Reports*, 7(1). <https://doi.org/10.1038/s41598-017-00057-3>

Paramsothy, S., Kamm, M. A., Kaakoush, N. O., Walsh, A. J., van den Bogaerde, J., Samuel, D., Leong, R. W. L., Connor, S., Ng, W., Paramsothy, R., Xuan, W., Lin, E., Mitchell, H. M., & Borody, T. J. (2017). Multidonor intensive faecal microbiota transplantation for active ulcerative colitis: a randomised placebo-controlled trial. *The Lancet*, 389(10075), 1218–1228. [https://doi.org/10.1016/S0140-6736\(17\)30182-4](https://doi.org/10.1016/S0140-6736(17)30182-4)

Park, J. H., Peyrin-Biroulet, L., Eisenhut, M., & Shin, J. II. (2017). IBD immunopathogenesis: A comprehensive review of inflammatory molecules. In *Autoimmunity Reviews* (Vol. 16, Issue 4, pp. 416–426). Elsevier B.V. <https://doi.org/10.1016/j.autrev.2017.02.013>

Pascal, V., Pozuelo, M., Borruel, N., Casellas, F., Campos, D., Santiago, A., Martinez, X., Varela, E., Sarrabayrouse, G., Machiels, K., Vermeire, S., Sokol, H., Guarner, F., & Manichanh, C. (2017). A microbial signature for Crohn's disease. *Gut*, 66(5), 813–822. <https://doi.org/10.1136/gutjnl-2016-313235>

Pastushenko, I., & Blanpain, C. (2019). EMT Transition States during Tumor Progression and Metastasis. In *Trends in Cell Biology* (Vol. 29, Issue 3, pp. 212–226). Elsevier Ltd. <https://doi.org/10.1016/j.tcb.2018.12.001>

Pawlik, T. M., Raut, C. P., & Rodriguez-Bigas, M. A. (2004). Colorectal carcinogenesis: MSI-H versus MSI-L. *Disease Markers*, 20(4–5), 199–206. <https://doi.org/10.1155/2004/368680>

Pawlikowska, M., Jędrzejewski, T., Piotrowski, J., & Kozak, W. (2016). Fever-range hyperthermia inhibits cells immune response to protein-bound polysaccharides derived from *Coriolus versicolor* extract. *Molecular Immunology*, 80, 50–57. <https://doi.org/10.1016/j.molimm.2016.10.013>

- Pece, S., & Gutkind, J. S. (2002). E-cadherin and Hakai: Signalling, remodeling or destruction? In *Nature Cell Biology* (Vol. 4, Issue 4, pp. E72–E74). Nature Publishing Group. <https://doi.org/10.1038/ncb0402-e72>
- Peri, A. K., Wilgenbus, P., Dahl, U., Semb, H., & Christofori, G. (1998). A causal role for E-cadherin in the transition from adenoma to carcinoma. *Nature*, *392*(6672), 190–193. <https://doi.org/10.1038/32433>
- Perry, D. A., Amaranthus, M. P., Borchers, J. G., Borchers, S. L., & Brainerd, R. E. (1989). Bootstrapping in Ecosystems. *BioScience*, *39*(4), 230–237. <https://doi.org/10.2307/1311159>
- Peterson, L. W., & Artis, D. (2014). Intestinal epithelial cells: Regulators of barrier function and immune homeostasis. In *Nature Reviews Immunology* (Vol. 14, Issue 3, pp. 141–153). Nat Rev Immunol. <https://doi.org/10.1038/nri3608>
- Pinho, S. S., Oliveira, P., Cabral, J., Carvalho, S., Huntsman, D., Gärtner, F., Seruca, R., Reis, C. A., & Oliveira, C. (2012). Loss and recovery of Mgat3 and GnT-III mediated E-cadherin N-glycosylation is a mechanism involved in epithelial-Mesenchymal-Epithelial transitions. *PLoS ONE*, *7*(3). <https://doi.org/10.1371/journal.pone.0033191>
- Pinho, S. S., & Reis, C. A. (2014). E-cadherin Glycosylation in Cancer. In *Glycoscience: Biology and Medicine* (pp. 1–6). Springer Japan. https://doi.org/10.1007/978-4-431-54836-2_54-1
- Pizer, E S, Lax, S. F., Kuhajda, F. P., Pasternack, G. R., & Kurman, R. J. (1998). Fatty acid synthase expression in endometrial carcinoma: correlation with cell proliferation and hormone receptors. *Cancer*, *83*(3), 528–537.
- Pizer, Ellen S., Thupari, J., Han, W. F., Pinn, M. L., Chrest, F. J., Frehywot, G. L., Townsend, C. A., & Kuhajda, F. P. (2000). Malonyl-Coenzyme-A Is a Potential Mediator of Cytotoxicity Induced by Fatty-Acid Synthase Inhibition in Human Breast Cancer Cells and Xenografts. *Cancer Research*, *60*(2).
- Price, L. A., Wenner, C. A., Sloper, D. T., Slaton, J. W., & Novack, J. P. (2010). Role for toll-like receptor 4 in TNF-alpha secretion by murine macrophages in response to

- polysaccharide Krestin, a *Trametes versicolor* mushroom extract. *Fitoterapia*, 81(7), 914–919. <https://doi.org/10.1016/j.fitote.2010.06.002>
- Queiroz, E. A. I. F., Fortes, Z. B., Da Cunha, M. A. A., Barbosa, A. M., Khaper, N., & Dekker, R. F. H. (2015). Antiproliferative and pro-apoptotic effects of three fungal exocellular β -glucans in MCF-7 breast cancer cells is mediated by oxidative stress, AMP-activated protein kinase (AMPK) and the Forkhead transcription factor, FOXO3a. *International Journal of Biochemistry and Cell Biology*, 67, 14–24. <https://doi.org/10.1016/j.biocel.2015.08.003>
- Radisky, E. S., & Radisky, D. C. (2010). Matrix metalloproteinase-induced epithelial-mesenchymal transition in breast cancer. In *Journal of Mammary Gland Biology and Neoplasia* (Vol. 15, Issue 2, pp. 201–212). Springer. <https://doi.org/10.1007/s10911-010-9177-x>
- Rahman, M., Chan, A. P. K., & Tai, I. T. (2011). A peptide of sparc interferes with the interaction between Caspase8 and Bcl2 to resensitize Chemoresistant tumors and enhance their regression in vivo. *PLoS ONE*, 6(11). <https://doi.org/10.1371/journal.pone.0026390>
- Ramos, G. P., & Papadakis, K. A. (2019). Mechanisms of Disease: Inflammatory Bowel Diseases. In *Mayo Clinic Proceedings* (Vol. 94, Issue 1, pp. 155–165). Elsevier Ltd. <https://doi.org/10.1016/j.mayocp.2018.09.013>
- Rashid, S., Unyayar, A., Mazmanci, M. A., McKeown, S. R., Banat, I. M., & Worthington, J. (2011). A study of anti-cancer effects of *Funalia trogii* in vitro and in vivo. *Food and Chemical Toxicology*, 49(7), 1477–1483. <https://doi.org/10.1016/j.fct.2011.02.008>
- Reinhold, W. C., Reimers, M. A., Lorenzi, P., Ho, J., Shankavaram, U. T., Ziegler, M. S., Bussey, K. J., Nishizuka, S., Ikediobi, O., Pommier, Y. G., & Weinstein, J. N. (2010). Multifactorial regulation of E-cadherin expression: An integrative study. *Molecular Cancer Therapeutics*, 9(1), 1–16. <https://doi.org/10.1158/1535-7163.MCT-09-0321>
- Reisenauer, K. N., Tao, Y., Das, P., Song, S., Svatek, H., Patel, S. D., Mikhail, S., Ingros,

- A., Sheesley, P., Masi, M., Boari, A., Evidente, A., Kornienko, A., Romo, D., & Taube, J. (2021). Epithelial-mesenchymal transition sensitizes breast cancer cells to cell death via the fungus-derived sesterterpenoid ophiobolin A. *Scientific Reports*, *11*(1), 10652. <https://doi.org/10.1038/s41598-021-89923-9>
- Ricciardi, M. R., Licchetta, R., Mirabilii, S., Scarpari, M., Parroni, A., Fabbri, A. A., Cescutti, P., Reverberi, M., Fanelli, C., & Tafuri, A. (2017). Preclinical antileukemia activity of tramesan: A newly identified bioactive fungal metabolite. *Oxidative Medicine and Cellular Longevity*, *2017*. <https://doi.org/10.1155/2017/5061639>
- Roda, G., Chien Ng, S., Kotze, P. G., Argollo, M., Panaccione, R., Spinelli, A., Kaser, A., Peyrin-Biroulet, L., & Danese, S. (2020). Crohn's disease. *Nature Reviews Disease Primers*, *6*(1), 1–19. <https://doi.org/10.1038/s41572-020-0156-2>
- Rodríguez-Alonso, A., Casas-Pais, A., Roca-Lema, D., Graña, B., Romay, G., & Figueroa, A. (2020). Regulation of epithelial-mesenchymal plasticity by the E3 ubiquitin-ligases in cancer. *Cancers*, *12*(11), 1–24. <https://doi.org/10.3390/cancers12113093>
- Rodríguez-Rigueiro, T., Valladares-Ayerbes, M., Haz-Conde, M., Aparicio, L. A., & Figueroa, A. (2011). Hakai reduces cell-substratum adhesion and increases epithelial cell invasion. *BMC Cancer*, *11*. <https://doi.org/10.1186/1471-2407-11-474>
- Roeten, M. S. F., Cloos, J., & Jansen, G. (2018). Positioning of proteasome inhibitors in therapy of solid malignancies. In *Cancer Chemotherapy and Pharmacology* (Vol. 81, Issue 2, pp. 227–243). Springer Verlag. <https://doi.org/10.1007/s00280-017-3489-0>
- Röhrig, F., & Schulze, A. (2016). The multifaceted roles of fatty acid synthesis in cancer. In *Nature Reviews Cancer* (Vol. 16, Issue 11, pp. 732–749). Nature Publishing Group. <https://doi.org/10.1038/nrc.2016.89>
- Roig, A. I., Eskiocak, U., Hight, S. K., Kim, S. B., Delgado, O., Souza, R. F., Spechler, S. J., Wright, W. E., & Shay, J. W. (2010). Immortalized Epithelial Cells Derived From Human Colon Biopsies Express Stem Cell Markers and Differentiate In Vitro.

Gastroenterology, 138(3). <https://doi.org/10.1053/j.gastro.2009.11.052>

Rossen, N. G., Fuentes, S., Van Der Spek, M. J., Tijssen, J. G., Hartman, J. H. A., Duflou, A., Löwenberg, M., Van Den Brink, G. R., Mathus-Vliegen, E. M. H., De Vos, W. M., Zoetendal, E. G., D'Haens, G. R., & Ponsioen, C. Y. (2015). Findings From a Randomized Controlled Trial of Fecal Transplantation for Patients With Ulcerative Colitis. *Gastroenterology*, 149(1), 110-118.e4. <https://doi.org/10.1053/j.gastro.2015.03.045>

Rossi, P., Diffrancia, R., Quagliariello, V., Savino, E., Tralongo, P., Randazzo, C. L., & Berretta, M. (2018). B-glucans from *Grifola frondosa* and *Ganoderma lucidum* in breast cancer: An example of complementary and integrative medicine. In *Oncotarget* (Vol. 9, Issue 37, pp. 24837–24856). Impact Journals LLC. <https://doi.org/10.18632/oncotarget.24984>

Russo, E., Giudici, F., Fiorindi, C., Ficari, F., Scaringi, S., & Amedei, A. (2019). Immunomodulating Activity and Therapeutic Effects of Short Chain Fatty Acids and Tryptophan Post-biotics in Inflammatory Bowel Disease. In *Frontiers in Immunology* (Vol. 10, p. 2754). Frontiers Media S.A. <https://doi.org/10.3389/fimmu.2019.02754>

Rutgeerts, P., Sandborn, W. J., Feagan, B. G., Reinisch, W., Olson, A., Johanns, J., Travers, S., Rachmilewitz, D., Hanauer, S. B., Lichtenstein, G. R., de Villiers, W. J. S., Present, D., Sands, B. E., & Colombel, J. F. (2005). Infliximab for Induction and Maintenance Therapy for Ulcerative Colitis. *New England Journal of Medicine*, 353(23), 2462–2476. <https://doi.org/10.1056/nejmoa050516>

Růžička, K., Zhang, M., Campilho, A., Bodi, Z., Kashif, M., Saleh, M., Eeckhout, D., El-Showk, S., Li, H., Zhong, S., Jaeger, G. De, Mongan, N. P., Hejátko, J., Helariutta, Y., & Fray, R. G. (2017). Identification of factors required for m6A mRNA methylation in Arabidopsis reveals a role for the conserved E3 ubiquitin ligase HAKAI. *New Phytologist*, 215(1), 157–172. <https://doi.org/10.1111/nph.14586>

Sahu, M. K., Kaushik, K., Das, A., & Jha, H. (2020). In vitro and in silico antioxidant and antiproliferative activity of rhizospheric fungus *Talaromyces purpureogenus* isolate-ABRF2. *Bioresources and Bioprocessing*, 7(1), 14.

<https://doi.org/10.1186/s40643-020-00303-z>

- Saleh, M. H., Rashedi, I., & Keating, A. (2017). Immunomodulatory properties of *coriolus versicolor*: The role of polysaccharopeptide. *Frontiers in Immunology*, 8(SEP), 1087. <https://doi.org/10.3389/fimmu.2017.01087>
- Santos Arteiro, J. M., Martins, M. R., Salvador, C., Candeias, M. F., Karmali, A., & Caldeira, A. T. (2012). Protein-polysaccharides of *Trametes versicolor*: Production and biological activities. *Medicinal Chemistry Research*, 21(6), 937–943. <https://doi.org/10.1007/s00044-011-9604-6>
- Sarlos, P., Kovesdi, E., Magyari, L., Banfai, Z., Szabo, A., Javorhazy, A., & Melegh, B. (2014). Genetic update on inflammatory factors in ulcerative colitis: Review of the current literature. *World Journal of Gastrointestinal Pathophysiology*, 5(3), 304. <https://doi.org/10.4291/wjgp.v5.i3.304>
- Saxena, S., Chhibber, M., & Singh, I. P. (2019). Fungal Bioactive Compounds in Pharmaceutical Research and Development. *Current Bioactive Compounds*, 15(2), 211–231. <https://doi.org/10.2174/1573407214666180622104720>
- Scaioli, E., Liverani, E., & Belluzzi, A. (2017). The imbalance between N-6/N-3 polyunsaturated fatty acids and inflammatory bowel disease: A comprehensive review and future therapeutic perspectives. In *International Journal of Molecular Sciences* (Vol. 18, Issue 12). MDPI AG. <https://doi.org/10.3390/ijms18122619>
- Schneider, M. R., Dahlhoff, M., Horst, D., Hirschi, B., Trülzsch, K., Müller-Höcker, J., Vogelmann, R., Allgäuer, M., Gerhard, M., Steininger, S., Wolf, E., & Kolligs, F. T. (2010). A Key Role for E-cadherin in Intestinal Homeostasis and Paneth Cell Maturation. *PLoS ONE*, 5(12), e14325. <https://doi.org/10.1371/journal.pone.0014325>
- Schulthess, J., Pandey, S., Capitani, M., Rue-Albrecht, K. C., Arnold, I., Franchini, F., Chomka, A., Ilott, N. E., Johnston, D. G. W., Pires, E., McCullagh, J., Sansom, S. N., Arancibia-Cárcamo, C. V., Uhlig, H. H., & Powrie, F. (2019). The Short Chain Fatty Acid Butyrate Imprints an Antimicrobial Program in Macrophages. *Immunity*, 50(2), 432-445.e7. <https://doi.org/10.1016/j.immuni.2018.12.018>

- Sekhon, B. K., Sze, D. M. Y., Chan, W. K., Fan, K., Li, G. Q., Moore, D. E., & Roubin, R. H. (2013). PSP activates monocytes in resting human peripheral blood mononuclear cells: Immunomodulatory implications for cancer treatment. *Food Chemistry*, *138*(4), 2201–2209. <https://doi.org/10.1016/j.foodchem.2012.11.009>
- Shi, B. J., Nie, X. H., Chen, L. Z., Liu, Y. L., & Tao, W. Y. (2007). Anticancer activities of a chemically sulfated polysaccharide obtained from *Grifola frondosa* and its combination with 5-Fluorouracil against human gastric carcinoma cells. *Carbohydrate Polymers*, *68*(4), 687–692. <https://doi.org/10.1016/j.carbpol.2006.08.003>
- Shi, L., Godfrey, W. R., Lin, J., Zhao, G., & Kao, P. N. (2007). NF90 regulates inducible IL-2 gene expression in T cells. *Journal of Experimental Medicine*, *204*(5), 971–977. <https://doi.org/10.1084/jem.20052078>
- Shnyreva, A. V., Shnyreva, A. A., Espinoza, C., Padrón, J. M., & Trigos, Á. (2018). Antiproliferative activity and cytotoxicity of some medicinal wood-destroying mushrooms from Russia. *International Journal of Medicinal Mushrooms*, *20*(1), 1–11. <https://doi.org/10.1615/IntJMedMushrooms.2018025250>
- Shomori, K., Yamamoto, M., Arifuku, I., Teramachi, K., & Ito, H. (2009). Antitumor effects of a water-soluble extract from Maitake (*Grifola frondosa*) on human gastric cancer cell lines. *Oncology Reports*, *22*(3), 615–620. https://doi.org/10.3892/or_00000480
- Shores, D. R., Binion, D. G., Freeman, B. A., & Baker, P. R. S. (2011). New insights into the role of fatty acids in the pathogenesis and resolution of inflammatory bowel disease. In *Inflammatory Bowel Diseases* (Vol. 17, Issue 10, pp. 2192–2204). Inflamm Bowel Dis. <https://doi.org/10.1002/ibd.21560>
- Shurbaji, M. S., Kalbfleisch, J. H., & Thurmond, T. S. (1996). Immunohistochemical detection of a fatty acid synthase (OA-519) as a predictor of progression of prostate cancer. *Human Pathology*, *27*(9), 917–921. [https://doi.org/10.1016/S0046-8177\(96\)90218-X](https://doi.org/10.1016/S0046-8177(96)90218-X)
- Sidiq, T., Yoshihama, S., Downs, I., & Kobayashi, K. S. (2016). Nod2: A critical regulator

- of ileal microbiota and Crohn's disease. In *Frontiers in Immunology* (Vol. 7, Issue SEP, p. 1). Frontiers Media S.A. <https://doi.org/10.3389/fimmu.2016.00367>
- Siegel, R. L., Torre, L. A., Soerjomataram, I., Hayes, R. B., Bray, F., Weber, T. K., & Jemal, A. (2019). Global patterns and trends in colorectal cancer incidence in young adults. *Gut*, *68*(12), 2179–2185. <https://doi.org/10.1136/gutjnl-2019-319511>
- Sima, P., Vannucci, L., & Vetvicka, V. (2014). Effects of glucan on bone marrow. In *Annals of Translational Medicine* (Vol. 2, Issue 2). AME Publishing Company. <https://doi.org/10.3978/j.issn.2305-5839.2014.01.06>
- Sivanandhan, S., Khusro, A., Paulraj, M. G., Ignacimuthu, S., & Al-Dhabi, N. A. (2017). Biocontrol properties of basidiomycetes: An overview. In *Journal of Fungi* (Vol. 3, Issue 1). MDPI AG. <https://doi.org/10.3390/jof3010002>
- Slots, J. (2017). Periodontitis: facts, fallacies and the future. In *Periodontology 2000* (Vol. 75, Issue 1, pp. 7–23). Blackwell Munksgaard. <https://doi.org/10.1111/prd.12221>
- Soares, R., Meireles, M., Rocha, A., Pirraco, A., Obiol, D., Alonso, E., Joos, G., & Balogh, G. (2011). Maitake (D fraction) mushroom extract induces apoptosis in breast cancer cells by BAK-1 gene activation. *Journal of Medicinal Food*, *14*(6), 563–572. <https://doi.org/10.1089/jmf.2010.0095>
- Sokol, H., Pigneur, B., Watterlot, L., Lakhdari, O., Bermúdez-Humarán, L. G., Gratadoux, J. J., Blugeon, S., Bridonneau, C., Furet, J. P., Corthier, G., Grangette, C., Vasquez, N., Pochart, P., Trugnan, G., Thomas, G., Blottière, H. M., Doré, J., Marteau, P., Seksik, P., & Langella, P. (2008). Faecalibacterium prausnitzii is an anti-inflammatory commensal bacterium identified by gut microbiota analysis of Crohn disease patients. *Proceedings of the National Academy of Sciences of the United States of America*, *105*(43), 16731–16736. <https://doi.org/10.1073/pnas.0804812105>
- Somineni, H. K., & Kugathasan, S. (2019). The Microbiome in Patients With Inflammatory Diseases. In *Clinical Gastroenterology and Hepatology* (Vol. 17, Issue 2, pp. 243–255). W.B. Saunders. <https://doi.org/10.1016/j.cgh.2018.08.078>

- Sonnenburg, J. L., & Bäckhed, F. (2016). Diet-microbiota interactions as moderators of human metabolism. In *Nature* (Vol. 535, Issue 7610, pp. 56–64). Nature Publishing Group. <https://doi.org/10.1038/nature18846>
- Spehlmann, M. E., Begun, A. Z., Saroglou, E., Hinrichs, F., Tiemann, U., Raedler, A., & Schreiber, S. (2012). Risk factors in German twins with inflammatory bowel disease: Results of a questionnaire-based survey. *Journal of Crohn's and Colitis*, 6(1), 29–42. <https://doi.org/10.1016/j.crohns.2011.06.007>
- Srivastava, S., Kedia, S., Kumar, S., Pratap Mouli, V., Dhingra, R., Sachdev, V., Tiwari, V., Kurrey, L., Pradhan, R., & Ahuja, V. (2015). Serum Human Trefoil Factor 3 is a Biomarker for Mucosal Healing in Ulcerative Colitis Patients with Minimal Disease Activity. *Journal of Crohn's and Colitis*, 9(7), 575–579. <https://doi.org/10.1093/ecco-jcc/jjv075>
- Stamets, P., & Zwickey, H. (2014). Medicinal Mushrooms: Ancient Remedies Meet Modern Science. *Integrative Medicine: A Clinician's Journal*, 13(1), 46.
- Stappenbeck, T. S., & McGovern, D. P. B. (2017). Paneth Cell Alterations in the Development and Phenotype of Crohn's Disease. *Gastroenterology*, 152(2), 322–326. <https://doi.org/10.1053/j.gastro.2016.10.003>
- Su, J., Su, L., Li, D., Shuai, O., Zhang, Y., Liang, H., Jiao, C., Xu, Z., Lai, Y., & Xie, Y. (2018). Antitumor Activity of Extract From the Sporoderm-Breaking Spore of *Ganoderma lucidum*: Restoration on Exhausted Cytotoxic T Cell With Gut Microbiota Remodeling. *Frontiers in Immunology*, 9, 1765. <https://doi.org/10.3389/fimmu.2018.01765>
- Sveen, A., Bruun, J., Eide, P. W., Eilertsen, I. A., Ramirez, L., Murumagi, A., Arjama, M., Danielsen, S. A., Kryeziu, K., Elez, E., Tabernero, J., Guinney, J., Palmer, H. G., Nesbakken, A., Kallioniemi, O., Dienstmann, R., & Lothe, R. A. (2018). Colorectal cancer consensus molecular subtypes translated to preclinical models uncover potentially targetable cancer cell dependencies. *Clinical Cancer Research*, 24(4), 794–806. <https://doi.org/10.1158/1078-0432.CCR-17-1234>
- Taghavi, M., Mortaz, E., Khosravi, A., Vahedi, G., Folkerts, G., Varahram, M.,

- Kazempour-Dizaji, M., Garssen, J., & Adcock, I. M. (2018). Zymosan attenuates melanoma growth progression, increases splenocyte proliferation and induces TLR-2/4 and TNF- α expression in mice. *Journal of Inflammation (United Kingdom)*, *15*(1). <https://doi.org/10.1186/s12950-018-0182-y>
- Takao, K., & Miyakawa, T. (2015). Genomic responses in mouse models greatly mimic human inflammatory diseases. *Proceedings of the National Academy of Sciences of the United States of America*, *112*(4), 1167–1172. <https://doi.org/10.1073/pnas.1401965111>
- Takeichi, M. (1988). The cadherins: cell-cell adhesion molecules controlling animal morphogenesis. *Development (Cambridge, England)*, *102*(4), 639–655.
- Talvensaari-Mattila, A., Pääkkö, P., & Turpeenniemi-Hujanen, T. (2003). Matrix metalloproteinase-2 (MMP-2) is associated with survival in breast carcinoma. *British Journal of Cancer*, *89*(7), 1270–1275. <https://doi.org/10.1038/sj.bjc.6601238>
- Tanaka, T., Kohno, H., Suzuki, R., Yamada, Y., Sugie, S., & Mori, H. (2003). A novel inflammation-related mouse colon carcinogenesis model induced by azoxymethane and dextran sodium sulfate. *Cancer Science*, *94*(11), 965–973. <https://doi.org/10.1111/j.1349-7006.2003.tb01386.x>
- Tanase, C., Cosarcă, S., & Muntean, D. L. (2019). A critical review of phenolic compounds extracted from the bark of woody vascular plants and their potential biological activity. In *Molecules* (Vol. 24, Issue 6). MDPI AG. <https://doi.org/10.3390/molecules24061182>
- Tang, A., Li, N., Li, X., Yang, H., Wang, W., Zhang, L., Li, G., Xiong, W., Ma, J., & Shen, S. (2012). Dynamic activation of the key pathways: linking colitis to colorectal cancer in a mouse model. *Carcinogenesis*, *33*(7), 1375–1383. <https://doi.org/10.1093/carcin/bgs183>
- Tanikawa, T., Wilke, C. M., Kryczek, I., Chen, G. Y., Kao, J., Núñez, G., & Zou, W. (2012). Interleukin-10 ablation promotes tumor development, growth, and metastasis. *Cancer Research*, *72*(2), 420–429. <https://doi.org/10.1158/0008-5472.CAN-10->

- Thiery, J. P. (2002). Epithelial–mesenchymal transitions in tumour progression. *Nature Reviews Cancer*, 2(6), 442–454. <https://doi.org/10.1038/nrc822>
- Tilg, H., Van Montfrans, C., Van den Ende, A., Kaser, A., Van Deventer, S. J. H., Schreiber, S., Gregor, M., Ludwiczek, O., Rutgeerts, P., Gasche, C., Koningsberger, J. C., Abreu, L., Kuhn, I., Cohard, M., LeBeaut, A., Grint, P., & Weiss, G. (2002). Treatment of Crohn’s disease with recombinant human interleukin 10 induces the proinflammatory cytokine interferon γ . *Gut*, 50(2), 191–195. <https://doi.org/10.1136/gut.50.2.191>
- Torres, J., Mehandru, S., Colombel, J. F., & Peyrin-Biroulet, L. (2017). Crohn’s disease. In *The Lancet* (Vol. 389, Issue 10080, pp. 1741–1755). Lancet Publishing Group. [https://doi.org/10.1016/S0140-6736\(16\)31711-1](https://doi.org/10.1016/S0140-6736(16)31711-1)
- Ullman, T. A., & Itzkowitz, S. H. (2011). Intestinal inflammation and cancer. *Gastroenterology*, 140(6), 1807-1816.e1. <https://doi.org/10.1053/j.gastro.2011.01.057>
- Uniken Venema, W. T. C., Voskuil, M. D., Dijkstra, G., Weersma, R. K., & Festen, E. A. M. (2017). The genetic background of inflammatory bowel disease: from correlation to causality. In *Journal of Pathology* (Vol. 241, Issue 2, pp. 146–158). John Wiley and Sons Ltd. <https://doi.org/10.1002/path.4817>
- Vacante, M., Ciuni, R., Basile, F., & Biondi, A. (2020). The liquid biopsy in the management of colorectal cancer: An overview. In *Biomedicines* (Vol. 8, Issue 9). MDPI AG. <https://doi.org/10.3390/biomedicines8090308>
- Valverde, M. E., Hernández-Pérez, T., & Paredes-López, O. (2015). Edible mushrooms: improving human health and promoting quality life. *International Journal of Microbiology*, 2015, 376387. <https://doi.org/10.1155/2015/376387>
- Van Der Jeught, K., Xu, H. C., Li, Y. J., Lu, X. Bin, & Ji, G. (2018). Drug resistance and new therapies in colorectal cancer. In *World Journal of Gastroenterology* (Vol. 24, Issue 34, pp. 3834–3848). Baishideng Publishing Group Co., Limited. <https://doi.org/10.3748/wjg.v24.i34.3834>

- Van Dongen, J., Slagboom, P. E., Draisma, H. H. M., Martin, N. G., & Boomsma, D. I. (2012). The continuing value of twin studies in the omics era. In *Nature Reviews Genetics* (Vol. 13, Issue 9, pp. 640–653). Nature Publishing Group.
<https://doi.org/10.1038/nrg3243>
- Venegas, D. P., De La Fuente, M. K., Landskron, G., González, M. J., Quera, R., Dijkstra, G., Harmsen, H. J. M., Faber, K. N., & Hermoso, M. A. (2019). Short chain fatty acids (SCFAs) mediated gut epithelial and immune regulation and its relevance for inflammatory bowel diseases. In *Frontiers in Immunology* (Vol. 10, Issue MAR). Frontiers Media S.A. <https://doi.org/10.3389/fimmu.2019.00277>
- Venkatakrishnan, K., Chiu, H. F., & Wang, C. K. (2019). Extensive review of popular functional foods and nutraceuticals against obesity and its related complications with a special focus on randomized clinical trials. In *Food and Function* (Vol. 10, Issue 5, pp. 2313–2329). Royal Society of Chemistry.
<https://doi.org/10.1039/c9fo00293f>
- Vleminckx, K., Vakaet, L., Mareel, M., Fiers, W., & Van Roy, F. (1991). Genetic manipulation of E-cadherin expression by epithelial tumor cells reveals an invasion suppressor role. *Cell*, *66*(1), 107–119. [https://doi.org/10.1016/0092-8674\(91\)90143-M](https://doi.org/10.1016/0092-8674(91)90143-M)
- Vodenkova, S., Buchler, T., Cervena, K., Veskrnova, V., Vodicka, P., & Vymetalkova, V. (2020). 5-fluorouracil and other fluoropyrimidines in colorectal cancer: Past, present and future. In *Pharmacology and Therapeutics* (Vol. 206). Elsevier Inc.
<https://doi.org/10.1016/j.pharmthera.2019.107447>
- Wan, J. M., Sit, W. H., Yang, X., Jiang, P., & Wong, L. L. (2010). Polysaccharopeptides derived from *Coriolus versicolor* potentiate the S-phase specific cytotoxicity of Camptothecin (CPT) on human leukemia HL-60 cells. *Chinese Medicine*, *5*.
<https://doi.org/10.1186/1749-8546-5-16>
- Wang, H., Cai, Y., Zheng, Y., Bai, Q., Xie, D., & Yu, J. (2017). Efficacy of biological response modifier lentinan with chemotherapy for advanced cancer: a meta-analysis. *Cancer Medicine*, *6*(10), 2222–2233. <https://doi.org/10.1002/cam4.1156>

- Wang, H. X., Ng, T. B., Liu, W. K., Ooi, V. E. C., & Chang, S. T. (1996). Polysaccharide-peptide complexes from the cultured mycelia of the mushroom *Coriolus versicolor* and their culture medium activate mouse lymphocytes and macrophages. *International Journal of Biochemistry and Cell Biology*, 28(5), 601–607. [https://doi.org/10.1016/1357-2725\(95\)00157-3](https://doi.org/10.1016/1357-2725(95)00157-3)
- Wang, J., Dong, B., Tan, Y., Yu, S., & Bao, Y. X. (2013). A study on the immunomodulation of polysaccharopeptide through the TLR4-TIRAP/MAL-MyD88 signaling pathway in PBMCs from breast cancer patients. *Immunopharmacology and Immunotoxicology*, 35(4), 497–504. <https://doi.org/10.3109/08923973.2013.805764>
- Wang, Q., Wang, F., Xu, Z., & Ding, Z. (2017). Bioactive mushroom polysaccharides: A review on monosaccharide composition, biosynthesis and regulation. In *Molecules* (Vol. 22, Issue 6). MDPI AG. <https://doi.org/10.3390/molecules22060955>
- Wang, Y. Y., Kuhajda, F. P., Li, J., Finch, T. T., Cheng, P., Koh, C., Li, T., Sokoll, L. J., & Chan, D. W. (2004). Fatty acid synthase as a tumor marker: its extracellular expression in human breast cancer. *Journal of Experimental Therapeutics & Oncology*, 4(2), 101–110.
- Wang, Y., Zhang, L., Ren, H., Ma, L., Guo, J., Mao, D., Lu, Z., Lu, L., & Yan, D. (2021). Role of Hakai in m6A modification pathway in *Drosophila*. *Nature Communications*, 12(1), 1–15. <https://doi.org/10.1038/s41467-021-22424-5>
- Wang, Z., Dong, B., Feng, Z., Yu, S., & Bao, Y. (2015). A study on immunomodulatory mechanism of Polysaccharopeptide mediated by TLR4 signaling pathway. *BMC Immunology*, 16(1). <https://doi.org/10.1186/s12865-015-0100-5>
- Wasser, S. P. (2011). Current findings, future trends, and unsolved problems in studies of medicinal mushrooms. In *Applied Microbiology and Biotechnology* (Vol. 89, Issue 5, pp. 1323–1332). <https://doi.org/10.1007/s00253-010-3067-4>
- Weber, C. R., Nalle, S. C., Tretiakova, M., Rubin, D. T., & Turner, J. R. (2008). Claudin-1 and claudin-2 expression is elevated in inflammatory bowel disease and may

- contribute to early neoplastic transformation. *Laboratory Investigation*, *88*(10), 1110–1120. <https://doi.org/10.1038/labinvest.2008.78>
- Weete, J. D., Abril, M., & Blackwell, M. (2010). Phylogenetic distribution of fungal sterols. *PLoS ONE*, *5*(5). <https://doi.org/10.1371/journal.pone.0010899>
- Wei, X., Yang, Z., Rey, F. E., Ridaura, V. K., Davidson, N. O., Gordon, J. I., & Semenkovich, C. F. (2012). Fatty acid synthase modulates intestinal barrier function through palmitoylation of mucin 2. *Cell Host and Microbe*, *11*(2), 140–152. <https://doi.org/10.1016/j.chom.2011.12.006>
- Wen, J., Lv, R., Ma, H., Shen, H., He, C., Wang, J., Jiao, F., Liu, H., Yang, P., Tan, L., Lan, F., Shi, Y. G., He, C., Shi, Y., & Diao, J. (2018). Zc3h13 Regulates Nuclear RNA m6A Methylation and Mouse Embryonic Stem Cell Self-Renewal. *Molecular Cell*, *69*(6), 1028-1038.e6. <https://doi.org/10.1016/j.molcel.2018.02.015>
- Weng, C. H., Chen, L. Y., Lin, Y. C., Shih, J. Y., Lin, Y. C., Tseng, R. Y., Chiu, A. C., Yeh, Y. H., Liu, C., Lin, Y. T., Fang, J. M., & Chen, C. C. (2019). Epithelial-mesenchymal transition (EMT) beyond EGFR mutations per se is a common mechanism for acquired resistance to EGFR TKI. *Oncogene*, *38*(4), 455–468. <https://doi.org/10.1038/s41388-018-0454-2>
- Wenner, C. A., Martzen, M. R., Lu, H., Verneris, M. R., Wang, H., & Slaton, J. W. (2012). Polysaccharide-K augments docetaxel-induced tumor suppression and antitumor immune response in an immunocompetent murine model of human prostate cancer. *International Journal of Oncology*, *40*(4), 905–913. <https://doi.org/10.3892/ijo.2011.1292>
- Wheelock, M. J., Shintani, Y., Maeda, M., Fukumoto, Y., & Johnson, K. R. (2008). Cadherin switching. In *Journal of Cell Science* (Vol. 121, Issue 6, pp. 727–735). J Cell Sci. <https://doi.org/10.1242/jcs.000455>
- Whittaker, R. H. (1969). New concepts of kingdoms of organisms. *Science*, *163*(3863), 150–160. <https://doi.org/10.1126/science.163.3863.150>
- Wilson, J. C., Furlano, R. I., Jick, S. S., & Meier, C. R. (2016). Inflammatory Bowel Disease and the Risk of Autoimmune Diseases. *Journal of Crohn's and Colitis*,

10(2), 186–193. <https://doi.org/10.1093/ecco-jcc/jjv193>

Wirtz, S., Popp, V., Kindermann, M., Gerlach, K., Weigmann, B., Fichtner-Feigl, S., & Neurath, M. F. (2017). Chemically induced mouse models of acute and chronic intestinal inflammation. *Nature Protocols*, *12*(7), 1295–1309.
<https://doi.org/10.1038/nprot.2017.044>

Wolf, A. M. D., Fontham, E. T. H., Church, T. R., Flowers, C. R., Guerra, C. E., LaMonte, S. J., Etzioni, R., McKenna, M. T., Oeffinger, K. C., Shih, Y.-C. T., Walter, L. C., Andrews, K. S., Brawley, O. W., Brooks, D., Fedewa, S. A., Manassaram-Baptiste, D., Siegel, R. L., Wender, R. C., & Smith, R. A. (2018). Colorectal cancer screening for average-risk adults: 2018 guideline update from the American Cancer Society. *CA: A Cancer Journal for Clinicians*, *68*(4), 250–281.
<https://doi.org/10.3322/caac.21457>

Wound Healing Tool - ImageJ-macros - MRI's Redmine.pdf. (n.d.). Retrieved June 10, 2020, from http://dev.mri.cnrs.fr/projects/imagej-macros/wiki/Wound_Healing_Tool

Xia, J., Dai, L., Wang, L., & Zhu, J. (2020). Ganoderic acid DM induces autophagic apoptosis in non-small cell lung cancer cells by inhibiting the PI3K/Akt/mTOR activity. *Chemico-Biological Interactions*, *316*, 108932.
<https://doi.org/10.1016/j.cbi.2019.108932>

Xiao, Y., Huang, Q., Wu, Z., & Chen, W. (2020). Roles of protein ubiquitination in inflammatory bowel disease. In *Immunobiology* (Vol. 225, Issue 6, p. 152026). Elsevier GmbH. <https://doi.org/10.1016/j.imbio.2020.152026>

Xu, H., Zou, S., & Xu, X. (2017). The β -glucan from *Lentinus edodes* suppresses cell proliferation and promotes apoptosis in estrogen receptor positive breast cancers. *Oncotarget*, *8*(49), 86693–86709.
<https://doi.org/10.18632/oncotarget.21411>

Yalchin, M., Baker, A. M., Graham, T. A., & Hart, A. (2021). Predicting colorectal cancer occurrence in ibd. In *Cancers* (Vol. 13, Issue 12). MDPI AG.
<https://doi.org/10.3390/cancers13122908>

- Yang, J., Antin, P., Berx, G., Blanpain, C., Brabletz, T., Bronner, M., Campbell, K., Cano, A., Casanova, J., Christofori, G., Dedhar, S., Derynck, R., Ford, H. L., Fuxe, J., García de Herreros, A., Goodall, G. J., Hadjantonakis, A. K., Huang, R. J. Y., Kalchauer, C., ... Sheng, G. (2020). Guidelines and definitions for research on epithelial–mesenchymal transition. In *Nature Reviews Molecular Cell Biology* (Vol. 21, Issue 6). Nature Research. <https://doi.org/10.1038/s41580-020-0237-9>
- Yang, Y., Zhou, H., Liu, W., Wu, J., Yue, X., Wang, J., Quan, L., Liu, H., Guo, L., Wang, Z., Lian, X., & Zhang, Q. (2018). Ganoderic acid a exerts antitumor activity against MDA-MB-231 human breast cancer cells by inhibiting the Janus kinase 2/signal transducer and activator of transcription 3 signaling pathway. *Oncology Letters*, 16(5), 6515–6521. <https://doi.org/10.3892/ol.2018.9475>
- Ye, X., & Weinberg, R. A. (2015). Epithelial-Mesenchymal Plasticity: A Central Regulator of Cancer Progression. In *Trends in Cell Biology* (Vol. 25, Issue 11, pp. 675–686). Elsevier Ltd. <https://doi.org/10.1016/j.tcb.2015.07.012>
- Yu, Q., Zhang, S., Chao, K., Feng, R., Wang, H., Li, M., Chen, B., He, Y., Zeng, Z., & Chen, M. (2016). E3 ubiquitin ligase RNF183 is a novel regulator in inflammatory bowel disease. *Journal of Crohn's and Colitis*, 10(6), 713–725. <https://doi.org/10.1093/ecco-jcc/jjw023>
- Zbar, A. P., Simopoulos, C., & Karayiannakis, A. J. (2004). Cadherins: An integral role in inflammatory bowel disease and mucosal restitution. In *Journal of Gastroenterology* (Vol. 39, Issue 5, pp. 413–421). J Gastroenterol. <https://doi.org/10.1007/s00535-004-1335-8>
- Zeissig, S., Bürgel, N., Günzel, D., Richter, J., Mankertz, J., Wahnschaffe, U., Kroesen, A. J., Zeitz, M., Fromm, M., & Schulzke, J. D. (2007). Changes in expression and distribution of claudin 2, 5 and 8 lead to discontinuous tight junctions and barrier dysfunction in active Crohn's disease. *Gut*, 56(1), 61–72. <https://doi.org/10.1136/gut.2006.094375>
- Zeng, F., Hon, C.-C., Sit, W.-H., Chow, K. Y.-C., Hui, R. K.-H., Law, I. K.-M., Ng, V. W.-L., Yang, X.-T., Leung, F. C.-C., & Wan, J. M.-F. (2005). Molecular characterization of *Coriolus versicolor* PSP-induced apoptosis in human promyelotic leukemic HL-60

- cells using cDNA microarray. *International Journal of Oncology*, 27(2), 513–523.
- Zhang, H., Morisaki, T., Matsunaga, H., Sato, N., Uchiyama, A., Hashizume, K., Nagumo, F., Tadano, J., & Katano, M. (2000). Protein-bound polysaccharide PSK inhibits tumor invasiveness by down-regulation of TGF- β 1 and MMPs. *Clinical and Experimental Metastasis*, 18(4), 343–352.
<https://doi.org/10.1023/A:1010897432244>
- Zhang, Henan, Shao, Q., Wang, W., Zhang, J., Zhang, Z., Liu, Y., & Yang, Y. (2017). Characterization of Compounds with Tumor-Cell Proliferation Inhibition Activity from Mushroom (*Phellinus baumii*) Mycelia Produced by Solid-State Fermentation. *Molecules*, 22(5). <https://doi.org/10.3390/molecules22050698>
- Zhang, J., Tang, Q., Zhou, C., Jia, W., Da Silva, L., Nguyen, L. D., Reutter, W., & Fan, H. (2010). GLIS, a bioactive proteoglycan fraction from *Ganoderma lucidum*, displays anti-tumour activity by increasing both humoral and cellular immune response. *Life Sciences*, 87(19–22), 628–637. <https://doi.org/10.1016/j.lfs.2010.09.026>
- Zhang, M., Zhang, Y., Zhang, L., & Tian, Q. (2019). Mushroom polysaccharide lentinan for treating different types of cancers: A review of 12 years clinical studies in China. In *Progress in Molecular Biology and Translational Science* (Vol. 163, pp. 297–328). Elsevier B.V. <https://doi.org/10.1016/bs.pmbts.2019.02.013>
- Zhang, Q. W., Lin, L. G., & Ye, W. C. (2018). Techniques for extraction and isolation of natural products: A comprehensive review. In *Chinese Medicine (United Kingdom)* (Vol. 13, Issue 1, p. 20). BioMed Central Ltd. <https://doi.org/10.1186/s13020-018-0177-x>
- Zhang, X., Zhang, S., Yan, X., Shan, Y., Liu, L., Zhou, J., Kuang, Q., Li, M., Long, H., & Lai, W. (2021). m6A regulator-mediated RNA methylation modification patterns are involved in immune microenvironment regulation of periodontitis. *Journal of Cellular and Molecular Medicine*, 25(7), 3634–3645.
<https://doi.org/10.1111/jcmm.16469>
- Zhang, Y., Sun, D., Meng, Q., Guo, W., Chen, Q., & Zhang, Y. (2017). *Grifola frondosa* polysaccharides induce breast cancer cell apoptosis via the mitochondrial-

- dependent apoptotic pathway. *International Journal of Molecular Medicine*, 40(4), 1089–1095. <https://doi.org/10.3892/ijmm.2017.3081>
- Zhao, X., Fan, J., Zhi, F., Li, A., Li, C., Berger, A. E., Boorgula, M. P., Barkataki, S., Courneya, J. P., Chen, Y., Barnes, K. C., & Cheadle, C. (2015). Mobilization of epithelial mesenchymal transition genes distinguishes active from inactive lesional tissue in patients with ulcerative colitis. *Human Molecular Genetics*, 24(16), 4615–4624. <https://doi.org/10.1093/hmg/ddv192>
- Zheng, L., Kelly, C. J., Battista, K. D., Schaefer, R., Lanis, J. M., Alexeev, E. E., Wang, R. X., Onyiah, J. C., Kominsky, D. J., & Colgan, S. P. (2017). Microbial-Derived Butyrate Promotes Epithelial Barrier Function through IL-10 Receptor-Dependent Repression of Claudin-2. *The Journal of Immunology*, 199(8), 2976–2984. <https://doi.org/10.4049/jimmunol.1700105>
- Zheng, S. G., Xu, Z., & Wang, J. (2019). A protective role of IFN- γ in T cell-mediated colitis by regulation of Treg/Th17 via induction of indoleamine-2,3-deoxygenase. *The Journal of Immunology*, 202(1 Supplement).
- Zhong, L., Yan, P., Lam, W. C., Yao, L., & Bian, Z. (2019). Coriolus Versicolor and Ganoderma Lucidum Related Natural Products as an Adjunct Therapy for Cancers: A Systematic Review and Meta-Analysis of Randomized Controlled Trials. *Frontiers in Pharmacology*, 10, 703. <https://doi.org/10.3389/fphar.2019.00703>
- Zhu, L., Shi, T., Zhong, C., Wang, Y., Chang, M., & Liu, X. (2017). IL-10 and IL-10 Receptor Mutations in Very Early Onset Inflammatory Bowel Disease. *Gastroenterology Research*, 10(2), 65–69. <https://doi.org/10.14740/gr740w>
- Ziogas, D. C., Terpos, E., Kastritis, E., & Dimopoulos, M. A. (2017). An overview of the role of carfilzomib in the treatment of multiple myeloma. *Expert Opinion on Pharmacotherapy*, 18(17), 1883–1897. <https://doi.org/10.1080/14656566.2017.1404575>

Appendixes

Appendix A

Funding sources

This work has been supported by the following institutions:

- Center for Industrial Technological Development (CDTI, Interconecta Program, 2015), co-funded by the Fondo Europeo de Desarrollo Regional (FEDER) “A way of Making Europe”). In collaboration with CZ Veterinaria, S.A. and Hifas da Terra S.L companies.
- Instituto de Salud Carlos III (ISCIII, Spain) and Plan Estatal I + D + i. Grant agreements PI13/00250 and PI18/00121 by Fondo Europeo de Desarrollo Regional (FEDER) “A way of Making Europe”.
- Axencia Galega de Innovación, Xunta de Galicia. Ayudas del Programa de Consolidación y Estructuración de Unidades de Investigación Competitivas Modalidad Grupo con Potencial Crecimiento. (IN607B2020/14).
- Fundación Profesor Novoa Santos – Beca Post-Especialización 2018
- Diputación de A Coruña - (BINV-CS) BOLSAS INVESTIGACIÓN 2018- Área de ciencias da saúde.
- Universidad de A Coruña - Programa inMOTION. Ayudas para estancias predoctorales INDITEX-UDC 2019

Appendix B

Publications related to the present thesis

- **Roca-Lema D**, Castosa R, Martinez-Iglesias O, Casas-Pais A, Díaz-Díaz A, Iglesias P, Santamarina I, Graña B, Calvo L, Valladares-Ayerbes M, Concha Á, Figueroa A. Hakai overexpression effectively induces tumour progression and metastasis in vivo. *Sci Rep*. 2018 Feb 22;8(1):3466. doi: 10.1038/s41598-018-21808-w. PMID: 29472634; PMCID: PMC5823865. ***Co-first author**
- **Roca-Lema D**, Martinez-Iglesias O, Fernández de Ana Portela C, Rodríguez-Blanco A, Valladares-Ayerbes M, Díaz-Díaz A, Casas-Pais A, Prego C, Figueroa A. *In Vitro* Anti-proliferative and Anti-invasive Effect of Polysaccharide-rich Extracts from *Trametes Versicolor* and *Grifola Frondosa* in Colon Cancer Cells. *Int J Med Sci*. 2019 Jan 1;16(2):231-240. doi: 10.7150/ijms.28811. PMID: 30745803; PMCID: PMC6367522.

Research Paper

In Vitro Anti-proliferative and Anti-invasive Effect of Polysaccharide-rich Extracts from *Trametes Versicolor* and *Grifola Frondosa* in Colon Cancer Cells

Daniel Roca-Lema^{1*}, Olaia Martínez-Iglesias^{1*}, Catalina Fernández de Ana Portela², Arturo Rodríguez-Blanco², Manuel Valladares-Ayerbes³, Andrea Díaz-Díaz¹, Alba Casas-Pais¹, Cecilia Prego⁴ and Angélica Figueroa¹✉

1. Epithelial Plasticity and Metastasis Group, Instituto de Investigación Biomédica de A Coruña (INIBIC), Complejo Hospitalario Universitario de A Coruña (CHUAC), Sergas, Universidade da Coruña (UDC).
2. Hifas da Terra SL, Pontevedra, Spain.
3. Department of Medical Oncology, Hospital Universitario Reina Sofía, Córdoba, Spain.
4. CZ Veterinaria SA, Pontevedra, Spain.

*These authors contributed equally to this work.

✉ Corresponding author: Angélica Figueroa, Epithelial Plasticity and Metastasis Group, Instituto de Investigación Biomédica (INIBIC), Complejo Hospitalario Universitario A Coruña (CHUAC), Sergas, Universidade da Coruña (UDC), As Xubias, 15006, A Coruña, Spain. Ph: +34-981-176399. angelica.figueroa.conde-valvis@sergas.es

© Ivyspring International Publisher. This is an open access article distributed under the terms of the Creative Commons Attribution (CC BY-NC) license (<https://creativecommons.org/licenses/by-nc/4.0/>). See <http://ivyspring.com/terms> for full terms and conditions.

Received: 2018.07.27; Accepted: 2018.11.05; Published: 2019.01.01

Abstract

Colorectal cancer (CRC) is one of leading causes of mortality in western countries and novel treatment strategies are required. The medicinal application of mushrooms has been used in traditional medicine in many oriental countries. Polysaccharide-rich extracts obtained from certain medicinal mushroom species have shown antitumor effects in different experimental models. In the present study, we have developed polysaccharide-rich extracts from *Trametes versicolor* (TV) and *Grifola frondosa* (GF) fruit bodies. We aim to evaluate the anticancer effects of these polysaccharide-rich extracts in LoVo and HT-29 human colon cancer cells. The *in vitro* effects were determined by cytotoxicity assay, proliferation assay, wound healing assay and invasion assay. Moreover, the effect on anchorage independent-cell growth was also determined. Our results showed that TV and GF extracts did inhibit human colon cell proliferation and induce cytotoxicity. Furthermore, both fungal extracts significantly inhibited oncogenic potential, cell migration and invasion in colon cancer cells. In addition, extracts induce a more epithelial phenotype, observed by phase contrast images, together with an increase expression of the E-cadherin epithelial marker, detected by western-blotting analyses. Moreover, by using gelatin zymography assays, it was detected a decrease of MMP-2 enzyme activity, a crucial metalloproteinase important for the degradation of the extracellular matrix. Finally, the combination of the extracts with one the most clinical used agents for colorectal cancer, 5-fluorouracil, increases cell cytotoxicity. Taken together our results underscore a potential antitumor effect of polysaccharide-rich extracts obtained from TV and GF in human colon cancer cells lines. These finding may contribute to the reported health effects of fungal extracts.

Key words: Colon cancer, invasion, proliferation, Fungal extracts

Introduction

Colorectal cancer (CRC) is one of the leading causes of mortality in Western countries [1, 2]. Around 90% of cancer-related deaths are due to

metastasis [3]. The metastatic process is constituted of a number of sequential events required in order for the tumour cell to successfully metastasize. In the

metastatic cascade, epithelial cells detach from the primary tumour, migrate, acquire the ability to invade and spread throughout the body to finally settle down in a second site. During this metastatic cascade, other important changes take place such as the alteration of cell-cell contacts and cell-matrix adhesions.

Complementary and alternative medicines have appeared as a promising strategy to treat a broad number of diseases. Indeed, natural products are emerging as potent sources for food supplements to improve cancer outcomes and patient quality of life [4]. Important research lines of evidences have demonstrated that medicinal mushrooms have a potent anti-neoplastic activity, including anti-proliferative and anti-angiogenesis properties. It has been reported that certain species of higher Basidiomycetes, including *Trametes versicolor* (TV) and *Grifola frondosa* (GF), produce several metabolites with anti-proliferative, antioxidant, antiviral, antimicrobial and immunomodulatory therapeutic effects [5, 6].

Grifola frondosa is an edible mushroom with an established immunological effect. Indeed, it has already been reported the effect of GF extracts in human clinical trials in breast cancer patients [7]. For example, β -(1,3)(1,6)-glucan extract from GF induces anti-tumour activity by enhancing hematopoiesis and activating the host immune system [8]. Besides, Z-fraction polysaccharide from GF inhibits tumour growth in BALB/c mice inoculated with colon cancer cell lines [9]. On the other hand, *Trametes versicolor* also has immunomodulatory effect and specific extracts are used in human cancer therapy in breast cancer prevention. However, the molecular mechanism involved in the antitumor action is still not clear. Recent evidences suggest that polysaccharides extracts can directly affect the viability of human tumour cells, independently of the immune system. For example, polysaccharide-enriched extracts from GF induce toxicity and apoptosis in human breast and gastric cancer cells while slightly affecting the growth of normal liver cells [10, 11]. Moreover, polysaccharides from GF are able to modulate tumour progression in human breast cancer cells by modifying the expression of genes such as *IGFBP-7*, involved in migration and metastasis [12, 13]. The potential effect of polysaccharides-enriched extracts from GF and TV in human colon carcinoma has not been extensively studied and whether they could play a role in tumour progression and metastasis is also unknown.

Colon tumour cells start to dedifferentiate and acquire enhanced migratory capabilities in order to metastasize. A critical molecular hallmark during dedifferentiation process is the loss of E-cadherin at cell-cell contacts, during a program named

epithelial-to-mesenchymal transition (EMT). Loss of E-cadherin is associated to the progression from benign to malignant tumour. Indeed, it was reported that *in vitro* re-expression of E-cadherin protein in E-cadherin negative tumour cells inhibit cell growth and block invasiveness [14, 15]. On the other hand, cell motility is also associated to the proteolytic activity of matrix metalloproteinases (MMPs). MMPs are a family of zinc-dependent endopeptidases implicated in the proteolytic degradation of the extracellular matrix (ECM) and in the cleavage of cell surface receptors. MMPs play an important role in proliferation, cancer migration and invasion [16]. The two gelatinase MMPs (MMP-2 and MMP-9) are able to degrade collagen type IV playing a critical role in tumour invasiveness [17].

In the present study, we aim to evaluate the anticancer effect of polysaccharide-rich extracts from *Trametes versicolor* and *Grifola frondosa* in human colon cancer cells. We particularly show that both extracts inhibit cell proliferation, oncogenic potential, migration and invasion. Moreover, their antitumor action may be due to the increase E-cadherin protein expression and the reduction of MMP-2 activity. Finally, we also show that the combination of 5-Fluorouracil, a common clinical drug used for colorectal cancer, together with the polysaccharide-rich extracts increases cell cytotoxicity suggesting a potential clinical benefit for colon cancer.

Material and methods

Material

Fruiting bodies from *Grifola frondosa* and *Trametes versicolor* were produced at Hifas da Terra S.L. plant and ground using industrial blenders. The resulting material was extracted with distilled water at a ratio of 1:12 (w/v) for *Grifola frondosa* and 1:10 (w/v) for *Trametes versicolor* at 80°C for 30 minutes and filtrated with Whatman No. 1 filter paper. The obtained residue was again extracted applying the same procedure and both filtrates were combined and lyophilized. *Grifola frondosa* extract presented a total Glucan content of 45 % (w/w), representing 10.20 % and 34.80 % of α -Glucans and β -glucans, respectively (w/w; β -Glucan Assay Kit Yeast & Mushroom, Megazyme). *Grifola frondosa* extract is present in several MicoSalud® products of Hifas da Terra S.L. *Trametes versicolor* extract presented a total Glucan content of 74.30 % (w/w); where α -Glucans and β -glucans represented 8.7 % and 65.60 % (w/w), respectively. *Trametes versicolor* extract is present in several MicoSalud® products of Hifas da Terra S.L., including Mico-Corio PSK®. Stock solutions of both extracts were re-suspended in distilled water at

50mg/ml and stored at -20°C. 5-Fluorouracil (5-Fu) was purchased from Sigma-Aldrich.

Cell lines

Human colon carcinoma LoVo and HT-29 cells were grown with F-12K Medium (Kaighn's Modification of Ham's F-12 Medium) and McCoy's 5a Medium Modified, respectively. Cells were supplemented with penicillin/streptomycin (50U/ml) and 10% heat-inactivated fetal bovine serum and were grown in a humidified incubator at 37°C with 5% CO₂. Cells were authenticated with the StemElite ID system (Promega) and monthly tested for mycoplasma to ensure free-contamination cultures.

Cytotoxicity assay

For cytotoxicity assays, 1×10^4 cells were plated per well into a 96-well plate and cultured during 24 h. Then, cells were treated with 10, 50, 100, 250 or 1000 µg/ml of extracts from *Trametes versicolor* or *Grifola frondosa* for 24, 48 or 72 h. Viability was measured by using a MTT [3-(4,5-dimethylthiazol-2-yl)-2,5-diphenyltetrazolium bromide] colorimetric cell viability assay kit (Sigma Aldrich, St Louis, MO). Cells were treated with 0.5 mg/ml of MTT for 3 hours. Then, medium was removed and 100 µl of DMSO was added to each well and shaken for 10-15 min. Absorbance was measured at 570 and 630 nm using a Multiskan Plus Reader (Thermo Fisher, MA, USA). Experiments were repeated at least three times and 6 wells were used for each treatment. The half-maximal inhibitory concentration (IC₅₀) values were calculated from dose-response curves constructed using GraphPad Prism software. Results are expressed as mean ± S.D and as fold change compared to untreated cells. To study the effect of the combination of fungal extracts with 5-fluorouracil (5-Fu), cells were treated with different concentrations of 5-Fu (5, 10, 100 and 1000 ng/ml), dissolved in fresh medium, in combination with 250 µg/ml of fungal extracts. After 72 h of incubation with extracts and 5-Fu, cells were treated with 0.5 mg/ml of MTT for 3 hours and cell viability was calculated as previously mentioned.

Proliferation Assay

For proliferation assays, 1×10^4 LoVo cells were plated per well into a 96-well plate and after 24 h cells were treated with 10 or 100 µg/ml of different fungal extracts during 48 h. Then, cells were treated with 10 mM BrdU for 2 h. BrdU incorporation into newly synthesized DNA was measured using a cell proliferation colorimetric immunoassay kit (Roche) according to the manufacturer's instructions. Data are the average of three independent experiments

performed six times. Results are expressed as mean ± S.D and fold change is represented compared to untreated cells.

Soft agar anchorage-independent cell growth

For soft agar-colony formation assay, 5×10^3 LoVo cells/well were cultured into a 12-well plate in medium containing 0.375% low-melting agarose (Sigma Aldrich, St Louis, MO). This agarose was layered over 0.6% agarose. Each well was allowed to solidify and subsequently covered with 150 µl culture media in presence or absence of the indicated fungal extracts (10, 100 or 250 µg/ml). Fungal extracts were refreshed every 3 days. After 21 days, cells were fixed and stained with 0.2% crystal violet in 5% formalin solution. Colonies were counted in Olympus microscope (magnification 40x) and whole wells were photographed. Experiments were repeated two times plated in triplicates. Results are expressed as mean ± SD and fold change is represented compared to untreated cells.

Wound healing assay

Cells were seeded at a high density (7×10^5 cells/ml) in 24-well plates containing Culture-Inserts (Ibidi) and allowed to adhere overnight. Then, cells were treated for 2 h with 10 µg/ml of mitomycin C and inserts were removed. Cells were treated with 10 or 100 µg/ml of fungal extracts and wound healing was maintained during 24, 48 and 72 h. Photographs were taken in Nikon Eclipse-Ti microscope (magnification 100x) at the indicated times. Quantification of the distance after cell migration was determined by using ImageJ program, using the MRI Wound Healing Tool. Experiments were repeated at least two times in replicates and results are expressed as mean ± S.D and fold change is represented compared to untreated cells.

Invasion assay

For invasion assays, cells were cultured in Ham's F-12K medium with FBS 1% with the fungi extracts (10 or 100 µg/ml) for 48 h. Then, LoVo cells (3×10^5 cells/well) were seeded in a cell invasion chamber (Cell invasion assay kit, Chemicon International) in a 24-well plate containing 8-µm pore size polycarbonate membrane covered with a thin layer of extracellular matrix as described [19]. After 72 h, filters were fixed and stained with crystal violet following the manufacturer's specifications. Cells were counted by photographing five-fields in an Olympus microscope (magnification 200x). Experiments were performed in triplicates for each condition and repeated at least two times. Results are expressed as mean ± S.D and fold induction is represented compared to untreated cells.

Phase contrast microscopy

For phase-contrast images, 1×10^5 LoVo cells were plated per well in a 12-well plate and cultured for 24 h before treatment with 10 or 100 $\mu\text{g}/\text{ml}$ of *Trametes versicolor* or *Grifola frondosa* extracts for 48 h. Then, cells were fixed with 4% paraformaldehyde in phosphate-buffered saline (PBS) for 20 min. Phase-contrast images were acquired using Nikon Eclipse-Ti microscope with 100x magnification.

Western blotting

For protein extraction, 8×10^5 LoVo cells were plated in 60mm dishes, and after 24 h cells were treated with 100 or 250 $\mu\text{g}/\text{ml}$ of fungal extracts for 72 h. Then, whole cell extracts were prepared for protein extraction as previously described [18]. Briefly, cells were lysed for 30 min in 0.3 ml of 1% Triton X-100 lysis buffer (20 mM Tris-HCL [pH 7.5], 150 mM NaCl, and 1% Triton X-100) containing 5 $\mu\text{g}/\text{ml}$ leupeptin, 50 mM phenylmethylsulfonyl fluoride, and 7.2 trypsin inhibitor units for aprotinin. After centrifugation at 14000 g for 10 min, twenty micrograms of the supernatants were loaded in 10% polyacrilamide SDS-PAGE. Western blotting was performed as previously described [19]. For western blotting, antibodies used are: monoclonal E-cadherin antibody (BD 610182), and monoclonal GAPDH antibody (Invitrogen, 39-8600). Experiments were repeated at least three times. Images were quantified by densitometry and results are expressed as mean \pm S.D and fold induction is represented compared to untreated cells.

Gelatin zymography

Zymogram technique was used to detect matrix metalloproteinase 2 and 9 (MMP-2 and MMP-9) activity. Cells were seeded in 60 mm dishes and incubated with 100 or 250 $\mu\text{g}/\text{ml}$ of fungi extracts for 72h. The last 24 h, cells were grown in 1 ml of serum-free medium. Medium was collected, centrifuged and loaded, using cell number for normalization. Samples were run in a 10% polyacrilamide gels containing gelatin (0.05%) under non-reducing conditions. SDS was removed by extensively washing in 2.5% Triton X-100 and metalloproteinase activity was reactivated by incubating the gel in a buffer containing 40 mM Tris-HCl pH 7.5; 0.1 M benzamidine (SIGMA) and 10 mM CaCl_2 , for 72 h. The gel was stained with Coomassie Blue R250 in a 10% acetic acid, 50% methanol solution overnight, and then, destained in 10% acetic acid, 50% methanol, until bands were clearly visible. Protease activity appeared as clear bands against a blue background where MMP-2 or MMP-9 has digested gelatin substrate. Gels were

photographed and quantified with Amersham Imager 600 equipment. Experiment was repeated three times and quantification is expressed as mean \pm SD.

Statistical analysis

Statistical significance was determined with GraphPad Prism software applying ANOVA or Kruskal-Wallis test. Shapiro-Wilk test was used to check a normal distribution and Levene test to determine the equality of variances. Results are expressed as means \pm SD. Significance of the Student *t*-test among the experimental groups indicated in the figures is shown as * $p < 0.05$, ** $p < 0.01$ and *** $p < 0.001$.

Results

Effect of TV and GF extracts on cell viability and proliferation in human colon cancer cells

To determine the effect of TV and GF fungal extracts on cancer cell viability, two different human colon cancer cell lines were selected. LoVo colon cells, derived from a metastatic site, and HT-29, a colorectal adenocarcinoma cell line with an epithelial morphology. Cells were treated at different concentrations ranging from 10 $\mu\text{g}/\text{ml}$ to 250 $\mu\text{g}/\text{ml}$ for 24 h, 48 h and 72 h. TV extract did not show any significant effect on cell viability after 24 h of treatment in LoVo cells. However, slightly reduction was detected after 48 h, and significantly decrease was shown after 72h, up to 40% reduction at a lower concentration (10 $\mu\text{g}/\text{ml}$), (Figure 1A). On the other hand, no significant effect was detected while treating HT-29 cells with TV extracts after 24 h, 48 h and 72 h (Figure 1B). GF treatment showed its inhibitory effect on LoVo cell viability at earlier times than TV extract by using higher concentrations (100 $\mu\text{g}/\text{ml}$ and 250 $\mu\text{g}/\text{ml}$). After 72 h of GF treatment, markedly reduction on cell viability was seen at a lower concentration (40% reduction compared to untreated cells using 10 $\mu\text{g}/\text{ml}$), (Figure 1C). Finally, the most prominent cytotoxicity effect was observed using GF extract in HT-29 cells. In these cells, at a low concentration of 50 $\mu\text{g}/\text{ml}$ GF extract, it was already observed a strong decrease after 24 h, 48 h and 72 h. This inhibitory effect on cytotoxicity reached up to 60-70% reduction after 72 h of GF treatment with 100 $\mu\text{g}/\text{ml}$ concentration, and similar results were observed with the concentration of 250 $\mu\text{g}/\text{ml}$ at any of the tested times (24 h, 48 h and 72h) (Figure 1D). Moreover, no cytotoxicity effect of the TV and GF extracts was detected in a non-tumorigenic epithelial MDCK cell lines (data not shown). The IC_{50} values for TV and GF were determined for each colon cancer cell lines (Table 1). Taken together our results show a more potent cytotoxicity effect of GF extracts

compared to TV extracts in LoVo and HT-29 colon cancer cell lines.

Table 1. IC₅₀ values for both extracts were calculated and indicated for Lovo and HT29 cell lines.

LoVo		IC ₅₀ (µg/ml)	
	24h		72h
<i>T. versicolor</i>	-		224,02
<i>G. frondosa</i>	934,82		127,12
HT-29		IC ₅₀ (µg/ml)	
	24h		72h
<i>T. versicolor</i>	-		-
<i>G. frondosa</i>	44,09		21,07

To analyse the effects of TV and GF extracts in colon cancer growth, LoVo cells were treated with increasing concentrations (10 µg/mg and 100 µg/ml) of each extract for 48 h and then proliferation was measured by BrdU assay. Quantification of BrdU incorporation confirmed that exposure to lower concentrations (10 µg/ml) of TV resulted in a significantly growth inhibition (up to 45% compared to untreated cells). Moreover, treatment with 10 µg/ml of GF extract produced up to 50-60% inhibition, while this inhibitory effect was increased up to 80% inhibition at 100 µg/ml of GF extract (Figure 1E). Our results showed a stronger anti-proliferative effect of GF extract compared to TV extract in Lovo cells. Interestingly, effects of both fungal extracts are more markedly on proliferation than on toxicity, therefore exposure to lower concentrations resulted in a growth inhibition, avoiding cytotoxicity effect.

Effect of TV and GF extracts on anchorage-independent cell growth

Given the observed effect in cytotoxicity and proliferation of the fungi extracts on colon cancer cells, we wondered whether they could have a potential role on the inhibition of tumour progression. The ability of cancer cells to survive and proliferate in the absence of a solid substrate is an important characteristic for the acquisition of an invasive and metastatic phenotype. By using soft agar growth assays, we examined the effect of the TV and GF extracts on colony formation in LoVo cells. As shown in Figure 2, both extracts significantly reduced colony formation induced by LoVo tumour cells. The effect was even detected at the lowest concentration tested of 10 µg/ml for both extracts. These results indicate that TV and GF extracts reduce anchorage-independent cell growth, thus reducing the oncogenic potential in colon cancer cells.

Effect of TV and GF extracts on cell migration and invasion

Cell migration and invasion capabilities of tumour cells are important features of malignant tumours during tumour progression and metastasis. We examined whether TV and GF extracts can inhibit cell migration in LoVo cells by using wound-healing assays. Results showed 40% and 20% of wound closure in LoVo cells after treatment with GF extracts during 48 h and 72 h, respectively (Figure 3A). Concentrations of 10 µg/mg and 100 µg/ml of TV extracts reduce around 50% of the wound closure after 48h. Similar results were obtained after GF

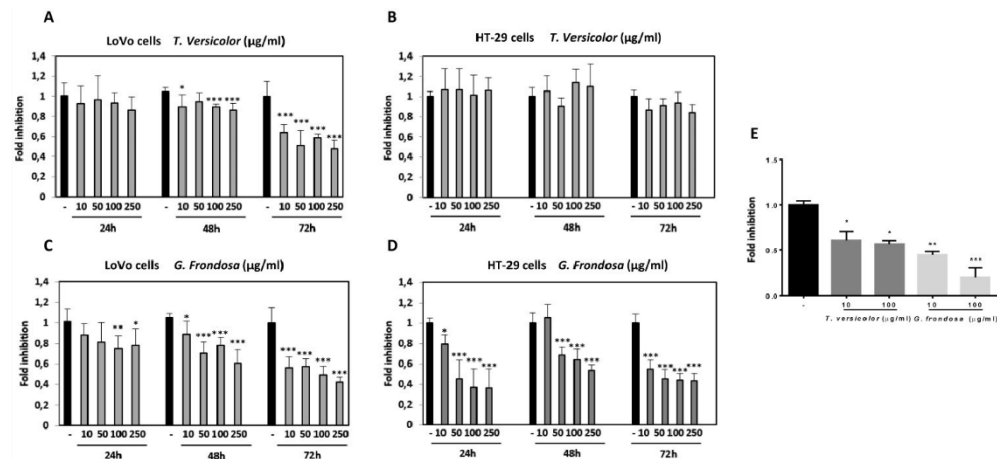


Fig 1. Effect of *Trametes versicolor* and *Grifola frondosa* extracts on viability of colon cancer cells. LoVo (A and C) and HT-29 cells (B and D) were treated with *Trametes versicolor* and *Grifola frondosa* extracts for 24, 48 and 72 h and MTT activity was determined. (E) Effect of fungi extracts on cell proliferation in LoVo cells was determined by a BrdU assay as described in Material and Methods. Data are the means \pm SD of three independent experiments (* $p < 0.05$, ** $p < 0.01$, *** $p < 0.001$)

treatment during 48 h treatment with 10 $\mu\text{g}/\text{mg}$ concentration (Figure 3A). Based on the observation that fungal extracts significantly inhibited LoVo cells migration, it is reasonable to hypothesize whether TV and GF may also affect cell invasion. To investigate the possible effect of the extracts on the invasive capacity, an invasion assays in LoVo cells was performed. It was previously reported that LoVo cells were able to cross through a matrigel matrix [20]. Our

results clearly showed that TV and GF extracts significantly attenuated the invasion capability of LoVo colon cancer cells (Figure 3B) after treatment with 10 or 100 $\mu\text{g}/\text{mg}$ of both extracts. These results pointed out that TV and GF extracts inhibited cell migration and invasion in LoVo cells at non-cytotoxic dosage (10 $\mu\text{g}/\text{mg}$), suggesting that both extracts might be potent and multiple functional agents to treat colon cancer progression and metastasis.

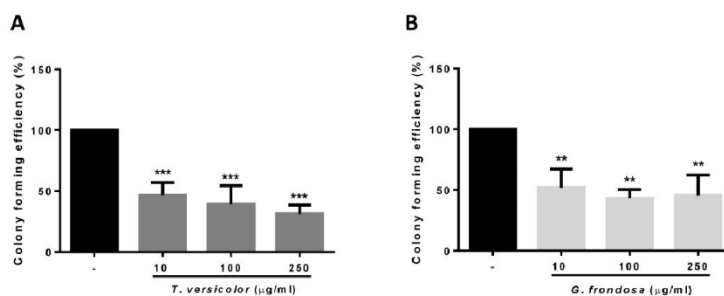


Fig 2. Effect of TV and GF extracts on anchorage-independent cell growth in soft agar. LoVo cells colonies were treated with *Trametes versicolor* (A) and *Grifola frondosa* (B) extracts for 21 days and the colony formation was determined by manual counting. Data are represented by the means \pm SD of two independent experiments (* $p < 0.05$, ** $p < 0.01$, *** $p < 0.001$)

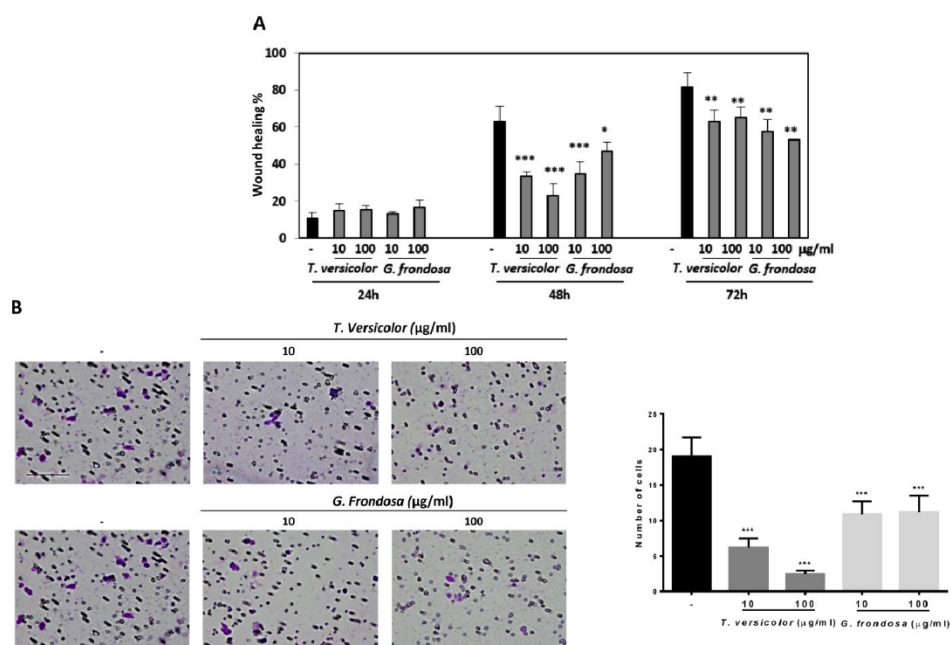


Fig 3. Effect of *Trametes versicolor* and *Grifola frondosa* extracts on cell migration and invasion in LoVo colon cancer cells. (A) LoVo cells were pre-treated for 2 h with mitomycin C to block proliferation and wound healing assay was followed for 3 days in presence or absence of the indicated concentrations of TV and GF extracts. Wound closure was quantified using ImageJ program. Data are represented by the means \pm SD in duplicates from two independent experiments. (B) Effect of TV and GF extracts on cell invasion in LoVo colon cancer cells. Cells were treated with the indicated concentrations of extracts for 48h. Cells were trypsinized and seeded in an invasion chamber as described in the Material and Methods. Migrated cells were stained, photographed and counted with a microscope at 200X. Scaled bar 627 μm . Data are the means \pm SD of three independent experiments (* $p < 0.05$, ** $p < 0.01$, *** $p < 0.001$).

Effect of TV and GF extracts on E-cadherin protein expression and MMP-2 activity

Next, we decided to study the possible molecular mechanisms by which migration and invasion could be regulated. To this end, first it was analysed the effect of TV and GF extracts on cellular morphology by phase-contrast microscopy. As shown in Figure 4, a more prominent epithelial morphology was observed in LoVo cells under TV and GF treatment (Figure 4A and B, respectively) compared to the fibroblast phenotype observed in non-treated cell. This morphology switch, from fibroblast to epithelial phenotype was accompanied by an increase in cell-cell adhesions, and a decrease number of membrane protrusions (Figure 4A and B, respectively). In addition, we evaluated the effect of the extracts on E-cadherin expression. E-cadherin is one of the best characterize cell adhesion molecules between epithelial cells, important for the establishment of tight cell-cell contacts. Indeed, loss of E-cadherin is lost during carcinoma development. The dedifferentiation process is linked to carcinoma-associated EMT, a crucial event for cellular migration and invasion of tumour cells. Moreover, E-cadherin loss is associated to tumour progression, invasion and metastasis. Then, we analysed E-cadherin protein expression by western blotting (Figure 4C, upper panel and Figure S1) and a statistical significant increase of E-cadherin protein expression was detected after treatment with TV and GF extracts in LoVo cells (Figure 4C, lower panel). Next, we tested whether fungal extracts may suppress metalloproteinase activity. It is known that the degradation of the extracellular matrix is a crucial event during tumour invasion and metastasis. The

gelatinases MMP-2 and MMP-9 are two members of the MMP family that have been extensively studied given their consistent association with tumour invasion and metastasis. MMP-2 and MMP-9 activity was measured by a zymogram assay and a significantly decrease on MMP-2 activity was detected after treatment with both fungal extracts (Figure 4D, upper panel and Figure S2). Although both fungal extracts were able to induce a strong reduction of MMP-2 activity, this reduction was more prominent using GF extract, reaching up to 60% decrease of MMP-2 activity with the lowest concentration tested at 100 $\mu\text{g}/\text{mg}$ (Figure 4D, lower panel).

TV and GF extracts increases the effect of 5-fluorouracil

5-fluorouracil (5-Fu) is a commonly used cytotoxic agent to treat colon cancer patients. The combination of 5-fluorouracil-based chemotherapy with other agents, such as natural products, has been extensively studied. However, the optimal combination regimen has not been determined. We examined the cytotoxicity effect of TV and GF fungal extracts in combination with 5-FU in LoVo cells. LoVo cells were treated with increasing concentrations of 5-Fu, alone or in combination with fungal extracts. MTT cytotoxicity assays showed an increase cytotoxicity effect at the lowest concentrations tested of 5-Fu (0,005 $\mu\text{g}/\text{ml}$) in combination with 250 $\mu\text{g}/\text{ml}$ of TV or GF fungal extracts. Indeed, the combination of 5-Fu with TV extracts was more evident (Figure 5). These results suggest a possible benefit of these fungal extracts in combination with 5-fluorouracil-based chemotherapy in colon cancer.

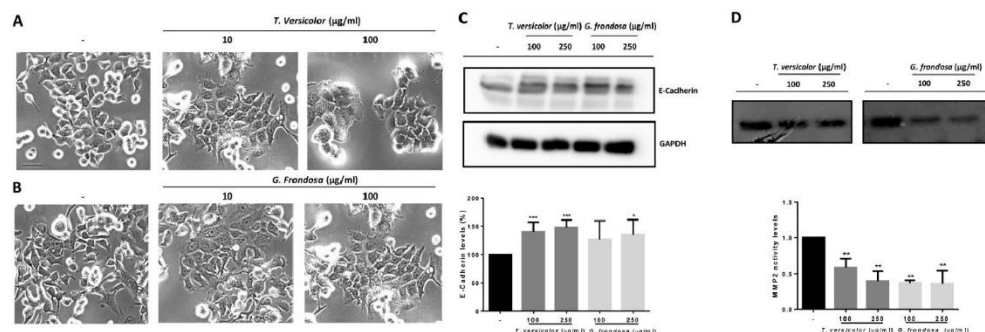


Fig 4. Effect of *Trametes versicolor* and *Grifola frondosa* extracts on cell morphology and invasion-related proteins. (A) Effect of TV extract on cell morphology of LoVo cells. **(B)** Effect of GF extract on cell phenotype in LoVo cells. (A and B) Phase-contrast microscopy images were taken after 48 h treatment with 10 $\mu\text{g}/\text{mg}$ or 100 $\mu\text{g}/\text{mg}$ of the indicated extracts. Scale bar 100 μm . **(C)** Effect of TV and GF extracts on E-cadherin protein expression. LoVo cells were treated with fungal extracts for 72 h and E-cadherin expression was determined by western-blot (upper panel). Western blot data are representative of three independent experiments and quantification by densitometry was represented (lower panel) **(D)** Effect of TV and GF extracts on the activity of metalloproteinases in LoVo colon cancer cells was determined by zymogram assay. LoVo cells were treated with the indicated concentrations of the indicated fungal extracts for 72 h and MMP2 activity is shown in upper panel. Quantification of three independent experiments is represented in the lower panel. Data are the means \pm SD of three independent experiments ($^*p<0.05$, $^{**}p<0.01$, $^{***}p<0.001$).

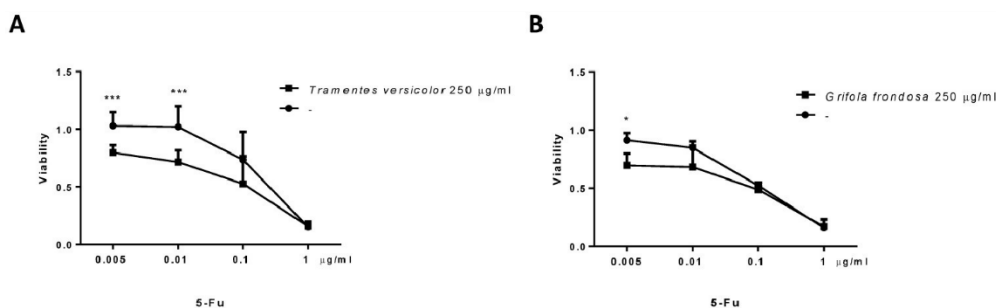


Fig 5. Effect of *Trametes versicolor* and *Grifola frondosa* extracts in combination with 5-Fluorouracil on cytotoxicity in LoVo colon cancer cells. (A) LoVo cells were treated with the indicated concentration of *Trametes versicolor* extract in combination with increasing concentrations of 5-Fluorouracil. **(B)** LoVo cells were treated with the indicated concentration of *Grifola frondosa* extract in combination with increasing concentrations of 5-Fluorouracil. Cell viability was measured as indicated in material and methods. Data are represented as means \pm SD of three independent experiments (* $p < 0.05$, ** $p < 0.01$, *** $p < 0.001$).

Discussion

Basidiomycete mushrooms have been shown to exert therapeutic anticancer properties, primarily because they contain a number of biologically active compounds. This effect is mainly linked to the presence of polysaccharides and their derivatives. Certain species of medicinal mushrooms produce bioactive compounds with antitumor activity that could work as adjuvants together with cancer chemotherapy. Indeed, polysaccharide-rich extracts from *Grifola frondosa* and *Trametes versicolor* species have already shown to play relevant clinical benefits in cancer patients [21, 22]. Recent evidence suggested a direct antitumor effect of polysaccharides-extracts in cancer cells independently of its action on the immune system. In this study, we used polysaccharide-rich extracts from GF and TV in order to investigate the possible molecular mechanism involved in the antitumor action in human colon cancer cell lines. Our results show that polysaccharide-rich extracts from GF and TV were capable not only to directly inhibit tumour cell proliferation in human colon carcinoma cells but also to inhibit anchorage-independent cell growth, cell migration and invasion, which are characteristics that facilitates the metastatic process in multiple carcinoma types [14]. Both extracts were able to induce an epithelial phenotype by increasing epithelial E-cadherin proteins marker, while the Vimentin mesenchymal marker was almost not detected in LoVo cells. Importantly, loss of E-cadherin during the acquisition of invasive characteristics has been linked to the metastatic process of colon tumour cells [23, 24]. In addition, we also observed that both extracts significantly decreased MMP-2 activity. Importantly, MMP-2 degrade extracellular matrix and promote cell growth and invasion in colorectal cancer and low levels of MMP-2 are associated with survival in breast carcinoma [25-27]. It has been reported that

MMPs activity may be regulated at different levels such as transcription, mRNA half-life, secretion, localization, regulation by proteolytic cleavage, proteinase inhibitors or post-translational modification (such as phosphorylation, or acetylation). However, further studies are needed to determine the most probable mechanism by which MMP-2 activity is regulated by these two TV and GF extracts. The fact that both extracts are able to decrease MMP-2 activity and increase E-cadherin protein levels may explain, at least in part, the mechanism by which they may inhibit cell migration and invasiveness in human colon cancer cells. However, other previous studies using TV extracts were reported to have different effect. For example, a reduction in MMP-9 activity but no changes for MMP-2 activity was observed by using aqueous extracts from TV in mouse mammary carcinoma [28]. On the other hand, an inhibition of both enzymes was detected by using protein-bound polysaccharide-K extracted from TV in human pancreatic and gastric cancer cell lines [29]. Interestingly in both studies it is shown how anti-migratory activity was not linked to anti-proliferative activity. In this study, the developed polysaccharides-rich extracts from GF and TV showed an anti-proliferative and anti-migratory action in human colon cancer cells, further supporting the potential benefit of the extracts in human colon cancer treatment.

Not many studies have reported a direct effect of polysaccharides-rich extracts from GF and TV in colon cancer cells and, in general, the reported investigations were performed in murine cancer cells with different results. For example, a heteropolysaccharide (MZF) from GF did not affect cell proliferation *in vitro* using mouse colon-26 cells [30]. On the other hand, although TV polysaccharide-rich extracts were shown to decrease cell viability in a human colon carcinoma cell line by

inhibiting apoptosis [31], no effect on cell proliferation was observed in human pancreatic and gastric cancer cell lines [29]. A water extract from TV, similar to the developed in the present study, did not show cytotoxicity effect in mouse mammary carcinoma even at a higher concentration (2 mg/mL) [28]. It is important to note that in this reported study, polysaccharide content was only 8.34 % (w/w) while in our study a higher-relative fraction of bioactive-polysaccharides was obtained (45 to 74% in glucans content). These differences may explain the different cytotoxicity effect in different cell lines, but also it may be influenced by the fruit body composition or the extraction procedures performed. Our data suggest that the extracts obtained in the present study may affect cancer cell proliferation and reinforces the critical importance of the production techniques used to observe these effects in cancer cells. Finally, the combination of 5-fluorouracil together with each polysaccharide-rich extracts increases cell cytotoxicity. These data suggest a potential adjuvant role for these extracts together with certain chemotherapeutic agents such as 5-Fu. Taken all together, the potential antitumor effect of the polysaccharide-rich GF and TV extracts in other human cancer cells and *in vivo* model systems awaits to be elucidated. Moreover, future clinical trials are needed to further evaluate safety and efficacy of these two newly developed GF and TV extracts.

Supplementary Material

Supplementary figures.

<http://www.medsci.org/v16p0231s1.pdf>

Acknowledgments

This work has been supported by the Center for Industrial Technological Development (CDTI, Interconecta Program, 2015), co-funded by the Fondo Europeo de Desarrollo Regional (FEDER) “A way of Making Europe” and by the companies CZ Veterinaria, S.A. and Hifas da Terra S.L. Roca-Lema has been supported by post-specialization fellowship from Fundación Profesor Novoa Santos, Diaz-Diaz has been supported by FPU contract (FPU014/02837) from Ministerio de Educación Cultura y Deporte from Spain and Casas-Pais has been supported by a predoctoral contract (IN606A-2017/013) from Axencia Galega de Innovación (GAIN)-Consellería de Economía, Empleo e Industria from Xunta de Galicia, Spain.

Competing Interests

The authors have declared that no competing interest exists.

References

- Siegel RL, Miller KD, Jemal A. Cancer statistics, 2018. *CA Cancer J Clin.* 2018;68(1):7-30.
- Jemal A, Ward EM, Johnson CJ, Cronin KA, Ma J, Ryerson B, et al. Annual Report to the Nation on the Status of Cancer, 1975-2014, Featuring Survival. *J Natl Cancer Inst.* 2017;109(9).
- Zheng H, Kang Y. Multilayer control of the EMT master regulators. *Oncogene.* 2014;33(14):1755-63.
- Guggenheim AG, Wright KM, Zwickey HL. Immune Modulation From Five Major Mushrooms: Application to Integrative Oncology. *Integr Med (Encinitas).* 2014;13(1):32-44.
- Shnyreva AV, Shnyreva AA, Espinoza C, Padrón JM, Trigos Á. Antiproliferative Activity and Cytotoxicity of Some Medicinal Wood-Destroying Mushrooms from Russia. *Int J Med Mushrooms.* 2018;20(1):1-11.
- Kim M, Jee SC, Sung JS, Kadam AA. Anti-proliferative applications of laccase immobilized on super-magnetic chitosan-functionalized halloysite nanotubes. *Int J Biol Macromol.* 2018;118(Pt A):228-37.
- Deng C, Lin H, Seidman A, Fornier M, D'Andrea G, Wesa K, et al. A phase I/II trial of a polysaccharide extract from *Grifola frondosa* (Maitake mushroom) in breast cancer patients: immunological effects. *J Cancer Res Clin Oncol.* 2009;135(9):1215-21.
- Masuda Y, Inoue M, Miyata A, Mizuno S, Nanba H. Maitake beta-glucan enhances therapeutic effect and reduces myelosuppression and nephrotoxicity of cisplatin in mice. *Int Immunopharmacol.* 2009;9(5):620-6.
- Masuda Y, Ito K, Konishi M, Nanba H. A polysaccharide extracted from *Grifola frondosa* enhances the anti-tumor activity of bone marrow-derived dendritic cell-based immunotherapy against murine colon cancer. *Cancer Immunol Immunother.* 2010;59(10):1531-41.
- Cui FJ, Li Y, Xu YY, Liu ZQ, Huang DM, Zhang ZC, et al. Induction of apoptosis in SGC-7901 cells by polysaccharide-peptide GFPS1b from the cultured mycelia of *Grifola frondosa* GF9801. *Toxicol In Vitro.* 2007;21(3):417-27.
- Zhang Y, Sun D, Meng Q, Guo W, Chen Q. *Grifola frondosa* polysaccharides induce breast cancer cell apoptosis via the mitochondrial-dependent apoptotic pathway. *Int J Mol Med.* 2017;40(4):1089-95.
- Alonso EN, Orozco M, Eloy Nieto A, Balogh GA. Genes related to suppression of malignant phenotype induced by Maitake D-Fraction in breast cancer cells. *J Med Food.* 2013;16(7):602-17.
- Alonso EN, Ferronato MJ, Gandini NA, Fermento ME, Obiol DJ, López Romero A, et al. Antitumoral Effects of D-Fraction from *Grifola frondosa* (Maitake) Mushroom in Breast Cancer. *Nutr Cancer.* 2017;69(1):29-43.
- Aparicio LA, Blanco M, Castosa R, Concha Á, Valladares M, Calvo L, et al. Clinical implications of epithelial cell plasticity in cancer progression. *Cancer Lett.* 2015;366(1):1-10.
- Wong SHM, Fang CM, Chuah LH, Leong CO, Ngai SC. E-cadherin: Its dysregulation in carcinogenesis and clinical implications. *Crit Rev Oncol Hematol.* 2018;121:11-22.
- Cialeli C, Theocharis AD, Karamanos NK. Roles of matrix metalloproteinases in cancer progression and their pharmacological targeting. *FEBS J.* 2011;278(1):16-27.
- Egeblad M, Werb Z. New functions for the matrix metalloproteinases in cancer progression. *Nat Rev Cancer.* 2002;2(3):161-74.
- Diaz-Diaz A, Casas-Pais A, Calamia V, Castosa R, Martínez-Iglesias O, Roca-Lema D, et al. Proteomic Analysis of the E3 Ubiquitin-Ligase Hakai Highlights a Role in Plasticity of the Cytoskeleton Dynamics and in the Proteasome System. *J Proteome Res.* 2017;16(8):2773-88.
- Rodríguez-Rigueiro T, Valladares-Ayerbes M, Haz-Conde M, Aparicio LA, Figueroa A. Hakai reduces cell-substratum adhesion and increases epithelial cell invasion. *Bmc Cancer.* 2011;11.
- Ji Q, Liu X, Han Z, Zhou L, Sui H, Yan L, et al. Resveratrol suppresses epithelial-to-mesenchymal transition in colorectal cancer through TGF- β 1/Smads signaling pathway mediated Snail/E-cadherin expression. *BMC Cancer.* 2015;15:97.
- Eliza WL, Fai CK, Chung LP. Efficacy of Yun Zhi (*Coriolus versicolor*) on survival in cancer patients: systematic review and meta-analysis. *Recent Pat Inflamm Allergy Drug Discov.* 2012;6(1):78-87.
- Kodama N, Komuta K, Nanba H. Can maitake MD-fraction aid cancer patients? *Altern Med Rev.* 2002;7(3):236-9.
- Nieto MA. Epithelial plasticity: a common theme in embryonic and cancer cells. *Science.* 2013;342(6159):1234-850.
- Ye X, Weinberg RA. Epithelial-Mesenchymal Plasticity: A Central Regulator of Cancer Progression. *Trends Cell Biol.* 2015;25(11):675-86.
- Talvensaari-Mattila A, Pääkkö P, Turpeenniemi-Hujanen T. Matrix metalloproteinase-2 (MMP-2) is associated with survival in breast carcinoma. *Br J Cancer.* 2003;89(7):1270-5.
- Dong W, Li H, Zhang Y, Yang H, Guo M, Li L, et al. Matrix metalloproteinase 2 promotes cell growth and invasion in colorectal cancer. *Acta Biochim Biophys Sin (Shanghai).* 2011;43(11):840-8.
- López-Otin C, Matrisian LM. Emerging roles of proteases in tumour suppression. *Nat Rev Cancer.* 2007;7(10):800-8.
- Luo KW, Yue GC, Ko CH, Lee JK, Gao S, Li LF, et al. In vivo and in vitro anti-tumor and anti-metastasis effects of *Coriolus versicolor* aqueous extract on mouse mammary 4T1 carcinoma. *Phytomedicine.* 2014;21(8-9):1078-87.

SCIENTIFIC REPORTS

OPEN

Hakai overexpression effectively induces tumour progression and metastasis *in vivo*

Received: 16 November 2017
Accepted: 12 February 2018
Published online: 22 February 2018

Raquel Castosa¹, Olaia Martínez-Iglesias¹, Daniel Roca-Lema¹, Alba Casas-Pais¹, Andrea Díaz-Díaz¹, Pilar Iglesias^{1,2}, Isabel Santamarina³, Begoña Graña³, Lourdes Calvo³, Manuel Valladares-Ayerbes⁴, Ángel Concha² & Angélica Figueroa¹

At early stages of carcinoma progression, epithelial cells undergo a program named epithelial-to-mesenchymal transition characterized by the loss of the major component of the adherens junctions, E-cadherin, which in consequence causes the disruption of cell-cell contacts. Hakai is an E3 ubiquitin-ligase that binds to E-cadherin in a phosphorylated-dependent manner and induces its degradation; thus modulating cell adhesions. Here, we show that Hakai expression is gradually increased in adenoma and in different TNM stages (I-IV) from colon adenocarcinomas compared to human colon healthy tissues. Moreover, we confirm that Hakai overexpression in epithelial cells drives transformation in cells, a mesenchymal and invasive phenotype, accompanied by the downregulation of E-cadherin and the upregulation of N-cadherin, and an increased proliferation and an oncogenic potential. More importantly, for the first time, we have studied the role of Hakai during cancer progression *in vivo*. We show that Hakai-transformed MDCK cells dramatically induce tumour growth and local invasion in nude mice and tumour cells exhibit a mesenchymal phenotype. Furthermore, we have detected the presence of micrometastasis in the lung mice, further confirming Hakai role during tumour metastasis *in vivo*. These results lead to the consideration of Hakai as a potential new therapeutic target to block tumour development and metastasis.

Carcinoma is the most common type of cancer and arises from the transformation of epithelial cells. Around 90% of cancer related deaths are consequence of metastasis. At early stages of tumour progression and carcinoma metastasis, epithelial tumour cells activate a crucial program named epithelial-to-mesenchymal transition (EMT), which is frequently observed in human carcinoma. EMT is a highly controlled program firstly reported during embryogenesis (EMT type I), and also described in wound healing and tissue repair (EMT type II). Apart from these physiological EMT, this program can also occur during pathological conditions such as organ fibrosis and tumour progression (EMT type III). Cancer-EMT is characterized by the disruption of cell-cell contacts, cell-substratum adhesions and apical-basal polarity, accompanied by the reorganization of the cytoskeleton. All these changes cause the loss of epithelial phenotype and the acquisition of a mesenchymal phenotype, which includes a gain of migratory and invasive capabilities, important for the dissemination of cancer cells¹⁻³. One of the best-characterized hallmarks of the EMT is the loss of E-cadherin in epithelial cells⁴⁻⁶. E-cadherin is the prototype member of classical cadherins at adherens junctions in epithelial cells, and its loss is associated to the progression from adenoma to carcinoma therefore, from benign tumour to malignant tumour^{6,7}. In addition to the loss of the epithelial E-cadherin protein, the mesenchymal marker N-cadherin is upregulated during EMT, and this switch between cadherins is also considered as a hallmark of cancer-related EMT program⁸.

It has been extensively studied the mechanism whereby E-cadherin is downregulated during EMT in cancer^{9,10}. Hakai is the first post-translational regulator described for the E-cadherin stability¹¹. Hakai, a new class of the three families of RING-finger type E3 ubiquitin-ligases, contains a novel domain called HYB (Hakai pTyr-binding) whereby interacts with the tyrosine-phosphorylated E-cadherin by Src, inducing its ubiquitination

¹Epithelial Plasticity and Metastasis Group, Instituto de Investigación Biomédica de A Coruña (INIBIC), Complejo Hospitalario Universitario de A Coruña (CHUAC), Universidade da Coruña (UDC), Sergas, Spain. ²Pathology Department, INIBIC, CHUAC, Sergas, UDC, Spain. ³Clinical and Translational Oncology Group, INIBIC, CHUAC, Sergas, UDC, Spain. ⁴Department of Medical Oncology, Hospital Universitario Reina Sofía, Córdoba, Spain. Raquel Castosa, Olaia Martínez-Iglesias and Daniel Roca-Lema contributed equally to this work. Correspondence and requests for materials should be addressed to A.F. (email: angelica.figueroa.conde-valvis@sergas.es)

and degradation, which in turn causes the alteration of cell–cell contacts^{11–13}. The ubiquitination system frequently signals for protein degradation into lysosome or proteasome pathway system. It is generally believed that cytosolic and nuclear proteins are mainly degraded via proteasome, while membrane proteins are routed for destruction into lysosome¹⁴. Indeed, lysosomal targeting of E-cadherin is the described mechanism for the downregulation of cell–cell adhesion during EMT¹⁵. In addition to Hakai action on cell–cell contacts, it has been described its involvement in the reduction of the cell–substratum adhesions and the increase of epithelial cell invasion *in vitro*¹⁶. Moreover, we have previously reported that Hakai expression is increased in human colon and gastric adenocarcinoma compared to its adjacent healthy epithelial tissue, further supporting Hakai role during tumour progression^{17–19}. Hakai is also involved in the regulation of cell proliferation in an E-cadherin-independent manner, suggesting that ubiquitinated novel substrates by Hakai wait to be elucidated¹⁷. Indeed, Cortactin and DOK1 were recently identified as a novel Hakai-interacting and ubiquitinated proteins in Src-phosphorylation-dependent manner. However, the physiological relevance of these interactions is not defined yet¹².

Despite Hakai ubiquitin-dependent functions, it has been proposed that Hakai may be involved in several cellular processes in an ubiquitin-independent manner^{17,20–23}. According to this, in a proteomics analysis of *Arabidopsis thaliana*, Hakai was identified as an interacting protein of several post-transcriptional regulators, including N6-methyladenosine (m⁶A) writer complex members²⁴. m⁶A is an important mRNA modification found in eukaryotes which is involved in processes such as splicing, mRNA stability, mRNA export and others. In this model, Hakai is functionally necessary for mRNA methylation, suggesting a possible similar role in mammals²⁵. On the other hand, Hakai interacts with the RNA-binding protein PSF (*Polypyrimidine tract binding protein associated Splicing Factor*). Indeed, Hakai overexpression increase the binding of PSF to mRNA transcripts encoding specific cancer-related proteins^{17,20}. Up to date, most of the publications related to the role of Hakai on E-cadherin expression were reported in an *in vitro* model system. Apart from the described role of Hakai in *A. thaliana*, other *in vivo* study was performed in *Drosophila melanogaster* where Hakai function was described to be most crucial at early stages of embryogenesis²⁶. In our study, we have extended our previous results to examine Hakai function in cancer progression by using human tissue samples from patients at different stages of colon cancer progression and the Hakai functional role *in vivo* by using a mice xenograft tumour model. By using Madin-Darby Canine Kidney (MDCK) cells, an established model system to study cell–cell adhesions, we have reported that Hakai overexpression induces tumour progression and micrometastasis *in vivo*.

Results

Hakai expression levels in different colon cancer TNM stages. By using human colon carcinoma samples, we have previously reported that Hakai expression levels were higher in colon cancer tissues than in adjacent normal epithelial tissues¹⁹. Here, we extend our previous analysis comparing pairs of human colon healthy tissues to adenoma and to different TNM stages (I–IV) from colon adenocarcinomas, as shown in a representative image (Fig. 1A). The quantification of the signal intensity of Hakai immunohistochemistry staining is shown in Fig. 1B. Staining intensities of Hakai in cancer cells were gradually increased in all stages I–IV compared to healthy normal epithelium. Moreover, the mesenchymal N-cadherin marker is upregulated in advance colon carcinoma progression compared to healthy colon tissues and the E-cadherin loss is associated to the progression from adenoma to carcinoma. However, we did not detect significant differences in protein expression in the other reported substrate for Hakai, Cortactin, during colon carcinoma development (Supplementary Fig. 1). Furthermore, we have also analysed Hakai mRNA levels showing a significant increase in TNM stage III and IV compared to healthy tissues, indicating that the transcriptional regulation of mRNA Hakai may be a late event during tumour progression (Fig. 1C). Taken together our results suggest the potential use of Hakai as novel biomarker for colon cancer progression.

Hakai promotes tumour formation and proliferation *in vivo*. Given that Hakai expression in human colon adenocarcinoma is highly upregulated compared to normal tissues suggesting its contribution to tumour progression, we decided to further study the possible role of Hakai during tumour progression *in vivo*. For this purpose, we used an established system, a normal epithelial Madin-Darby Canine Kidney (MDCK) cell line^{27,28}. As previously reported, we confirmed that Hakai overexpression in MDCK cells (Hakai-MDCK clone 4 and clone 11) transformed the normal epithelial phenotype of MDCK into a mesenchymal morphology¹⁷ (Supplementary Fig. 2A), accompanied by the decrease of protein expression of Hakai substrates, E-cadherin and Cortactin, and a robust increase of the mesenchymal marker N-cadherin (Supplementary Figs 2B and 3). As mentioned, this cadherin switch (between E- and N-cadherins), observed when Hakai is overexpressed in MDCK cells, is a classical event seen during cancer-related EMT program. Moreover, we confirmed that Hakai-MDCK cells acquire the ability to invade and exhibit oncogenic potential (Supplementary Fig. 2C, D). On the other hand, important efforts were made to obtain stable transfection to knocking-down Hakai in several epithelial cell lines, however, we failed to do so suggesting that Hakai protein may be crucial for cell survival. MDCK and Hakai-MDCK cells were injected subcutaneously into the flank of nude mice to get further insights into the possible role of Hakai during tumour progression *in vivo*. Hakai-MDCK cells formed primary tumours in all injection sites whereas parental MDCK cells were unable to do so, as shown in Fig. 2A. Tumour growth induced by Hakai-MDCK cells was measured showing an increased tumour volume 38 days post-injection. Palpable tumours were detected in the mice injecting 5×10^6 Hakai-MDCK cells on day 18 post-injection (Fig. 2B). All mice injected with MDCK cells were tumour-free, on the contrary, local tumour in Hakai-MDCK inoculated mice appeared after 18 days and all mice showed tumours after 22 days post injection. After 38 days all mice were euthanized (Fig. 2C). Histological analysis of the tumour xenografts further confirmed the biological effect of Hakai overexpression. Interestingly, while injecting 5×10^6 MDCK cells, we observed a teratoma formation (Fig. 2D), however, these findings were not observed by injecting 1×10^6 MDCK cells (data not shown). Our results are in concordance with previous reported results on which adjacent MDCK cells maintain the ability to regenerate kidney

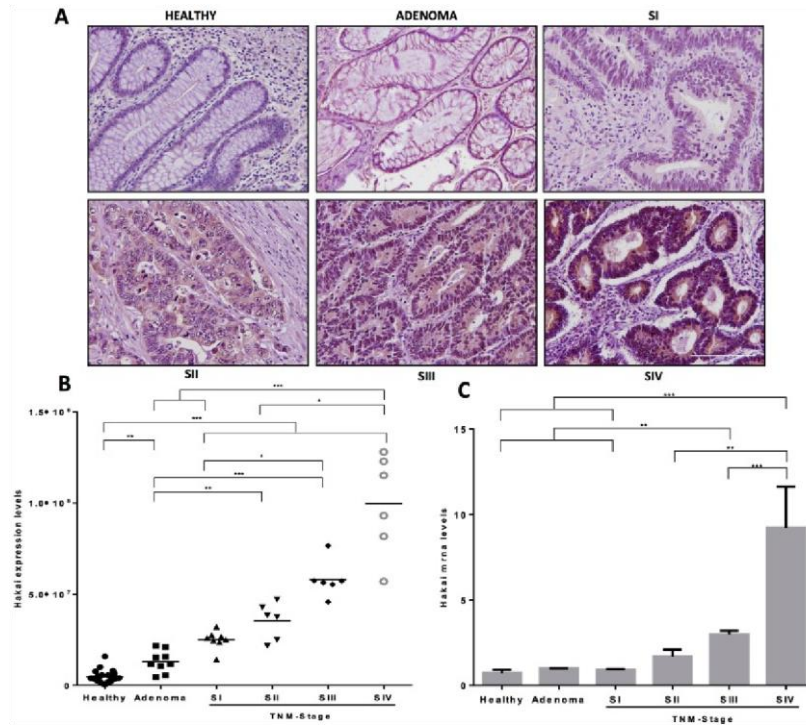


Figure 1. Hakai expression levels in human samples from colorectal cancer patients. (A) Representative immunoreactivity of Hakai in normal colonic mucosa, adenoma, and colorectal cancer (TNM stages I-IV). Images were obtained with a 20x objective. Scale bar 125 μ m. (B) Statistical quantification of Hakai staining intensity in epithelial cancer cells at different colon cancer stages and in adenoma and normal colon tissues (normal colonic mucosa, $n = 26$; adenoma, $n = 10$; colorectal cancer, $n = 20$ of all stages). Five photographs of each tissue were quantified. Data are represented as scatter plot. Values are means \pm SEM of staining intensity signal scoring per area. Calibration and quantification of the images were performed with ImageJ software. Kruskal-Wallis with Tukey correction test analyses show statistical differences in colorectal cancer (TNM, SI-IV) respect to paired healthy samples (* $p < 0.05$; ** $p < 0.01$; *** $p < 0.001$). (C) Hakai mRNA expression levels normalized to control RPL13A mRNA were measured in normal colonic mucosa, adenoma, and colorectal cancer (normal colonic mucosa, $n = 12$; adenoma, $n = 3$; colorectal cancer, $n = 12$ of all stages).

tubule-like structures *in vivo* by using athymic nude mice, keeping joined junctions and retained regional differentiation²⁹. In contrast, tumours induced by Hakai-MDCK cells showed a significant change to undifferentiated and spindle-shape carcinoma cells. Cell morphology of Hakai-MDCK xenografts was dramatically changed showing an increase in nucleus size with an irregular size and shape, and prominent nucleoli. On the contrary, a reduction of the cytoplasm size is seen. All these morphological changes are characteristic of cancerous cells (Fig. 2D).

Growth potential quantification of these tumours was characterized by studying Ki67 immunohistochemistry and mitotic index. Tumours originated by Hakai-MDCK cells were highly proliferative with more than 80% of positive cells for Ki67 labelling (Fig. 3A). These results were confirmed with the quantification of mitotic index, a parameter commonly used in clinical diagnosis, showing an extraordinary high number of cells in mitosis detected in Hakai-MDCK tumour sections stained with H&E (Fig. 3B, arrows). In conclusion, a marked increase of both proliferation markers in Hakai-MDCK tumours was observed supporting that Hakai-MDCK cells arise tumours with an extremely high proliferative rate.

Hakai induces local invasion and tumour cells exhibit a mesenchymal phenotype. In order to further evaluate the *in vivo* role of Hakai during invasion and metastasis, we first performed H&E staining of the tumour sections. After 38 days, blood vessels were infiltrated with tumour Hakai-MDCK cells (Fig. 3C, upper pan l), erythrocytes or leukocytes (Fig. 3C, lower panel), although no specific immunoreactivity was detected

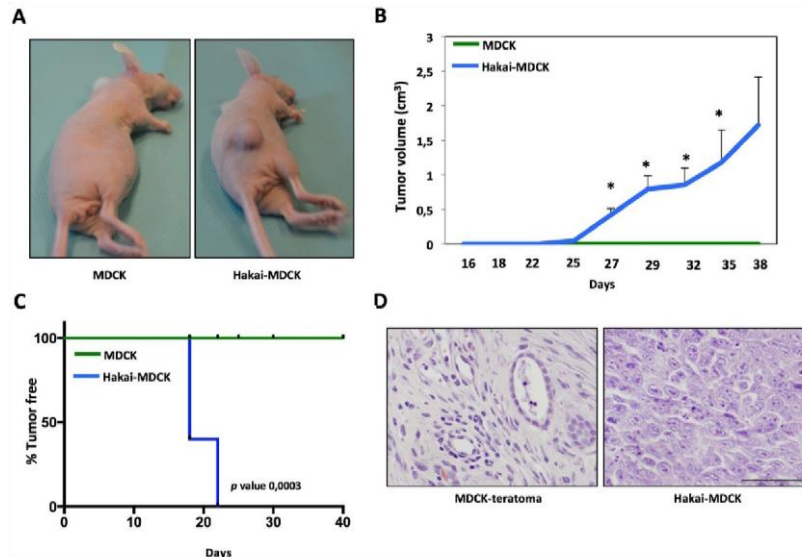


Figure 2. Hakai induces tumour formation *in vivo*. (A) Representative photographs after 38 days of subcutaneous injection of 5×10^6 MDCK or Hakai-MDCK into nude mice cells (MDCK, $n = 4$; Hakai-MDCK, $n = 5$). (B) Tumour growth in nude mice injected with MDCK or Hakai-MDCK. Tumours were measured twice a week, as described in Materials and Methods and results are represented as mean \pm SEM ($*P < 0,05$). (C) Tumour-free survival of MDCK or Hakai-MDCK cells in nude mice. p value was calculated with Breslow test and is indicated in the figure. (D) Representative H&E staining of teratoma and tumours originated by MDCK or Hakai-MDCK cells, respectively. Pictures were taken with a 40x objective, scale bar 500 μ m.

using anti-HA antibody to specifically detect of Hakai-MDCK (Supplementary Fig. 4). It was determined that 60% of the mice showed infiltrating Hakai-MDCK cells in blood vessels (Fig. 3C), and invading the adjacent muscle (Fig. 3D) further supporting the implication of Hakai on invasion *in vivo*. Furthermore, 20% of the mice showed an extent of primary tumour invasion (Fig. 3E), a fact of particular relevance which suggests the extremely aggressive behaviour of the Hakai-MDCK cells, as mice with locally invasive tumours are more likely to develop metastases and also tend to have a worse prognosis. Then, we also studied the possible Hakai influence on E-cadherin-mediated cell-cell contacts. First, we confirmed that Hakai-MDCK cells in xenograft mouse model continued to express higher Hakai levels compared to the MDCK injected cells (Fig. 4A, left panel and Supplementary Fig. 5A, left panel). We also analysed E-cadherin expression as its loss is a prerequisite and hallmark of EMT, and critical for the invasive and malignant phenotype^{30,31}. The expression of the epithelial marker E-cadherin was found to be completely disappeared in Hakai-MDCK injected cells *in vivo*, whereas remaining E-cadherin at cell-cell contacts was detected in the teratoma formation by MDCK-injected cells (Fig. 4A, right panel and Supplementary Fig. 5A, right panel). Moreover, Hakai-MDCK tumours were robustly positive for N-cadherin mesenchymal marker whereas MDCK teratomas were negative (Fig. 4B, left panel and Supplementary Fig. 5B, left panel). This cadherin switch was described as a hallmark of cancer-related EMT program⁸. Finally, we also extended our study by analysing the expression of another *in vitro* described substrate for Hakai, Cortactin. As expected, Cortactin expression was reduced in Hakai-MDCK xenograft tumours compared to MDCK-injected cells, supporting *in vivo* the previous *in vitro* reported action of Hakai in the ubiquitination and degradation of Cortactin (Fig. 4B, right panel and Supplementary Fig. 5, right panel)¹². Interestingly, Hakai-MDCK xenograft tumours show Cortactin expression only in the cytoplasm, whereas in MDCK teratoma is also highly enriched in the nucleus. Taken all together these results indicate that Hakai-MDCK exhibits a mesenchymal phenotype and induce local invasion *in vivo*.

Hakai overexpression produces lung micrometastasis *in vivo*. Finally, to determine whether Hakai may promote cancer metastasis, lung, kidney and liver tissues were analysed by H&E staining. Metastasis to distant sites was not observed neither with Hakai-MDCK nor MDCK cells (Fig. 5A). This result was probably due to short timing analysis for the *in vivo* study, as 38 days after injection of cells may not be enough to allow cells to settle down and form macrometastasis. Moreover, no specific signal was detected in lung and liver tissues by using HA antibody (Supplementary Fig. 6). Therefore, we decided to further determine the possible existence of micrometastasis by analysing the presence of DNA of Hakai-MDCK in lung. For this purpose, HA-tagged Hakai primers in Hakai-MDCK cells was measured by using two different specific primers: one designed for HA epitope

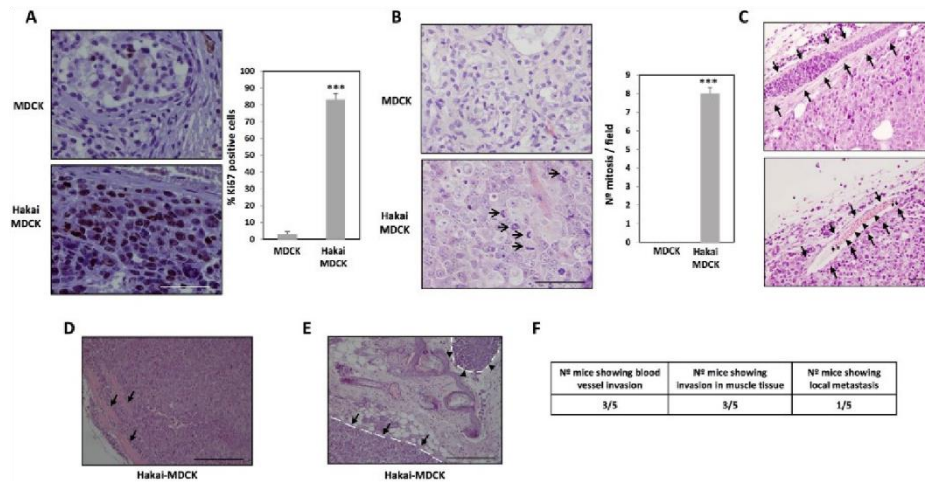


Figure 3. Hakai action on tumour proliferation and invasion in a mouse xenograft model. (A) Immunohistochemistry for ki67 expression in teratoma and tumours originated by MDCK or Hakai-MDCK cells, respectively (MDCK, $n = 2$; Hakai-MDCK, $n = 5$, five pictures per each were taken). Representative images were taken with the 40x objective (*left panel*) and the quantification of the percentage of positive cells is shown (*right panel*). Scale bar, 500 μm . (B) Mitotic cells in MDCK and Hakai-MDCK xenografts (MDCK, $n = 2$; Hakai-MDCK, $n = 5$, five pictures per each were taken). Mitotic cells in representative images of H&E staining taken with a 40x objective (*left panel, arrows*) and the corresponding mitosis quantification in xenografts (*right panel*). Scale bar, 500 μm . (C) H&E staining in the upper panel shows an infiltrated blood vessel with tumour cells originated by Hakai-MDCK injection, and in the bottom panel a blood vessel containing leukocytes (asterisks) and erythrocytes (arrowheads) is shown. Blood vessels are indicated with arrows. Photograph was taken with a 20x objective. Scale bar, 100 μm . (D) H&E staining showing muscle infiltration by Hakai-MDCK cells. Picture was taken with a 10x objective. Muscle is indicated with arrows. Scale bar, 500 μm (E) H&E staining showing primary tumour (arrows) and a local metastasis (arrowheads) originated by Hakai-MDCK cells are indicated with a discontinuous line. Connective tissue is found between the primary tumour and the local metastasis. Picture was taken with a 10x objective. Scale bars, 500 μm . Quantifications are shown as mean \pm SEM ($***P < 0,001$). (F) Table including the number of animals containing infiltrated tumour cells in blood vessels (C), in muscle tissue (D) or a local metastasis (E). H&E stained sections were examined under microscopy and the number of animals with tumour cells into blood vessels, muscle tissue or with local metastasis were counted.

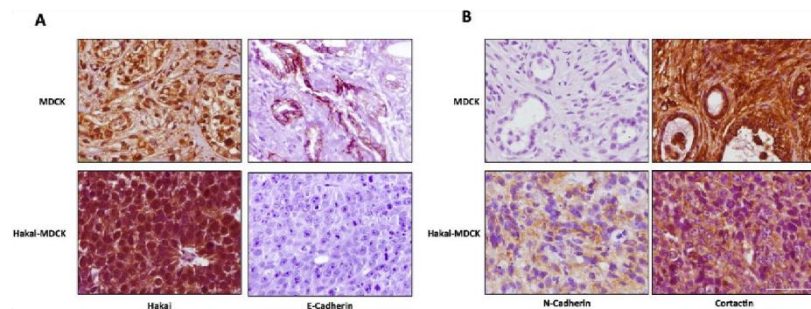


Figure 4. Hakai overexpression induces tumours with mesenchymal phenotype in xenografts mouse model. (A) Immunohistochemical staining for E-cadherin and Hakai in tumours originated by MDCK and Hakai-MDCK cells (MDCK, $n = 2$; Hakai-MDCK, $n = 5$). Representative images were taken with a 40x objective. Scale bar, 125 μm . (B) Representative immunoreactivity of N-cadherin and Cortactin in tumours originated by MDCK or Hakai-MDCK cells (MDCK, $n = 2$; Hakai-MDCK, $n = 5$). Representative images were taken with a 40x objective. Scale bar, 125 μm .

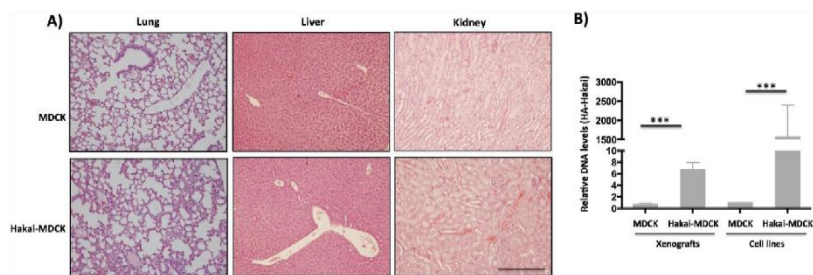


Figure 5. Hakai induces lung micrometastasis in nude mice. **(A)** Analysis of macrometastasis presence in lung, liver and kidney. MDCK or Hakai-MDCK cells were inoculated into the flank of nude mice and after 38 days the indicated organs were excised, fixed and stained with H&E in order to detect macrometastasis. Representative pictures were taken with a 10x objective. Scale bar, 500 μ m. **(B)** The presence of tumour cells into the mice lung was assessed by quantitative PCR analysis of HA-Hakai sequences as indicated in Materials and Methods. Tumour xenografts from MDCK and Hakai-MDCK injected cells ($n = 4$ and $n = 5$ respectively) were measured and MDCK and HA-MDCK cell line were used as negative and positive controls, respectively (***) ($P < 0,001$).

and the second primer for Hakai. After 38 days post-injection, micrometastases were detected in the lung of the Hakai-MDCK xenograft mouse model while no detection was found in MDCK cells xenografts. MDCK and Hakai-MDCK cell lines were used as negative and positive controls respectively (Fig. 5B), further confirming that Hakai induces lung micrometastasis. Taken together, our results underscore an important role of Hakai during tumour progression and metastasis *in vivo*.

Discussion

In this study, we describe for the first time the role of Hakai *in vivo*. Our findings indicate that Hakai protein expression gradually increases during human colon cancer progression. Interestingly, in benign colon adenoma samples, protein expression is statistically enhanced compared to normal tissues. These data suggest that Hakai may not only be involved in the malignant progression of human colon cancer but also at early stages of tumorigenesis by acting on cell proliferation¹⁷. When analysing Hakai mRNA levels, it is shown a statistically significant increase in TNM-stages III and IV compared to normal and adenoma human colon tissues, further suggesting that the regulation of Hakai at transcriptional level may be a late event during tumour progression. Therefore, our data highlight the potential use of Hakai as a biomarker during colon cancer progression. However, further investigations are required to elucidate whether Hakai expression could be correlated with patient survival and/or associated with poor outcome or other clinic-pathologic characteristics of colorectal cancer patients.

In keeping with previous reports, during EMT the loss of the epithelial E-cadherin protein is accompanied by an upregulation of the mesenchymal marker N-cadherin. Loss of E-cadherin-mediated cell adhesion coincides with the transition from well differentiated adenoma to invasive carcinoma in a transgenic mouse model⁷. We also confirm the downregulation of E-cadherin and upregulation of N-cadherin during colon cancer progression. Our results also show that no loss of E-cadherin was observed in human colon adenoma compared to normal healthy adjacent tissues, as previously reported³². Therefore, other levels of regulation could be involved, as for example, the loss of E-cadherin may be regulated by hypermethylation on E-cadherin promoter at early event during colon cancer development³³. As Hakai expression is gradually increased during tumour progression, our results underscore that Hakai could contribute to an invasive phenotype in colon adenocarcinoma by downregulating E-cadherin at early stages of tumour progression. Moreover, our group has previously published that knocking-down Hakai, by using a small interference RNA, blocked proliferation in MCF7 and HEK-293 cells, accompanied by the reduction of the expression of the important cell cycle regulator cyclin D1. Furthermore, by using a mutant of the RING-finger domain (Hakai- Δ RING), necessary for Hakai E3 ubiquitin-ligase activity, we showed that this domain was necessary for Hakai effect on proliferation. According to the demonstrated role of Hakai E3 ubiquitin-ligase activity on proliferation *in vitro*, it was studied Hakai expression in two different human tissues. Certainly, increased Hakai expression was detected in the germinal centres of lymph node, where lymphocytes are actively proliferating, and in the proliferative phase of the endometrium, while low expression was observed in the secretory phase¹⁷. Moreover, it has been also published that Wilm's tumor 1-associating protein (WTAP) forms a complex with several proteins, including Hakai, which is required for cell cycle progression. Indeed, silencing Hakai expression in this model with a small interference RNA reduced proliferation with G2/M accumulation²⁴. Moreover, by analysing the functional role of the Hakai homologue in *Drosophila melanogaster*, Kaido *et al.* demonstrated that Hakai null mutants died during larval stages²⁶.

Interestingly, it has been suggested that Hakai protein may be particularly relevant at early stages of EMT. Janda *et al.* reported that the cooperation between Ras and TGF β to activate EMT enhanced E-cadherin endocytosis and lysosomal degradation. They demonstrated that E-cadherin is downregulated at post-translational level at initial phases of EMT whereas the loss of E-cadherin via transcriptional repression is a late event during EMT³⁴. On the other hand, in *Drosophila melanogaster*, it was demonstrated that Hakai function is most vital at early stages of embryogenesis and its contribution decreases at later stages²⁶, and in *Arabidopsis thaliana*, Hakai

is required for methylation of mRNA (m6A)²⁵, which is described as an essential process for the earliest stages of pattern formation in plants³⁵⁻³⁷. All these publications further support that Hakai may act on early stages of EMT during carcinoma progression by its action as a post-translational regulator of E-cadherin. However, novel research lines are needed to determine whether Hakai may act on other novel unidentified substrates or as a post-transcriptional regulator by its influence on mRNA stability, m6A process or others, given that in different model systems Hakai is mainly localized in the nucleus^{17,25,26}. Therefore, future investigations regarding to the molecular mechanism by which Hakai influences carcinoma progression will contribute to open a novel direction for therapeutic intervention against cancer.

Cortactin is a cytoskeleton protein and one of the major substrates for Src kinase. It is required for cell migration and it is present in cell-motility structures such as lamellipodia and invadopodia, opening a great interest in tumour invasion. Although cortactin is overexpressed in many types of cancers such as head and neck squamous carcinoma, oral squamous carcinoma, breast cancer or melanoma, we could not find any regulation in protein levels in human colon cancer tissues³⁸⁻⁴¹. It has been reported that subcellular localization and activity is determinant for cortactin-mediated cell migration. Indeed, it was shown that cortactin is regulated by various post-translational modifications, such as acetylation. *Ito et al.* demonstrated that acetylated form of cortactin is mainly localized in the nucleus and this acetylated-cortactin decreases cell migration by inhibiting its binding to Keap1 protein in the cytoplasm^{42,43}. These interesting findings elucidate for the first time the opposite effect on cellular migration depending on the subcellular localization of cortactin. Therefore, it is plausible that Hakai may also influence the migratory capabilities that are important for the dissemination of cancer cells by its action on cortactin localization.

Given the important reported role of the E3 ubiquitin-ligase Hakai during carcinoma metastasis *in vitro* and *in vivo*, the development of novel inhibitors against the E3 ubiquitin-ligase Hakai appears to be an attractive strategy for therapeutic interventions. So far, the FDA has approved very few drugs targeting members of the ubiquitin pathway, which include the proteasome inhibitors bortezomib, carfilzomib and ixazomib. However these drugs are limited to specific hematopoietic malignancies, and clinical trials testing their use for solid tumours have been so far disappointing^{44,45}. Indeed, a recent publication demonstrated that in epithelial cells undergoing EMT, the proteasome activity is decreased and the proteasome inhibitors induced EMT⁴⁶. According to this, we have recently demonstrated a specific downregulation of several proteasome subunits in Hakai-MDCK epithelial cells compared to non-transformed MDCK cells²³. Taken together and given that Hakai expression is enhanced in human tumour progression in colon adenocarcinoma compared to normal tissues (Fig. 1), our results reinforce that proteasome inhibitors may not be an effective treatment for epithelial tumours that follow EMT and we propose the E3 ubiquitin-ligase Hakai as a better therapeutic target against cancer in specific molecular subtypes of colorectal cancer already defined^{47,48}.

Materials and Methods

Mice and human tissues samples. Animal experiments were performed in the Experimental Surgery Unit-Technological formation centre from INIBIC-CHUAC in compliance with the European Community Law (86/609/EEC) and the Spanish law (R.D. 53/2013), with approval of the Experimental Animal Ethics Committee from Xerencia de Xestión Integrada A Coruña (XXIAC). Colon cancer biopsies were obtained from the Pathological Anatomy department from the Complejo Hospitalario Universitario A Coruña (CHUAC), under informed consent from all patients signed and research investigation was approved by the Research Ethics Committee from A Coruña-Ferrol and performed following standard ethical procedures of the Spanish regulation (Ley Orgánica de Investigación Biomédica, 14 July 2007). Paraffin samples were provided by CHUAC Biobank integrated in the Spanish Hospital Platform Biobanks Network.

Antibodies and materials. The rabbit polyclonal anti-Hakai antibody (Hakai-2498) was provided by Dr. Fujita. For immunohistochemistry Anti-E-cadherin antibody (24E10), from Cell Signaling, was used. Anti-Cortactin antibody (05-180) was from Millipore. Anti-N-cadherin (ab18203) was from Abcam. Anti-Ki67 monoclonal antibody (clone MIB-1, code M7240) was from DAKO. For nude mice immunohistochemistry, antibodies were used at dilution 1/400 for E-cadherin, 1/250 for Hakai, 1/150 for Ki67, 1/100 for N-Cadherin, 1/50 for Cortactin. For human immunohistochemistry Hakai dilution was 1/700.

Cell lines. MDCK cells were cultured in Dulbecco's Modified Eagle Medium (DMEM) containing 1% penicillin/streptomycin, 1% glutamax and 10% of heat-inactivated fetal bovine serum (FBS). MDCK stably expressing Hakai cells (Hakai-MDCK) were provided by Dr. Fujita¹⁷ and were cultured in presence of the selection antibiotic G418 (800 µg/ml). In the present work, Hakai-MDCK (clone 4) was used, however, all selected clones represented comparable phenotypes and results¹⁷. Cells were grown at 37 °C in a humidified incubator with 5% CO₂. Cells were also tested regularly for mycoplasma contamination and all cells used were negative for mycoplasma test.

Real-time quantitative PCR (qRT-PCR). Ten sections of paraffin-embedded (FPPE) human colon cancer tissues (4 µm) were cut and deparaffinized in an eppendorf using xylene. Total RNA was extracted using the RNeasy FPPE Kit (Qiagen). Three adenomas, three colorectal cancer of every TNM stage and 12 healthy tissues were analysed. mRNA levels were analysed in technical triplicates by quantitative RT-PCR, following specifications of reverse transcriptase kit (NZYTech). Amplification was performed in a Light Cycler 480 and data was analysed by using the comparative C_T method. Primers used for Hakai amplification were F-CGCAGACGAATTCCTATAAAGC and R-CCTTCTTCATCACCAGGTGG and as control to monitor loading difference, RPL13A levels were measured using the following primers F-CAAGCGGATGAACCAAC and R-TGTGGGGCAGCATACTC.

Tumour xenograft in nude mice. Groups of athymic 6 weeks old mice (BALB/c, *nu/nu*) were used for xenograft assay. Mice were in a 12/12 hours light/dark cycle with water and food available ad libitum. Animals were always randomly distributed among the experimental groups. Five million MDCK or MDCK-Hakai cells 100 μ l DMEM without serum and antibiotic were injected subcutaneously into the flank ($n = 4$ mice for MDCK cells and $n = 5$ mice for Hakai-MDCK cells). Tumour volume was measured twice a week and animals were sacrificed 38 days after inoculation. Tumour volume was calculated as $pLW2/6^{49}$. Tumours, lungs, kidneys and livers were collected and then fixed in 4% PFA and embedded in paraffin blocks for histology and/or immunohistochemistry (IHC) analyses.

Histology and Immunohistochemistry. Sections (4 μ m) of tumours, lungs, kidneys and livers were deparaffinised, rehydrated and stained with haematoxylin and eosin (H&E) using standard procedures. Deparaffinised and hydrated sections (4 μ m) of tumours were also used for immunohistochemistry. Antigen retrieval was carried out with citrate or EDTA buffer following datasheet instructions and endogenous peroxidase activity was inhibited with peroxidase blocking (DakoCytomation). Samples were blocked for 1 hour at room temperature with 0.2% BSA and 0.1% Tx-100 and incubated overnight at 4 $^{\circ}$ C in a wet chamber with the primary antibody. Then, slides were incubated for 1 hour at room temperature with the secondary antibody and were revealed with DAB (DakoReal Envision kit). Then, slides were counterstained with Gill's Hematoxylin and mounted with DePeX (Serva). Pictures were taken with an Olympus microscope in the indicated objectives in figure legends. Sections of tumours and teratoma stained with H&E were used for number of mitosis quantification. The number of mitosis was counted in 10 high magnification fields (objective 40x) of each tumour or teratoma with an Olympus BX50 microscope as previously reported⁵⁰. Results are represented as mean \pm SEM and a representative photograph was taken of each condition. Twenty formalin-fixed and paraffin-embedded (FFPE) colon cancer tissues (4 μ m) of the I-IV TNM stages of colon cancer progression, ten adenomas and the corresponding adjacent normal colon tissues from the same patients were used for immunohistochemistry with anti-Hakai antibody. Five pictures of each section were taken with an Olympus microscope and the positive staining was quantified with Image J programme. Results are expressed as mean \pm SEM of each TNM-stage of the disease and are represented in a scatter plot graphic.

Quantification of lung invasion from *in vivo* mouse model. The presence of tumour cells in the lung mice was studied by real-time PCR⁵¹ using primers for HA epitope and Hakai present in ectopic HA-tagged Hakai expressed in MDCK-Hakai cells (5'-TCTGGGACGTCGTATGGGTA-3'; 5'-TTCTTCATCACCTTGCGGG-3'). Primers for mouse apolipoprotein B (*apob*) (5'-CGTGGGCTCCAGCATTCTA-3'; 5'-TCACCAGTCATTTCTGCCTTTG-3') were used as endogenous control⁵¹. MDCK and Hakai-MDCK cell lines were used as negative and positive controls, respectively. Lung DNAs were obtained with QIAamp DNA Mini Kit (Qiagen) as previously described⁵² and the quality and quantity of extracted DNA was determined by using Nanodrop ND-spectrophotometer (Thermo Fisher Scientific, MA, USA). The amplification and quantification of 100 ng DNA was carried out in technical triplicates by using a LightCycler 480 real-time lightcycler (Roche). Data analysis was performed and relative levels of expression were calculated by $2^{-\Delta\Delta Ct}$ method⁵³.

Statistical analysis. Statistical significance of data was determined by applying a two-tailed Student t-test. Shapiro-Wilk test was used to check a normal distribution and Levene test to assess the equality of variances. Results obtained are expressed as mean \pm SD or mean \pm SEM. Quantification of human IHQ did not follow a normal distribution therefore we used Kruskal-Wallis with Tukey correction test. Significance of the Student t-test and Kruskal-Wallis with Tukey correction test among the experimental groups indicated in the figures is shown as * $P < 0.05$, ** $P < 0.01$ and *** $P < 0.001$. Survival graphic in xenograft assay was made with GraphPad Prism software and the test of Breslow was used to calculate the p value.

References

1. Nieto, M. A. Epithelial plasticity: a common theme in embryonic and cancer cells. *Science* **342**, 1234850, <https://doi.org/10.1126/science.1234850> (2013).
2. Ye, X. & Weinberg, R. A. Epithelial-mesenchymal plasticity: a central regulator of cancer progression. *Trends Cell Biol* **25**, 675–686 (2015).
3. Aparicio, L. A. *et al.* Clinical implications of epithelial cell plasticity in cancer progression. *Cancer Lett* **366**, 1–10 (2015).
4. Christofori, G. New signals from the invasive front. *Nature* **441**, 444–450 (2006).
5. Yang, J. & Weinberg, R. A. Epithelial-mesenchymal transition: at the crossroads of development and tumor metastasis. *Dev Cell* **14**, 818–829 (2008).
6. Thiery, J. P., Acloque, H., Huang, R. Y. & Nieto, M. A. Epithelial-mesenchymal transitions in development and disease. *Cell* **139**, 871–890 (2009).
7. Peril, A. K., Wilgenbus, P., Dahl, U., Semb, H. & Christofori, G. A causal role for E-cadherin in the transition from adenoma to carcinoma. *Nature* **392**, 190–193 (1998).
8. Hazan, R. B., Qiao, R., Keren, R., Badano, I. & Suyama, K. Cadherin switch in tumor progression. *Ann N Y Acad Sci* **1014**, 155–163 (2004).
9. Lee, J. Y. & Kong, G. Roles and epigenetic regulation of epithelial-mesenchymal transition and its transcription factors in cancer initiation and progression. *Cell Mol Life Sci* **73**, 4643–4660 (2016).
10. Aparicio, L. A., Abella, V., Valladares, M. & Figueroa, A. Posttranscriptional regulation by RNA-binding proteins during epithelial-to-mesenchymal transition. *Cellular and Molecular Life Sciences* **70**, 4463–4477 (2013).
11. Fujita, Y. *et al.* Hakai, a c-Cbl-like protein, ubiquitinates and induces endocytosis of the E-cadherin complex. *Nat Cell Biol* **4**, 222–231 (2002).
12. Mukherjee, M. *et al.* Structure of a novel phosphotyrosine-binding domain in Hakai that targets E-cadherin. *EMBO J* **31**, 1308–19 (2012).
13. Cooper, J. A., Kaneko, T. & Li, S. S. Cell regulation by phosphotyrosine-targeted ubiquitin ligases. *Mol Cell Biol* **35**, 1886–1897 (2015).
14. Hunter, T. The age of cross talk: phosphorylation, ubiquitination, and beyond. *Mol Cell* **28**, 730–738 (2007).

15. Palacios, F., Tushir, J., Fujita, Y. & D'Souza-Schorey, C. Lysosomal targeting of E-cadherin: a unique mechanism for the down-regulation of cell-cell adhesion during epithelial to mesenchymal transitions. *Mol Cell Biol* **25**, 389–402 (2005).
16. Rodriguez-Rigueiro, T., Valladares-Ayerbes, M., Haz-Conde, M., Aparicio, L. A. & Figueroa, A. Hakai reduces cell-substratum adhesion and increases epithelial cell invasion. *BMC Cancer* **11**, 474, <https://doi.org/10.1186/1471-2407-11-474> (2011).
17. Figueroa, A. *et al.* Novel roles of Hakai in cell proliferation and oncogenesis. *Molecular Biology of the Cell* **20**, 3533–3542 (2009).
18. Rodriguez-Rigueiro, T. *et al.* A novel procedure for protein extraction from formalin-fixed paraffin-embedded tissues. *Proteomics* **11**, 2555–2559 (2011).
19. Abella, V. *et al.* miR-203 regulates cell proliferation through its influence on Hakai expression. *PLoS One* **7**, e25268, <https://doi.org/10.1371/journal.pone.0052568> (2012).
20. Figueroa, A., Fujita, Y. & Gorospe, M. Hacking RNA Hakai promotes tumorigenesis by enhancing the RNA-binding function of PSE. *Cell Cycle* **8**, 3648–3651 (2009).
21. Gong, E., Park, E. & Lee, K. Hakai acts as a coregulator of estrogen receptor alpha in breast cancer cells. *Cancer Sci* **101**, 2019–25 (2010).
22. Aparicio, L. A., Valladares, M., Blanco, M., Alonso, G. & Figueroa, A. Biological influence of Hakai in cancer: a 10-year review. *Cancer Metastasis Rev* **31**, 375–386 (2012).
23. Diaz-Diaz, A. *et al.* Proteomic analysis of the E3 ubiquitin-ligase Hakai highlights a role in plasticity of the cytoskeleton dynamics and in the proteasome system. *J Proteome Res* **16**, 2773–2788 (2017).
24. Horiuchi, K. *et al.* Identification of Wilms' tumor 1-associating protein complex and its role in alternative splicing and the cell cycle. *J Biol Chem* **288**, 33292–33302 (2013).
25. Růžička, K. *et al.* Identification of factors required for m(6) A mRNA methylation in Arabidopsis reveals a role for the conserved E3 ubiquitin ligase HAKAI. *New Phytol* **215**, 157–172 (2017).
26. Kaido, M., Wada, H., Shindo, M. & Hayashi, S. Essential requirement for RING finger E3 ubiquitin ligase Hakai in early embryonic development of Drosophila. *Genes Cells* **14**, 1067–1077 (2009).
27. Andrew, D. J. & Ewald, A. J. Morphogenesis of epithelial tubes: Insights into tube formation, elongation, and elaboration. *Dev Biol* **341**, 34–55 (2010).
28. Moreno-Bueno, G. *et al.* The morphological and molecular features of the epithelial-to-mesenchymal transition. *Nat Protoc* **4**, 1591–1613 (2009).
29. Rindler, M. J., Chuman, L. M., Shaffer, L. & Saier, M. H. Retention of differentiated properties in an established dog kidney epithelial cell line (MDCK). *J Cell Biol* **81**, 635–648 (1979).
30. Thiery, J. P. Epithelial-mesenchymal transitions in tumour progression. *Nat Rev Cancer* **2**, 442–454 (2002).
31. Vleminkx, K., Vakaet, L., Mareel, M., Fiers, W. & van Roy, F. Genetic manipulation of E-cadherin expression by epithelial tumor cells reveals an invasion suppressor role. *Cell* **66**, 107–119 (1991).
32. Berkhout, M. *et al.* Loss of extracellular E-cadherin in the normal mucosa of duodenum and colon of patients with familial adenomatous polyposis. *Hum Pathol* **37**, 1389–1399 (2006).
33. Wheeler, J. M. *et al.* Hypermethylation of the promoter region of the E-cadherin gene (CDH1) in sporadic and ulcerative colitis associated colorectal cancer. *Gut* **48**, 367–371 (2001).
34. Janda, E. *et al.* Raf plus TGFbeta-dependent EMT is initiated by endocytosis and lysosomal degradation of E-cadherin. *Oncogene* **25**, 7117–7130 (2006).
35. Zhong, S. *et al.* MTA is an Arabidopsis messenger RNA adenosine methylase and interacts with a homolog of a sex-specific splicing factor. *Plant Cell* **20**, 1278–1288 (2008).
36. Bodi, Z., Bottley, A., Archer, N., May, S. T. & Fray, R. G. Yeast m6A Methylated mRNAs Are Enriched on Translating Ribosomes during Meiosis, and under Rapamycin Treatment. *PLoS One* **10**, e0132090, <https://doi.org/10.1371/journal.pone.0132090> (2015).
37. Shen, L. *et al.* N(6)-methyladenosine RNA modification regulates shoot stem cell fate in Arabidopsis. *Dev Cell* **38**, 186–200 (2016).
38. MacGrath, S. M. & Koleske, A. J. Cortactin in cell migration and cancer at a glance. *J Cell Sci* **125**, 1621–1626 (2012).
39. Ni, Q. F. *et al.* Cortactin promotes colon cancer progression by regulating ERK pathway. *Int J Oncol* **47**, 1034–1042 (2015).
40. Weaver, A. M. Cortactin in tumor invasiveness. *Cancer Lett* **265**, 157–166 (2008).
41. Clark, E. S. & Weaver, A. M. A new role for cortactin in invadopodia: regulation of protease secretion. *Eur J Cell Biol* **87**, 581–590 (2008).
42. Zhang, X. *et al.* HDAC6 modulates cell motility by altering the acetylation level of cortactin. *Mol Cell* **27**, 197–213 (2007).
43. Ito, A. *et al.* The subcellular localization and activity of cortactin is regulated by acetylation and interaction with Keap1. *Sci Signal* **8**, ra120, <https://doi.org/10.1126/scisignal.aad0667> (2015).
44. Aghajanian, C. *et al.* A phase II evaluation of bortezomib in the treatment of recurrent platinum-sensitive ovarian or primary peritoneal cancer: a Gynecologic Oncology Group study. *Gynecol Oncol* **115**, 215–220 (2009).
45. Rosenberg, J. E. *et al.* Phase II study of bortezomib in patients with previously treated advanced urothelial tract transitional cell carcinoma: CALGB 90207. *Ann Oncol* **19**, 946–950 (2008).
46. Banno, A. *et al.* Downregulation of 26S proteasome catalytic activity promotes epithelial-mesenchymal transition. *Oncotarget* **7**, 21527–21541 (2016).
47. Isella, C. *et al.* Selective analysis of cancer-cell intrinsic transcriptional traits defines novel clinically relevant subtypes of colorectal cancer. *Nat Commun* **8**, 15107, <https://doi.org/10.1038/ncomms15107> (2017).
48. Guinney, J. *et al.* The consensus molecular subtypes of colorectal cancer. *Nat Med* **21**, 1350–1356 (2015).
49. Minn, A. J. *et al.* Genes that mediate breast cancer metastasis to lung. *Nature* **436**, 518–524 (2005).
50. Meijer, G. A. & Baak, J. P. Quantification of proliferative activity in colorectal adenomas by mitotic counts: relationship to degree of dysplasia and histological type. *J Clin Pathol* **48**, 620–625 (1995).
51. Fujiki, Y. *et al.* Quantification of green fluorescent protein by *in vivo* imaging, PCR, and flow cytometry: comparison of transgenic strains and relevance for fetal cell microchimerism. *Cytometry A* **73**, 11–118 (2008).
52. Lin, J. *et al.* High-quality genomic DNA extraction from formalin-fixed and paraffin-embedded samples deparaffinized using mineral oil. *Anal Biochem* **395**, 265–267 (2009).
53. Livak, K. J. & Schmittgen, T. D. Analysis of relative gene expression data using real-time quantitative PCR and the 2(-Delta Delta C(T)) Method. *Methods* **25**, 402–408 (2001).

Acknowledgements

This work has been supported by Plan Estatal I+D+I 2013–2016, co-funded by the Instituto Carlos III (ISCIII, Spain) – Fondo Europeo de Desarrollo Regional (FEDER) “A way of Making Europe” (P113/00250). Diaz-Diaz has been supported by FPU contract (FPU014/02837) from Ministerio de Educación Cultura y Deporte from Spain and Casas-Pais has been supported by a predoctoral contract (IN606A-2017/013) from Axencia Galega de Innovación (GAIN)-Consellería de Economía, Empleo e Industria from Xunta de Galicia, Spain.

Appendix C

Summary of the thesis in Spanish

Capítulo Uno

Introducción

El cáncer es una de las principales causas de mortalidad y morbilidad en el mundo, con aproximadamente 19,3 millones de casos nuevos en 2020. Se espera que el número de casos nuevos aumente en las próximas dos décadas hasta 30,2 millones al año en 2040. El número de muertes relacionadas con tumores en 2020, según los datos proporcionados por la OMS, asciende a 9,96 millones. Los tumores responsables del mayor número de muertes en todo el mundo son el cáncer de pulmón (18,0% de todas las muertes por cáncer), el cáncer colorrectal (9,4%), el cáncer de hígado (8,3%) y el cáncer de estómago (7,7%). El cáncer colorrectal (CCR) es el cuarto tipo de cáncer con mayor incidencia a nivel mundial para ambos sexos y todas las edades según el Observatorio Global del Cáncer (GLOBOCAN) en su último informe de 2020.

La etiología del CCR es multifactorial, siendo el resultado de una compleja interacción entre la susceptibilidad genética y diferentes factores biológicos y ambientales. Algunos de estos factores de riesgo son modificables como, por ejemplo: dieta, disbiosis microbiana intestinal, consumo de grasas, obesidad, tabaquismo, alcohol, colecistectomía o radiación. Otros sin embargo no lo son, entre ellos se encontrarían: edad, presencia de enfermedad inflamatoria intestinal y antecedentes personales de adenomas y/o CCR.

La gran mayoría de los casos de cáncer colorrectal (>90%) corresponden a adenocarcinomas, tumores que se originan a partir de células epiteliales glandulares. Estas células forman una estructura epitelial que es de vital importancia para la salud del huésped y la homeostasis global. La mayoría de los cánceres colorrectales (CCR) se originan a partir de pólipos adenomatosos, que aparecen en el colon cuando se alteran los mecanismos que regulan la renovación de las células epiteliales. Se ha demostrado que la carcinogénesis colorrectal es un proceso de múltiples pasos en el que la acumulación de alteraciones genéticas en las células epiteliales les confiere una serie de capacidades biológicas que permiten el desarrollo tumoral. A medida que las células epiteliales sanas evolucionan progresivamente hacia un estado neoplásico, adquieren una serie de capacidades distintivas que les permitirán convertirse primero en tumorigénicas y finalmente en malignas. Estos ocho sellos distintivos del cáncer son: mantener la señalización proliferativa, evadir los supresores del crecimiento, resistir la muerte

celular, permitir la inmortalidad replicativa, inducir la angiogénesis, activar la invasión y la metástasis, reprogramar el metabolismo energético y evitar la destrucción inmunológica.

La capacidad de las células tumorales para invadir y metastatizar es uno de los elementos más distintivos del cáncer y se estima que el 90% de las muertes por cáncer están causadas por las metástasis. El principal mecanismo regulador que permite la activación de estas capacidades celulares es un proceso conocido como transición epitelio-mesenquimal (EMT). Durante la EMT, las células pierden su fenotipo epitelial y adquieren progresivamente un fenotipo mesenquimal caracterizado por cambios morfológicos y moleculares que aumentan la capacidad celular de invasión y migración a través de la matriz extracelular. El marcador mejor caracterizado del proceso EMT es la pérdida del marcador epitelial E-cadherina.

Uno de los mecanismos descritos implicados en la pérdida de E-cadherina es a través de la degradación de la E-cadherina, que se produce de manera dependiente de fosforilación y mediante un proceso de ubiquitinación. Esta ubiquitinación está mediada por una E3 ubiquitina-ligasa conocida como Hakai, descrita por primera vez en 2002 como el primer regulador postraduccionales de la estabilidad de la E-cadherina. Hasta la fecha, la E-cadherina es el único sustrato de Hakai descrito que está directamente involucrado en el proceso de EMT. Sin embargo, también se ha observado que Hakai interactúa con otras proteínas como el receptor estrogénico alfa (ER α) en cáncer de mama o Ajuba en carcinoma hepatocelular. Por otro lado, también se ha descrito que Hakai interactúa con el ARN y desempeña un papel regulador en la epitranscriptómica, durante la metilación de m⁶A. A través de este mecanismo, Hakai se ha relacionado con la regulación del microambiente inmunológico de la periodontitis, donde se cree que Hakai regula la citocina TNF- α y sus receptores.

El vínculo entre la inflamación y la tumorigénesis está bien establecido para el CCR y se ha descrito una vía específica de carcinogénesis asociada con inflamación crónica y enfermedad inflamatoria intestinal (EII). La EII es una enfermedad inflamatoria crónica que afecta al tracto gastrointestinal y comprende dos entidades clínicas principales: la enfermedad de Crohn (EC) y la colitis ulcerosa (CU). Tanto la EC como la CU son enfermedades complejas que implican una gran interrelación entre el sistema inmunológico, la microbiota intestinal y múltiples factores ambientales. La CU se caracteriza por una inflamación de la mucosa, que normalmente se inicia en el recto y

se extiende hasta el colon de forma continua. La inflamación en la CU se limita típicamente a la capa mucosa y causa daño superficial a la pared intestinal. La EC por su parte, es una enfermedad inflamatoria intestinal que puede afectar cualquier parte del tracto digestivo y se caracteriza por lesiones intermitentes parcheadas a lo largo del tracto digestivo. La EC se caracteriza por una inflamación transmural que conduce al desarrollo de fibrosis, estenosis y fístulas. En ambos casos se produce una disrupción de la barrera epitelial que conduce a una respuesta inflamatoria como parte del proceso fisiológico de cicatrización de heridas destinado a reparar el tejido dañado y restaurar la estructura normal y la funcionalidad del intestino. En este proceso de curación de heridas y reparación de tejidos está también implicado el proceso de EMT.

Las células epiteliales, por tanto, juegan un papel fundamental en la patogenia de la EII, desencadenando la respuesta inmune local y actuando como barrera protectora entre la luz intestinal y las células inmunes. En este sentido, existe una amplia gama de ácidos grasos de vital importancia en la fisiología de las células epiteliales intestinales, así como en sus procesos inflamatorios. Los ácidos grasos son una fuente de energía importante de las células de la mucosa intestinal y contribuyen considerablemente a la función y patología de las células epiteliales intestinales. La biosíntesis de estos ácidos grasos de cadena larga es catalizada por la sintasa de ácidos grasos (FASN). FASN se encuentra sobreexpresada en algunas lesiones benignas y preneoplásicas de los nevos de próstata, mama, pulmón, estómago, colon y piel, asociada a la progresión tumoral. Varios estudios también han documentado la sobreexpresión de esta proteína en los trastornos inflamatorios, especialmente en la CU.

Hipótesis y objetivos

La E3 ubiquitina-ligasa Hakai juega un papel importante durante la EMT y la progresión tumoral, regulando negativamente la E-cadherina en los contactos célula-célula. En base a los antecedentes descritos y los resultados previos obtenidos por nuestro grupo de investigación, se propone estudiar en profundidad la expresión de la E3 ubiquitina-ligasa Hakai en estadios tempranos de la progresión tumoral del CCR, así como su posible rol en la enfermedad inflamatoria intestinal (EII). La hipótesis general de este estudio sería:

- Hakai podría estar implicado en eventos tempranos de la progresión del CCR, así como estar involucrado en el desarrollo de procesos inflamatorios preneoplásicos como la EII.

Para confirmar esta hipótesis, proponemos los siguientes objetivos específicos:

- **Objetivo 1-** Analizar la expresión de Hakai en pares de tejidos sanos de colon humano en comparación con adenoma y con diferentes estadios TNM (I-IV) de adenocarcinomas de colon.
- **Objetivo 2-** Realizar un interactoma de Hakai para buscar potenciales nuevas proteínas que interactúen con Hakai involucradas en procesos inflamatorios.
- **Objetivo 3-** Estudiar el posible papel de Hakai *in vitro* por su acción sobre nuevas proteínas diana relacionadas con la inflamación en el cáncer colorrectal.
- **Objetivo 4-** Analizar *in vivo* el papel de Hakai en diferentes modelos animales de EII.
- **Objetivo 5-** Analizar la expresión de Hakai en muestras humanas de pacientes con CU y EC.

Resultados

Los resultados obtenidos previamente en nuestro grupo de investigación habían demostrado que Hakai estaba claramente sobreexpresado en los adenocarcinomas de colon humano en comparación con los tejidos normales. En este estudio, nos planteamos determinar si esta expresión de Hakai podría estar correlacionada con el estadiaje de la enfermedad. Por ello, mediante inmunohistoquímica se compararon pares de muestras de tejido sano adyacente con diferentes estadios (I-IV) TNM de adenocarcinomas de colon y adenoma. Los resultados mostraron que las intensidades de tinción de Hakai aumentaron gradualmente desde el tejido sano hasta el adenoma y los estadios I a IV del adenocarcinoma colorrectal. De este modo, Hakai se establecería como un posible biomarcador de progresión tumoral en CCR. Además, esta sobreexpresión de Hakai es apreciable incluso en las primeras etapas de la progresión

del tumor ya que su sobreexpresión fue significativa tanto en las muestras de adenoma como de adenocarcinoma estadio I.

El hecho de que la expresión de Hakai se encontrara alterada incluso en estadios muy tempranos del desarrollo tumoral, nos llevó a cuestionarnos si Hakai pudiera estar implicado en procesos previos al cáncer como las enfermedades inflamatorias intestinales. Se procedió por tanto a evaluar por inmunohistoquímica la expresión de Hakai en muestras de pacientes con enfermedad inflamatoria intestinal (EII), que incluye, tanto pacientes con colitis ulcerativa (CU) como con enfermedad de Crohn (EC). La intensidad de la tinción de Hakai en las muestras de EII se incrementó significativamente en comparación con el tejido normal adyacente, pero sin alcanzar el nivel de intensidad de tinción observada en las muestras de adenocarcinoma colorrectal estadio IV.

En vista de estos resultados, nos decidimos a estudiar el posible papel de Hakai en la EII, tanto *in vivo* como *in vitro*, así como tratar de identificar posibles nuevos targets de Hakai vinculados al proceso inflamatorio.

El estudio de la expresión *in vivo* de Hakai en diferentes modelos animales de EII, mostró una regulación clara de Hakai en diferentes condiciones inflamatorias, con una gran reducción de la expresión de Hakai en el epitelio inflamado de los ratones en comparación con ratones sanos. Estos resultados fueron confirmados posteriormente mediante un análisis de la base de datos Gene Expression Omnibus (GEO) del NCBI. En ella experimentos similares habían reportado una reducción en los niveles de mRNA de Hakai en el tejido inflamado de los mismos modelos animales evaluados.

Por otro lado, con el objetivo de identificar posibles targets de Hakai asociados a procesos inflamatorios, se llevó a cabo un interactoma de la proteína. En dicho interactoma se detectó, entre otras proteínas, la Ácido graso sintetasa (FASN), una proteína cuya sobreexpresión se ha asociado con el desarrollo de EII. El estudio *in vitro* del vínculo entre Hakai y FASN demostró que efectivamente ambas proteínas interactúan y que concretamente Hakai media la degradación de FASN vía lisosoma mediante ubiquitinación. Esta degradación además regula la acumulación celular de ácidos grasos mediada por FASN.

Con el fin de dar explicación a la reducción de la expresión de Hakai observada en los tejidos inflamados de los modelos animales inflamatorios, se planteó estudiar como afectaba a dicha expresión la presencia *in vitro* de diferentes citoquinas proinflamatorias como TNF- α , IL-6, IFN- γ , o stress oxidativo (H₂O₂). El tratamiento con estas citoquinas no modificó la expresión de Hakai, a excepción del caso del IFN- γ , en el cual los resultados mostraron una regulación negativa de la expresión de Hakai, especialmente a tiempos largos de exposición. Además, esta reducción en la expresión de Hakai ante el tratamiento con IFN- γ , conllevó una sobreexpresión de su target, FASN. Esta correlación inversa entre la expresión de Hakai y FASN fue igualmente observada en los tejidos inflamados del modelo animal AOM/DSS de CCR asociado a colitis. Podría establecerse, por tanto, un vínculo entre IFN- γ -Hakai-FASN de manera que el IFN- γ sería ser al menos en parte responsable de esta regulación negativa de Hakai y la consecuente sobreexpresión de FASN. Sin embargo, son necesarios más estudios para profundizar en el papel de Hakai en la EII tanto en modelos de ratones como en biopsias humanas con el fin de comprender mejor el mecanismo y las vías reguladoras que pueden influir en la homeostasis intestinal y su alteración en la EII.

Conclusiones

1. La expresión de Hakai aumenta gradualmente en el adenoma y en los estadios TNM (I a IV) del adenocarcinoma colorrectal en comparación con los tejidos de colon sano, siendo un posible nuevo biomarcador para la progresión del cáncer colorrectal.
2. FASN es una nueva proteína que interactúa con Hakai relacionada con la EII.
3. Hakai media la ubiquitinación y degradación de FASN a través del lisosoma, lo que regula la acumulación celular de lípidos mediada por FASN.
4. IFN- γ regula negativamente la expresión de Hakai *in vitro* y aumenta la expresión de FASN.
5. La expresión de Hakai está regulada negativamente en tejidos inflamatorios en diferentes modelos animales de EII.
6. FASN está incrementado en tejidos inflamados del modelo animal inflamatorio AOM/DSS, mientras los niveles de expresión de Hakai se encuentran reducidos.

7. La expresión de Hakai esta incrementada en el tejido inflamado de pacientes con CU y EC en comparación con el tejido sano adyacente.

Capítulo Dos

Introducción

Desde tiempos inmemoriales, los seres humanos han utilizado los hongos no sólo como alimento sino también como agentes medicinales. Prueba de ello es la larga tradición del uso de hongos como agentes terapéuticos en la medicina de los países orientales y la creciente variedad de productos obtenidos de diferentes especies de hongos que ayudan a mejorar el estado de salud. Los hongos poseen múltiples acciones medicinales, entre las que podemos encontrar: antitumorales, inmunomoduladoras, cardiovasculares, antibacterianas, antivirales, antifúngicas, antiparasitarias, o antioxidantes. Las propiedades terapéuticas de estos hongos se deben a varios de sus compuestos celulares, así como a ciertos metabolitos secundarios presentes en los cuerpos fructíferos, micelios y sus medios de cultivo. Estos metabolitos pueden ser de naturaleza muy variada: polisacáridos, proteínas, complejos formados por ambos o metabolitos de bajo peso molecular como compuestos fenólicos, triterpenoides, poliquétidos, lactonas, alcaloides, ácidos grasos y nucleótidos.

Las propiedades antitumorales de los hongos se describieron por primera vez en 1957 a partir de extractos de cuerpos fructíferos de *Boletus edulis* y otros *Homobasidiomicetos* sobre el sarcoma en ratones. Desde entonces, se ha demostrado que los hongos pertenecientes a una amplia variedad de especies, así como los extractos obtenidos de ellos, poseen efectos antitumorales. Los mecanismos de acción por los cuales los extractos fúngicos ejercen su actividad antineoplásica son muy diversos, pero se podrían agrupar principalmente en inmunomoduladores y de citotoxicidad. Por un lado, muchos extractos son capaces de intensificar la actividad del sistema inmune aumentando la infiltración de células T y dendríticas en los tumores, así como una mayor expresión de citocinas y quimiocinas. Otros extractos ejercen su actividad anticancerígena a través de mecanismos de citotoxicidad, como la detención del ciclo celular, la apoptosis o la inhibición de la migración. Estos mecanismos a su vez pueden presentarse de forma conjunta o de manera individual en función de las características y composición de cada extracto.

Hasta la actualidad se han identificado diversos compuestos con actividad antitumoral de diferente naturaleza: polisacáridos, proteínas, esteroides, glucopéptidos y otros complejos proteicos, alcaloides, compuestos fenólicos, etc. Entre todos ellos, los polisacáridos, especialmente los β -glucanos, han sido identificados como los principales responsables de este efecto y destacan claramente. Extractos ricos en polisacáridos han demostrado entre otros efectos, inducir la apoptosis a través de la acción sobre las vías dependientes de PI3K/Ak/mTOR, NF- κ B y p53, arresto del ciclo celular (fase G1) mediante la activación de p53 e inhibición de la fosforilación de STAT-3, reducción del potencial migratorio e invasivo de las células a través de la supresión de la actividad enzimática de MMP-2 y MMP-9, disminución de la quinasa de adhesión focal (FAK)/paxilina y regulación de la EMT a través de los factores de transcripción Snail y Slug. Por tanto, no hay duda de que los hongos y los productos derivados de ellos tienen un potencial muy grande para el tratamiento del cáncer. De hecho, varias empresas farmacéuticas ya se dedican a la producción de medicamentos contra el cáncer, así como fórmulas y suplementos para su prevención a partir de compuestos de origen fúngico.

Cinco filos diferentes, cada uno de los cuales incluye especies muy diferentes, componen el reino de los hongos: *Basidiomycota*, *Ascomycota*, *Zygomycota*, *Chytridiomycota* y *Glomeromycota*. Se cree que la gran mayoría, si no todas las especies de hongos basidiomicetos contienen polisacáridos biológicamente activos en sus cuerpos fructíferos, en sus micelios cultivados y en sus medios de cultivo. Los hongos medicinales pertenecientes al filo *Basidiomycota*, por tanto, representan una fuente abundante de productos naturales con actividades biológicas de interés que aún se encuentran en gran parte sin explotar. La división *Basidiomycota* o "phylum" comprende tres grupos o subdivisiones principales: *Agaricomycotina*, *Ustilaginomycotina* y *Pucciniomycotin*. En el presente estudio nos centraremos en dos especies de hongos pertenecientes a la subdivisión *Agaricomycotina*, *Trametes versicolor* del orden *Polyporales* y la familia *Polyporaceae*, y *Grifola frondosa* del orden *Polyporales* y la familia *Meripilaceae*.

Los principales componentes bioactivos de *Trametes versicolor* son los polisacaropéptidos (PSP). De todos ellos, el Polisacárido Péptido (PSP) y la Krestina o Polisacárido-K (PSK) son los componentes biológicamente más activos, ambos con una estructura formada por β -glucanos. Múltiples estudios avalan el efecto de los extractos de

Trametes versicolor sobre la carcinogénesis. A nivel inmunológico PSK actúa como agonista de los receptores tipo Toll, TLR2 y TLR4; PSP, por su parte aumenta los niveles de fosforilación de los factores de transcripción NF- κ B, p65, and c-Jun. Todos estos elementos están relacionados con la activación del sistema inmunológico, lo cual induce la producción de citocinas inflamatorias, necesarias para la activación de linfocitos T por células dendríticas y macrófagos. Además de sus efectos sobre el sistema inmunológico, también se ha demostrado que estos polisacaropéptidos ejercen su efecto a través de la toxicidad directa sobre células cancerosas. Por ejemplo, PSK es capaz de promover la apoptosis mediante la activación de la caspasa-3 y producir la fosforilación de p38 MAPK, que participa en una cascada de señalización involucrada en la apoptosis y la autofagia. Además, la caracterización molecular de PSP mostró que induce la apoptosis mediando la regulación positiva de factores de transcripción tempranos como AP-1, EGR1, IER2 e IER5 y la regulación negativa de la vía moduladora del cáncer NF- κ B. Otros mecanismos descritos para el efecto anticanceroso a través de toxicidad directa incluyen la interrupción de la progresión del ciclo celular y la detención en las fases G0, G0/G1, G1/S y G2/M, así como la inhibición de la migración e invasión celular mediante la inhibición de enzimas angiogénicas clave como metaloproteasas de la matriz.

Grifola frondosa, por su parte, también posee en su composición un elevado número de β -glucanos con actividad antitumoral. La administración oral de β -glucanos de *Grifola frondosa*, ha demostrado activar macrófagos y células dendríticas (DC), funcionalmente defectuosas en pacientes con tumores, induciendo a las células T colaboradoras y las células T citotóxicas a inhibir el crecimiento de las células tumorales. Otro estudio en pacientes con un extracto de polisacáridos de *Grifola frondosa* también mostró una mayor producción de citocinas proinflamatorias, incluidas IL-2, IL-10, TNF- α e IFN- γ por parte de subconjuntos de células T. Otro mecanismo de acción descrito para los β -glucanos de *Grifola frondosa* son sus funciones anticancerígenas a través de la regulación de diferentes vías tumorales. Por ejemplo, se ha descrito que extractos de *Grifola frondosa* pueden inducir apoptosis en células de cáncer de mama mediante la activación de genes proapoptóticos. Los mismos autores también documentaron la regulación a la baja de la vía de señalización PI3K-AKT bajo tratamiento con el mismo extracto. Otros estudios han reportado que los extractos disminuyeron las capacidades

migratorias e invasivas de células de cáncer de mama al aumentar la adhesión celular, medida por el aumento de la expresión del marcador epitelial E-Cadherina, y al disminuir el número de filopodios y lamelipodios. Estos efectos también fueron respaldados por una regulación a la baja de la actividad de MMP-2 y una reducción de la carga tumoral y las metástasis pulmonares en un modelo murino.

Hipótesis y objetivos

Como se mencionó anteriormente, los extractos de hongos representan una fuente muy importante de compuestos con potencial actividad antitumoral. Por otro lado, a pesar de los estudios disponibles, el mecanismo por el cual los extractos de hongos ejercen su efecto antitumoral es poco conocido. En particular, no se sabe bien cómo los extractos de hongos pueden afectar al proceso de la EMT. La hipótesis general para este trabajo sería:

- Los extractos fúngicos de diferentes especies autóctonas de Galicia podrían tener efecto antitumoral en células de CCR. Este efecto antitumoral podría ejercerse a través de la regulación EMT, un elemento clave en la progresión tumoral y la metástasis.

Para investigar esta hipótesis, en este estudio nos propusimos analizar el potencial antitumoral de diferentes especies de hongos autóctonos de Galicia. Para ello se proponen los siguientes objetivos específicos.

- **Objetivo 1-** Analizar el efecto de diferentes extractos de hongos sobre la viabilidad y proliferación de células cancerosas de colon.
- **Objetivo 2** - Seleccionar los extractos más prometedores por su acción sobre la viabilidad y proliferación celular para estudios posteriores.
- **Objetivo 3-** Determinar el efecto de extractos seleccionados sobre la reversión del proceso EMT, migración e invasión de células cancerosas de colon.
- **Objetivo 4-** Estudiar el posible efecto sinérgico con uno de los agentes más utilizados en la clínica para el cáncer colorrectal, el 5-fluorouracilo, en combinación con extractos de hongos seleccionados.

Resultados

La evaluación inicial se comenzó partiendo de 35 extractos fúngicos diferentes pertenecientes a 5 especies de hongos distintas: *Grifola frondosa* (GF), *Trametes versicolor* (TV), *Pleurotus ostreatus* (PO), *Ganoderma lucidum* (GL) and *Polyporus umbellatus* (PU). Tras evaluar el potencial citotóxico de cada extracto, así como su efecto sobre el fenotipo celular de las células de cáncer colorrectal, se identificaron dos extractos pertenecientes a las especies GF y TV como los más prometedores de cara a estudios más en profundidad. Ambos extractos además de reducir la viabilidad de células de cáncer colorrectal también demostraron afectar significativamente a la capacidad proliferativa de estas mismas células medida mediante ensayos de BrdU. Además, en relación con la posible vinculación entre el mecanismo de estos extractos con la EMT, se estudió el efecto de estos en distintos procesos celulares como la migración y la invasión celulares o el potencial oncogénico. Los resultados mostraron que ambos extractos fueron capaces de inhibir significativamente el potencial oncogénico, la migración celular y la invasión en las células CRC.

Con el objetivo de profundizar en el posible mecanismo responsable de los resultados observados, se estudió si alguno de los principales marcadores de la EMT podría estar siendo regulado por los extractos fúngicos. En este sentido, el marcador epitelial E-cadherina, cuya pérdida está considerada como un sello distintivo de la transición epitelio-mesenquimal, resultó estar regulado positivamente por el tratamiento con ambos extractos. Por otro lado, las metaloproteinasas, enzimas clave en el proceso de invasión y metástasis de carcinomas, también resultaron estar reguladas por el tratamiento con los extractos fúngicos de TV y GF. En concreto, el tratamiento tanto con TV como GF, redujo significativamente la actividad de la metaloproteinasa MMP-2.

Como los extractos habían mostrado un efecto significativo sobre la proliferación y viabilidad celular, planteamos la hipótesis de que algunas proteínas reguladoras del ciclo celular podrían estar reguladas por estos extractos y ser las responsables del efecto que detectamos. Por ello, evaluamos la expresión de proteínas con un papel importante en el control del ciclo celular y que habían sido descritas como supresoras de tumores o

relacionadas con la progresión tumoral. La proteína de la retinoblastoma fosforilada (pRb) es una proteína supresora de tumores alterada en muchos tipos de cáncer, normalmente implicada en la prevención de la proliferación celular, bloqueando la progresión del ciclo celular. p21 está regulado por el gen supresor de tumores p53, y también actúa regulando la detención del ciclo celular G0/G1. Finalmente, CDK2 es esencial para la transición G1/S en el ciclo celular. Los resultados mostraron una regulación positiva de la expresión de p21 y pRb ante el tratamiento con extractos de TV y GF. Estos resultados sugieren que el efecto antiproliferativo y antitumoral mostrado por los extractos puede explicarse por la regulación de p21 y pRb.

Finalmente, nuestros resultados también muestran que la combinación de los extractos con uno de los agentes más utilizados en la clínica para el cáncer colorrectal, el 5-fluorouracilo, aumenta la citotoxicidad celular, abriendo la puerta a nuevas investigaciones para el uso de extractos de hongos como tratamiento adyuvante en el cáncer.

Conclusiones

1. Los extractos fúngicos ejercen diferentes niveles de inhibición sobre la viabilidad celular y la proliferación en las células de cáncer de colon.
2. Se seleccionaron extractos de *Trametes versicolor* (TV) y *Grifola frondosa* (GF) por su efecto sobre la citotoxicidad celular y sobre un fenotipo de tipo celular más epitelial.
3. Los extractos de TV y GF inhiben significativamente el potencial oncogénico, la migración celular y la invasión en células de cáncer de colon.
4. Los extractos de TV y GF aumentan la expresión del marcador epitelial E-cadherina y reducen la actividad de la MMP-2.
5. La combinación de extractos de TV y GF con el agente quimioterápico, 5-fluorouracilo, aumenta la citotoxicidad celular.